USAAVLABS TECHNICAL REPORT 66-31

A PRESENTATION OF MEASURED AND CALCULATED FULL-SCALE ROTOR BLADE AERODYNAMIC AND STRUCTURAL LOADS

By

J. P. Rabbott, Jr.
A. A. Lizak
V. M. Paglino

July 1966

U. S. ARMY AVIATION MATERIEL LABORATORIES
FORT EUSTIS, VIRGINIA

CONTRACT DA 44-177-AMC-53(T)

UNITED AIRCRAFT CORPORATION
SIKORSKY AIRCRAFT DIVISION
STRATFORD, CONNECTICUT

Disclaimers

The findings in this report are not to be construed as an official Department of the Army position unless so designated by other authorized documents.

When Government drawings, specifications, or other data are used for any purpose other than in connection with a definitely related Government procurement operation, the United States Government thereby incurs no responsibility nor any obligation whatsoever; and the fact that the Government may have formulated, furnished, or in any way supplied the said drawings, specifications, or other data is not to be regarded by implication or otherwise as in any manner licensing the holder or any other person or corporation, or conveying any rights or permission, to manufacture, use, or sell any patented invention that may in any way be related thereto.

Trade names cited in this report do not constitute an official endorsement or approval of the use of such commercial hardware or software.

Disposition Instructions

Destroy this report when no longer needed. Do not return it to the originator.

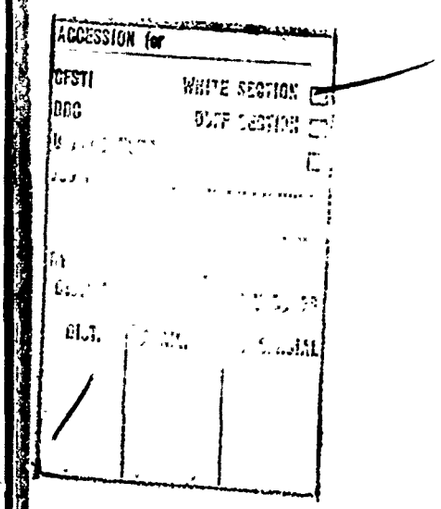

DEPARTMENT OF THE ARMY
U. S. ARMY AVIATION MATERIEL LABORATORIES
FORT EUSTIS, VIRGINIA 23604

This report has been reviewed by the U. S. Army Aviation Materiel Laboratories and is considered to be technically sound and accurate. It is published for the exchange of information and the stimulation of further understanding and research in rotary-wing aerodynamics.

Task 1P125901A14604

Contract DA 44-177-AMC-53(T)

USAAVLABS Technical Report 66-31

July 1966

A PRESENTATION OF MEASURED AND CALCULATED FULL-SCALE ROTOR BLADE AERODYNAMIC AND STRUCTURAL LOADS

SER-58398

by

J. P. RABBOTT, JR.
A. A. LIZAK
V. M. PAGLINO

Prepared by

UNITED AIRCRAFT CORPORATION
SIKORSKY AIRCRAFT DIVISION
STRATFORD, CONNECTICUT

for

U.S. ARMY AVIATION MATERIEL LABORATORIES
FORT EUSTIS, VIRGINIA

SUMMARY

A test of a set of Sikorsky CH-34 rotor blades was conducted in the NASA/Ames full-scale wind tunnel at speeds of from 110 to 175 knots. One blade of the set was instrumented to measure differential chordwise pressures and flapwise, chordwise, and torsional stress. The test results are presented, two- and three-dimensional pressure distributions are compared, and a correlation of airloads and blade stresses is made with a flexible blade aeroelastic theory, including both uniform and variable inflow assumptions.

At inboard radial stations where a direct comparison of measured and two-dimensional chordwise loadings could be made, the correlation was good. However, near the advancing blade tip, in a region of rapid change in loading, and therefore in shed vorticity, there is evidence of a requirement for including consideration of lifting surface effects in the calculation.

Correlation of measured section airload time histories with theory was generally good, with the principal discrepancy noted at high speed in the region of the advancing blade tip where a sharp, impulsive type of loading was measured. Inclusion of variable inflow improved the correlation on both advancing and retreating sides of the disk at speeds as high at 175 knots, but the need for a more rigorous treatment of theoretical shed vorticity is indicated, owing to the presence of a phase lag between measured and calculated loading.

Good correlation of measured and calculated vibratory blade stresses was shown. Inclusion of variable inflow tends to improve the correlation of flapwise stress time histories, but has a negligible effect on computed chordwise and torsion stress.

A comparison of wind tunnel and flight test results obtained from the same rotor blade set (both operating at 110 knots but at a different rotor propulsive force) showed generally good agreement, and the differences could reasonably be explained by the differences in rotor operating conditions.

FOREWORD

Mr. Robert Piper monitored this program for the U.S. Army Aviation Materiel Laboratories. The NASA/Ames Project Engineer for the wind tunnel testing was Mr. John McCloud, III. Mr. Lawrence Doyle of the Sikorsky Measurements Instrumentation Section was the principal instrumentation engineer and wrote the Instrumentation Section of this report. Grateful appreciation is extended to each for their valuable assistance in this program.

CONTENTS

ILLUSTRATIONS

TABLES

SYMBOLS

(For Text and Table I)

		Units
a_{1s}	Longitudinal first harmonic flapping with respect to the shaft	Degrees
A_{1s}	Lateral cyclic pitch	Degrees
b	Number of blades	—
b_{1s}	Lateral first harmonic flapping with respect to shaft	Degrees
B_{1s}	Longitudinal cyclic pitch with respect to the shaft	Degrees
c	Blade chord	Feet
C_N	Section normal force coefficient	—
D	Rotor drag	Pounds
E_o	Average lag angle	Degrees
E_1	First harmonic cosine amplitude of lag angle	Degrees
F_1	First harmonic sine amplitude of lag angle	Degrees
HP	Rotor shaft horsepower	—
L	Rotor lift	Pounds
M	Free-stream Mach number	—
$M_{(1.0,90)}$	Mach number of advancing blade tip	—
q	Free stream dynamic pressure	Pounds/square foot
r	Distance from center of rotation to blade radial station	Feet

		Units
R	Blade radius	Feet
V	Forward speed	Feet per second or knots
x	Distance from leading edge to blade chordwise station	Feet
α_r	Local blade section angle of attack	Degrees
α_s	Rotor shaft angle of attack	Degrees
β	Blade flapping angle with respect to shaft	Degrees
γ	Shed vorticity	Square feet per second
Γ	Trailing vorticity	Square feet per second
$\theta_{.75\,R}$	Blade collective pitch at 0.75R	Degrees
μ	Advance ratio, $V/\Omega R$	—
ρ	Air density	Slugs per cubic foot
σ	Blade solidity, $^{bc}/\pi R$	—
ψ	Azimuth angle	Degrees
Ω	Rotor angular velocity	Radians per second

For Remaining Tables

A (N)	Cosine components in terms of Fourier series
B (N)	Sine component in terms of Fourier series
N	Harmonic order, N = 1, 2, 3, . . .

$Y = A_0 - A_1 \cos\psi - B_1 \sin\psi - A_2 \cos 2\psi - B_2 \sin 2\psi$ . . . etc.

INTRODUCTION

During the design stage of rotary-wing aircraft, the ability to predict aerodynamic and, more important, overall dynamic structural blade loads is essential to achieve a structurally reliable and efficient rotor system. This is because the rotor is subjected to continuous fatigue loading, even during normal cruise flight. Early studies to measure the aerodynamic loads on a rotor include the wind tunnel tests of Reference 1 and the more recent flight tests of References 2 and 3. These tests covered the approximate speed range of 0 to 100 knots, and correlation of these test data with theory, as in References 1 and 4, showed that the assumption of uniform rotor inflow was inadequate to predict aerodynamic and structural loads, at least in the lower flight speeds, and that the effects of the trailing wake vorticity must be included in the theory, as covered in References 4 and 5.

The purpose of the present investigation was to extend the range of available aerodynamic and structural loading data to higher forward speeds. Therefore, the pressure-instrumented Sikorsky CH-34 full-scale rotor system, used in the study of Reference 2, was tested in the NASA/Ames full-scale wind tunnel at speeds of from 110 to 175 knots. An additional test was conducted at 110 knots to simulate a flight test condition of Reference 2. These data are presented and a comparison is made with computed aerodynamic and structural loads. For certain computations, both nonuniform and uniform rotor inflow were used.

This program was jointly sponsored by the United States Army Aviation Materiel Laboratories and Sikorsky Aircraft, and the tests were conducted by the Ames Research Center of the National Aeronautics and Space Administration.

DESCRIPTION OF FACILITIES AND EQUIPMENT

WIND TUNNEL

The full-scale wind tunnel located at the NASA Ames Research Center is of the closed-throat, closed-return type, with a test section 40 feet high and 80 feet wide. This tunnel has a nominal maximum speed capability of 200 knots and is powered by six 6000-horsepower electric motors. Model forces and moments are measured by a six-component mechanical balance, with the readings punched directly on IBM cards for processing.

ROTOR DRIVE AND CONTROL SYSTEM

The faired rotor drive and control system is shown as installed in the wind tunnel in Figure 1. The fully articulated rotor is mounted on a standard CH-34 transmission powered by a NASA 1500-horsepower variable-speed electric motor. The four-bladed hub is equipped with coincident flapping and lagging hinges located 1 foot from the center of rotation. Lagging motion is restrained by standard production hydraulic dampers. A terminal plate is mounted on the rotor head to accommodate instrumentation leads from the rotating system through the slip rings to the fixed system. All components are mounted on a triangular I-beam frame, and the complete assembly is enclosed in a streamlined fairing. The model was supported on the tunnel balance by means of two faired forward struts and one unfaired, telescoping tail strut. The rotor head, at zero angle of attack, was positioned 7 feet above the tunnel center line.

Certain modifications to the CH-34 control system were made to minimize pitch-lag coupling and to provide for adequate strength to react the anticipated control loads which, at the high speeds and advance ratios possible in the wind tunnel, were expected to be in excess of the CH-34 design loads. The swash plate, scissors, and control horn were redesigned. The CH-34 pushrods and primary control servos were replaced by units standard on the Sikorsky S-61 helicopter. The usual aircraft collective and cyclic pitch control sticks were replaced by three remotely operated electromechanical actuators which controlled rotor blade pitch through the standard aircraft linkage.

ROTOR BLADES

The test was conducted using a standard four-bladed CH-34 main rotor, one blade of which was modified only to the extent required for the necessary instrumentation. The remaining blades were balanced to match the instrumented blade. Rotor radius is 28 feet, and the blades are of -8 degrees aerodynamic twist with a blade chord of 16.4 inches. Airfoil contour is that of an NACA 0012, based on a chord of 16.0 inches

modified by a 0.4-inch trailing edge extension of 0.096 inch thickness. Figure 2 compares the basic airfoil shape, the tip cap region at 99 percent radius, and the inboard blade spar. The blade's physical properties are given in Figure 3; the blade frequency diagram, in Figure 4. The calculated blade natural frequencies at a rotor tip speed of 650 feet per second are as follows:

	CYCLES/REVOLUTION
1st Flapwise Mode:	1.03
2nd Flapwise Mode:	2.70
3rd Flapwise Mode:	4.98
4th Flapwise Mode:	7.71
1st Chordwise Mode:	0.24
2nd Chordwise Mode:	3.38
3rd Chordwise Mode:	9.00
1st Torsional Mode:	7.41

(The listed first flapwise and chordwise modes are sometimes referred to as the rigid body flapping and lagging frequencies. However, this is true only for an articulated blade with zero flap and lag hinge offset. For an articulated rotor with finite flapping and lag hinge offset, such as considered here, these are actually elastic modes.)

INSTRUMENTATION AND DATA ACQUISITION SYSTEM

One rotor blade of the set was instrumented with 56 electrical pressure gages, NASA type 49-TP and 6680-NS, (Reference 6) in order to provide measurements of instantaneous aerodynamic loads. The gages were located at nine radial stations as shown in Figure 5. The blade was also strain gaged to measure four flapwise, four chordwise, and three torsion stresses. As a safety precaution, five total stress gages were also provided and continuously monitored during testing (see Figure 5).

A master control console was used to provide rotor control and monitoring functions. The panel display consisted primarily of a rotor tachometer, gearbox oil pressure and temperature indicators, two dials for the resolved flapping angle, and three dial indicators for the control inputs. Three position toggle switches controlled servo actuators, and a servo position indicator system was utilized to set test conditions.

Blade flap and lag angles were measured by Baldwin-Lima-Hamilton angulators installed on the rotor head. A flapping resolver system was used to derive the first harmonic sine and cosine components electrically

from the output of one of two flapping transducers. These flapping components were displayed on the control console for use in setting trim conditions during testing.

Rotor power was derived from torsion strain gages located on the rotor shaft. Electrical signals were transmitted from the rotating to the non-rotating system through a 160-channel slip-ring assembly. Magnetic pickups were used to sense blade azimuth position.

Time-averaged six-component rotor performance data were recorded by the wind tunnel balance and processed by NASA/Ames wind tunnel equipment.

DATA REDUCTION FACILITY

In order to utilize automated electronic data processing techniques, the recording medium selected for all dynamic measurements was magnetic tape. A block diagram of the instrumentation is shown in Figure 6. The principal acquisition device was an Ampex Model 800B Magnetic Tape Recorder which has a capacity of 14 tracks of information.

The recording system was a narrow-band FM multiplex using standard IRIG subcarrier oscillators. Eight channels of information, IRIG bands 9 through 16, were recorded on individual tape tracks. A total of 10 direct record tracks were used for dynamic data. In addition, one track was used for audio comments, two others were used for main rotor azimuth reference contactors, and a final track contained a data run command to be used in processing. All dynamic measurements were recorded simultaneously to provide proper time correlation of the data.

The 56 pressure transducers in the instrumented blade were conditioned using CEC System D Amplifiers.

The strain gage instrumentation channels were conditioned by B & F Bridge Balance Units. The resulting signal outputs were then supplied to the subcarrier oscillators.

In order to provide for on-line monitoring of test conditions, a patch panel and an 18-channel CEC Datarite Oscillograph were provided. It was also necessary to observe specific signals continually during the entire test program. For this purpose, a 17-inch oscilloscope and a four-trace electronic switch were supplied and patched into the appropriate channels.

Operation of the recording system was accomplished by use of a single control unit. Features included selectable time duration data bursts

and an automatic calibration sequence using standard shunt resistance techniques.

DATA PROCESSING SYSTEM

The dynamic test data were processed at Sikorsky Aircraft by means of the technique block diagrammed in Figure 7. A single tape track, which contained a maximum of eight measurements in an FM multiplex, was played back into a bank of narrow-band FM discriminators (Model GFD-7, Data Controls Systems, Inc.). The discriminator outputs were then fed into normalizing amplifiers that scaled all measurements to a common signal level (10 volts = full scale). These data were presented to a solid-state multiplex with sample and hold amplifiers. The sampling rate of the multiplexer was controlled by special Sikorsky-designed hardware that utilized control signals from the analog tape. The control signals, 72 azimuth pulses per main rotor revolution, one azimuth pulse per main rotor revolution, and a data run command, were combined to generate 720 data sampling pulses for 10 data cycles within a given data burst. The multiplexer output was digitized by an eight Bit Binary Plus sign analog to digital converter and formated on digital tape through a Scientific Data Systems Computer, Model 910. This digital tape was then processed to final form by an IBM 7094 computer, with calibration constants incorporated in the digital computations.

FREQUENCY RESPONSE OF DATA SYSTEM AND MEASUREMENT ACCURACY

In considering data accuracy for a test of this type, both static and dynamic errors must be included. By a static error is meant the summation of the possible errors in each individual component of the data acquisition and processing system. This was arrived at by taking the square root of the sum of the squares of the possible deviations of each component, a standard statistical procedure. This resulted in a static system amplitude accuracy for strain gage measurements of 2.2 percent of full scale, and 4.1 percent of full scale for blade pressures.

The dynamic response of the data acquisition and reduction system must also be considered, as it could distort both the amplitude and the phase relationship of the data. There was no measurable amplitude distortion up to the tenth harmonic of rotor speed and a maximum of only 2 percent at the twentieth harmonic for either pressure or strain gage measurements. Figure 8 presents the phase lag of the system versus frequency for both pressure and strain gage measurements.

Any departure from linearity would indicate a phase distortion of the final waveform, but the nonlinearity of the curve is so small that no correction was applied to the data.

SIGN CONVENTIONS

The sign convention used is that a positive sign indicates:

Measurement	Direction
Flapwise bending moment	Upper surface in compression
Chordwise bending moment	Trailing edge in compression
Torsion Moment	Leading edge up
Pressure	Lift (upward)

$\theta_{75\,R}$	Leading edge up, average value
A_{1s}	Pitch reduction at ψ = 0 Degrees Azimuth
B_{1s}	Pitch reduction at ψ = 90 Degrees Azimuth
a_{1s}	Down flapping at ψ = 0 Degrees Azimuth
b_{1s}	Down flapping at ψ = 90 Degrees Azimuth
E_o	Blade span axis lagged behind line from center of rotation and lag hinge (average value)
E_l	Blade leading at ψ = 0 Degrees Azimuth
F_l	Blade leading at ψ = 90 Degrees Azimuth

TEST PROCEDURES, DATA RELIABILITY, AND DATA REPEATABILITY

PROCEDURE

The testing procedure was to set a desired tip speed (650 feet per second), shaft angle of attack, forward speed, and nominal rotor lift. Longitudinal and lateral cyclic pitch were adjusted to provide nominal zero first harmonic flapping with respect to the shaft. The actual first harmonic flapping angles are presented in Table I. A negative Fourier series is used to represent blade motions and all other harmonic amplitudes (for example, $\beta = a_0 - a_{1s}\cos\psi - b_{1s}\sin\psi - a_{2s}\cos 2\psi -$ etc.).

In anticipation of the high control loads that would be generated at high tunnel speeds, the control system was modified and strengthened as described previously. However, this modification resulted in an unusual control system kinematic coupling such that two adjacent blades had a slightly different cyclic pitch from the other two adjacent blades, which resulted in a "split" tip path plane whenever cyclic pitch was applied. The instrumented blade and the preceding blade (whose vortex system has the primary influence on the following blade) were always in plane, but the other two blades were flapped approximately one degree higher. Calculations based on the method of Reference 5 indicate that such a misalignment should have no significant influence on the measured pressure data.

RELIABILITY OF PRESSURE DATA

At each data point, an analog tape record was made for 10 rotor revolutions. Figure 9 shows a typical plot of differential pressure at 90 percent radius and 16.8 percent chord, a randomly chosen location. Curve 1 is a direct playback from the analog tape of a random cycle within the 10-cycle data burst. Curve 2 represents the same random cycle after being digitized in 5-degree increments. Curve 3 is an average of the 10 digitized cycles within the data burst. The figure demonstrates excellent cycle-to-cycle repeatability was well as accurate conversion from analog to digital information.

OVERALL REPEATABILITY OF DATA

At a tunnel speed of 150 knots and a shaft angle of zero, two completely independent runs were conducted at separate times to permit evaluation of overall data repeatability. Figure 10 compares time histories of airloads for three typical radial stations, and Figure 11 presents time histories of flapwise, chordwise, and torsional stress at 65 percent radius. Excellent repeatability is evidenced, particularly considering the slight difference in actual rotor lift and drag.

DESCRIPTION OF COMPUTATIONAL METHOD

The computational technique used (see Figure 12) is based on the aerodynamic approach of Reference 7 but is extended to include blade flexibility through the summation of normal modes of vibration and the incorporation of an option for including the influence of the trailing and shed wakes on rotor loads, using the method of Reference 4. Calculations are performed on an IBM 7094 and are initiated by inserting the blade's physical properties and rotor speed into a deck for computing the rotor blade's natural frequencies and mode shapes based on an extension of the Myklestad method for rotating beams (Reference 8). In this investigation, 4 flapwise, 3 chordwise, and 1 torsional mode shapes were used. These results, along with the required flight parameters (forward speed, tip speed, lift, and propulsive force), blade section aerodynamic data (Reference 7), and rotor inflow, are then inserted in the Normal Mode Transient Analysis program to calculate blade response. Determination of blade response by the normal mode method is described in References 9 and 10. Briefly, using arbitrary starting values, the transient response of the blade is calculated at finite azimuthal increments until the steady state is reached to within a specified tolerance. If the desired lift and propulsive force and/or blade flapping motions are not achieved, an automatic iteration is performed by adjusting rotor inflow and control positions, as indicated in Figure 12. Once convergence is achieved, the rotor blade aerodynamic and structural loads, blade motions, and control positions are printed out.

If the variable inflow option is exercised, the above results are used as input to the Cornell Aeronautical Laboratory variable inflow calculation method of Reference 4. This method represents the rotor wake as a series of discrete shed and trailing vortices, as illustrated schematically in Figure 13, taken from Reference 4. For the present calculations, 10 radial segments were used and calculations of inflow were made at 15-degree increments in azimuth, the minimum spacing provided in the method. The wake transport velocity is assumed to be equal to the vector sum of the mean rotor inflow velocity and the forward speed of the rotor. The variable induced velocity output is then introduced into the Transient Analysis Program and a new blade response is determined. This procedure can be repeated, but experience has shown that one iteration is adequate. For the correlation conditions of this report, both uniform and nonuniform inflow were used in the calculations. However for the tabulated theoretical results, only uniform inflow was assumed, unless otherwise noted.

It should be noted that in the following comparison of measured and computed loading using the variable inflow method of Reference 4, that when discrepancies are attributed to possible limitations in the theory, no

criticism of the theory of Reference 4 is intended. The intent is to emphasize that additional research in the very complicated field of rotor inflow determination is required, as discussed in References 14 and 15, to provide a more precise definition of the influence of the returning wake on rotor loading.

DISCUSSION OF WIND TUNNEL DATA

CHORDWISE LOADING

Figure 14 presents typical examples (complete pressure data are available in Reference 11) of differential blade pressure versus chordwise position at 175 knots for 90-degree increments in azimuth at 55, 75, 95, 97, and 99 percent radius. (Note that the measurements at 99 percent radius are on the tip cap and therefore are not for an NACA 0012 airfoil section; see Figure 2.) The load distributions are generally as expected, with the primary exception of the unusual pressure distribution at 95 percent radius and 90 degrees azimuth. These data were particularly carefully checked for validity. No definite explanation for this apparently peculiar behavior is available at this time, but two possibilities are present. First, this distribution may be partly a two-dimensional characteristic. The two-dimensional wind tunnel tests of Reference 12 on a production CH-34 rotor section indicate that at the Mach numbers under consideration, approximately 0.8, similar chordwise loadings may be encountered, but normally at a higher angle of attack, as shown in Figure 15. Second, the distribution may be influenced by a three-dimensional effect. Examination of the wake trajectory, computed by the method of Reference 4, shows that the tip vortex from the preceding blade is at about 88 percent radius and within 1 foot of the instrumented blade. If this representation is reasonably accurate, there could be a large chordwise variation in inflow at the instrumented blade due to the returning wake under the rotor which would suggest the necessity of the use of lifting surface theory for more accurate determination of chordwise load distribution. Harmonic analysis of the individual pressure gage output at this station showed a large variation in harmonic content with chordwise location, which would lend support to the latter hypothesis. An excellent discussion of this point is given in Reference 15. Further examination of this phenomenon is beyond the scope of the present report.

Figure 16 presents a comparison of the rotor chordwise load distribution with two-dimensional data from Reference 11, at 25, 55, and 75 percent radius. The radial stations and azimuth positions selected coincided approximately with data points in Reference 12 at the same Mach number and normal force coefficient, so interpolation would not be necessary. The correlation of two-dimensional and three-dimensional loading is generally good for these conditions, and additional comparisons may be made by interpolating between References 11 and 12.

SAMPLE BLADE ROOT MOTION COMPARISON

A correlation of measured and calculated blade root flapping motion is presented in Figure 17 for speeds of 110, 150, and 175 knots at a shaft angle of -5 degrees (forward tilt). It should be noted that here, and in all plotted correlations of theory and experiment, the theoretical first harmonic flapping angle with respect to the shaft has been made equal to the measured value. In the tabulated calculations, the first harmonic flapping angle is set equal to zero. The effect of out-of-trim flapping on computed airloads and blade stress is discussed in connection with Figures 21 and 29.

Correlation of theoretical and measured flapping in Figure 17 is good, and the effect of the inclusion of variable inflow is small. Harmonic analyses of all test conditions are presented in Table II.

No comparisons were made of the blade lag motion, as the higher harmonic content was negligible. The first harmonic measured values are listed in Table I.

CORRELATION OF ROTOR AIRLOADS

Figures 18 through 20 present a comparison of the measured time histories of section aerodynamic loading with computed airloads based both on uniform and variable inflow at α_s = -5 degrees and forward speeds of 110, 150, and 175 knots for radial stations of 25, 40, 55, 75, 85, 90, 95, and 97 percent radius. At 99 percent radius, only variable inflow theory is presented because this station is within the tip loss region for uniform inflow; therefore, the lift is assumed equal to zero. Also at 99 percent radius, NACA 0012 airfoil data were used in the theoretical calculations, for lack of information on the actual section characteristics. Complete time histories and harmonic analysis of airloads for the remaining test conditions are presented in Tables III through VIII and IX through XVII, respectively. The blade surface pressures were integrated to obtain section aerodynamic loading using the Gaussian technique of Reference 2, except for stations at 97 and 99 percent radius, where an averaged quadratic method was used. These pressure gages could not be located for structural reasons at chordwise locations compatible with the Gaussian method. The integrated loadings at 97 and 99 percent radius are not as well defined as at other stations, as only 4 and 3 pressure gages were installed, respectively, owing to space limitations.

At 110 knots, Figure 18, the correlation of loading is generally good out to 55 percent radius; but from 75 to 97 percent radius, the measured data show a sharp rise in the vicinity of 80 to 90 degrees azimuth which is not predicted by either theory. For all radial stations at this speed, however, the inclusion of variable inflow improves the correlation with experiment, particularly on the retreating side of the disk at the outboard stations.

Inspection of stations 95 and 97 percent radius, for example, shows a trend which is noticeable at higher speeds as well: a phase lag in the measured loading in the region of 120 degrees azimuth compared to either uniform or nonuniform inflow theories. This is a region of high rate of change of loading with azimuth and therefore one in which there is a rapid change in shed vorticity from the blade, which would imply that unsteady aerodynamic effects might be significant. As discussed under the section "Description of Computational Method", the variable inflow program used in this study incorporates shed as well as trailing vorticity in the wake and therefore should ideally account for the lift deficiency and phase lag associated with nonstationary flow. However, the method of Reference 4 has a minimum wake spacing of 15 degrees in azimuth, which is probably too coarse to represent the influence of the shed vorticity adequately in close proximity to the blade. In an attempt to assess whether unsteady effects are indeed significant, a very approximate calculation was made of the Theordorsen phase lag (Reference 13); the results indicate that

there could be a 5- to 10-degree phase lag in loading. This two-dimensional analysis, while not conclusive, does tend to support the hypothesis that a more exact treatment of the shed wake is needed in rotor aerodynamic theory. Reference 15 suggests that a 1- to 2-degree spacing is required near the blade, and presents a good discussion of lifting line versus lifting surface theory with respect to nonstationary flow effects. Another point to be kept in mind is that, in the computational method used, the wake trajectory time history is prespecified by the forward and mean inflow velocities and any change in wake positioning could have a significant influence on the computed inflow and loading. An interesting discussion of some of these problems is presented in References 14 and 15.

At 150 knots (Figure 19), correlation of experiment and theory at 25 to 55 percent radius is similar to the 110-knot case, but two differences may be noted. At 25 to 55 percent radius, the variable inflow calculations show a higher harmonic content than the experimental data. This effect will be seen to be more pronounced at 175 knots. It is postulated that this is due to the sensitivity of the calculated results when the blade is in close proximity to the zero core diameter line vortex which is assumed in the currently used theory. It is believed that a more precise definition of wake geometry and chordwise distribution of vorticity could improve correlation. The second point is that at 25 percent radius, within the reversed velocity region, the variable inflow calculations shows a positive lift as opposed to the measured negative lift and the calculated negative lift based on the assumption of uniform inflow. This will be discussed in more detail in connection with Figure 20. At radial stations outboard of 75 percent radius, the inclusion of nonuniform inflow improves the correlation with experiment on the retreating side of the disk as at 110 knots; but an additional effect is noticed, in comparison to the uniform inflow calculations, on the advancing side of the disk. Here, and in Figure 20 at 175 knots, the inclusion of variable inflow tends to increase the sharpness of the drop in loading more in line with the experimental results. However, the steep drop in loading on the advancing side (which is more evident in Figure 20 at 175 knots) is still substantially greater than either theory predicts. The phase lag in loading on the advancing side, previously discussed, is again evidenced here, similar to that of Reference 14, Figure 17 and 18. The high-frequency airload at 95 percent radius between 160 and 230 degrees azimuth may be due to the proximity to the blade of a strong tip vortex in practice, not accounted for by current theory, as discussed in Reference 15.

The correlation of theory and experiment at 175 knots ($\mu = .45$) is similar to that at 150 knots except that the differences noted (Figure 20) are more pronounced. At the inboard radial stations, the higher harmonic content of the variable inflow theory on the advancing blade is more exaggerated, probably due to inexact placement of the trailing

wakes, and the degree of correlation in the reversed flow region has deteriorated.

Subsequent to the preparation of Figures 18 through 20 further investigation of the computing program used (Reference 4) has indicated that the inconsistencies in the reverse flow region do not in fact exist and the variable inflow theory should also predict negative aerodynamic loading in the reverse flow region. However, precise definition of the airload distribution was not available in time for inclusion in this publication. Preliminary calculations show that only reverse flow airloads are influenced, and these differences do not affect computed blade stresses, to be discussed subsequently. To put this correlation discussion in proper perspective, it should be kept in mind that the variable inflow theory of Reference 4 was originally developed primarily for application at low advance ratio conditions where the reversed flow region is small, and the effects shown here would not be important.

On the advancing blade (for example, at 90 and 95 percent radius) an extremely rapid reduction in measured loading is evidenced, compared to theory. Reference 15 has postulated that this rapid change in loading is predominantly influenced by the tip vortex of the preceding blade; Reference 14, containing data obtained during the present tests under transient conditions, shows a similar impulsive type load.

The lack of agreement between theory and experiment for this impulsive type loading on the advancing blade at high speed is disturbing to the aerodynamicist, and indicates that substantial additional research is needed to understand rotor dynamic airloads properly. However, it should be remembered that the final result of importance to the designer of a structurally reliable rotor system is the ability to predict vibratory blade stresses; and as will be shown in the discussion of blade stresses, the rotor blade does not respond substantially to this impulsive type of aerodynamic loading, as the time duration is short compared to the natural period of the blade lower order flapwise modes of vibration. The character of the loading variation with azimuth at 97 and 99 percent radius of Figure 20 is seen to be quite different than at 95 percent. For example, the sharp peaks have been rounded off, similar to 99 percent radius at 150 knots in Figure 19. In each case, inclusion of variable inflow substantially improves the correlation of theory and experiment.

As discussed in connection with Figure 17, each of the theoretical calculations for which the data are plotted had first harmonic flapping set equal to the measured value, while for the tabulated calculations the first harmonic flapping is set equal to zero. For a rotor with zero flapping hinge offset, there would be no effect of flapping on airloads; but with a finite flapping offset selected to produce hub moment capability for control,

first harmonic flapping with respect to the shaft does influence the airload distribution. However, with the relatively small offset of the CH-34 rotor system (approximately 3.6 percent radius), the effects are small for small amounts of flapping. This can be seen from examination of Figure 21, which presents computed aerodynamic loading versus azimuth at 175 knots, based on uniform flow, for 25, 55, and 90 percent radial stations. Figure 21 represents the condition where the maximum differences in actual and trimmed flapping occurred; therefore, in the tabulated theoretical calculations, the effects of out-of-trim flapping will be less than shown here. The solid line represents first harmonic flapping trimmed to zero with respect to the shaft, while the dashed line has longitudinal and lateral flapping iterated equal to the experimentally measured values. As expected, the principal differences occur on the outboard advancing side when the combination of flapping velocity and dynamic pressure is greatest; the effect is primarily one per revolution, thereby producing a lateral moment for the lateral flapping case shown.

EFFECT OF NONUNIFORM INFLOW ON CALCULATED SECTION ANGLES OF ATTACK

The preceding discussion of correlation of theory and experiment showed that nonuniform inflow considerations based on the method of Reference 4 were significant on rotor airloads at speeds at least as high as 175 knots. Similar comparisons cannot be made on the basis of local blade section angle of attack owing to the lack of experimental section angle data. Therefore, Figures 22 through 24 were prepared to present a comparison of the theoretical local angle of attack contours over the rotor disk for both uniform and nonuniform inflow. These conditions correspond to those where the airload correlations were presented in Figures 18 through 20. Some general observations are apparent from Figures 22 through 24. The primary influence of the inclusion of variable inflow, as calculated by the method of Reference 4, is the substantially greater nonuniformity in computed angles of attack, particularly on the retreating side of the disk. Also, the angle of attack at the retreating tip is reduced by variable inflow in all cases; for example, a reduction from 6 to 4 degrees at 110 knots, from 9.5 to 5 degrees at 150 knots, and from 9 to 5 degrees at 175 knots. The inclusion of variable inflow tends to shift the region of maximum positive angles of attack inboard, notably in the regions of 225 and 315 degrees azimuth at approximately 50 percent radius, typically by 2 to 3 degrees. Further inboard radially, just outboard of the reversed flow region, the large negative angles of attack predicted by uniform inflow theory become positive (110 and 175 knots), or substantially less negative, as at 150 knots, when variable inflow theory is used.

CORRELATION OF BLADE STRESSES

BLADE STRESS TIME HISTORIES

Figures 25 through 27 compare measured blade stress time histories with calculated stress, for both uniform and variable inflow assumptions, at 110, 150, and 175 knots forward speed and -5-degree shaft angle. Stations at 0.375 and 0.65 radius were chosen for presentation, as these represent locations where flapwise, chordwise, and torsional data each were measured. Also, the 65 percent station is normally the critical stress station at the speeds and loadings considered in the present study. Data for the remaining test conditions are given in Tables XVIII through XXVI as blade stress time histories, and in Tables XXVII through XXXV as harmonics of blade stress. Although the figures are grouped in terms of forward speed for consistency, the discussion will consider each component of stress at a given speed separately so that trends for a given component may more easily be seen. The figures are reasonably self-explanatory, so only the more unusual features will be discussed in some detail.

FLAPWISE STRESS

The correlation of flapwise stress with azimuth is generally good at all speeds, as to general stress signature. The agreement on steady flapwise bending stress at the inboard station, 37.5 percent radius, is less than desirable, and the variable inflow calculation is less precise in this case than constant inflow. Inspection of Tables XXVIIa through XXXVa shows a maximum discrepancy between theory and experiment of steady bending stress of 1090 p.s.i. and an average deviation of less than 400 p.s.i.

Throughout the speed range, the principal harmonics of flapwise stress are the first through third, as seen by inspection of Figures 25a through 27a and Tables XXVIIa through XXXVa. At 110 knots for harmonics above the fourth, the stress amplitudes are generally less than 100 p.s.i. At 150 knots, harmonic amplitudes above the fifth are generally less than 100 p.s.i.; for 175 knots, 100 p.s.i. harmonic amplitudes are rarely found above the sixth. Compared in the following sketch are the experimental and calculated first three harmonics of flapwise stress in bar-graph form for the 65 percent radial station, at a shaft angle of -5 degrees.

HARMONIC AMPLITUDE p.s.i

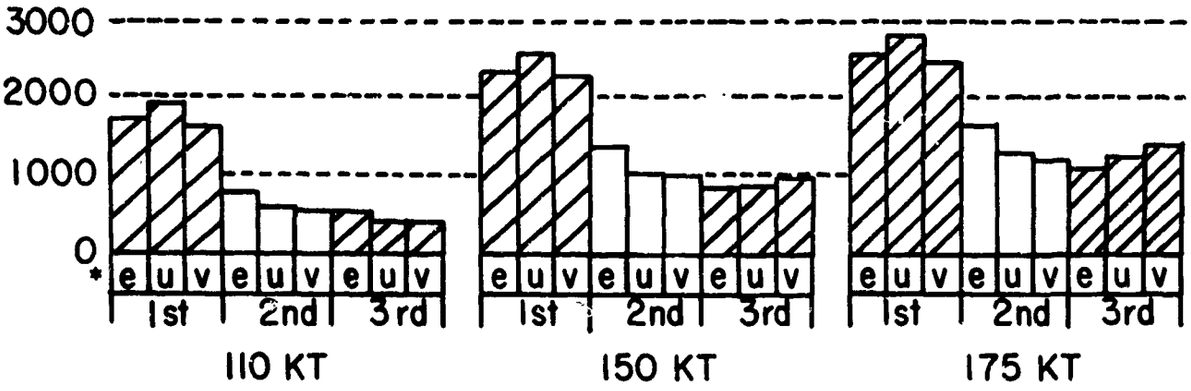

*NOTE : e = experimental; u = uniform inflow theory; v = variable inflow theory

It can be seen that, in general, the correlation of the lower harmonics, which predominantly participate in blade peak-to-peak stresses and therefore influence blade fatigue design, is good; the overall peak-to-peak correlation is shown in Figures 30 through 32. The higher harmonic content of the experimental data at 110 knots is small; but at 150 and 175 knots forward speed, there appears to be substantial harmonic response within the region of 90 to 180 degrees azimuth, not reflected in the calculations, which is attributed to the impulsive type of aerodynamic loading described previously in the "Correlation of Rotor Airloads" section. Because of the short time duration of the aerodynamic impulse compared to the period of the lower order modes, the correlation of measured and calculated blade flapwise stress is much better than the correlation of airloads. As with the airloads, the inclusion of variable inflow improves the correlation of theory and experiment, particularly in the advancing blade region. Examination of the frequency of blade response in the 90- to 180-degree azimuth region indicates that the response is primarily second-mode bending, which has a calculated natural frequency of 2.7 cycles per revolution.

Examination of Tables XXVIIa through XXXVa shows that for all three flight conditions in Figures 25a through 27a, both the measured data and the calculations based on uniform inflow show relatively insignificant harmonic content at frequencies above the fifth or sixth at stations inboard of 80 percent radius. At the 80 percent radial station it may be noted in the tables that measured seventh and/or eighth harmonics appear for some of the flight conditions which are substantially greater than 10 percent of the first harmonic (Tables XXXIa, XXXIIa, XXXVa). It is seen in these instances that the uniform inflow theory does not adequately predict these higher harmonics. At other flight conditions (Tables XXVIIa, XXXIIIa), where variable inflow calculations were performed, the measured seventh and eighth harmonics are small, while the variable inflow calculations predict these harmonics to be too large. A study was undertaken to evaluate the effects of variable inflow on computed seventh and eighth harmonic flapwise stress at 80 percent radius for Tables XXXIa, XXXIIa, and XXXVa, and it was found that in all cases the inclusion of variable inflow tended to increase the higher harmonic content over that predicted by uniform inflow, as would be expected physically, but that in at least one case the variable inflow predicted fourth and eighth harmonics larger than the first harmonic, which is much greater than anything measured. The study also showed that very small changes in wake geometry have a large effect on the predicted higher harmonics when the rotor disk is at small angles to the free stream (thus causing the assumed wake to pass very close to the rotor). Thus it seems that the variable inflow theory used in this study tends to increase the predicted higher harmonic content over that of uniform inflow, which is more comparable to experimental results, but does not yet pinpoint this content with sufficient accuracy. Reference 17 has shown that strong line vortex concentrations, as used in the current variable inflow calculations, can have a considerable influence on the higher harmonics and therefore higher modes of vibration. This suggests again that a better definition of the theoretical wake geometry and vortex field is required.

CHORDWISE STRESS TIME HISTORIES

Figures 25b through 27b present a comparison of measured and computed chordwise stress versus azimuth. As with the flapwise stress correlations, the figures are rather self-explanatory, so only the salient differences will be noted in the discussion herein. The degree of correlation of measured and computed time histories is less precise than with the flapwise stress discussed above, but this is mitigated by the fact that the chordwise stress amplitudes are only on the order of 40 percent of the flapwise stresses, and the agreement on vibratory stress amplitude (Figures 30 through 32) is good, a fact which is important for fatigue analysis. However, a better definition of the higher harmonics of chordwise stress is desirable, as these are reflected in the blade root shear

forces which determine aircraft vibration levels. It is noteworthy that the inclusion of variable inflow has little influence on computed chordwise stress.

One of the simplifying assumptions implicit in the theory used for the present correlation is that the lag damper moment, which primarily influences chordwise stress, is a linear function of the instantaneous lagging velocity. However, in practice, a typical damper response curve would be as in the sketch following:

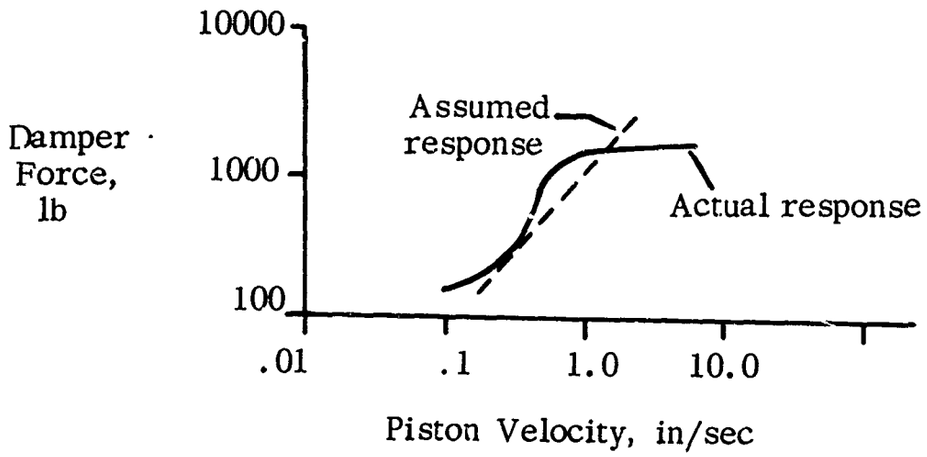

The influence of this simplifying assumption is currently under study independently at Sikorsky Aircraft.

The predominant harmonic of measured chordwise stress is the third, and both theoretical calculations agree reasonably well at this frequency. However, there are two discrepancies between theory and experiment that can be noted, particularly in Figures 26b and 27b, at 150 and 175 knots, respectively.

At 37.5 percent radius in Figure 26b, there is a small-amplitude, high-frequency component in the measured data which is not found in either

theory. Detailed harmonic analysis of these data showed that all harmonics greater than the fourth were substantially less than 10 percent of the fundamental, except for the twenty-first harmonic, which was 15 percent of the fundamental.

The calculated fourth-mode chordwise bending frequency at this tip speed is 18 cycles per revolution, which is close to this twenty-first harmonic. This may be an indication of a requirement for a more exact definition of the higher mode frequencies in the solution of the rotating beam equations into the normal modes of vibration.

At 65 percent radius, there is a sizeable 8-per-revolution frequency in the experimental data which is not reflected in the theory. The theoretical third-mode chordwise frequency is approximately 9 cycles per revolution, close to the measured response. Therefore, a small change in the computed third natural frequency (along with a better definition of the higher harmonic airloads) would probably improve the correlation.

TORSIONAL STRESS TIME HISTORIES

The torsional stresses measured at the loadings encountered during this program were of such low magnitude that the presentation must be considered qualitative in nature rather than quantitative; however, the results are presented for the sake of completeness, and a supplemental correlation is presented for quantitative evaluation of the theory under severe operating conditions. Figures 25c through 27c present torsional stress time histories for experiment, and both uniform and nonuniform inflow computations. The vertical scales have been grossly expanded, out of proportion to the measurement accuracy, to demonstrate qualitative trends (if the proper scale had been used, no appreciable variation of torsion stress with azimuth would be evident). Qualitatively, therefore, the predominant first and second harmonics of torsion stress from the figures and Tables XXVIIc through XXXVc are in good agreement, and a discussion of the correlation of the higher harmonics is not considered appropriate because of the very low levels under consideration. A more severe comparison of the ability of the Transient Analysis Theory to predict torsional stress time histories was presented in Reference 16, which discussed, among other items, similar correlations with test results obtained on a dynamically scaled model rotor at advance ratios as high as 1.0, a very severe operating condition. Figure 28, from Reference 16, compares measured and calculated torsion stress time histories at an advance ratio of 1.0 (dynamic equivalent forward speed of 300 knots), and the quantitative correlation with the theory of this report is seen to be quite good. As discussed in Reference 16, the disagreement between theory and experiment near zero azimuth is believed to be due to turbulent flow from the relatively large unfaired model rotor

head. It is interesting to note that the phase lag in measured and computed torsional stress of Figure 28 at 270 degrees azimuth, the region of maximum change in angle of attack, is similar to the previous full-scale aerodynamic loading data at 90 degrees azimuth at lower advance ratios such as in Figures 18 through 20.

EFFECT OF FLAPPING ON BLADE STRESS TIME HISTORIES

Figure 29 was prepared to show the theoretical effect of out-of-trim flapping on flapwise, chordwise, and torsional stress at 65 percent radius and 175 knots, the most severe case. The effects are seen to be minimal.

VIBRATORY BLADE STRESS AMPLITUDE

Figures 30 through 32 present measured and calculated total vibratory stress amplitude versus radius for flapwise, chordwise, and torsional bending for forward speeds of 110, 150, and 175 knots, respectively. As discussed previously, while the higher harmonic contents of blade stress are important in that they reflect on the harmonic content of root vibratory shear forces, the primary criterion for satisfactory blade structural reliability is the ability to predict blade stress amplitudes accurately. Figures 30 through 32 show excellent correlation of theory and experiment in this respect. The apparent discrepancy in torsional correlation is due to the overly expanded vertical stress scale previously discussed in conjunction with blade stress time histories but preserved here for consistency. The absolute difference in torsional stress amplitude correlation, on the order of 100 p.s.i., is of no practical importance.

DISCUSSION OF WIND TUNNEL AND FLIGHT TEST DATA

During the test, it was desired to duplicate, in the wind tunnel, a flight test condition previously conducted on this same rotor blade set, as reported in Reference 2. The condition chosen to be duplicated is listed in Reference 2 as Flight 18. Essentially the same value of rotor lift was achieved: 11,800 pounds for the wind tunnel data versus an estimated 11,500 pounds for the flight test data. (Reference 2 lists a range of aircraft gross weights, rather than specific values at each test point.) However, a greater rotor propulsive force was inadvertently produced in the wind tunnel: 2144 pounds versus an estimated flight test value of 1390 pounds (based on 36.5 square feet of parasite area for the H-34 helicopter). The increased propulsive force and the -9-degree rather than -7.2-degree shaft angle reported in Reference 2 thus represent a different inflow and loading for the rotors, so these differences should be kept in mind in the following comparison of wind tunnel and flight test data.

ROTOR AIRLOADS

Figure 33a presents the averaged aerodynamic loading versus spanwise station for wind tunnel and flight test data as well as theoretical calculations based on both uniform and nonuniform inflow assumptions simulating the wind tunnel operating condition. The wind tunnel data appear to be smoother than the flight test data, perhaps reflecting the more easily controlled conditions in the wind tunnel. The well defined and sharp drop-off in lift from 95 to 99 percent radius for the wind tunnel data is an indication of the existence of a very strong tip vortex, and supports the hypothesis of References 14 and 15 that simplifications in the existing variable inflow theories could be made by representing the trailing vorticity by a single tip vortex. (However, as discussed earlier, a more exact treatment of the shed vorticity is required.) Both theoretical airload distributions follow the wind tunnel results well. The only significant difference in the two calculations is that the variable inflow theory predicts the drop-off in lift toward the blade tip, which the constant inflow assumption precludes. Theoretical calculations based on flight test values of propulsive force have indicated that a higher propulsive force results in a lower average airload at the inboard stations and a higher average airload at the outboard stations. This is in agreement with the characteristics displayed by the wind tunnel and flight test data in Figure 33a.

Figure 33b presents a comparison of time histories of flight and wind tunnel airloads at comparable radial stations. (Wind tunnel data for 97 and 99 percent radius are listed in Table XXXVI, and harmonics of loading for all tunnel conditions are presented in Table XXXVII.) Discounting the difference in average loading (shown in Figure 33a), the agreement

between flight and tunnel airload time histories is generally good. The principal differences in loading signature are noted at 85 and 90 percent radius in the region of 120 degrees azimuth, where the flight test data show a sharper drop in lift. The principal harmonics of airload are the first through the fourth, and Table XXXVII, which presents measured and computed harmonics of the wind tunnel test conditions, shows good agreement with these harmonics, particularly when variable inflow is included. Therefore it appears that the major differences in loading of Figure 33b are probably attributable to the difference in operating condition, that is, rotor propulsive force and mean rotor inflow, rather than to differences between wind tunnel and flight testing.

BLADE STRESSES

Flapwise blade stress time histories are compared in Figure 33c. The stress signature is generally comparable, although the flight test data have a somewhat higher harmonic content and total amplitude than the wind tunnel results. If any significant variations of tunnel-induced upwash over the rotor disk were present, this would result in an increased harmonic content of blade stress rather than the reduction shown here, so the differences are attributed primarily to the different operating conditions and not to tunnel effects. The reduced flapwise stress amplitude for the wind tunnel data is in line with the results of Reference 18, which showed that at a given blade twist, a larger propulsive force generally reduces flapwise blade stress amplitudes. Table XXXIXa lists the harmonic content of flapwise stress for both wind tunnel data and theory and shows generally good agreement for the significant harmonics, which tends to support the validity of the wind tunnel data.

Chordwise blade stress time histories are presented in Figure 33d for the two radial stations at which comparisons can be made. Additional wind tunnel data are given in Tables XXVIII and XXXIXb for 65 and 85 percent radius. The correlation of wind tunnel and flight test chordwise stress is not as good as for the flapwise stresses. In addition to the difference in rotor propulsive force for the two tests, two other factors could influence the chordwise stress amplitude. These are possible differences in lag damper setting between the two tests and possible differences in flapping with respect to the shaft, which would introduce Coriolis moments in the chordwise direction. An examination of these factors is beyond the scope of the present study.

Figure 33e compares torsional stress time histories for both wind tunnel and flight data at 15 percent radius. (Additional wind tunnel data are presented in Tables XXXIII and XXXIXc for 37.5 and 65 percent radius.) As with previously presented torsion stress plots, the vertical scale has been exaggerated greatly because of the low stress levels encountered, but even at this scale the correlation is seen to be quite good.

CONCLUSIONS

Analysis of the results of full-scale experimental and theoretical rotor airload and blade stress correlations at speeds of from 110 to 175 knots leads to the following principal conclusions.

1. At several inboard radial stations where direct comparisons could be made, good agreement was obtained with two-dimensional and three-dimensional chordwise airload distributions. However, at the advancing blade tip where rapid fluctuations in loading are encountered, there is evidence that lifting surface theory may be required for an adequate prediction of chordwise pressures.

2. Correlation of airload time histories with theory was reasonably good, with the principal discrepancy occurring at high speed in the region of the advancing blade tip, where a much sharper drop-off in lift was measured than predicted (an impulsive type loading). Inclusion of variable inflow in the theory improved airload correlations on both the advancing and the retreating blades at speeds as high as 175 knots (advance ratio = 0.45), but improvements in the inflow theory are required. Evidence was shown for the need for treating the effects of shed vorticity more precisely.

3. Correlation of measured and calculated blade stress time histories was considerably better than the airload correlation, as the lower mode blade natural period is long compared to the duration of the measured impulsive type airload. Excellent correlation of blade vibratory stress amplitude versus radius was achieved. Inclusion of variable inflow in the theory tends to improve correlation with experiment of flapwise stress signature and amplitude, but has no significant effect on chordwise or torsion stresses.

A comparison of wind tunnel and flight test results at 110 knots forward speed and approximately equal rotor lift, but differing by approximately a factor of two in rotor propulsive force, leads to the following conclusions:

1. The wind tunnel data are somewhat better defined, particularly with respect to average airloads, probably owing to the ability to hold a given test condition more closely in the wind tunnel than in flight testing.

2. Agreement between flight test and wind tunnel test data was generally good, and the differences could reasonably be explained by the difference in rotor operating condition.

RECOMMENDATIONS

1. Current research on the development of variable inflow theory should be expanded to include operation at high forward speeds where reversed flow is significant as well as in the transition region. Also, a more rigorous treatment of nonstationary flow effects is needed.

2. Additional correlation of wind tunnel and flight test measurements should be made under conditions as closely identical as possible to substantiate further the correlations discussed herein.

REFERENCES

1. Rabbott, J. P., Jr., and Churchill, G. B., Experimental Investigation of the Aerodynamic Loading on a Helicopter Rotor Blade in Forward Flight, NACA RML56I07, Langley Aeronautical Laboratory, Langley Field, Virginia, October 1956.

2. Scheiman, J., A Tabulation of Helicopter Rotor Blade Differential Pressures, Stresses, and Motions as Measured in Flight, NASA TM X-952, Langley Research Center, Langley Station, Hampton, Virginia, March 1964.

3. Burpo, F., Measurement of Dynamic Airloads on a Full-Scale Semirigid Rotor, TREC Technical Report 62-42, U.S. Army Aviation Materiel Laboratories, Fort Eustis, Virginia, December 1962.

4. Piziali, R. A., and DuWaldt, F. A., A Method for Computing Rotary-Wing Airload Distributions in Forward Flight, TREC Technical Report 62-44, U.S. Army Aviation Materiel Laboratories, Fort Eustis, Virginia, November 1962.

5. Miller, R. H., Rotor Blade Harmonic Airloading, IAS Paper No. 62-82, Presented at the IAS 30th Annual Meeting, New York, January 1962.

6. Patterson, J. L., A Miniature Electrical Pressure Gage Utilizing a Stretched Flat Diaphragm, NACA TN 2659, Langley Aeronautical Laboratory, Langley Field, Virginia, 1952.

7. Tanner, W. H., Charts for Estimating Rotary Wing Performance in Hover and at High Forward Speeds, NASA CR-114, Sikorsky Aircraft Division of United Aircraft Corporation, Stratford, Connecticut, November 1964, SER-50379.

8. Myklestad, N. O., Fundamentals of Vibration Analysis, McGraw-Hill Book Company, Inc., New York, 1956.

9. Bisplinghoff, R. L., Ashley, H., and Halfman, R. L., Aeroelasticity, Addison-Wesley Publishing Co., Inc. Cambridge, Mass., 1955.

10. Miller, R. H., Aeroelastic Problems of VTOL Aircraft, Notes for a Special Summer Program on Aeroelasticity, Vol. III, Massachusetts Institute of Technology, 1958.

11. Rabbott, J. P., Jr., Lizak, A. A., Paglino, V. M., Tabulated CH-34 Blade Surface Pressures Measured at NASA/Ames Full Scale Wind Tunnel, SER-58399, Sikorsky Aircraft Division of United Aircraft Corporation, Stratford, Connecticut, December 1965.

12. Lizak, A. A., Two-Dimensional Wind Tunnel Tests of an H-34 Main Rotor Airfoil Section, TREC Technical Report 60-53, SER-58304, Sikorsky Aircraft Division of United Aircraft Corporation, Stratford, Connecticut, September 1960.

13. Scanlon, R. H., and Rosenbaum, R., Introduction to the Study of Aircraft Vibration and Flutter, The Macmillan Company, New York, 1951.

14. White, R. P., Jr., VTOL Periodic Aerodynamic Loadings, Paper Presented at the Symposium on the Noise and Loading Actions on Helicopters, V/STOL Aircraft, and Ground Effect Machines, August 30 — September 3, 1965. Institute of Sound and Vibration Research, University of Southampton, England.

15. Miller, R. H., Unsteady Airloads on Helicopter Rotor Blades, Fourth Cierva Memorial Lecture, Presented to the Royal Aeronautical Society, London, England, October 25, 1963.

16. Fradenburgh, E. A., and Segel, R. M., Model and Full Scale Compound Helicopter Research, Paper Presented before the American Helicopter Society Twenty-First Annual National Forum, Washington, D. C., May 12 — 14, 1965.

17. Bain, L. J., Comparison of Theoretical and Experimental Model Rotor Blade Vibratory Shear Forces, SER-50419, Sikorsky Aircraft Division of United Aircraft Corporation, Stratford, Connecticut, "In Publication".

18. Rabbott, J. P., Jr., A Study of the Optimum Rotor Geometry for a High Speed Helicopter, TREC Technical Report 62-53, SER-50254, U. S. Army Aviation Materiel Laboratories, Fort Eustis, Virginia, May 1962.

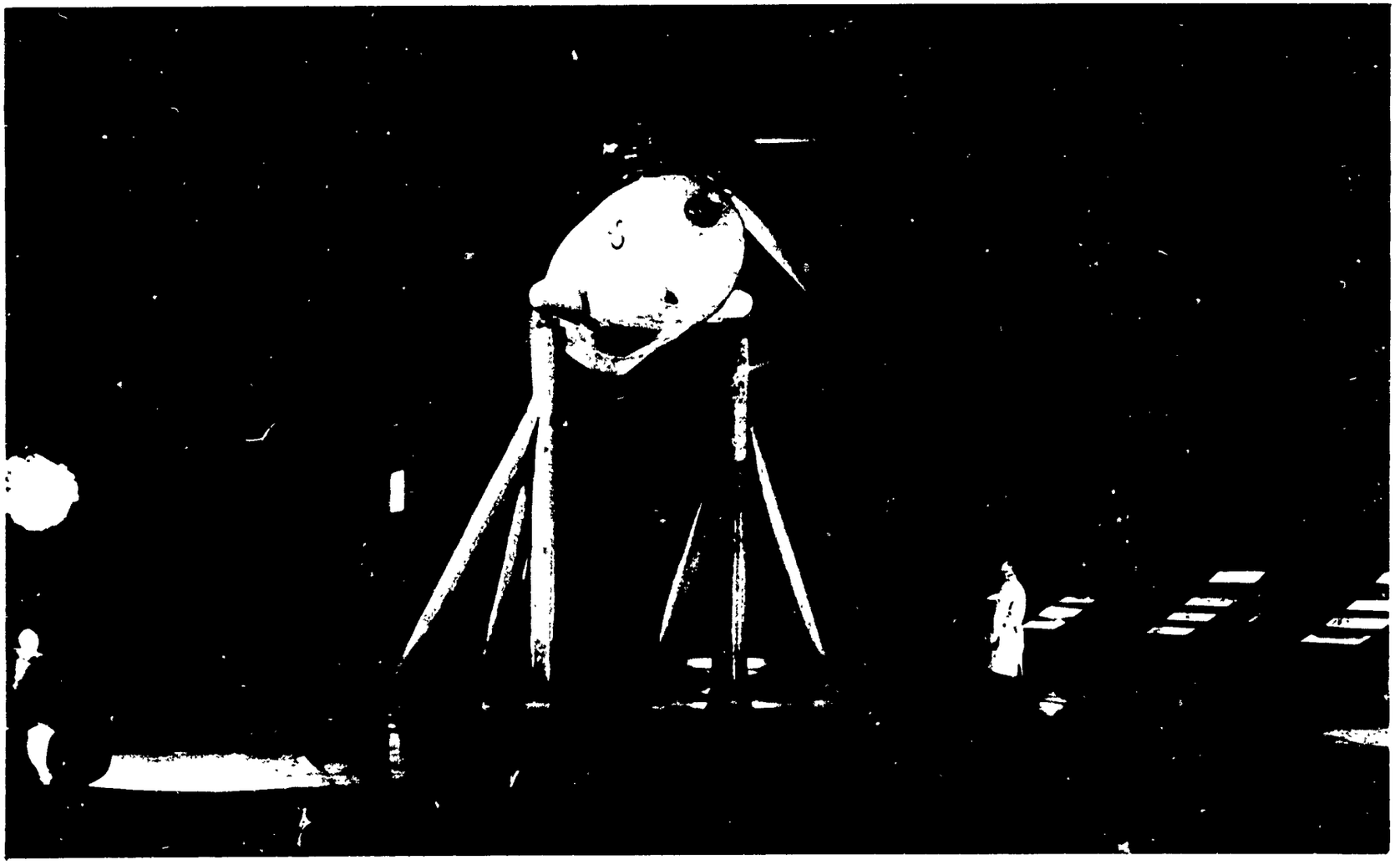

Figure 1. Sikorsky CH-34 Rotor Installed In NASA/Ames Full-Scale Wind Tunnel.

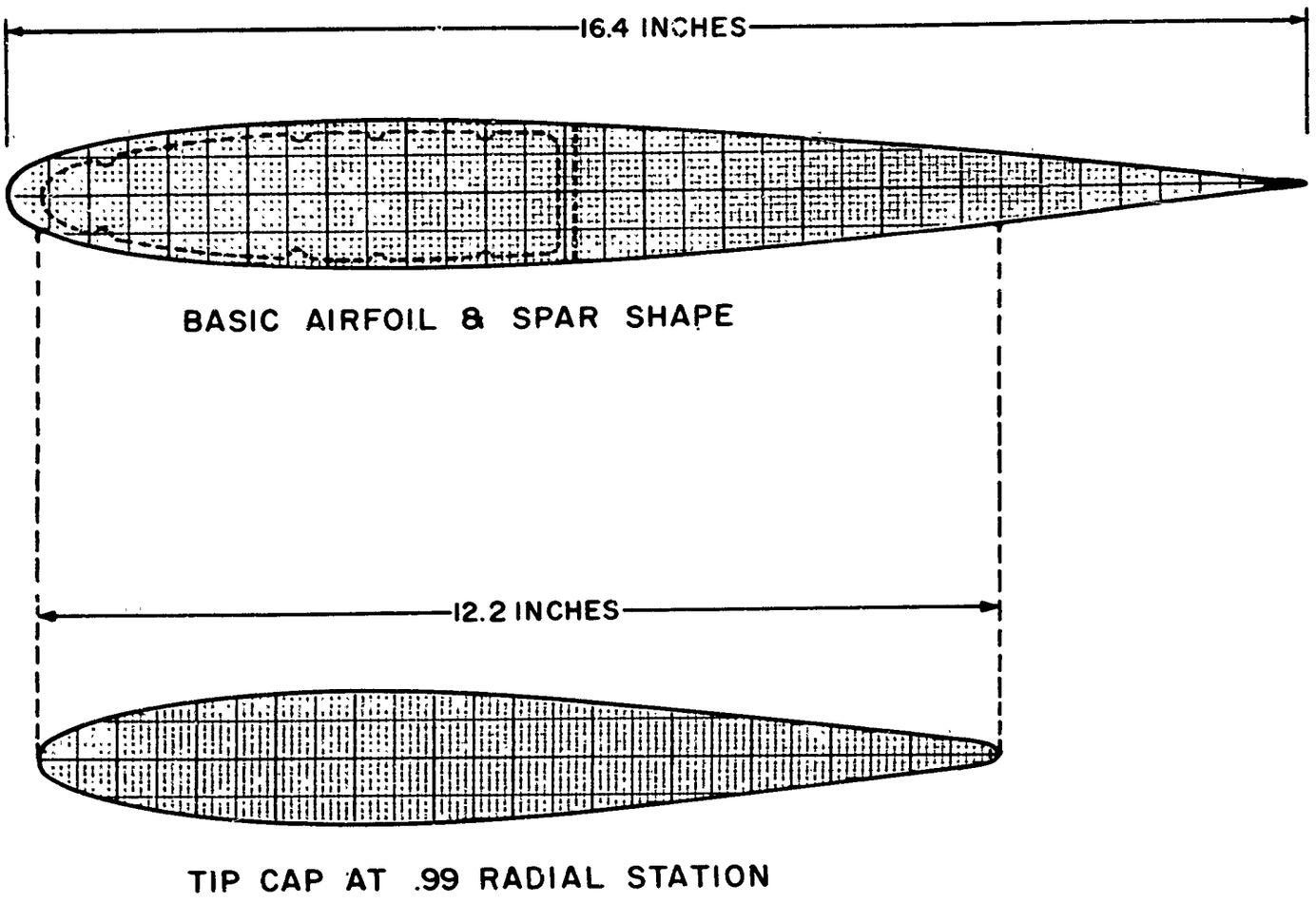

Figure 2. Comparison of Basic Airfoil, Spar, and Tip Cap Cross Section.

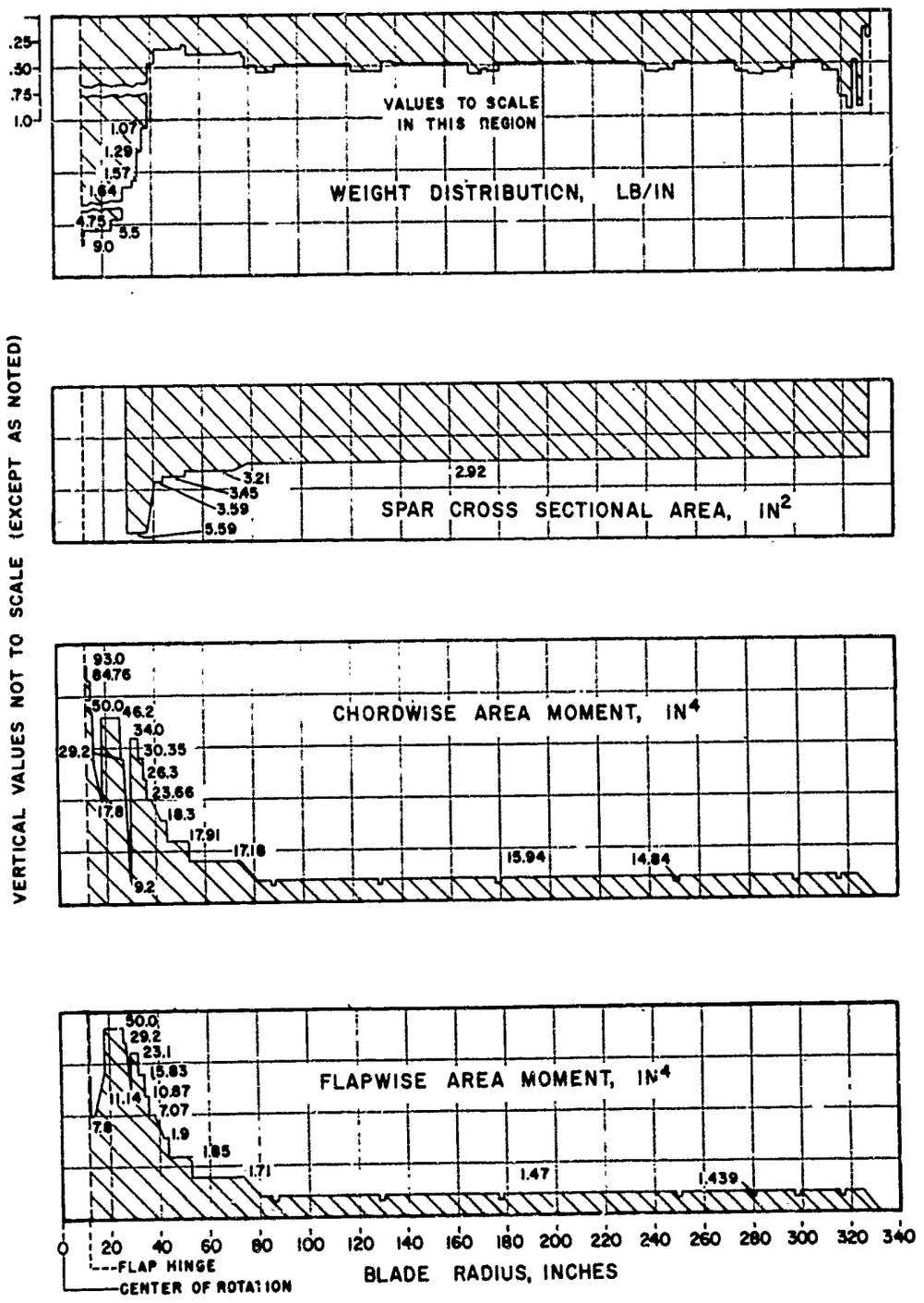

Figure 3. Blade Physical Properties.

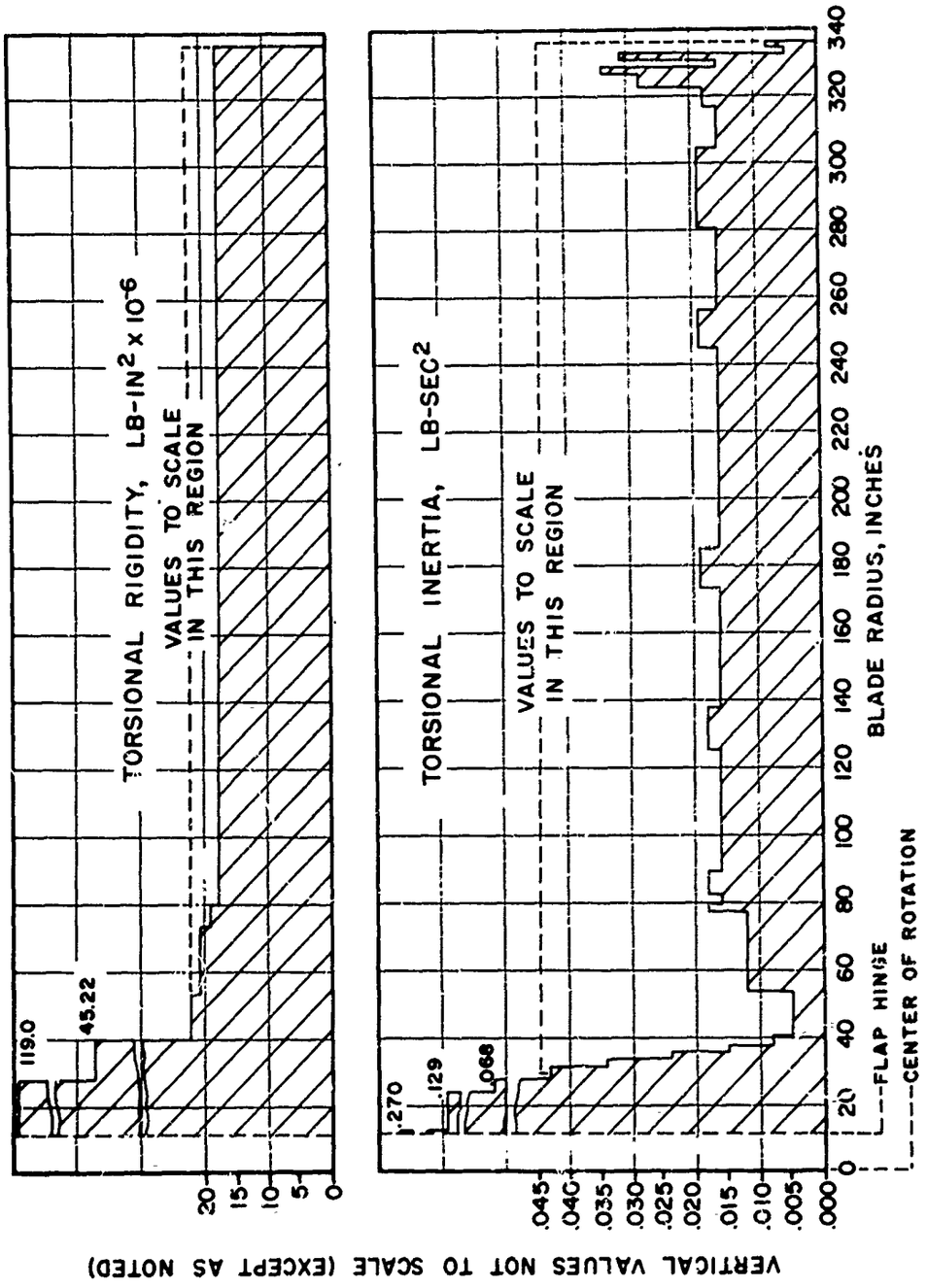

Figure 3. Concluded.

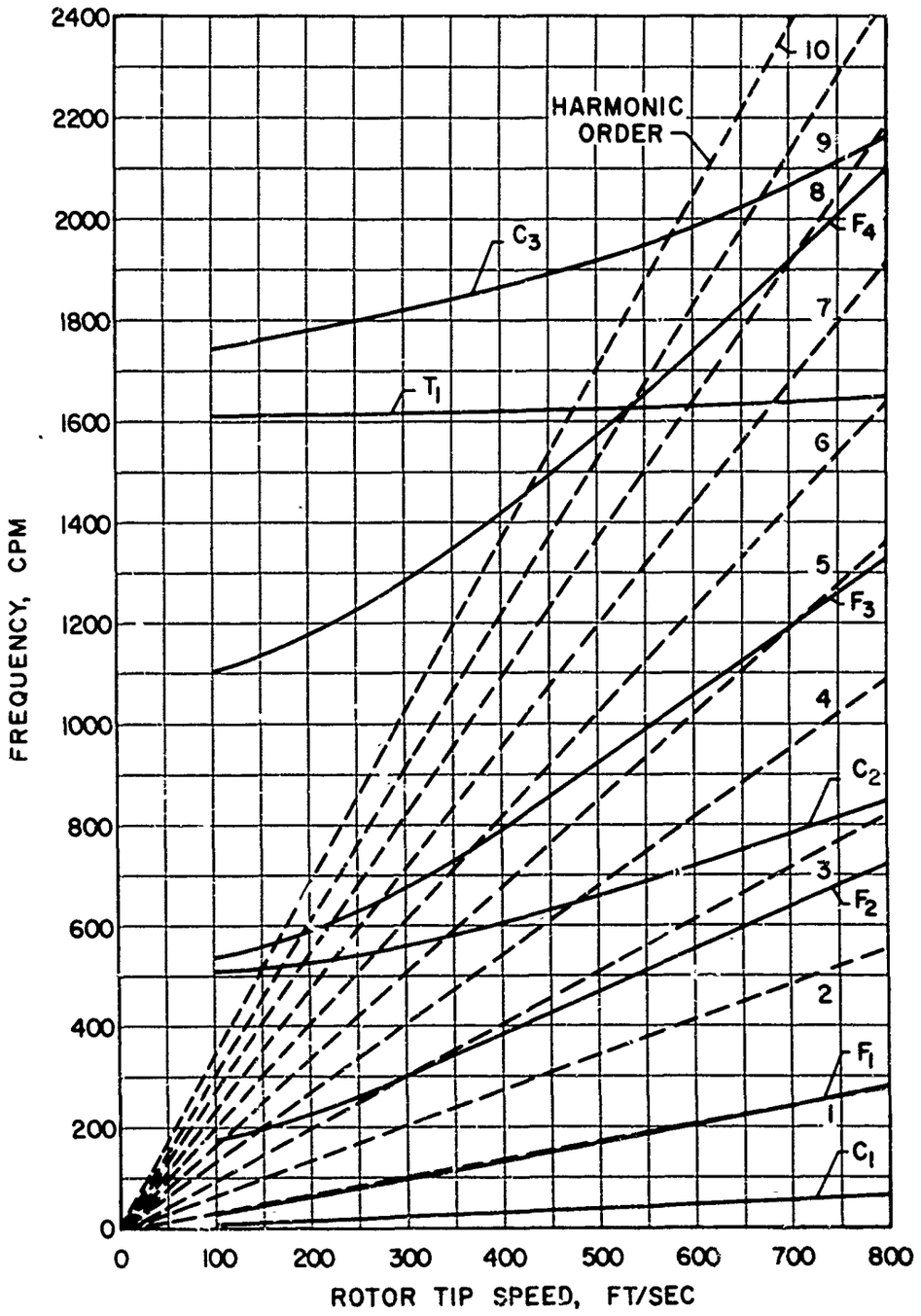

Figure 4. Blade Frequency Diagram.

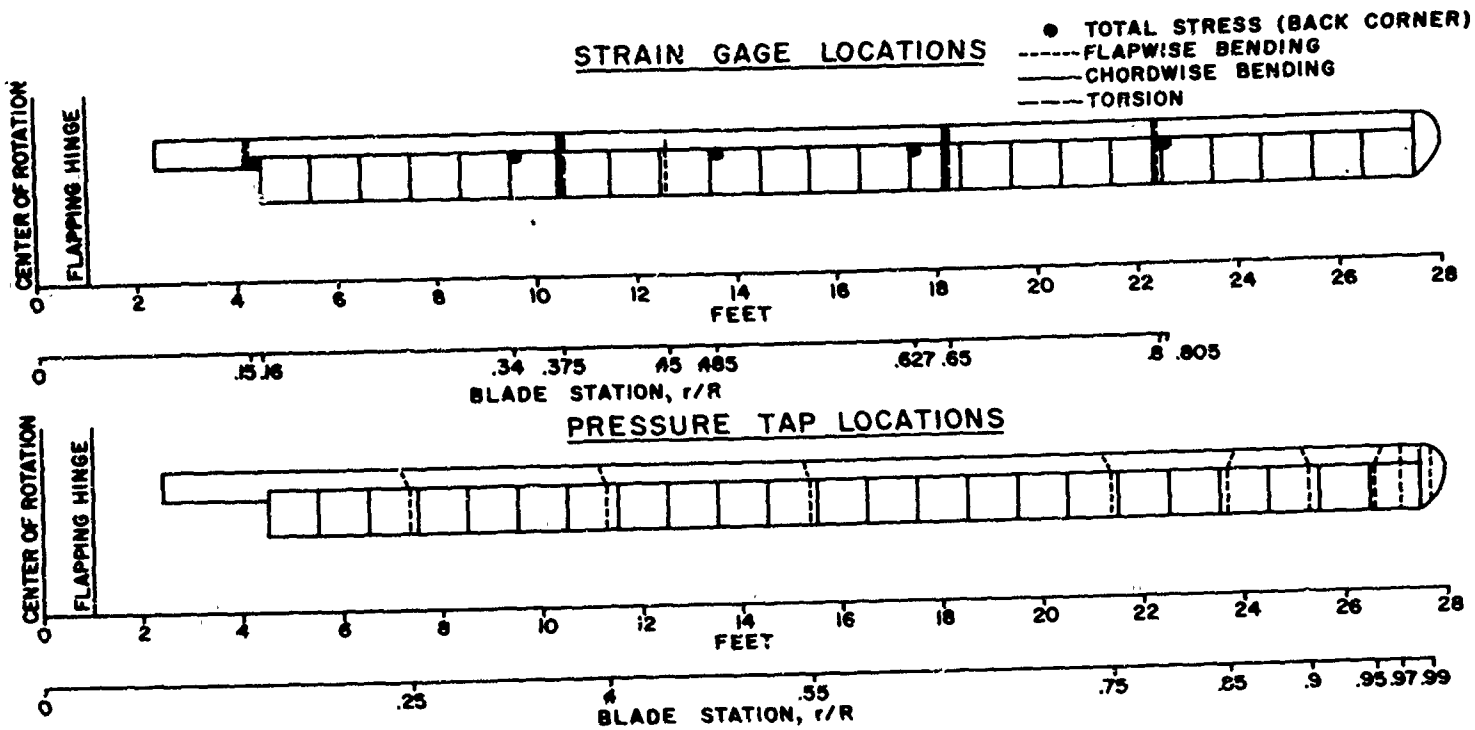

X/C AT r/R =	.25	.40	.55	.75	.85	.90	.95	.97	.99
	.042	.042	.017	.017	.017	.017	.017	.090	.101
	.158	.158	.090	.090	.040	.090	.090	.230	.290
	.300	.300	.168	.168	.090	.158	.168	.565	.737
	.600	.600	.233	.233	.130	.233	.233	.850	
	.910	.910	.335	.335	.168	.335	.335		
			.625	.625	.233	.625	.625		
			.915	.915	.335	.915	.915		
					.500				
					.625				
					.769				
					.915				

Figure 5. Location Of Blade Instrumentation.

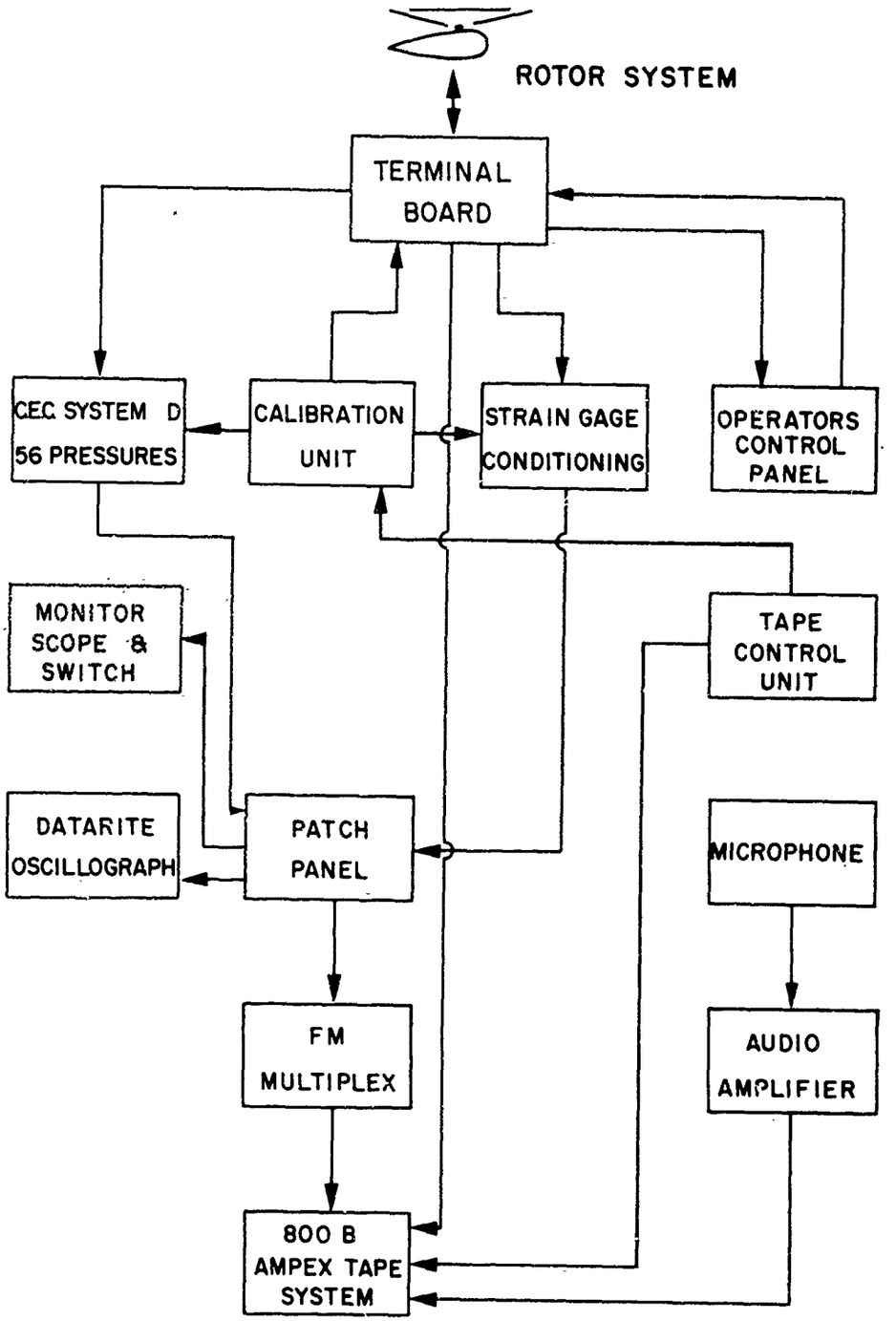

Figure 6. Data Acquisition Block Diagram.

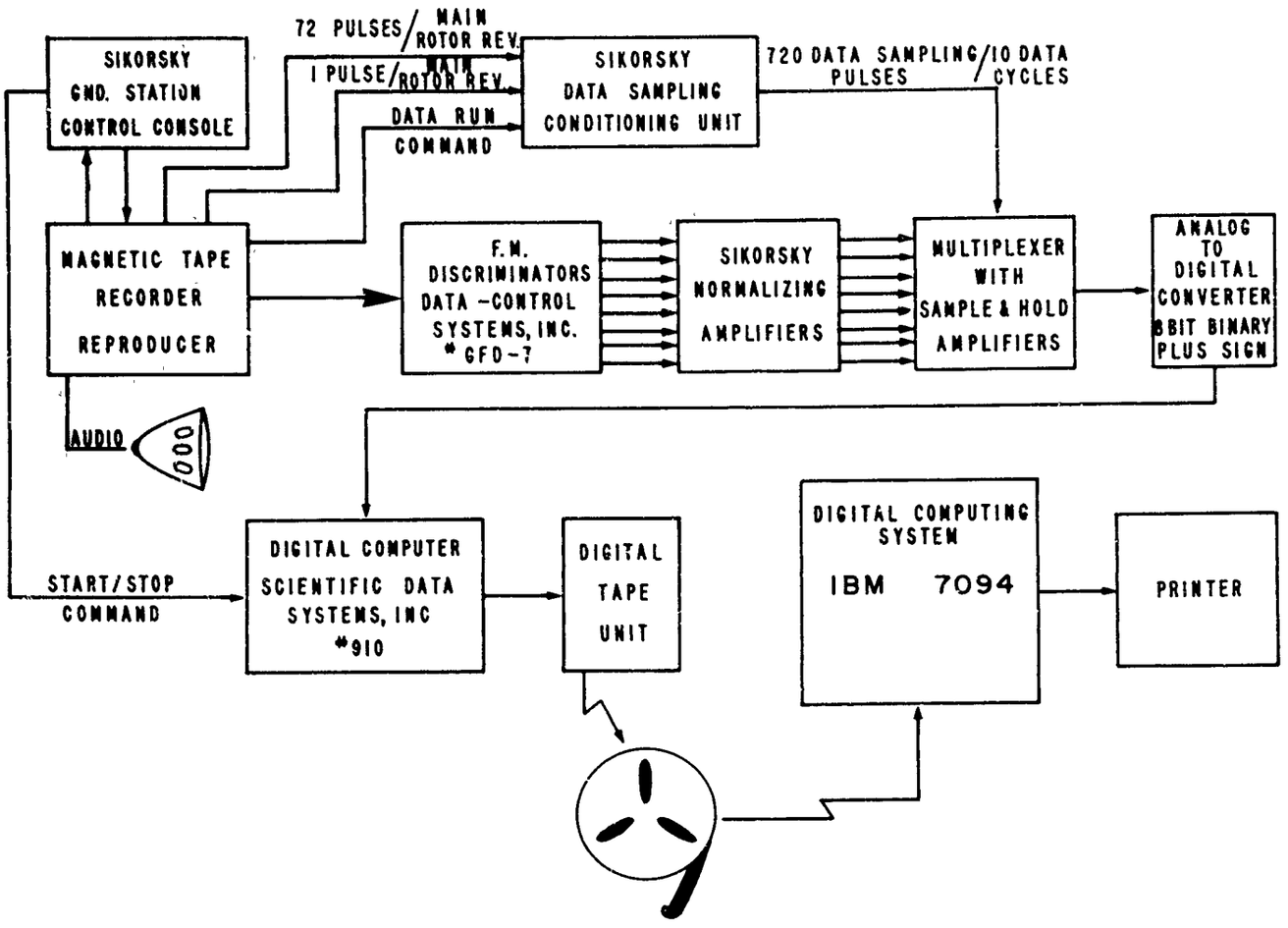

Figure 7. Data Processing System.

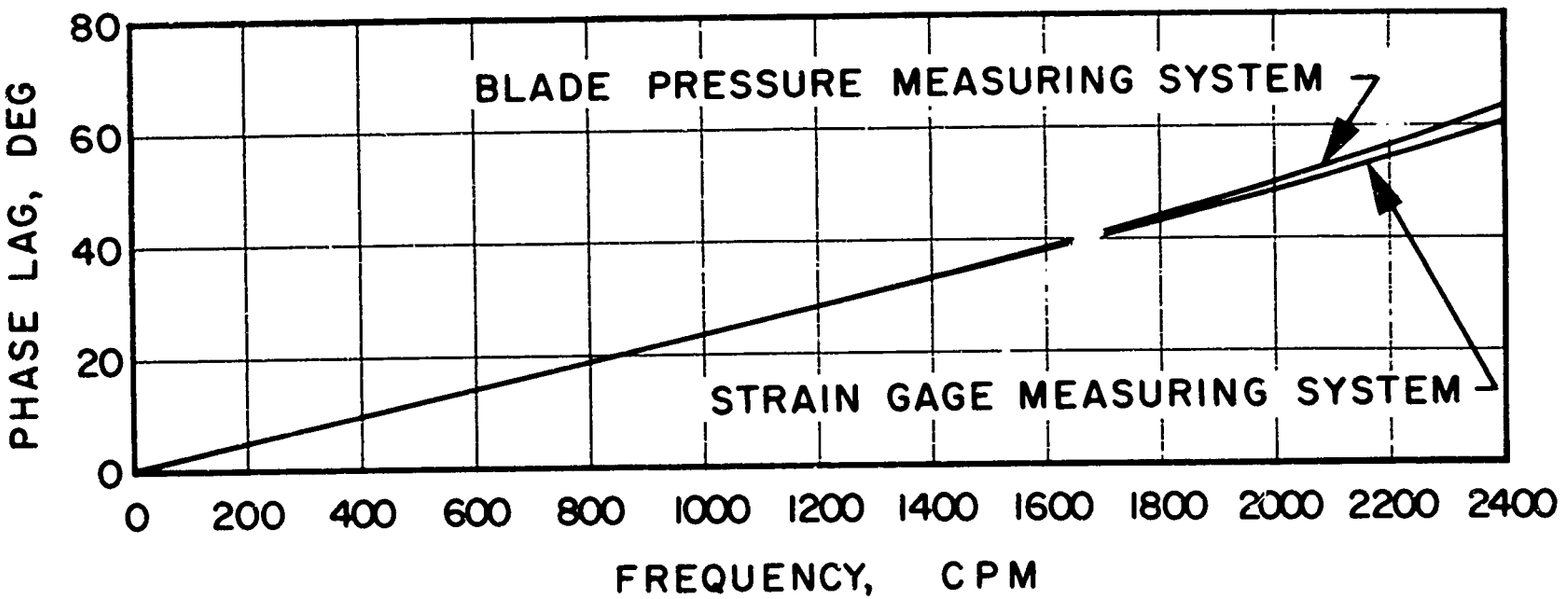

Figure 8. Phase Response of Data System .

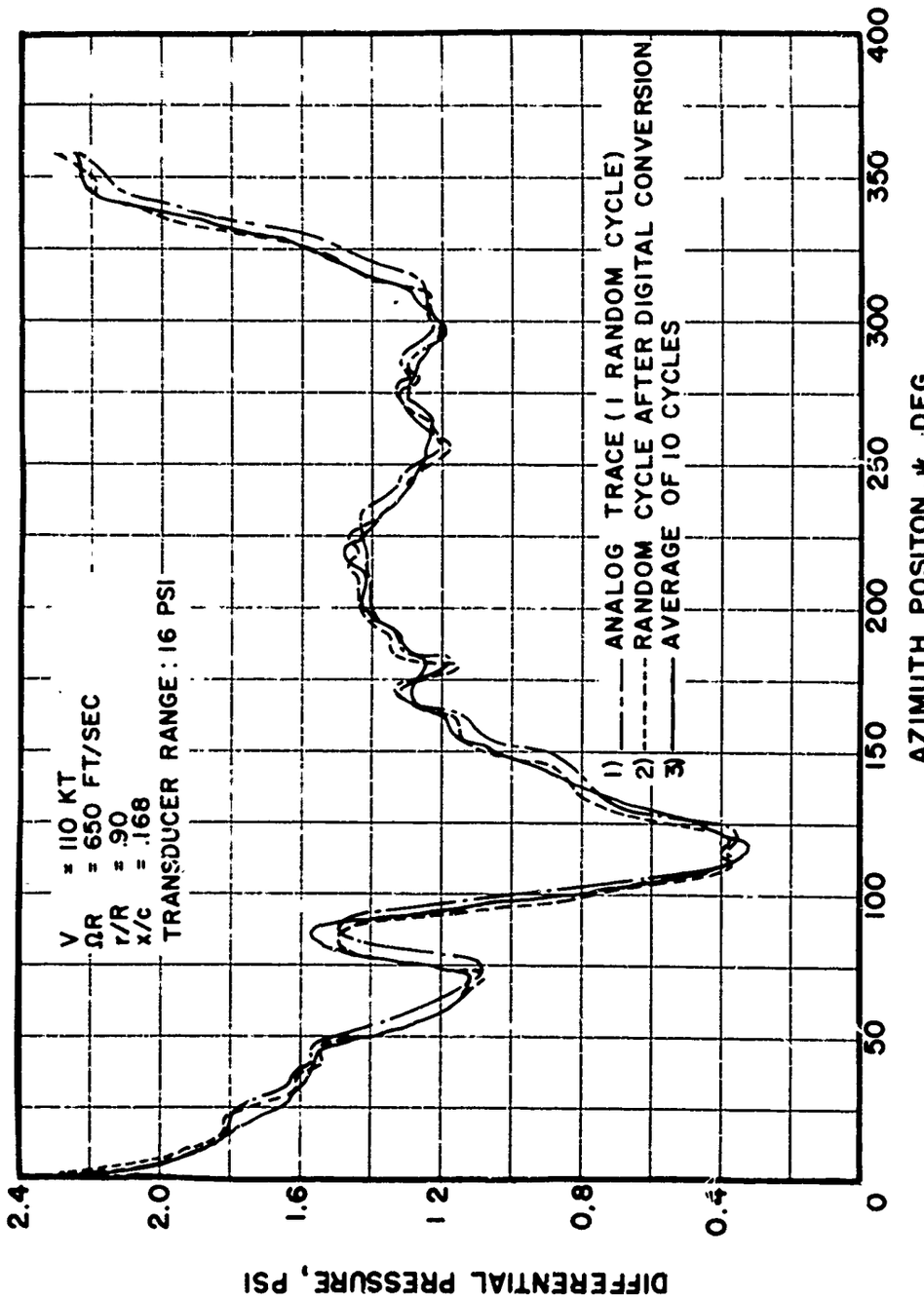

Figure 9. Sample Pressure Data Reliability.

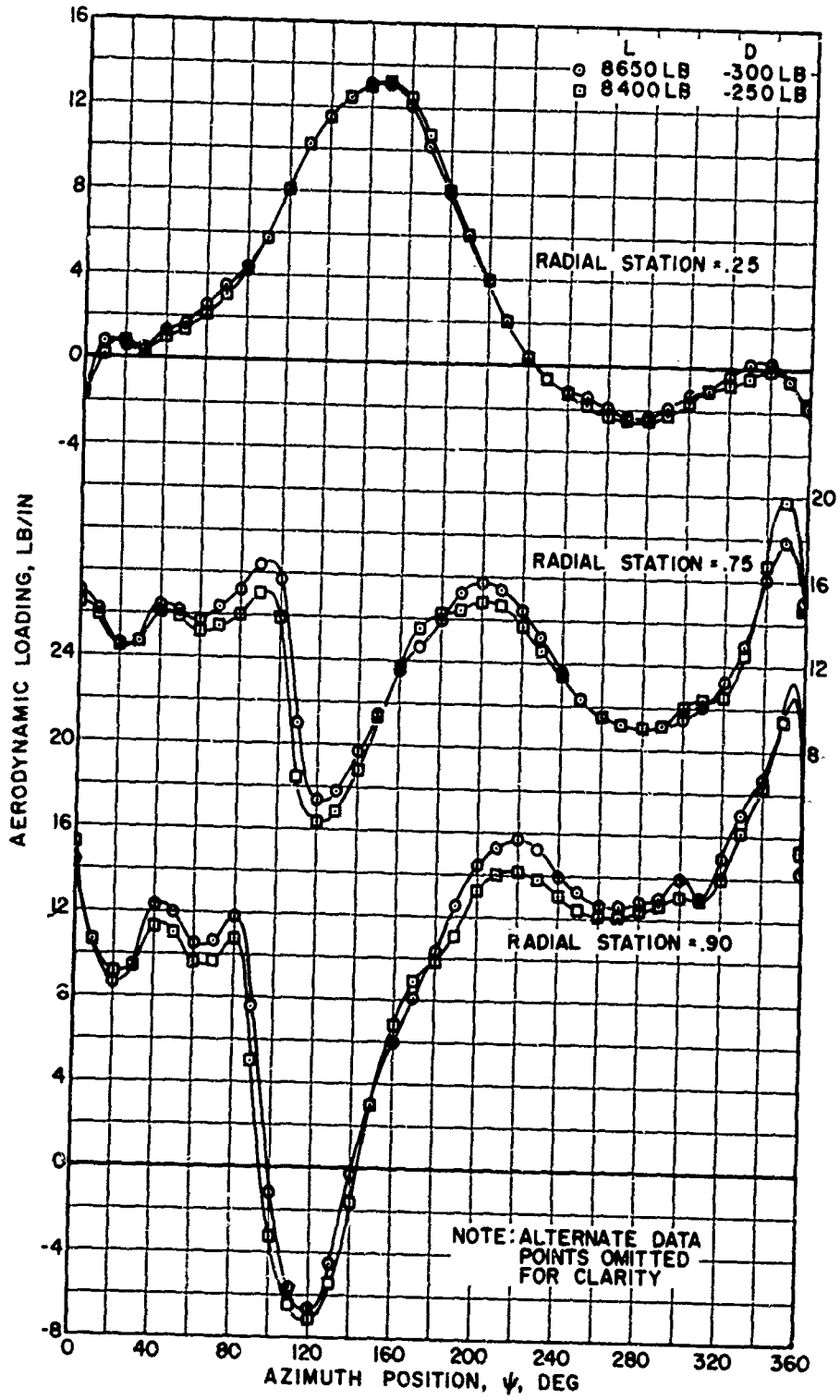

Figure 10. Sample Repeatability Of Airload Data.

$V = 150$ KT $\quad \alpha_s = 0°$

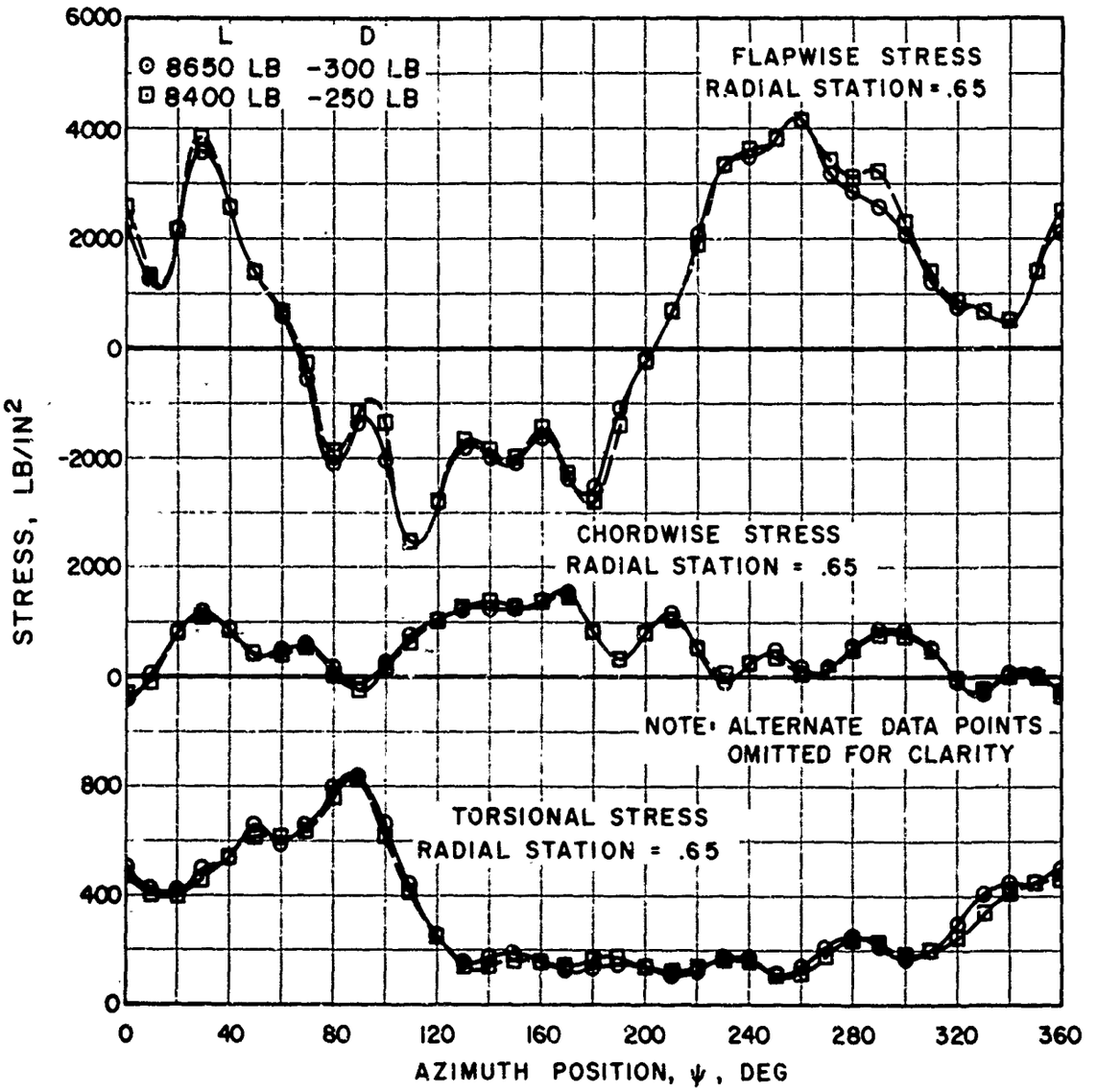

Figure 11. Sample Repeatability Of Blade Stress Data.

$V = 150$ KT $\quad \alpha_s = 0°$

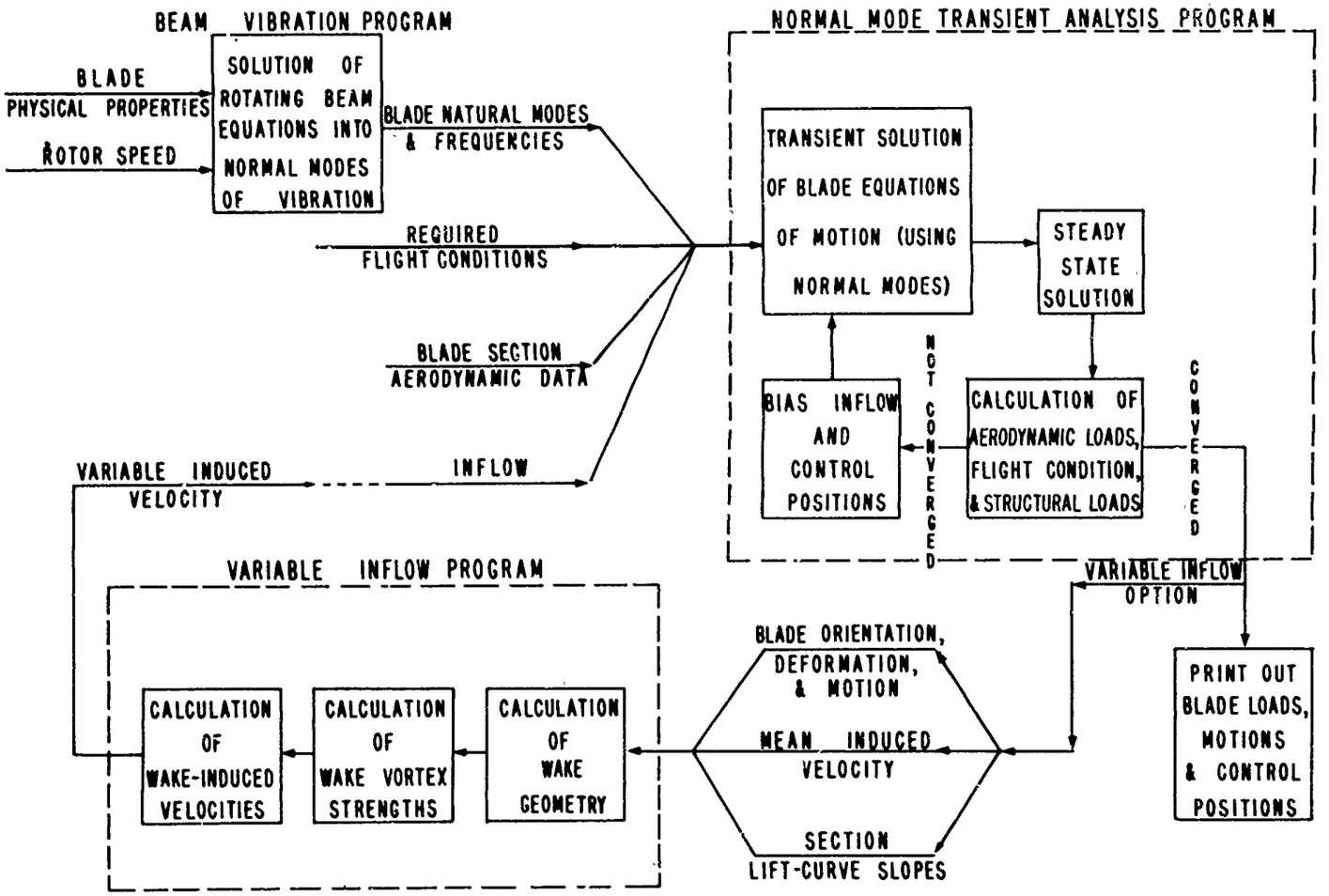

Figure 12. Flow Diagram for Computations.

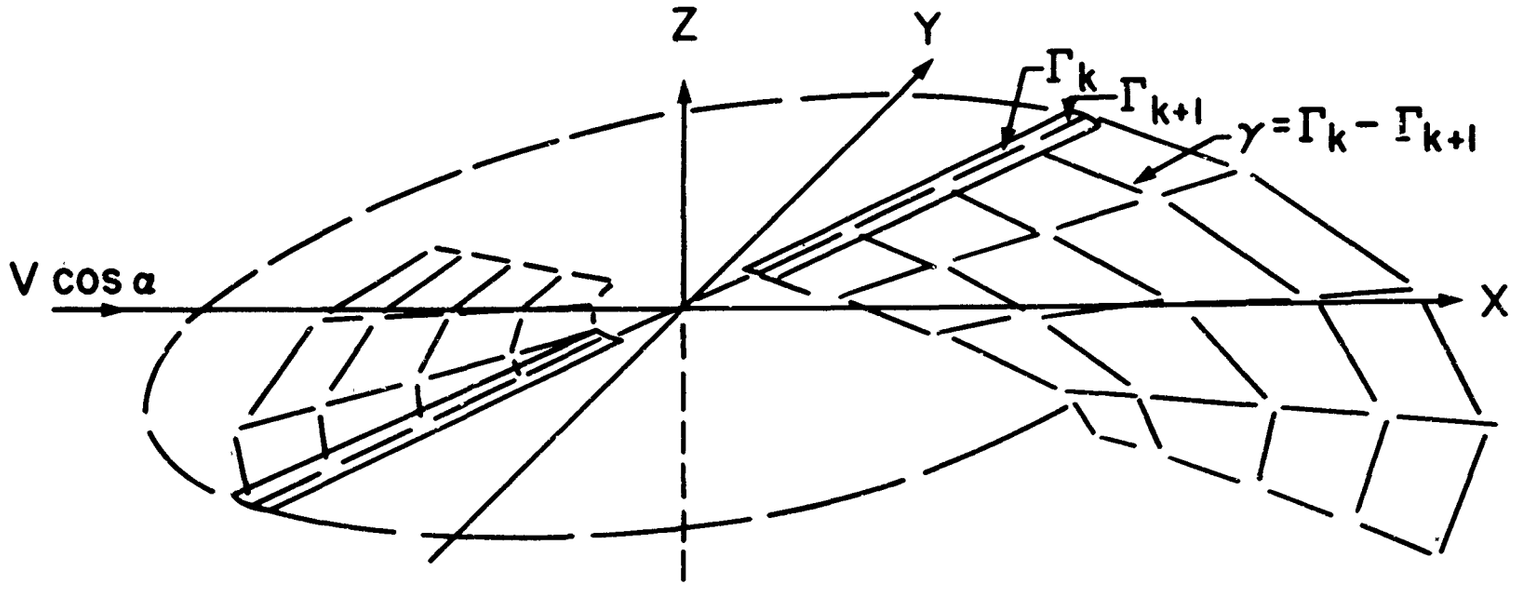

Figure 13. Pictorial Example Of The Initial Portion Of The Wake Of A Two-Bladed Rotor Divided Into Four Radial Segments (From Reference 4).

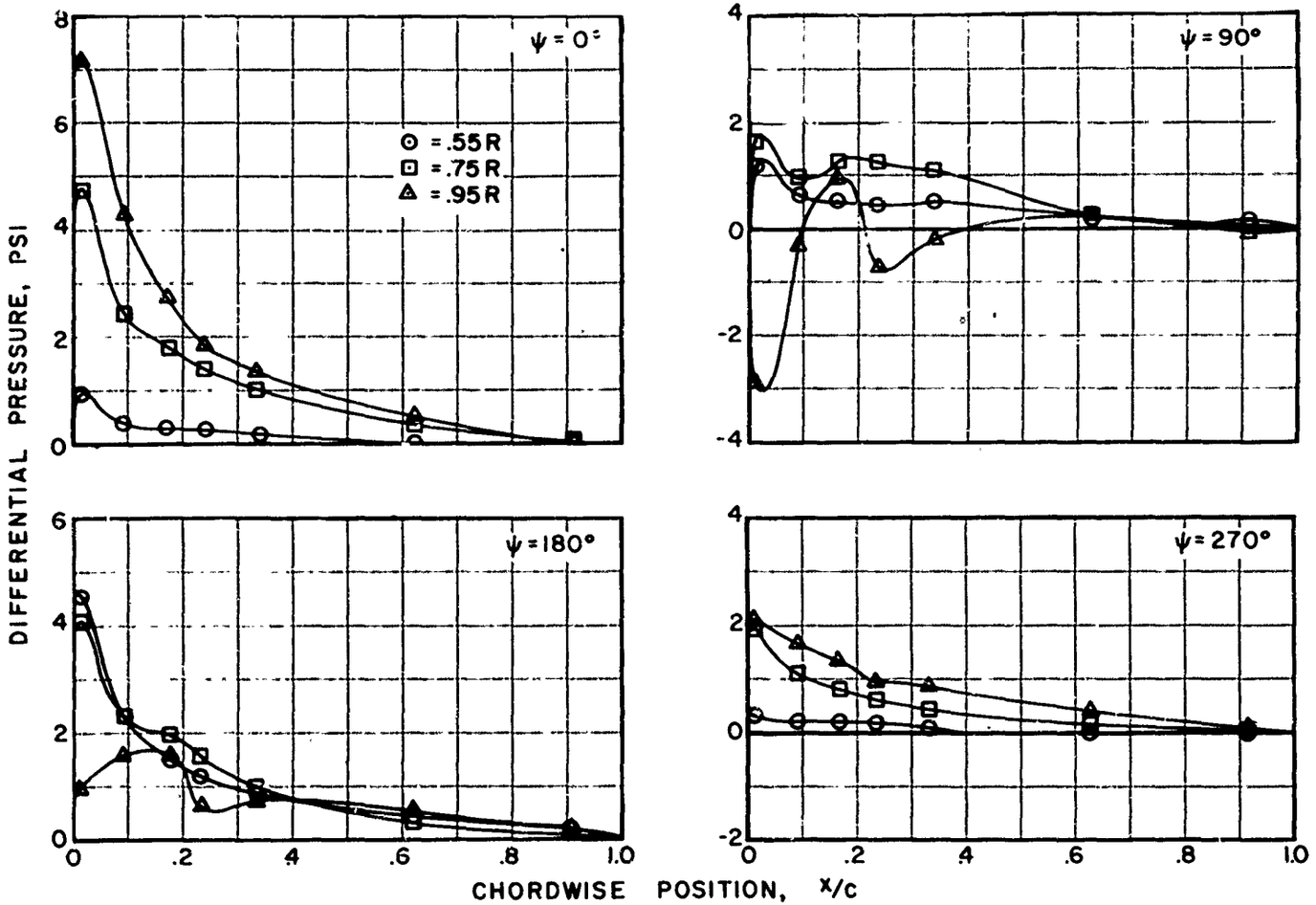

Figure 14. Sample Chordwise Pressure Distributions.

V = 175 KT α_s = -5° L = 7100 LB D = -250 LB

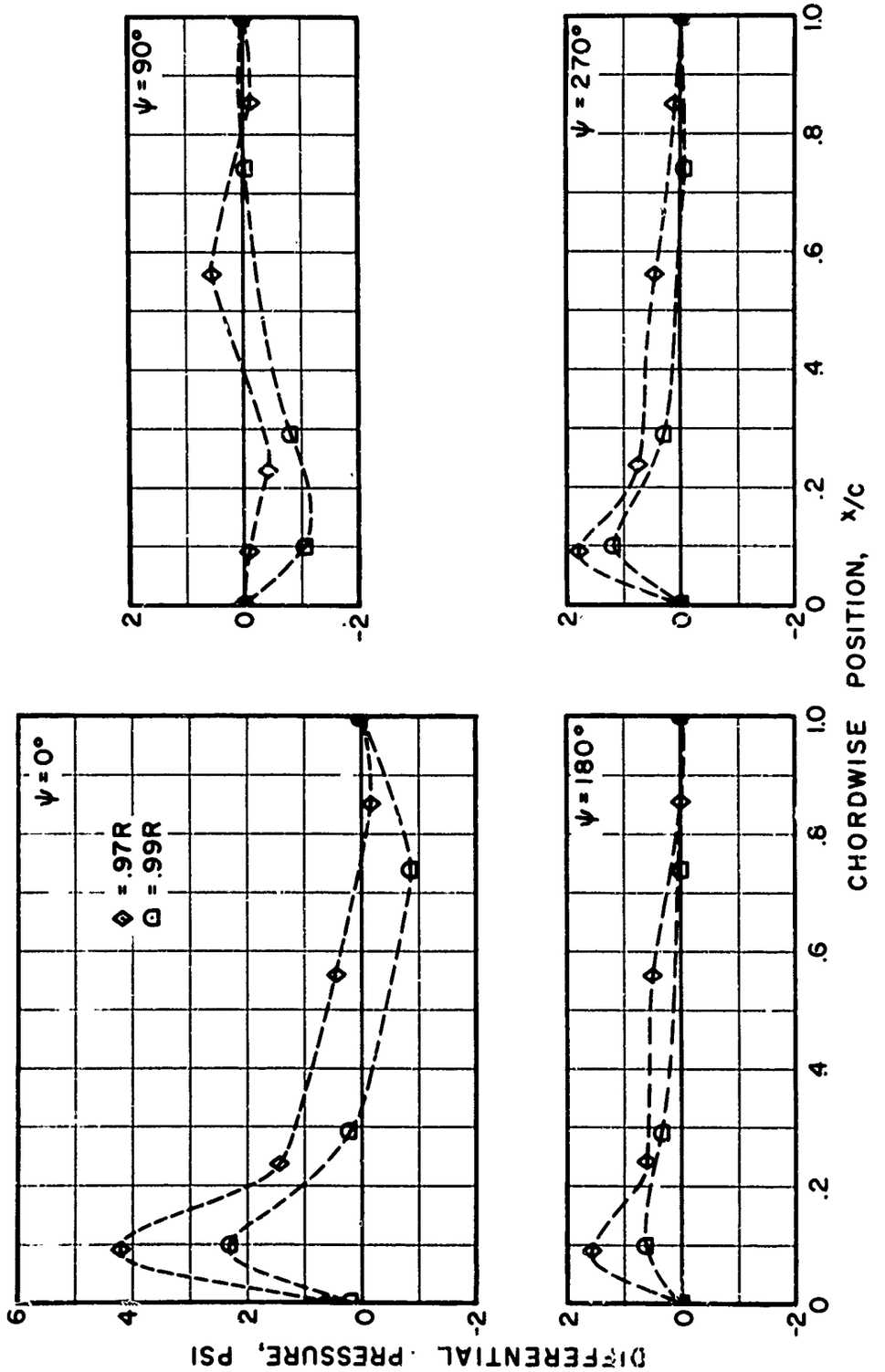

Figure 14. Concluded.

V = 175 KT α_s = -5° L = 7100 LB D = -250 LB

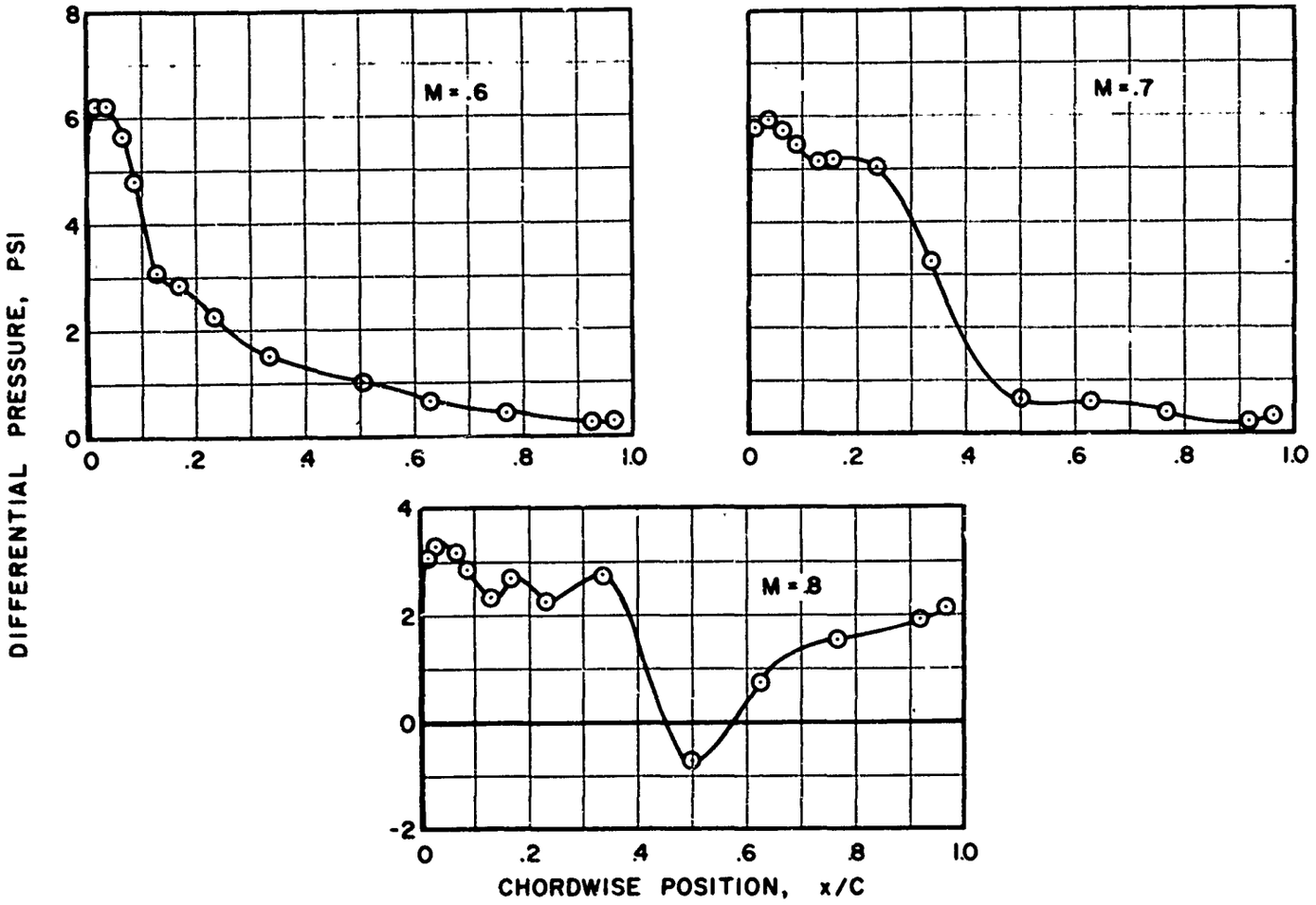

Figure 15. Sample 2-D Chordwise Loading At 4° Angle of Attack.

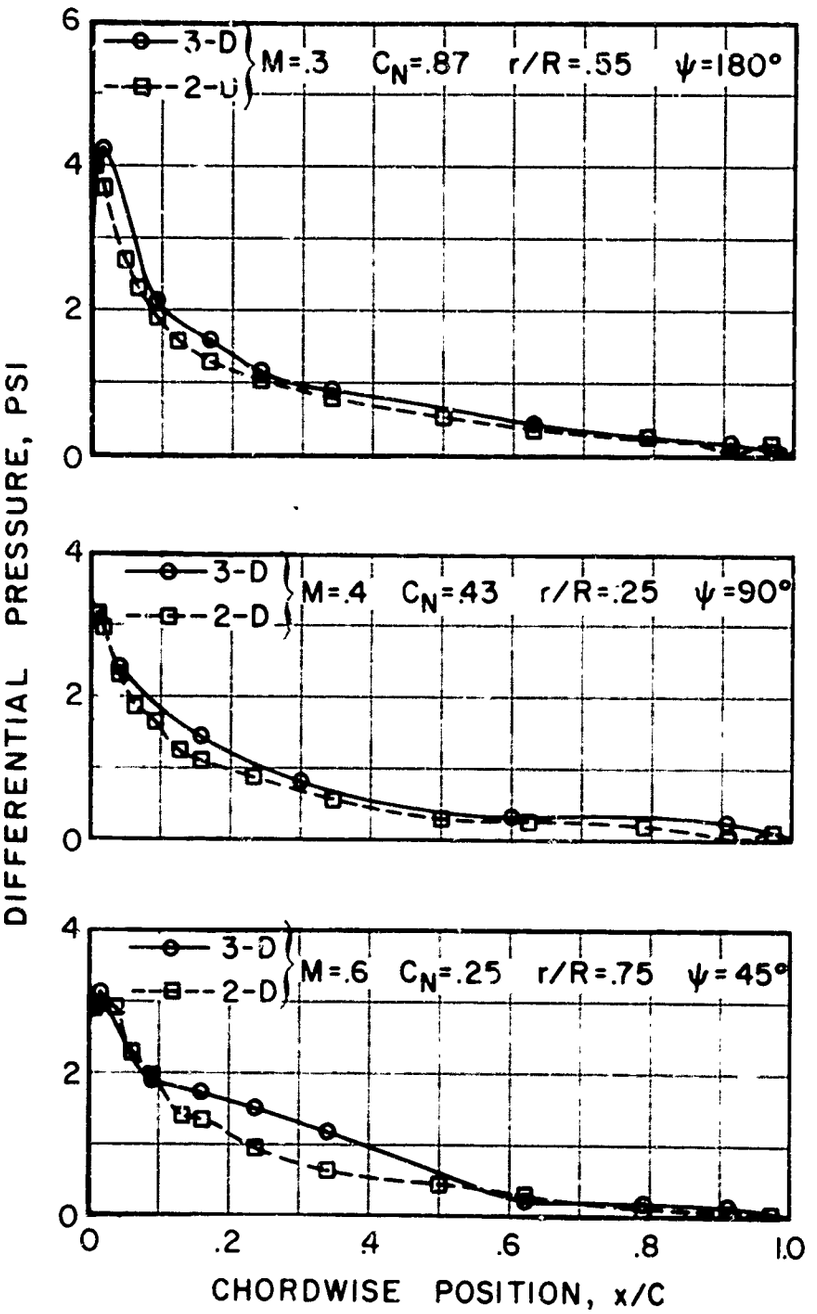

Figure 16. Comparison of 2-D and 3-D Chordwise Loading.

Note: 3 Dimensional Data Taken From Ames Tunnel

V = 175 KT $\alpha_S = +5°$

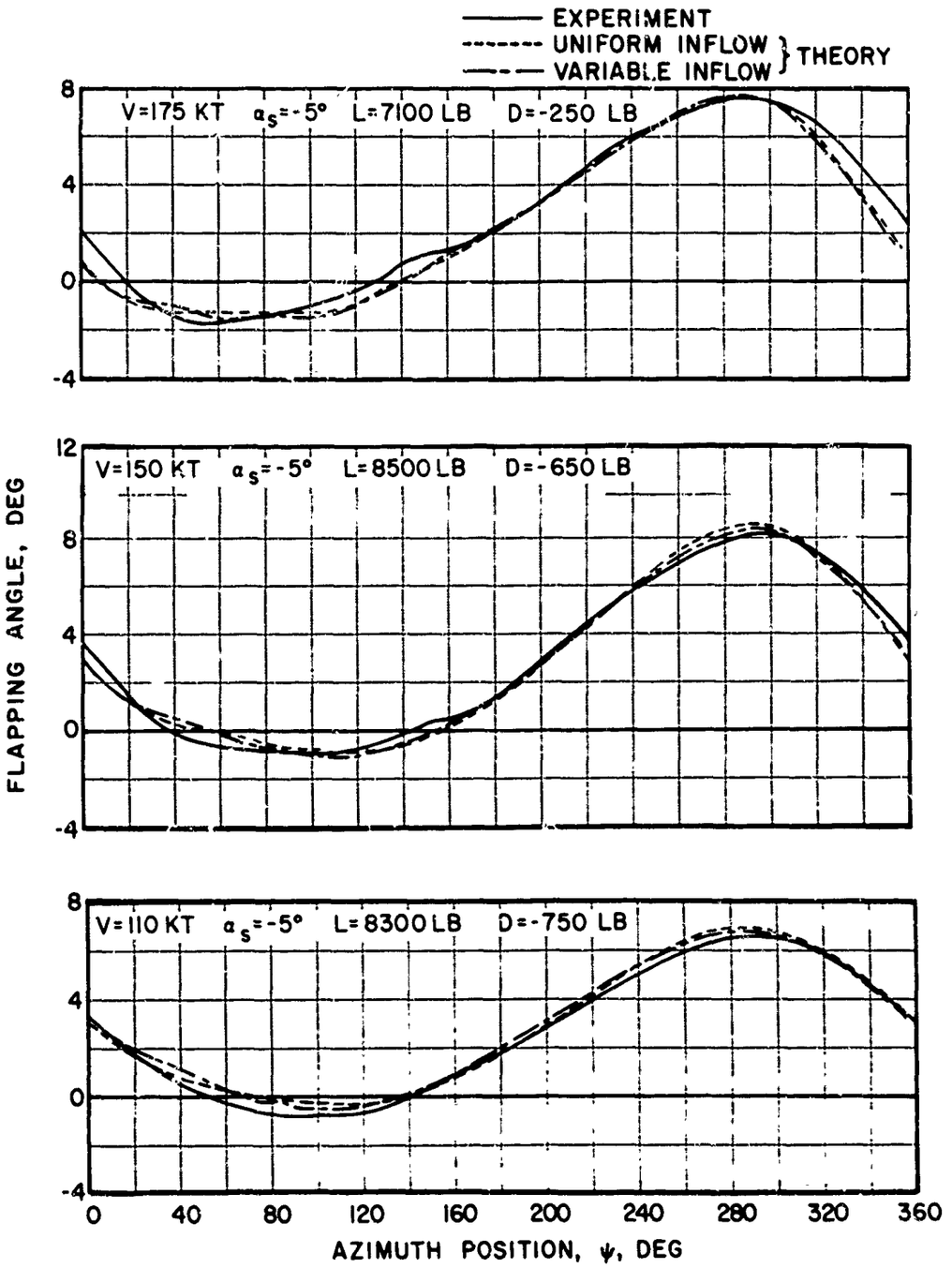

Figure 17. Sample Blade Root Flapping Motions.

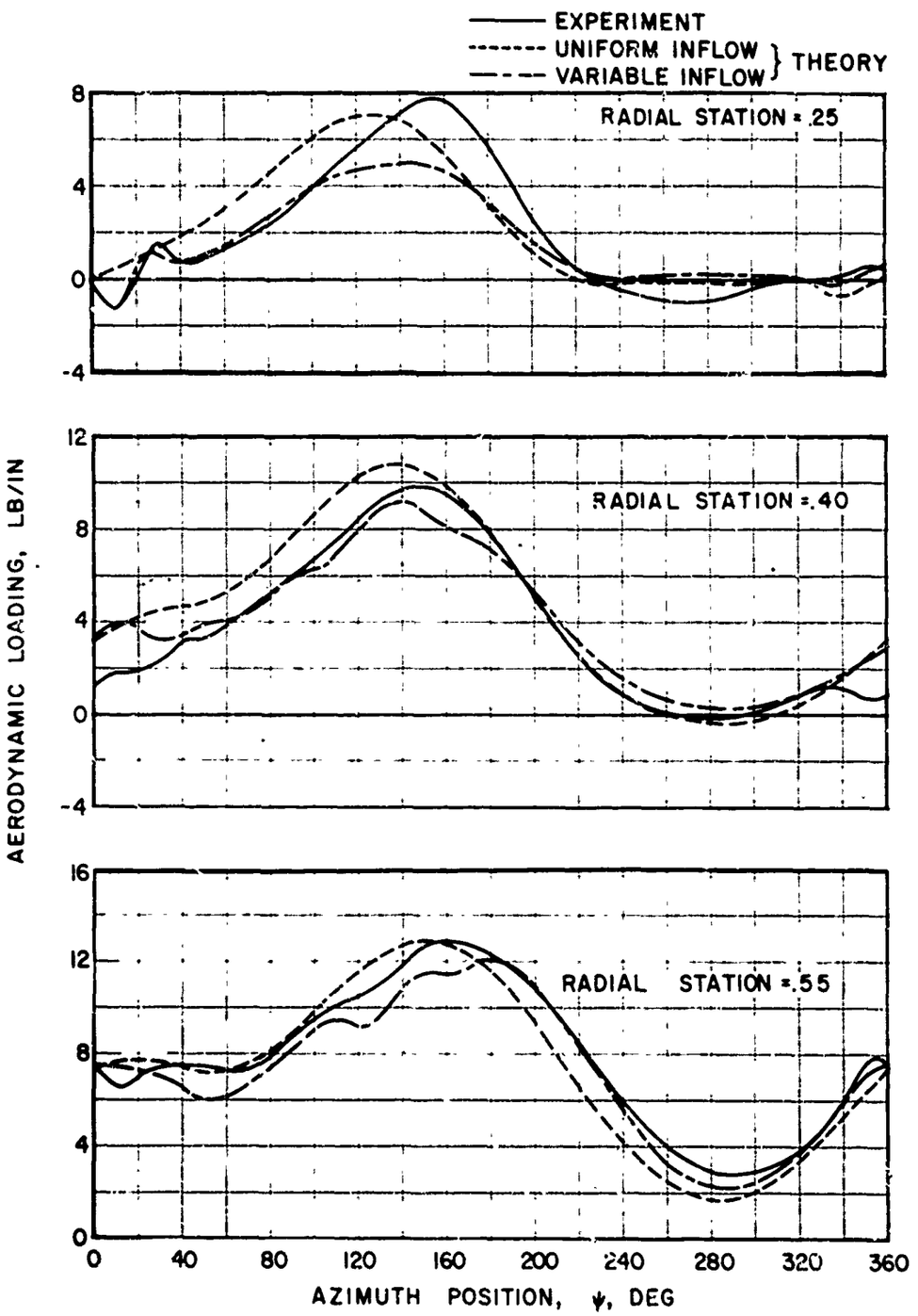

Figure 18. Section Aerodynamic Loading.

V = 110 KT α_s = -5° L = 8300 LB D = -750 LB

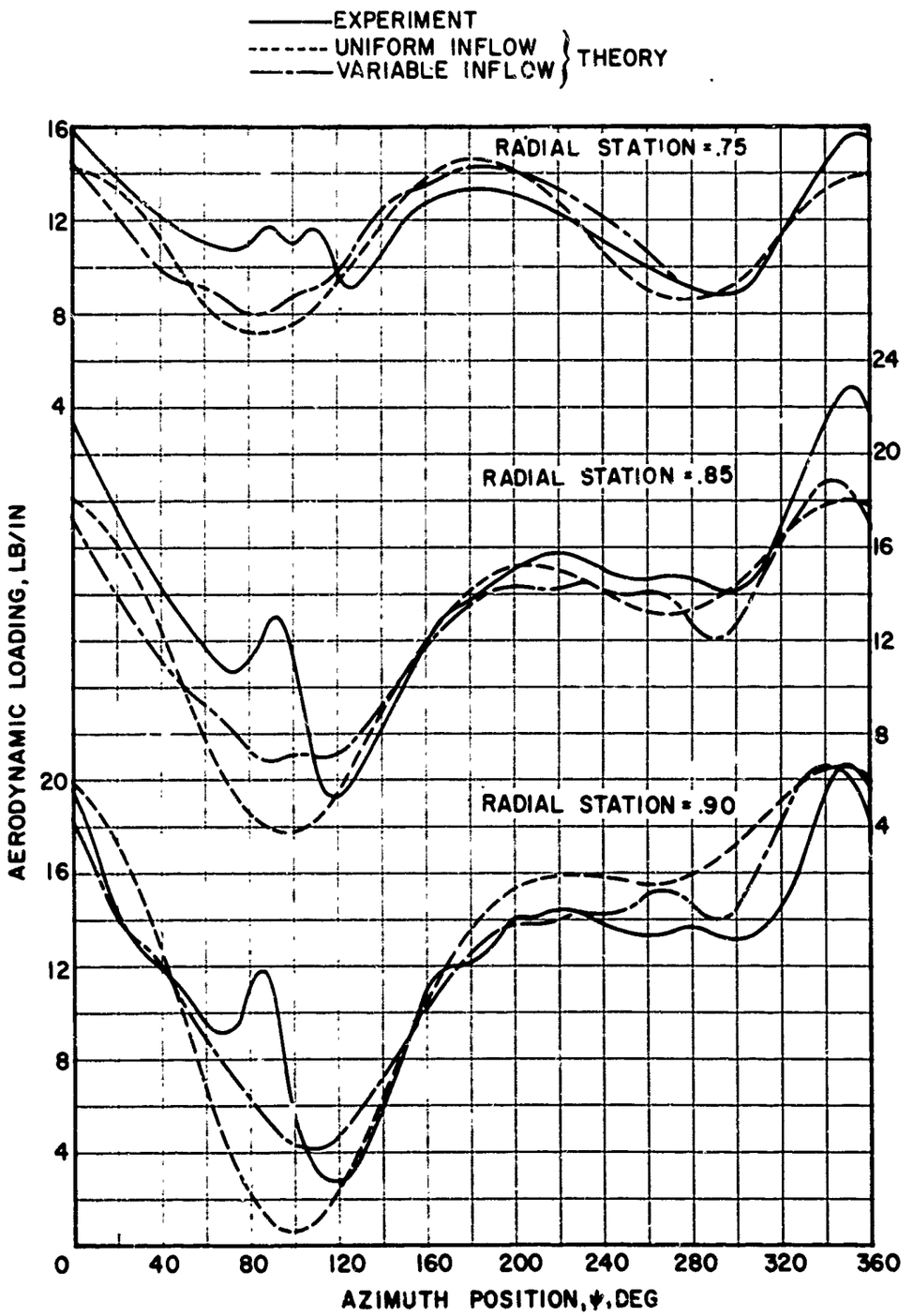

Figure 18. Continued.

V = 110 KT α_s = -5° L = 8300 LB D = -750 LB

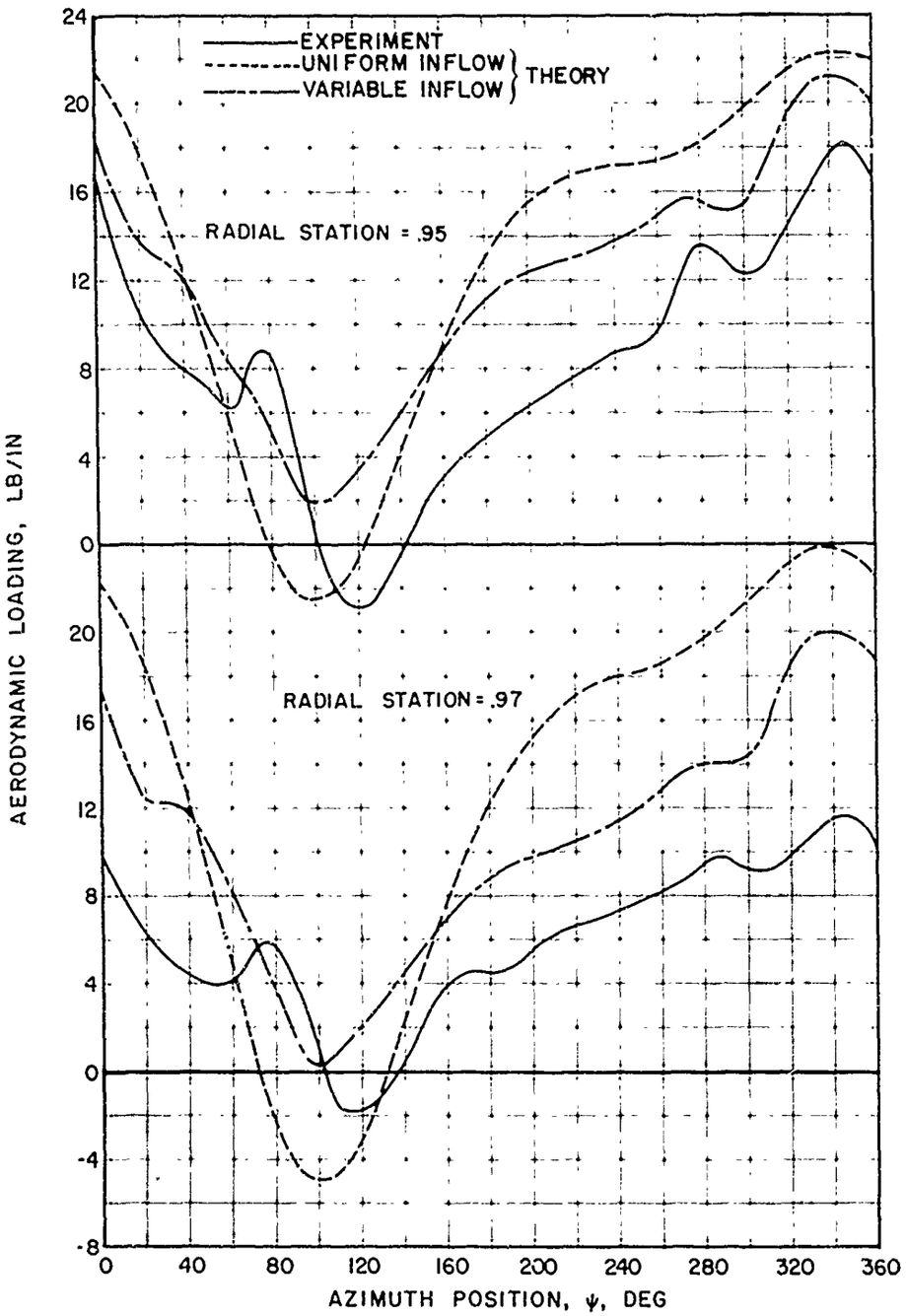

Figure 18. Continued.

V = 110 KT α_s = -5° L = 8300 LB D = -750 LB

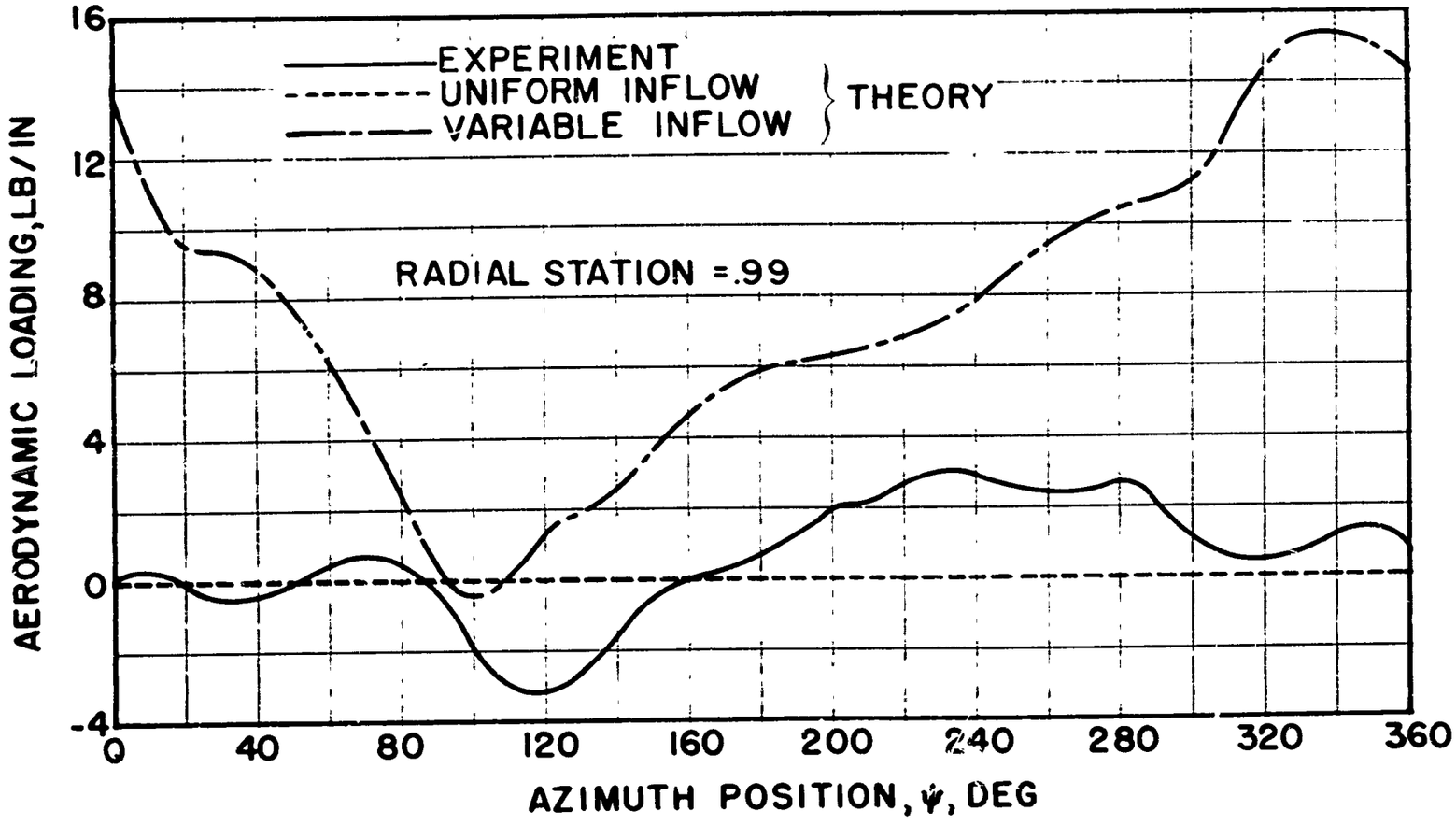

Figure 18. Concluded.

V = 110 KT α_s = -5° L = 8300 LB D = -750 LB

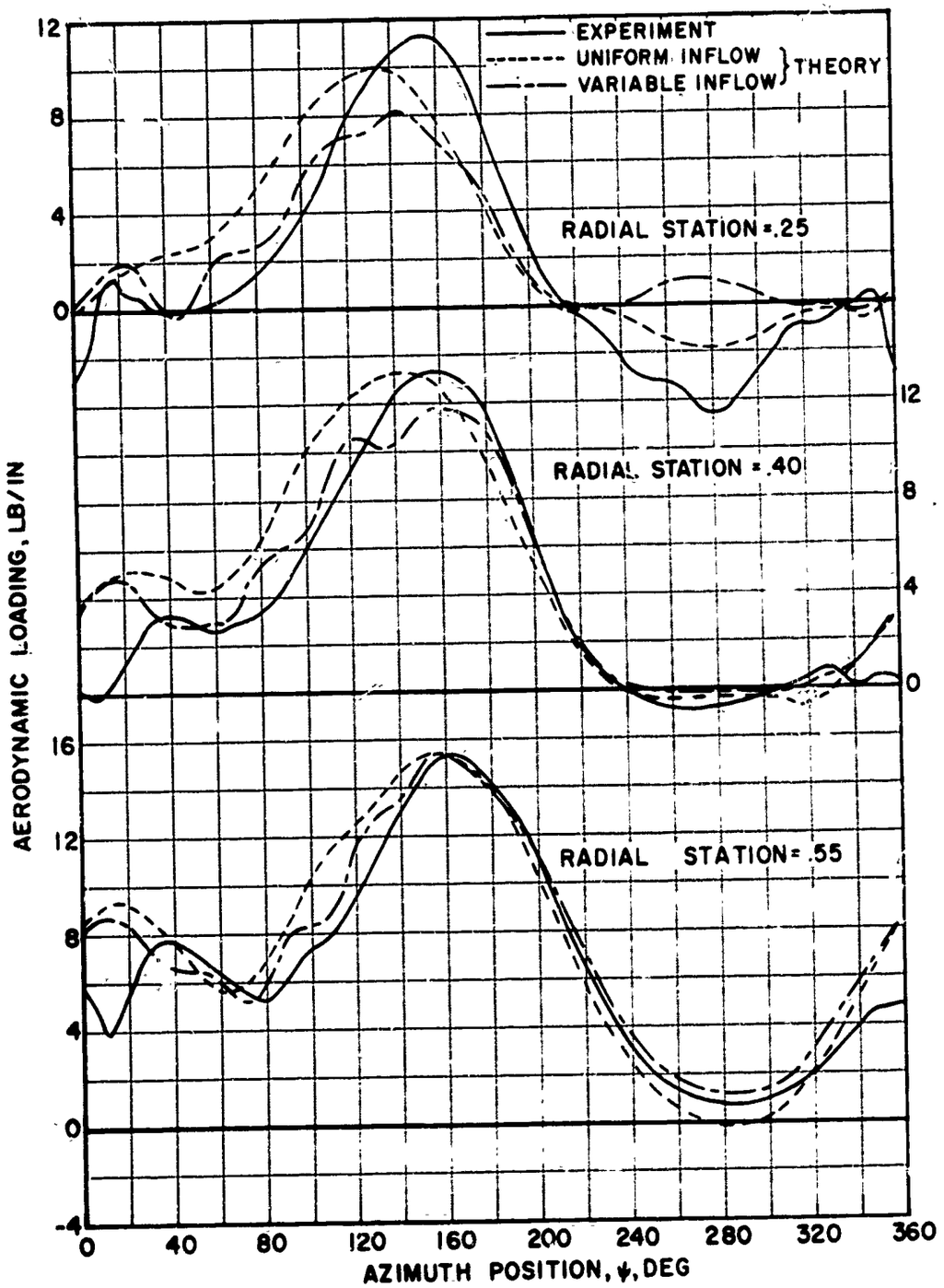

Figure 19. Section Aerodynamic Loading.

V = 150 KT α_s = -5° L = 8500 LB D = -650 LB

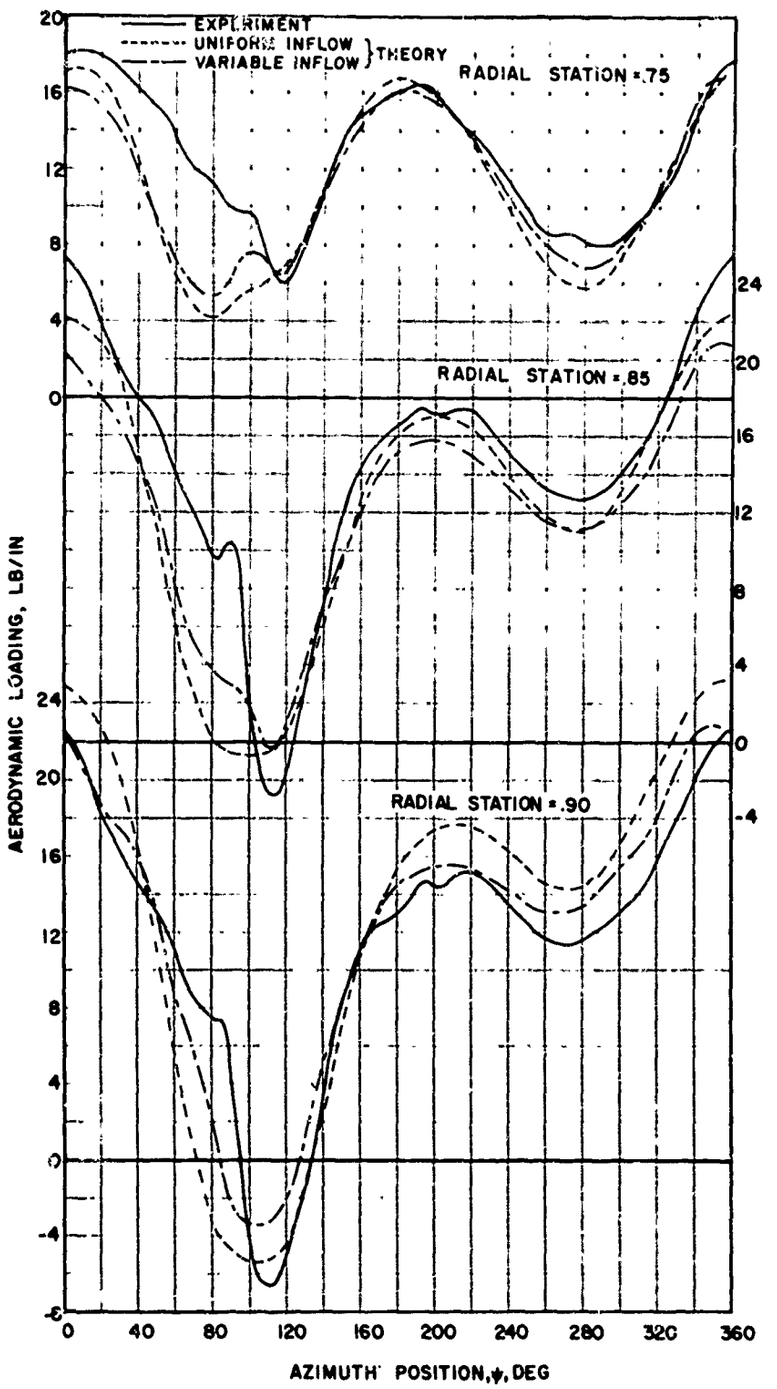

Figure 19. Continued.

V = 150 KT α_s = -5° L = 8500 LB D = -650 LB

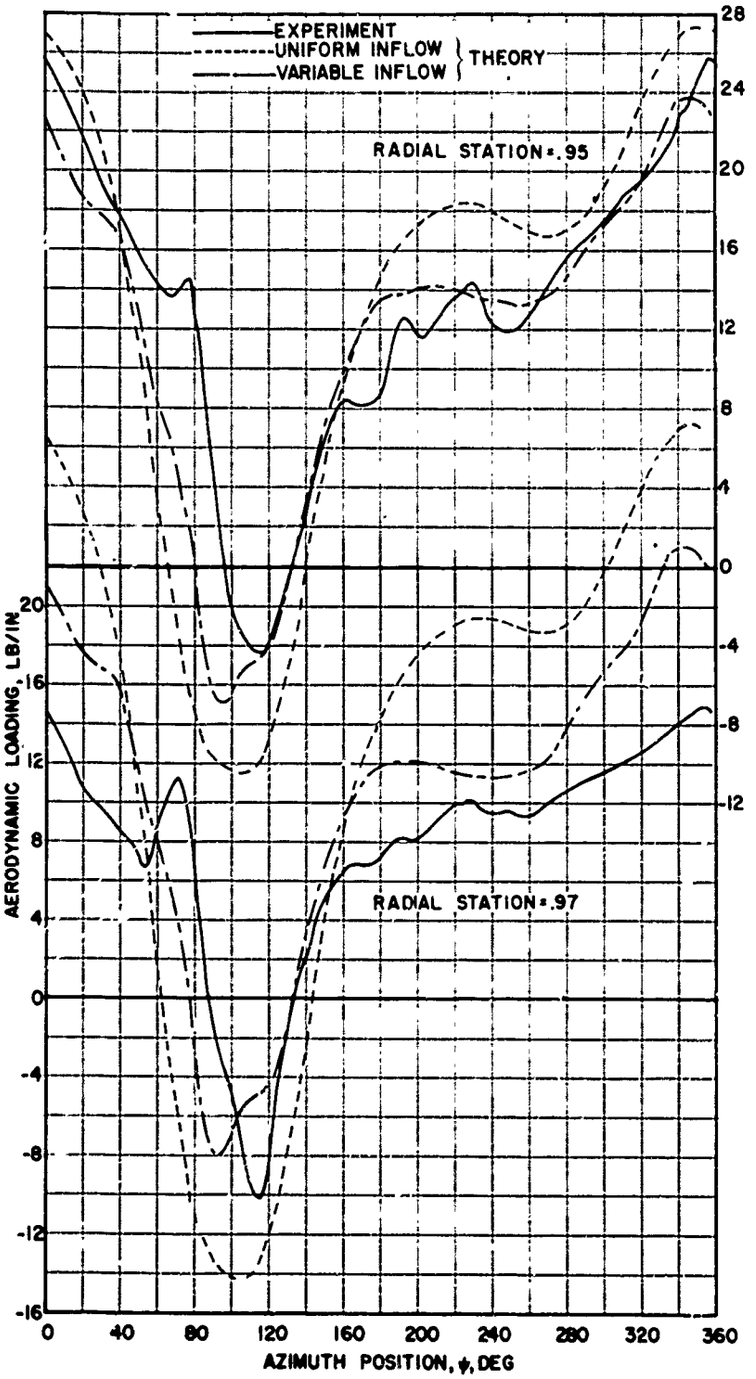

Figure 19. Continued.

V = 150 KT α_s = -5° L = 8500 LB D = -650 LB

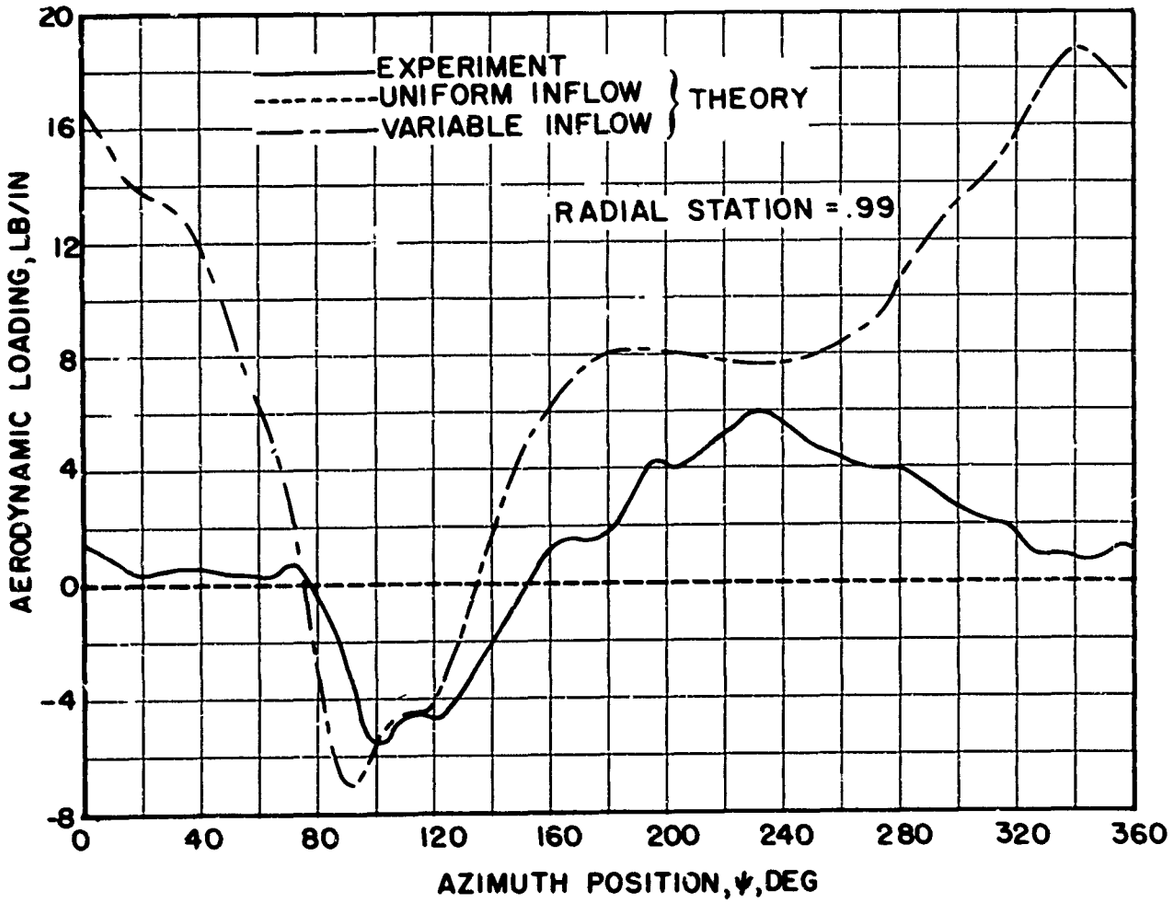

Figure 19. Concluded.

V = 150 KT α_s = -5° L = 8500 LB D = -650 LB

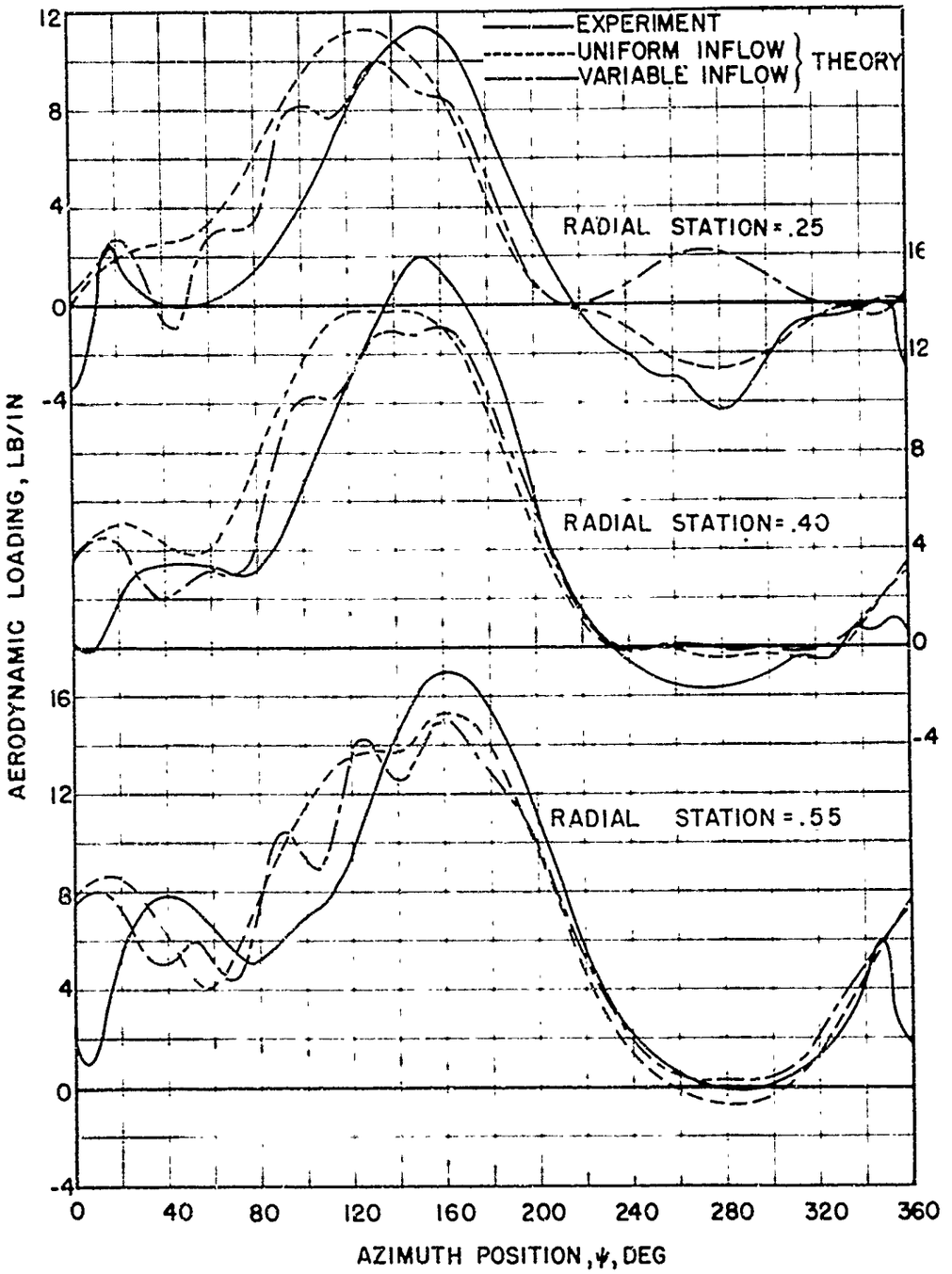

Figure 20. Section Aerodynamic Loading.

V = 175 KT α_s = -5° L = 7100 LB D = -250 LB

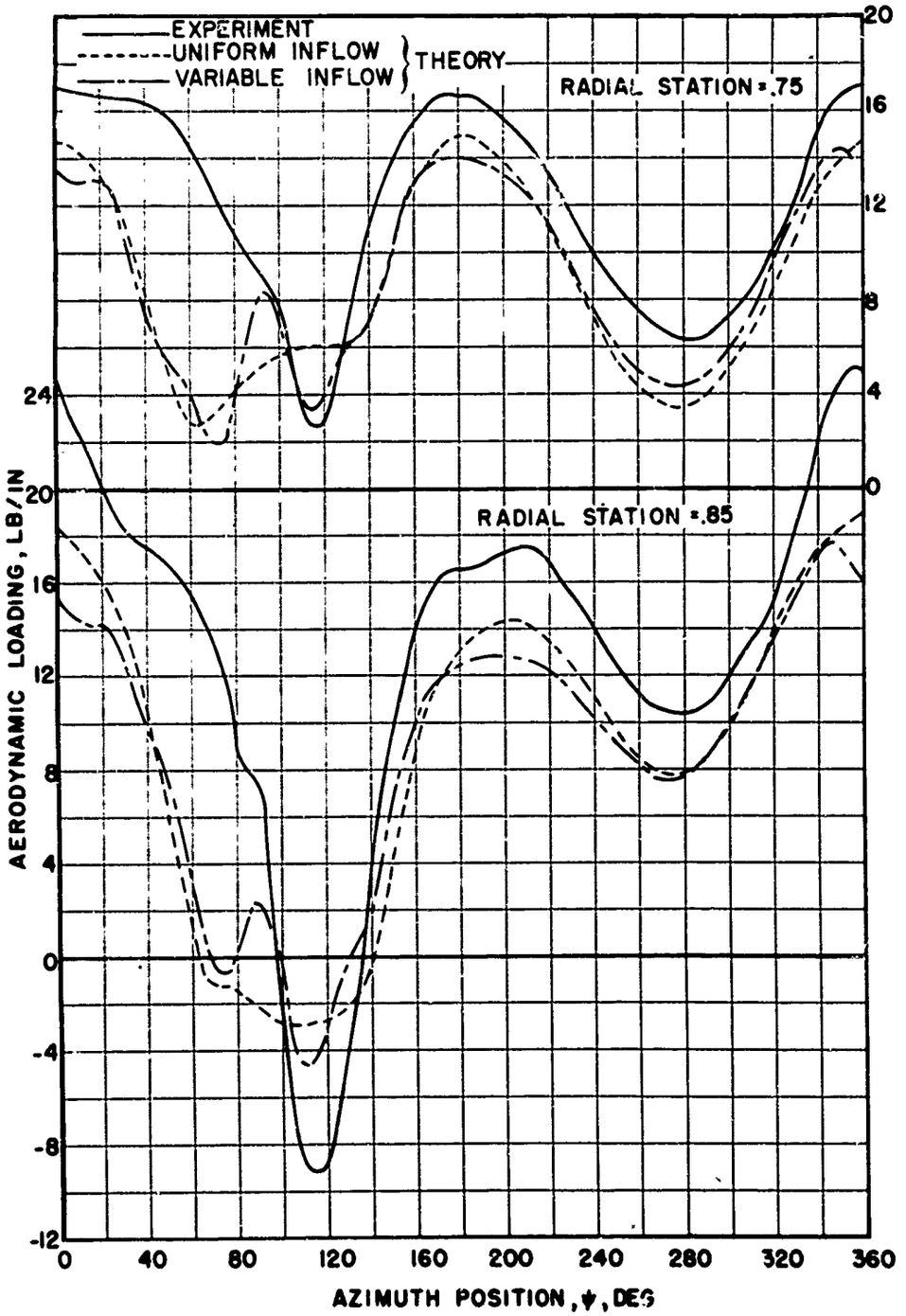

Figure 20. Continued.

V = 175 KT α_s = -5° L = 7100 LB D = -250 LB

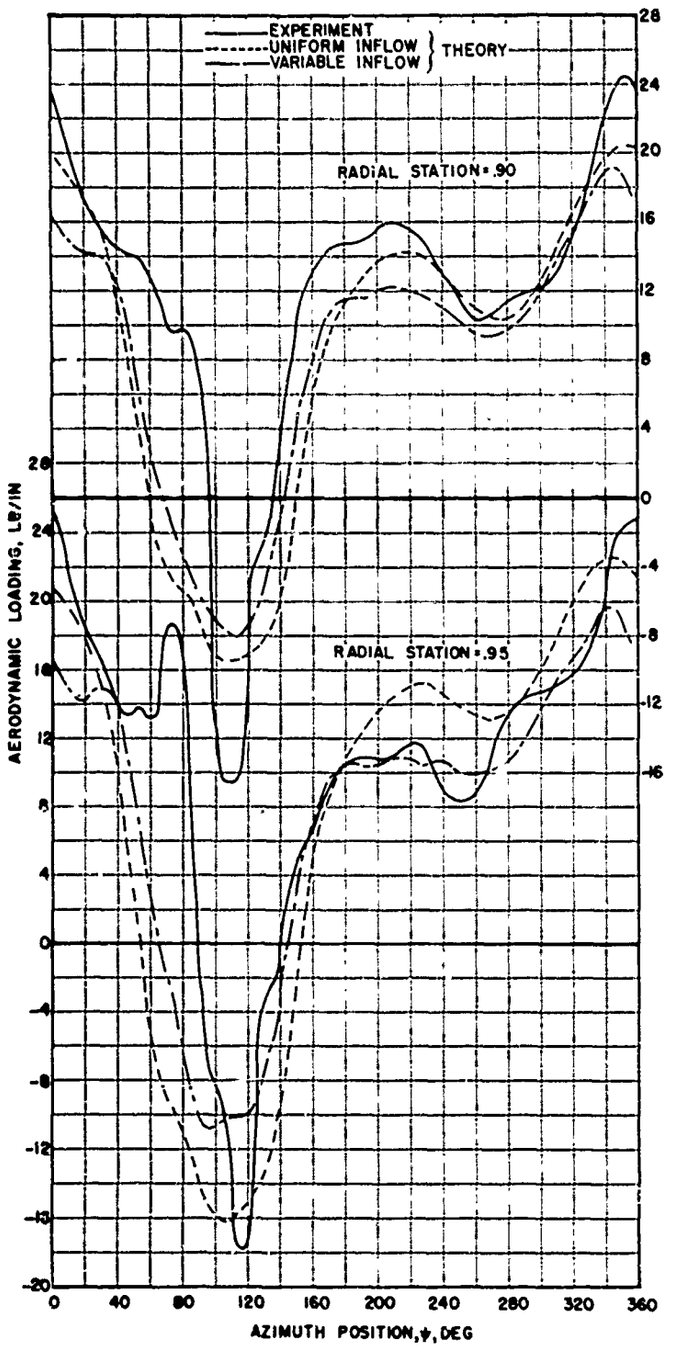

Figure 20. Continued.

V = 175 KT α_s = -5° L = 7100 LB D = -250 LB

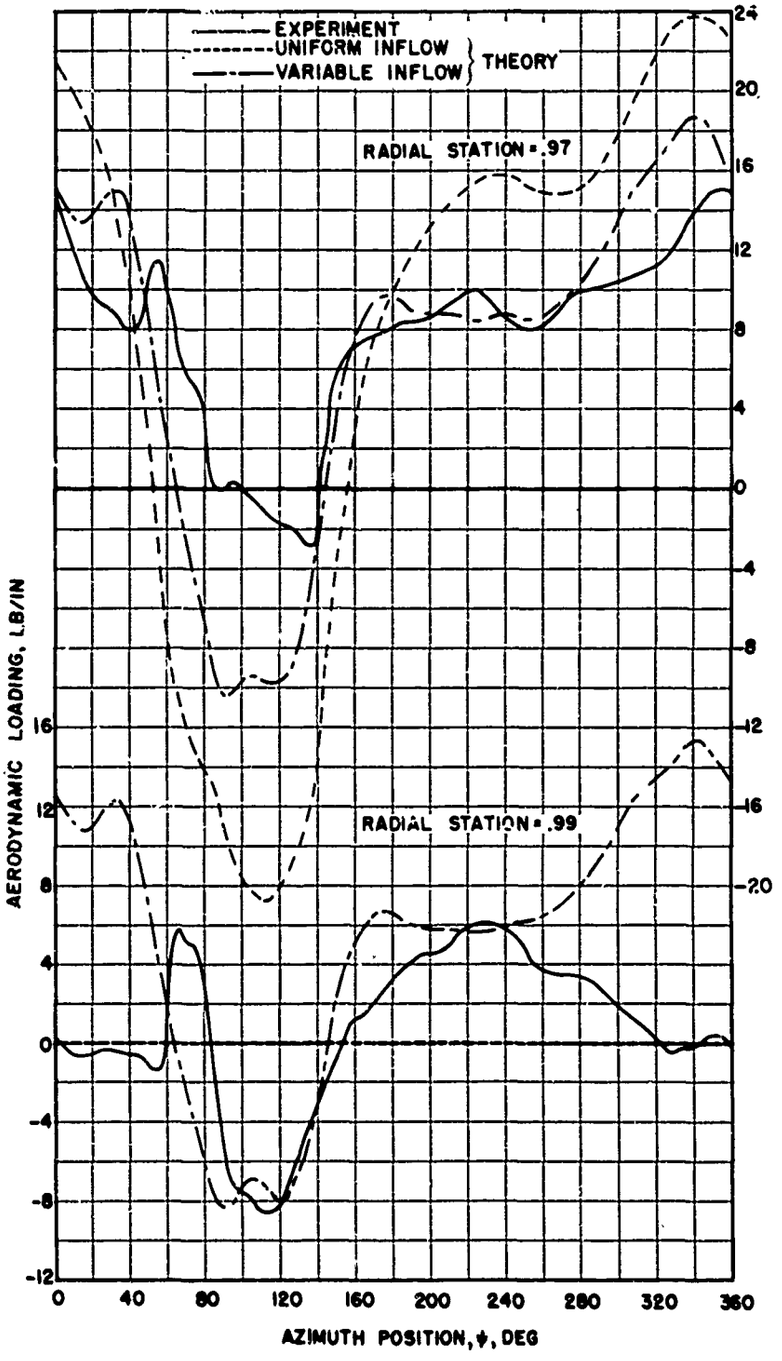

Figure 20. Concluded.

V = 175 KT α_s = -5° L = 7100 LB D = -250 LB

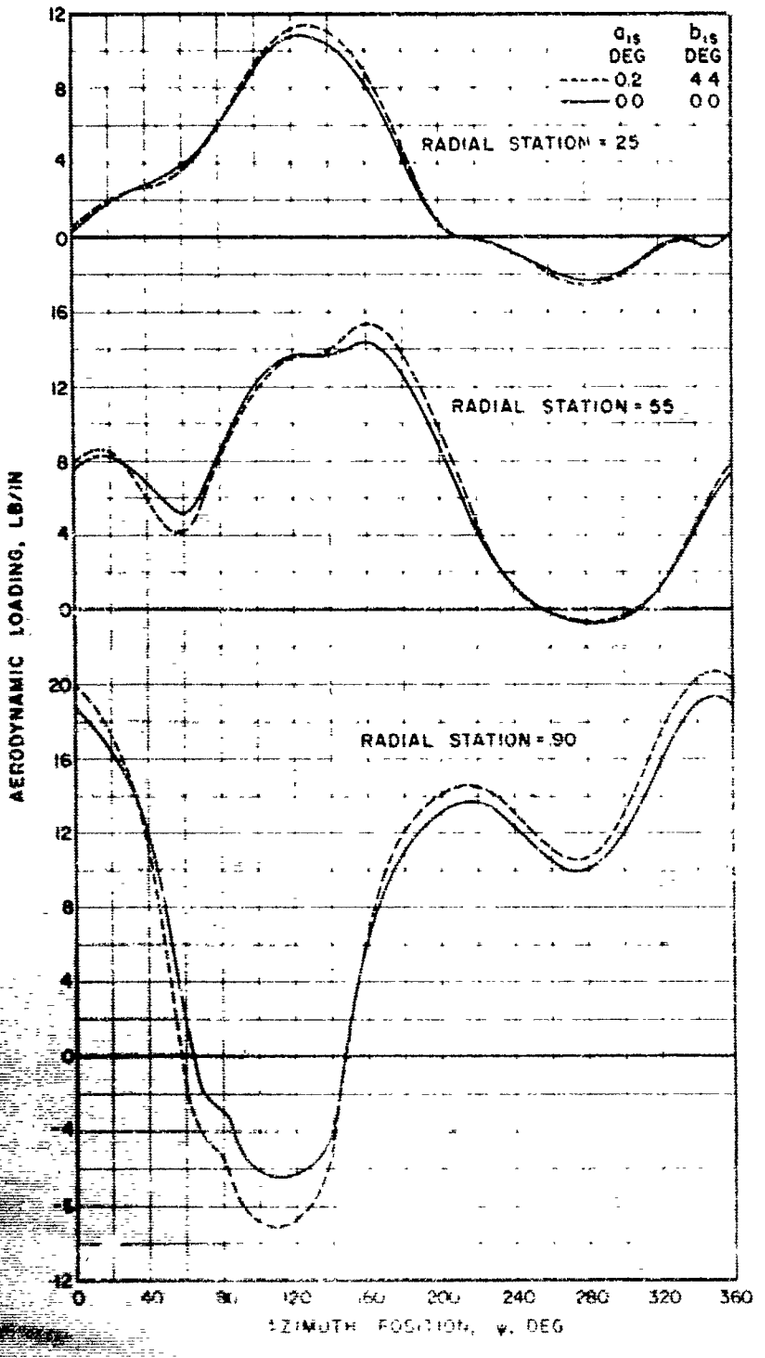

Figure 21. Theoretical Effect Of Blade Flapping On Aerodynamic Loading, Uniform Inflow

V_t = 175 KT a_s = -5° T = 7100 LB D = -250 LB

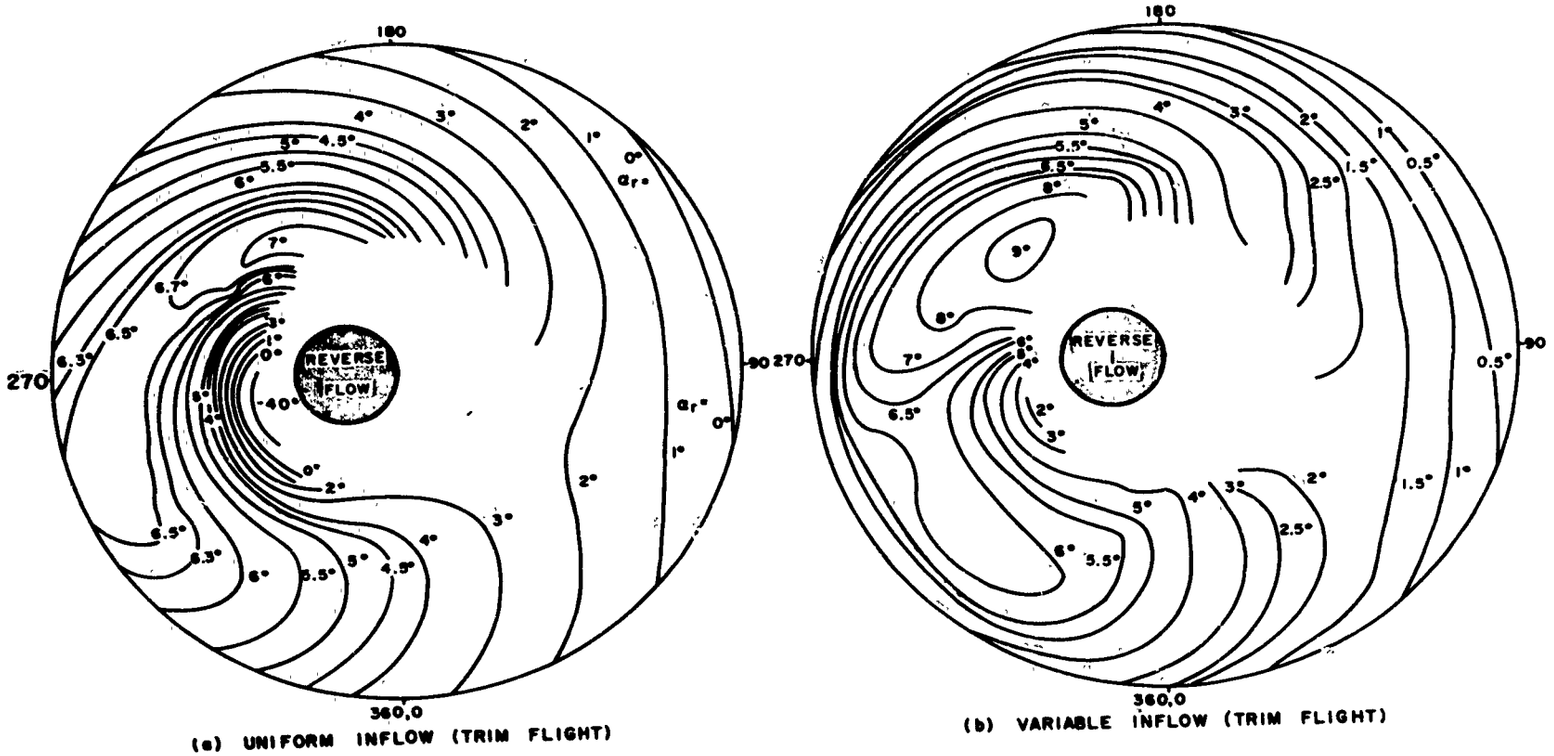

Figure 22. Theoretical Local Angle of Attack Distribution at 110 Kt.

α_s = -5° ΩR = 650 FT/SEC μ = .29 $M_{(1.0, 90)}$ = .73 L = 8300 LB D = -750 LB

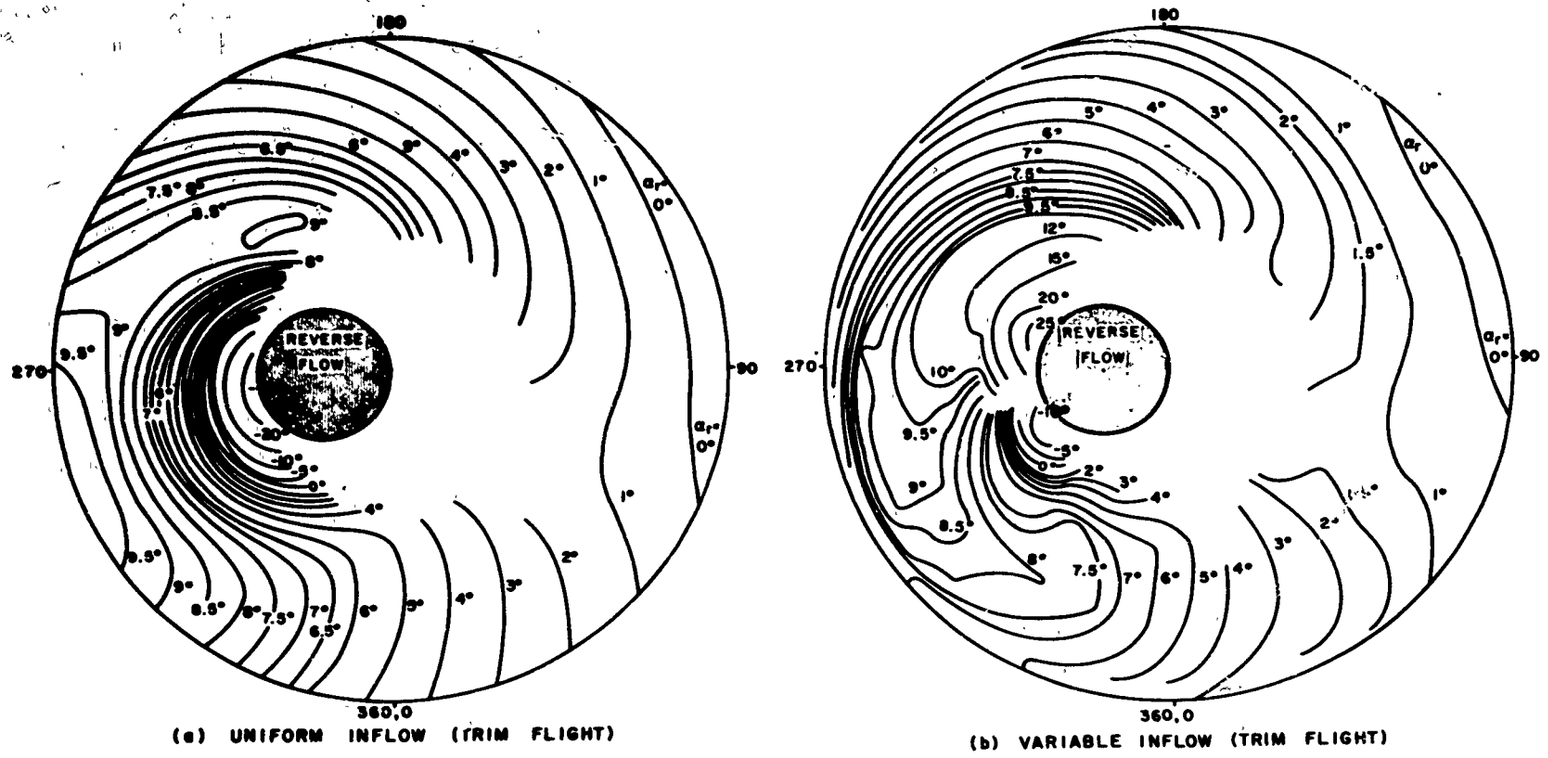

Figure 23. Theoretical Local Angle of Attack Distribution At 150 Kt.

α_s = -5° ΩR = 650 FT/SEC μ = .39 $M_{(1.0, 90)}$ = .79 L = 8500 LB D = -650 LB

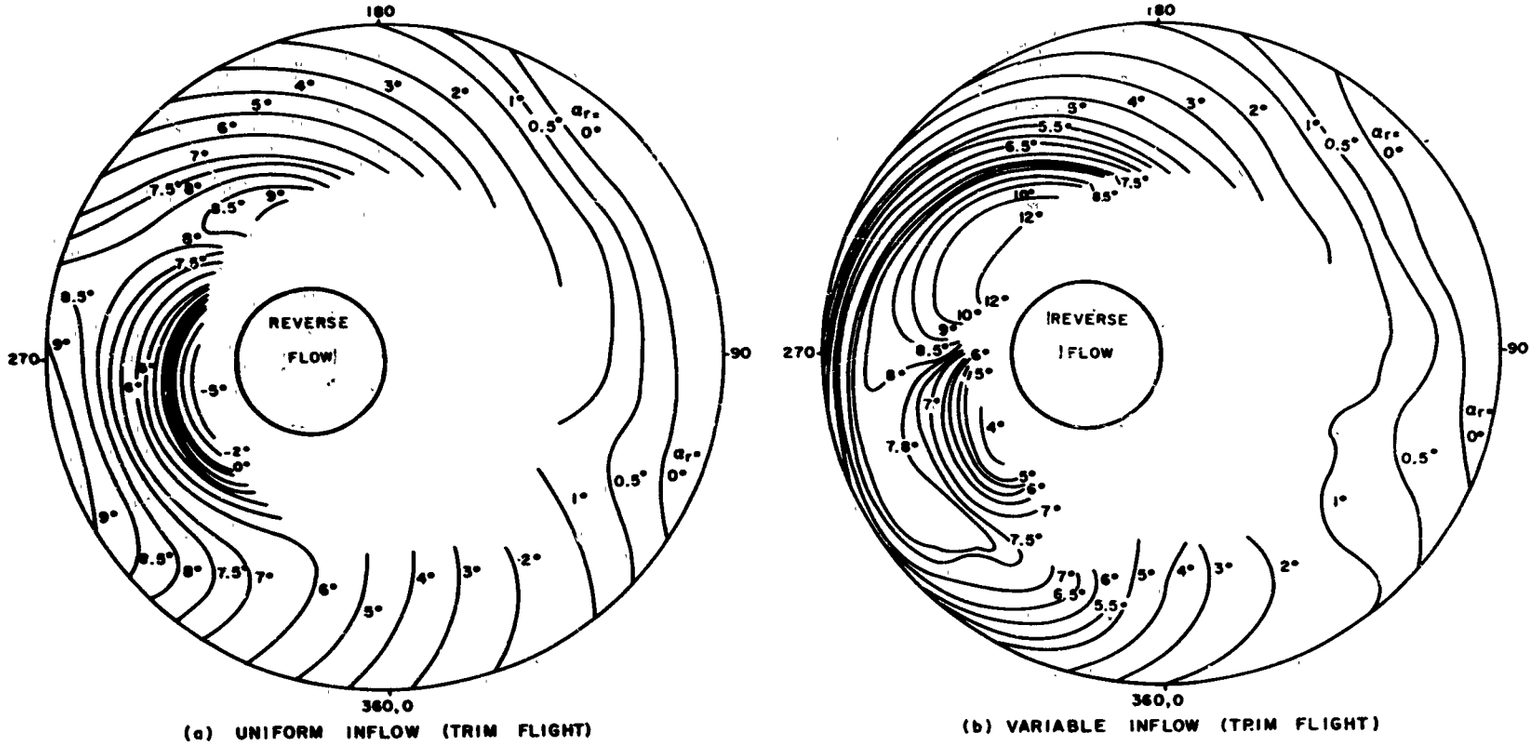

(a) UNIFORM INFLOW (TRIM FLIGHT)

(b) VARIABLE INFLOW (TRIM FLIGHT)

Figure 24. Theoretical Local Angle of Attack Distribution at 175 Kt.

α_s = -5° ΩR = 650 FT/SEC μ = .45 $M_{(1.0, 90)}$ = .83 L = 7100 LB D = -250 LB

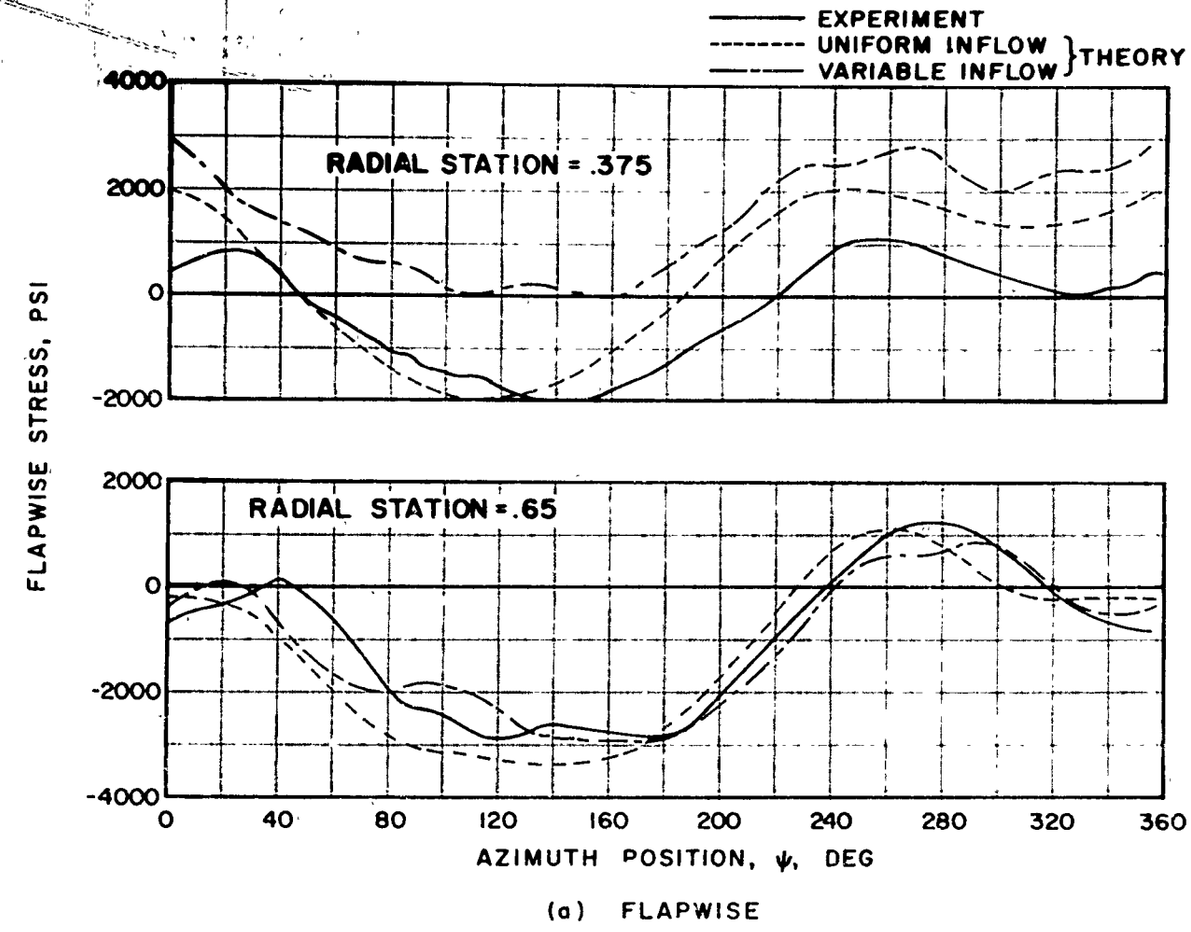

Figure 25. Blade Stress Time Histories.

V = 110 KT α_s = -5° L = 8300 LB D = -750 LB

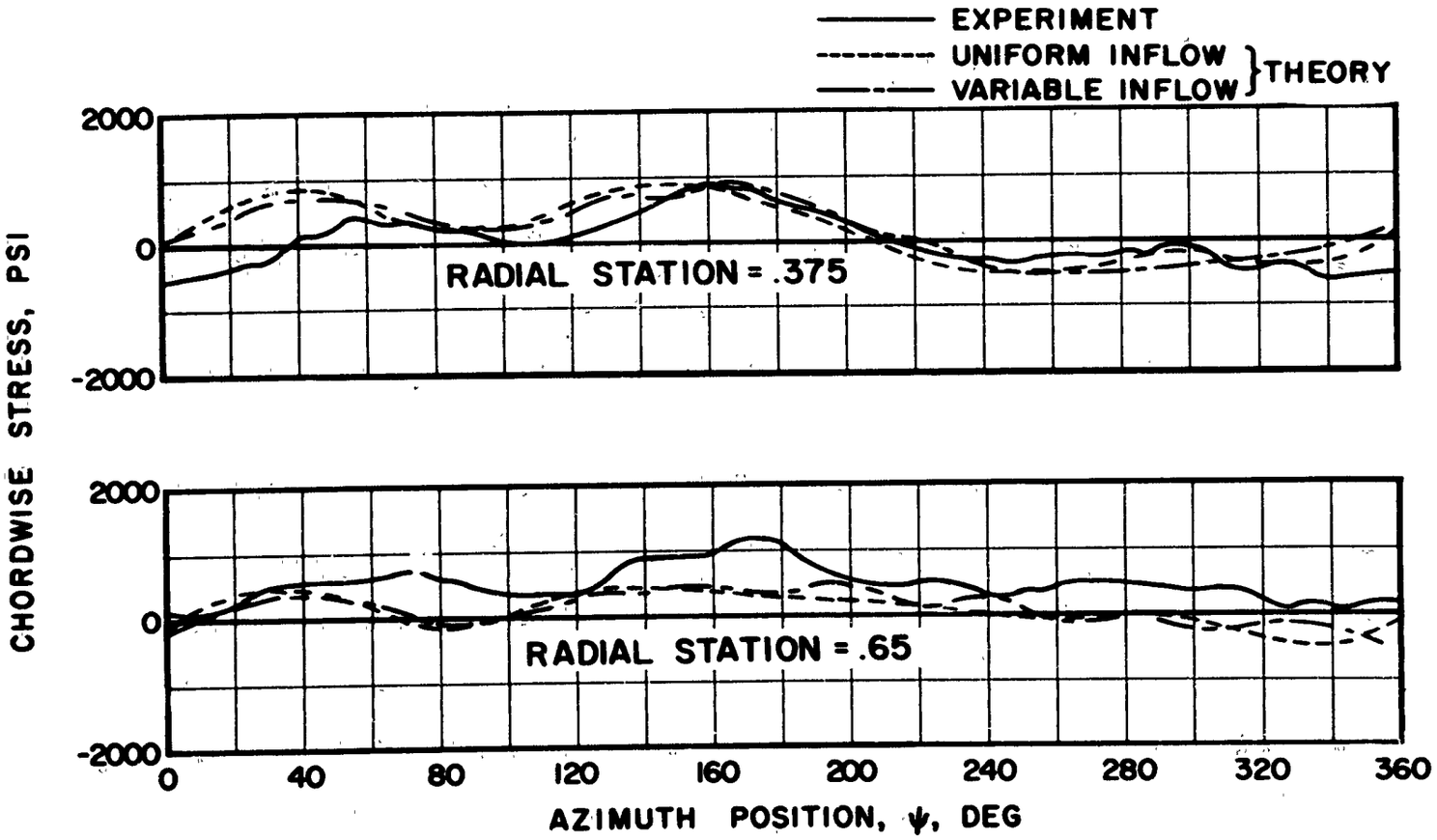

(b) CHORDWISE

Figure 25. Continued.

V = 110 KT α_s = -5° L = 8300 LB D = -750 LB

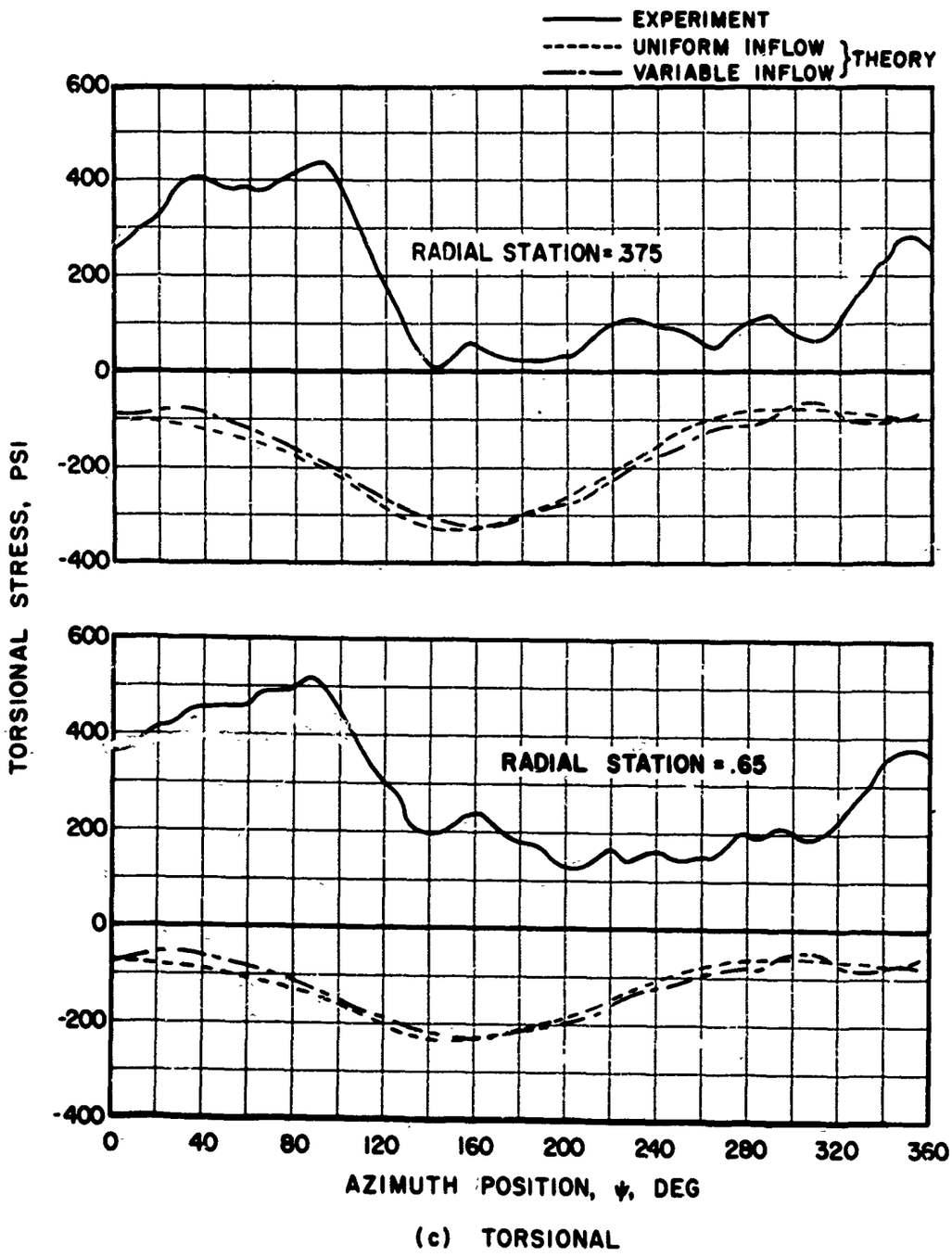

(c) TORSIONAL

Figure 25. Concluded.

V = 110 KT α_s = -5° L = 8300 LB D = -750 LB

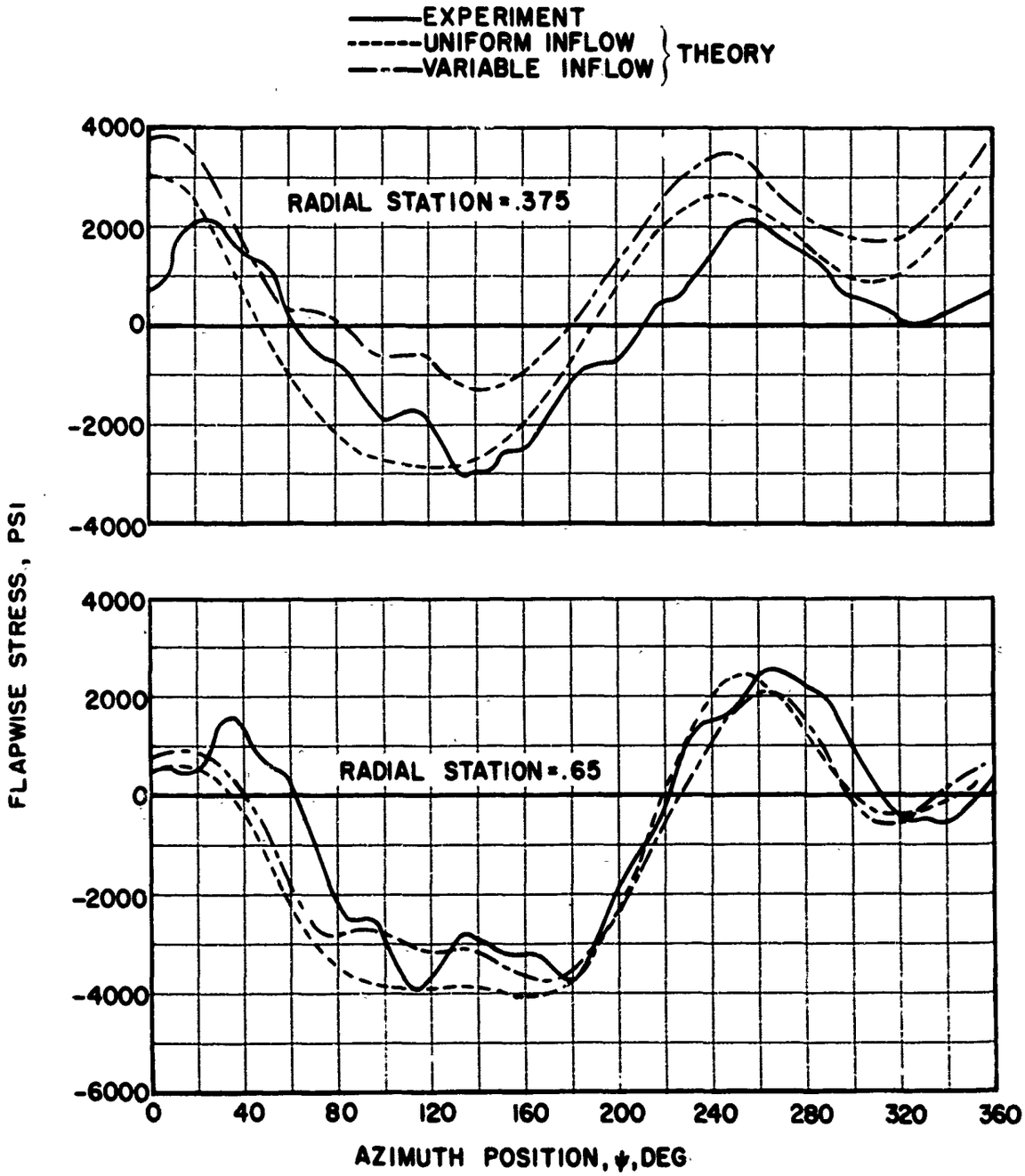

(a) FLAPWISE

Figure 26. Blade Stress Time Histories.

V = 150 KT α_s = -5° L = 8500 LB D = -650 LB

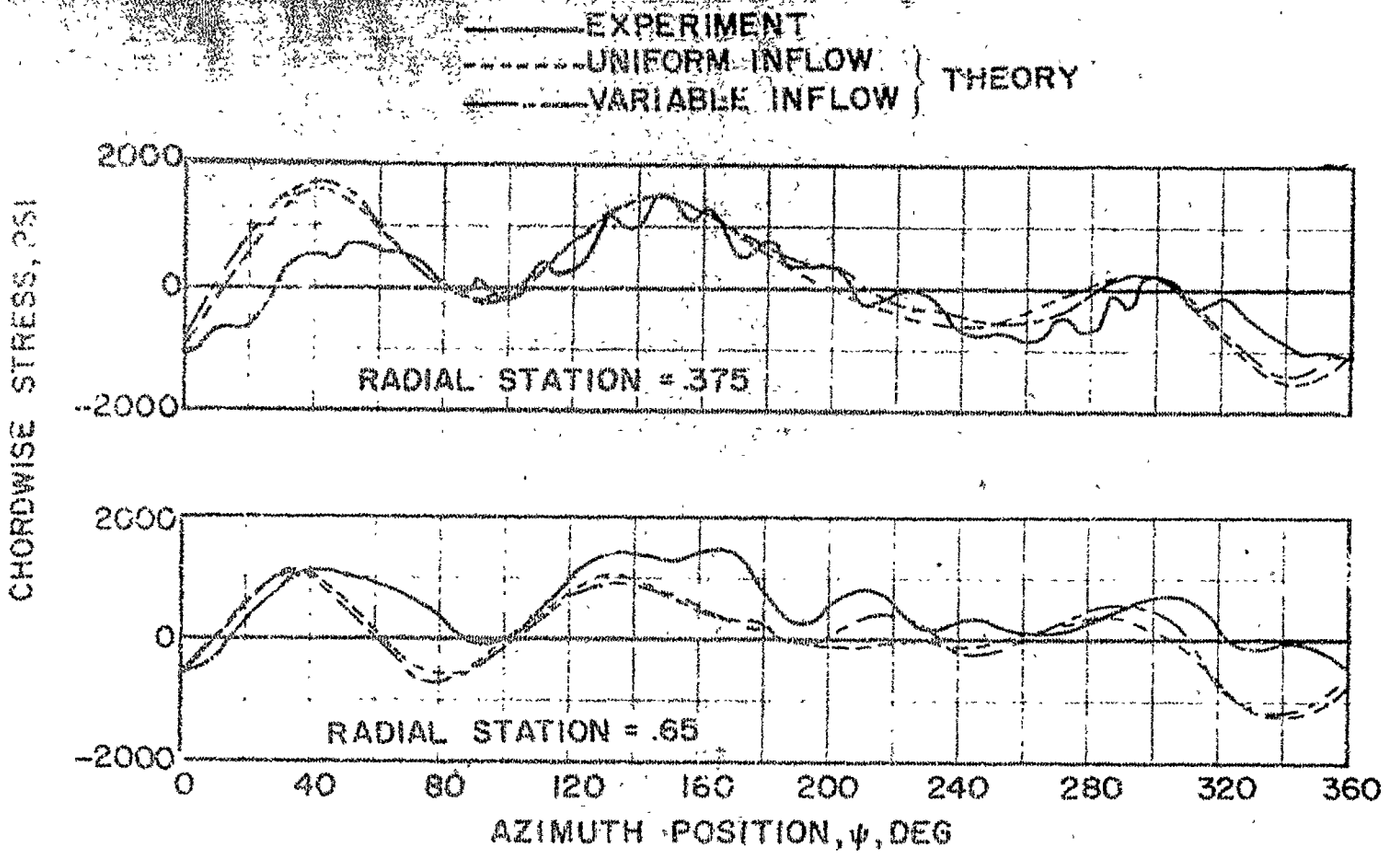

(b) CHORDWISE

Figure 26. Continued.

V = 150 KT α_s = -5° L = 8500 LB D = -650 LB

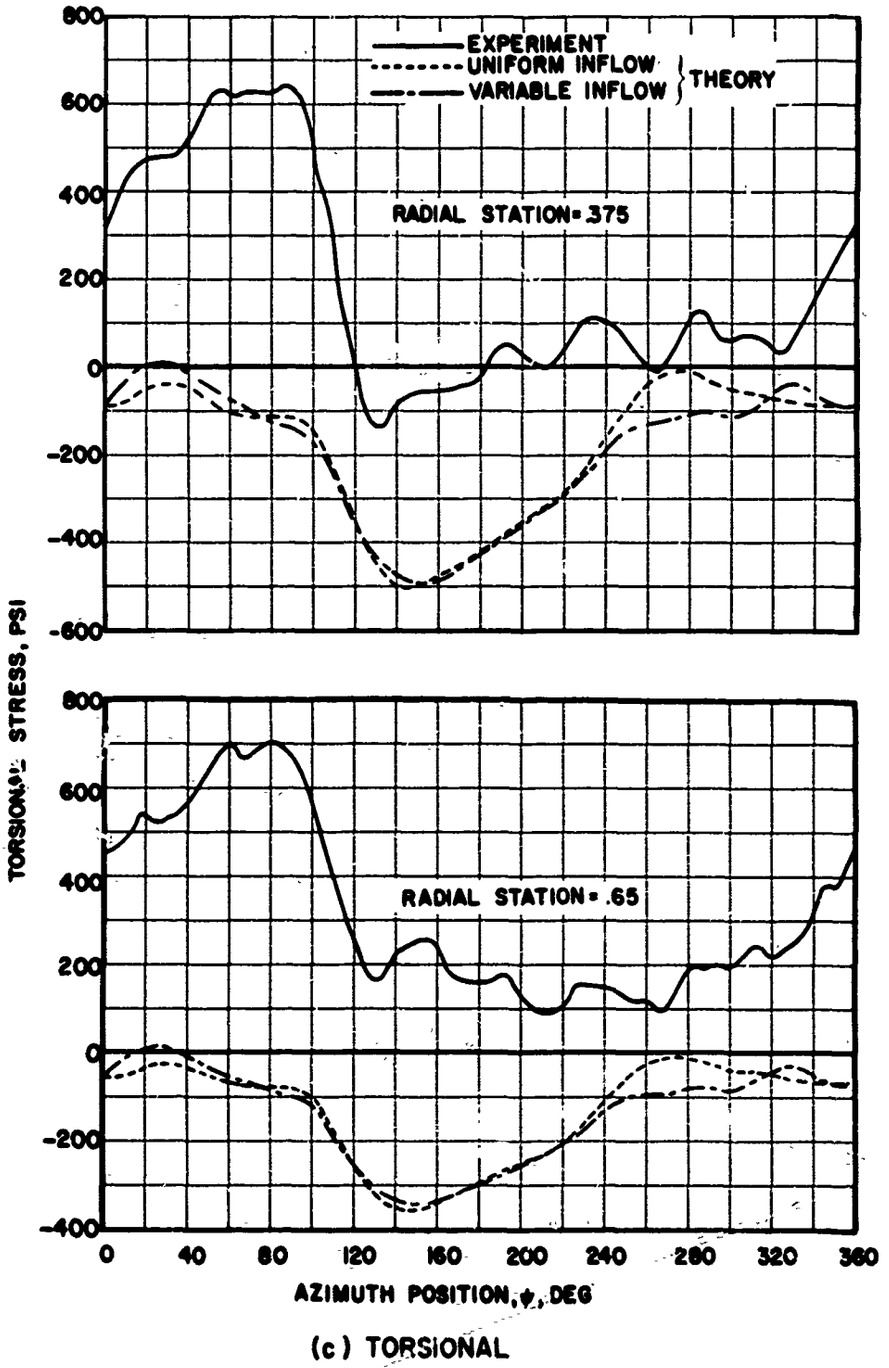

(c) TORSIONAL

Figure 26. Concluded.

V = 150 KT α_s = -5° L = 8500 LB D = -650 LB

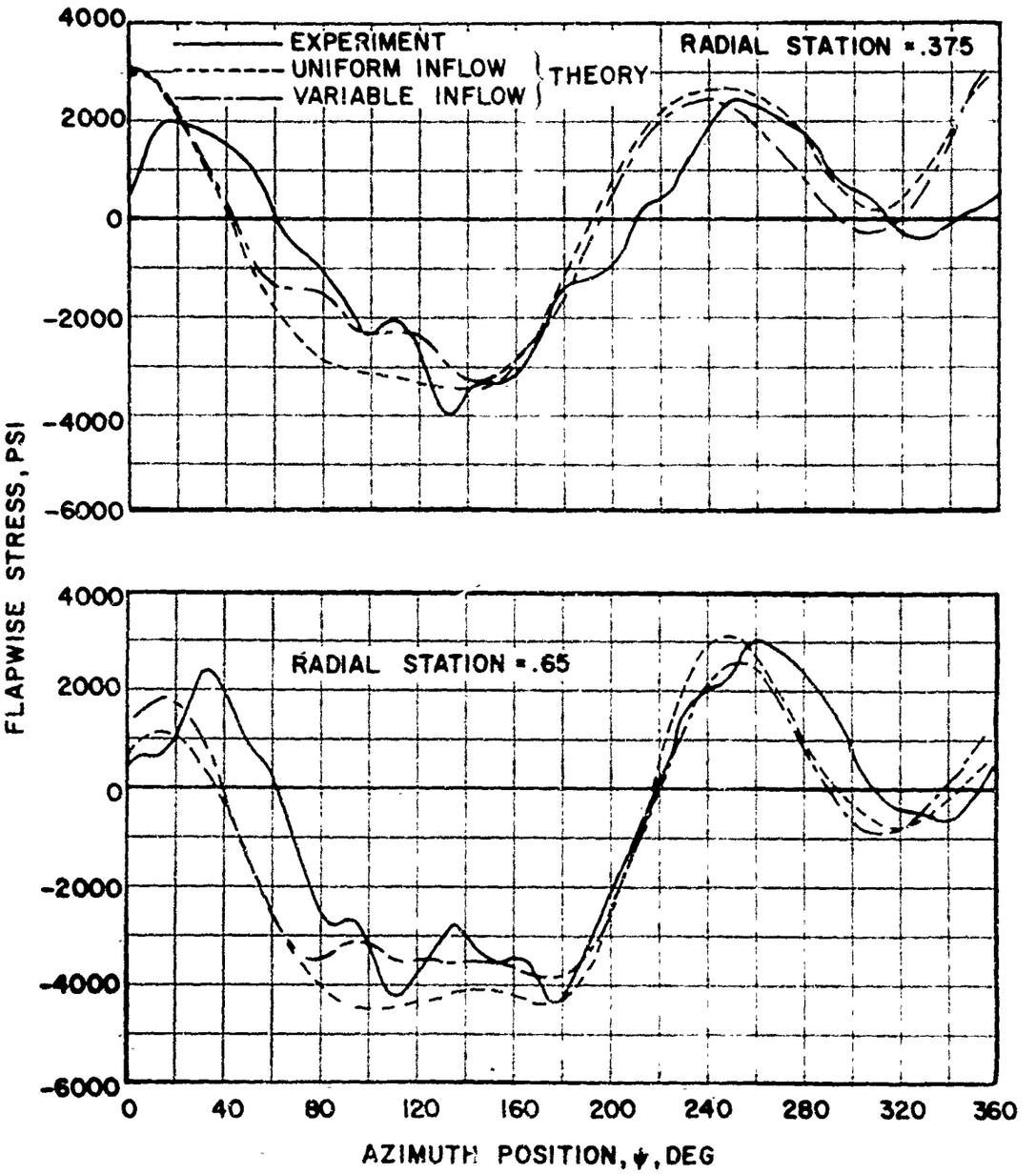

(a) FLAPWISE

Figure 27. Blade Stress Time Histories.

V = 175 KT α_s = -5° L = 7100 LB D = -250 LB

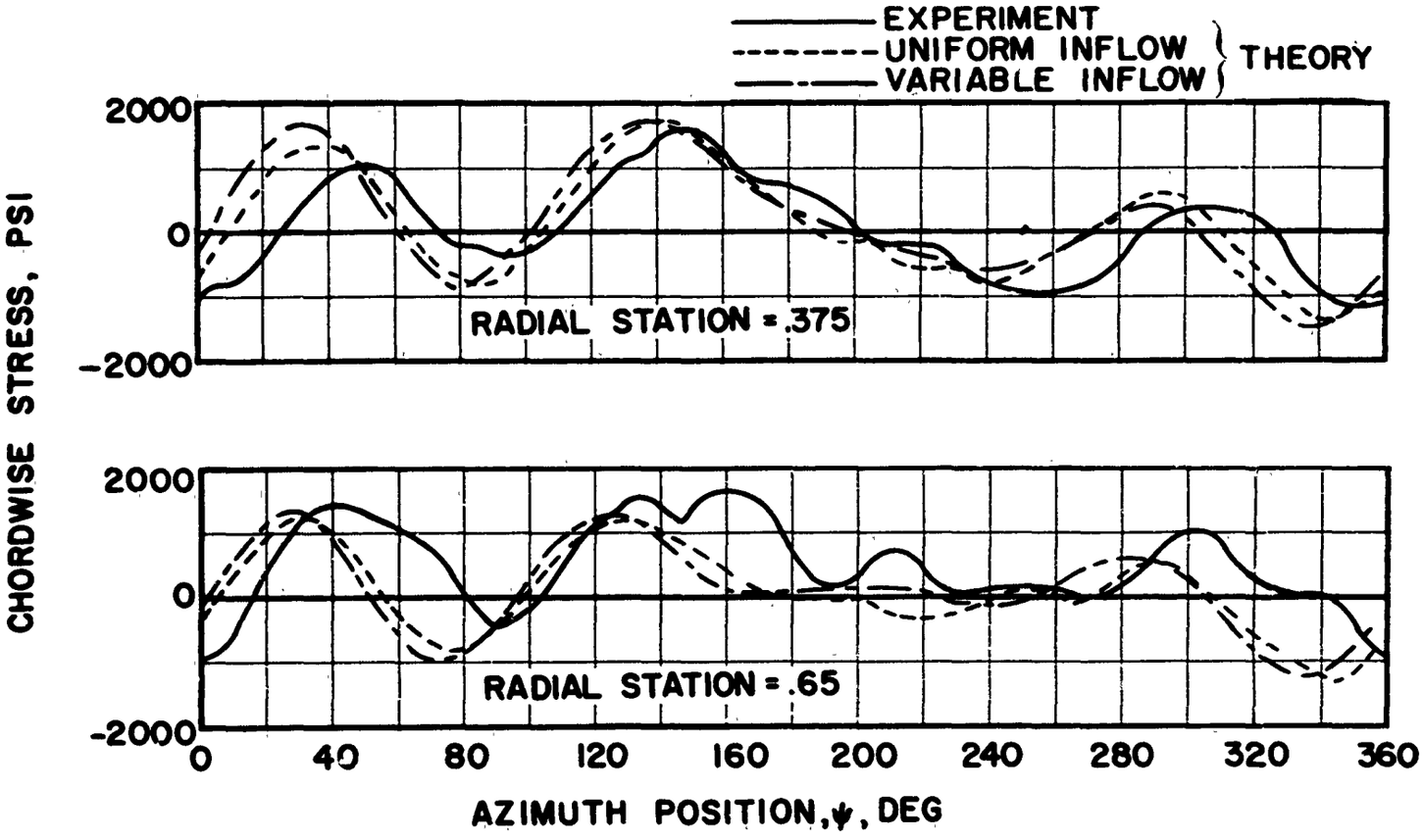

(b) CHORDWISE

Figure 27. Continued.

V = 175 KT α_s = -5° L = 7100 LB D = -250 LB

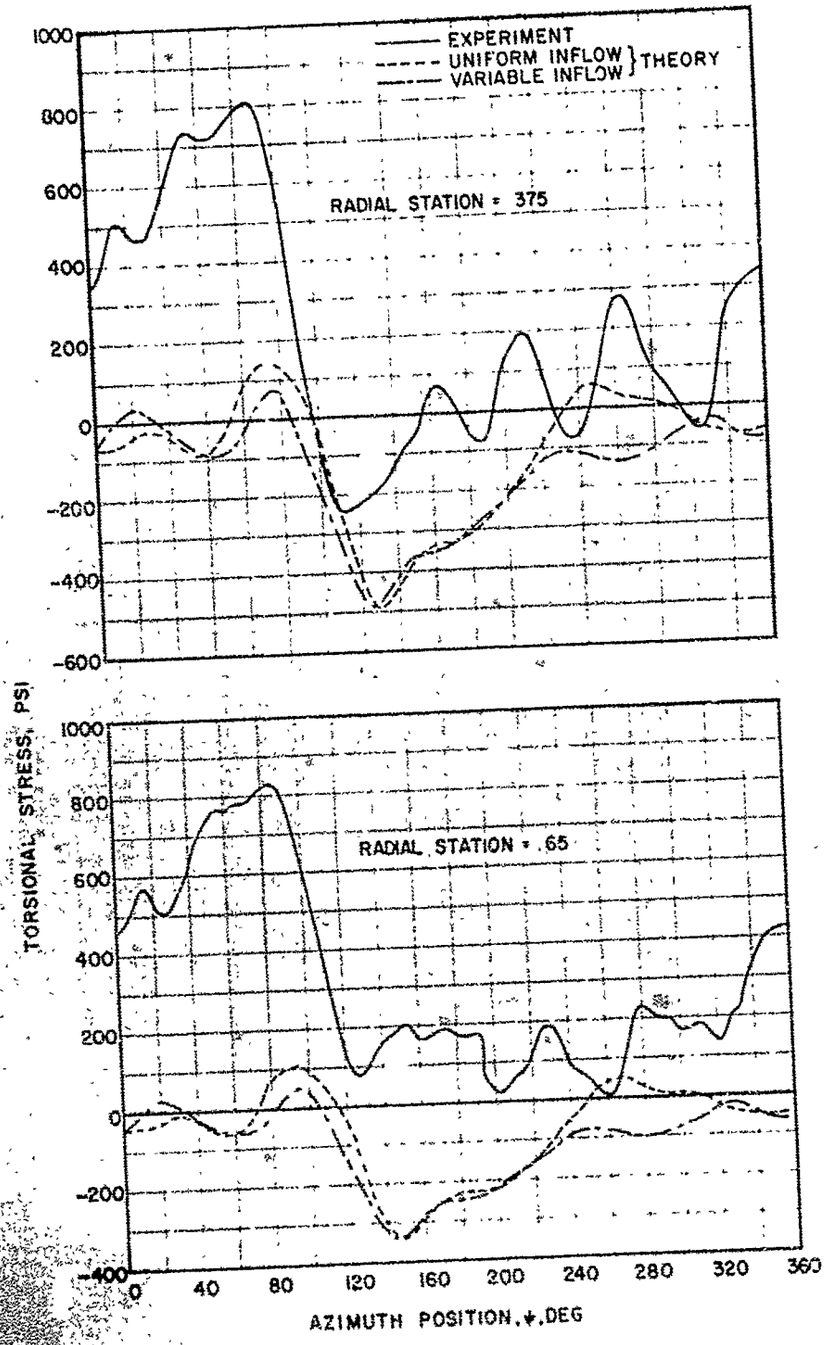

(c) TORSIONAL

Figure 27. Concluded.

V = 175 KT α_s = -5° L = 7100 LB D = -250 LB

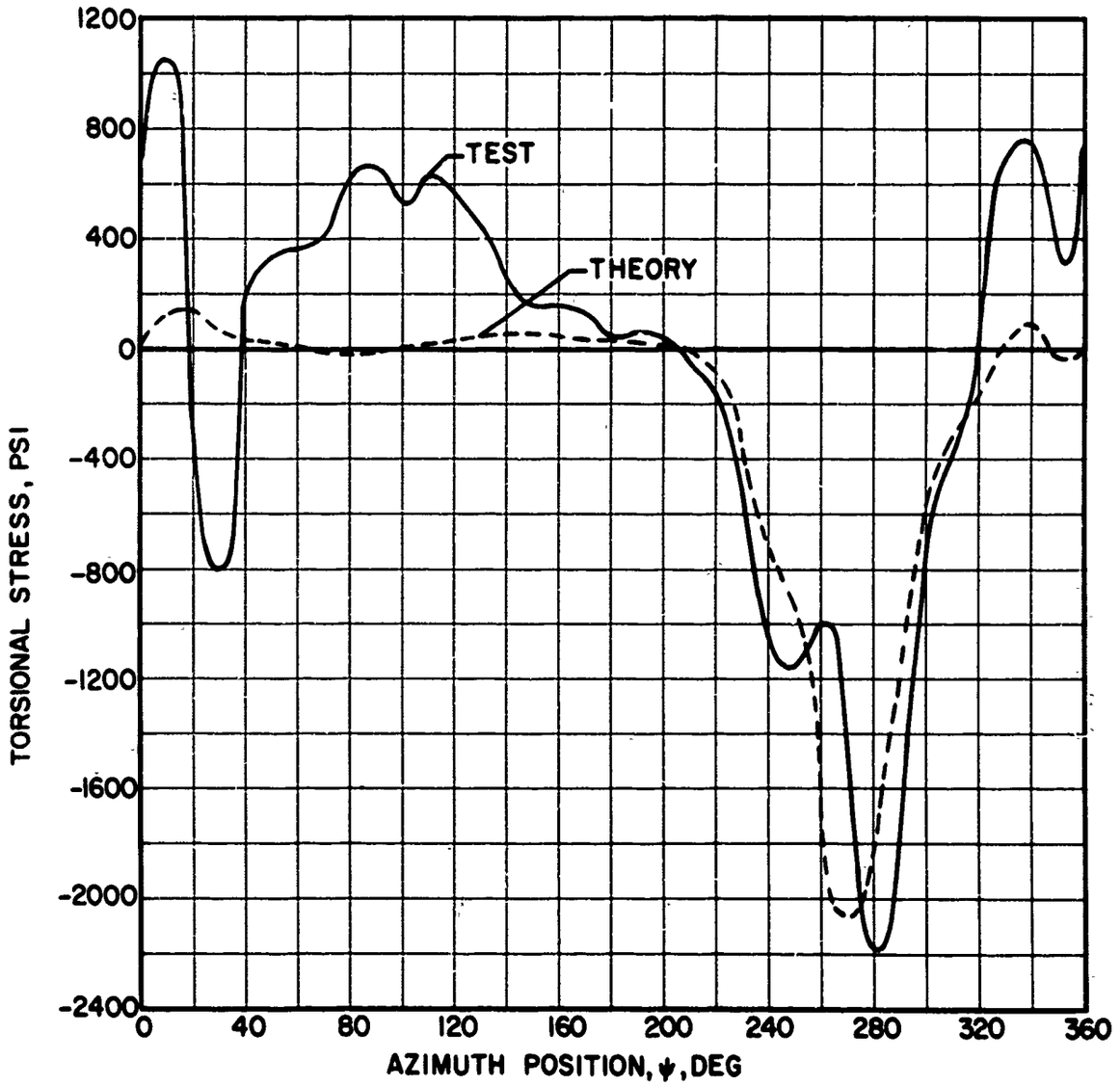

Figure 28. Azimuthal Variation of Torsional Stress (Reference 16).

$\mu = 1.0 \quad C_{L/\sigma} \approx 0 \quad \theta_{.75R} = -2°$

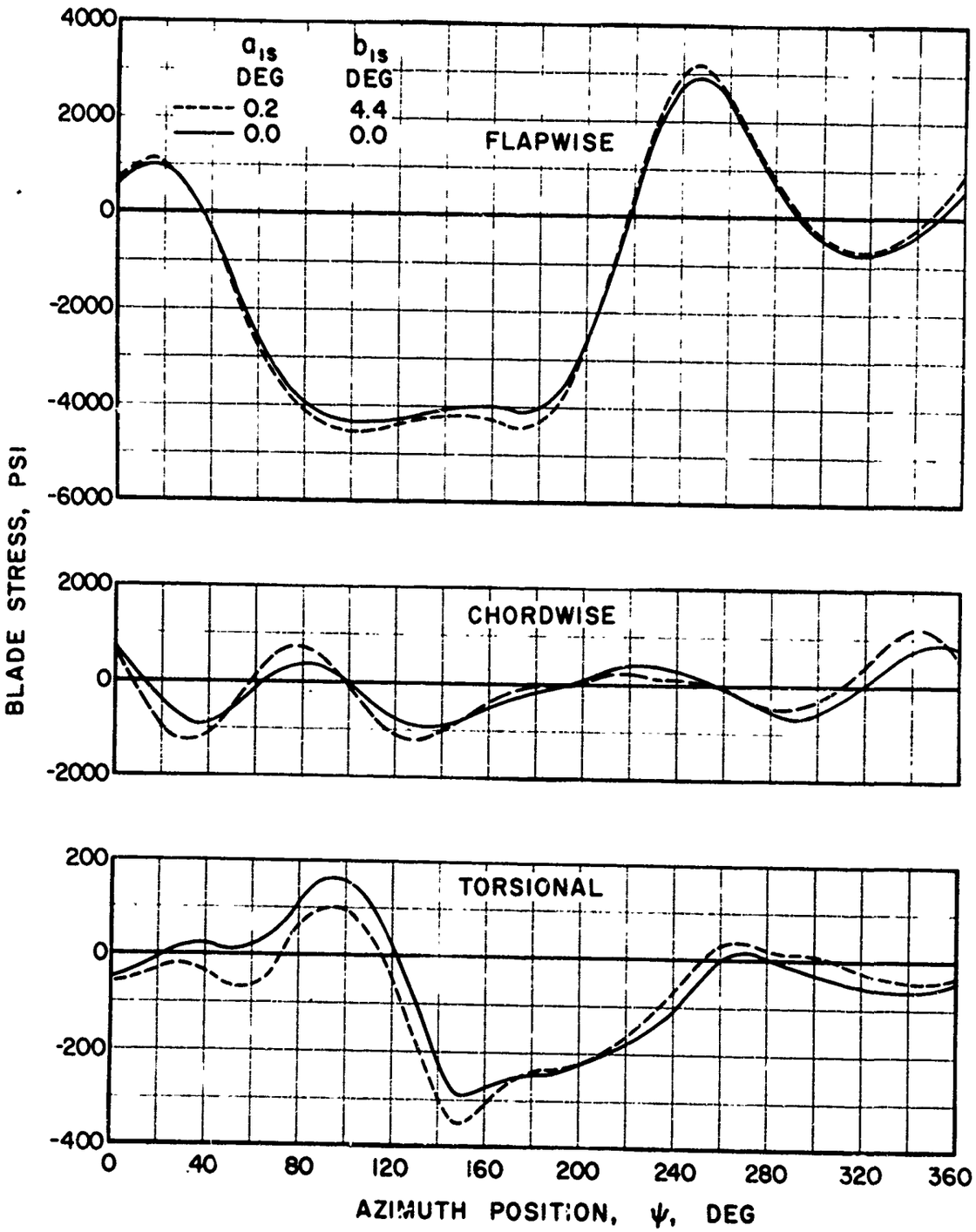

Figure 29. Theoretical Effect Of Blade Flapping On Blade Stress At 65% Radius.
Uniform Inflow
V = 175 KT α_s = -5° L = 7100 LB D = -250 LB

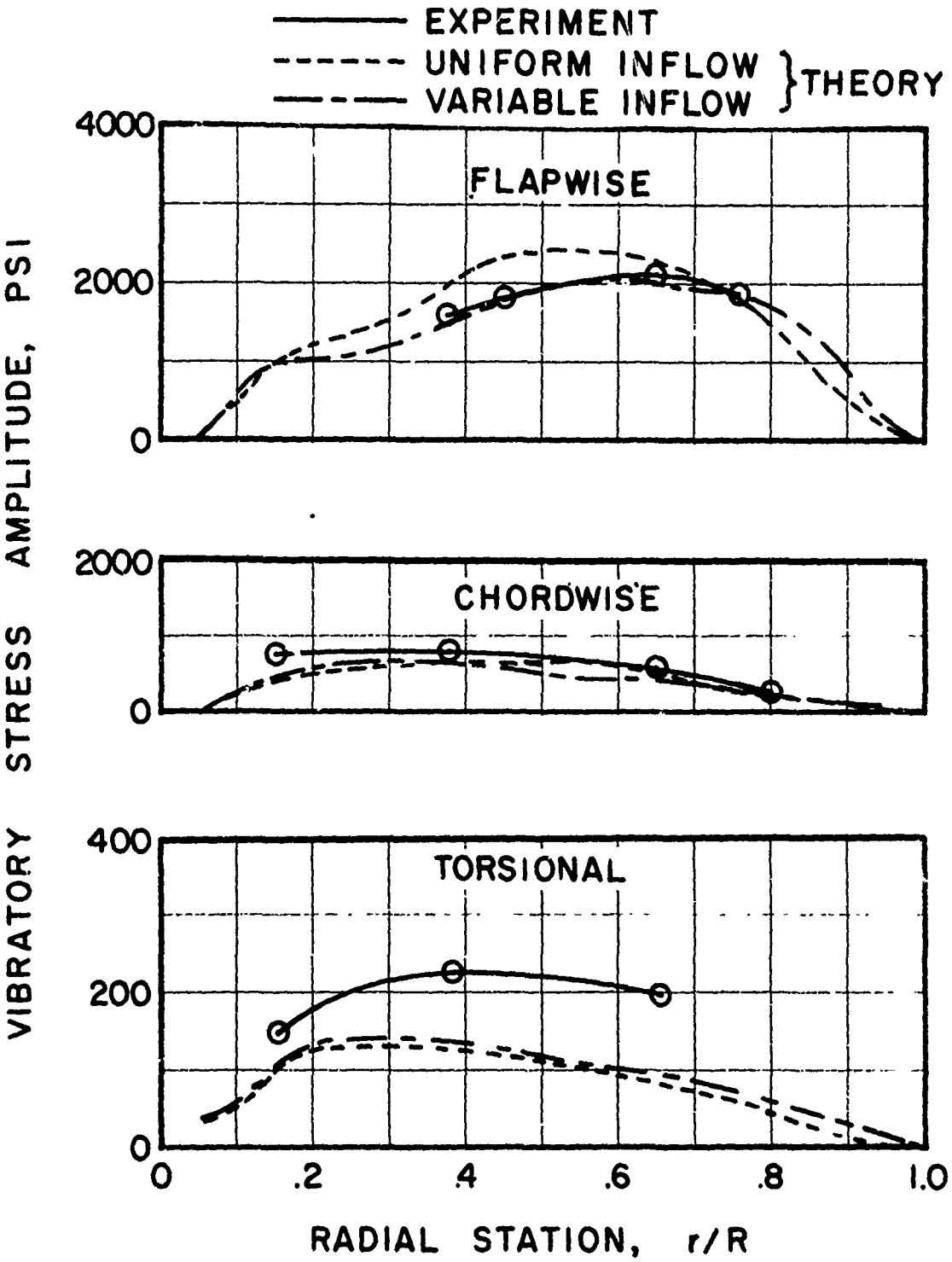

Figure 30. Vibratory Stress Envelope.

V = 110 KT α_s = -5° L = 8300 LB D = -750 LB

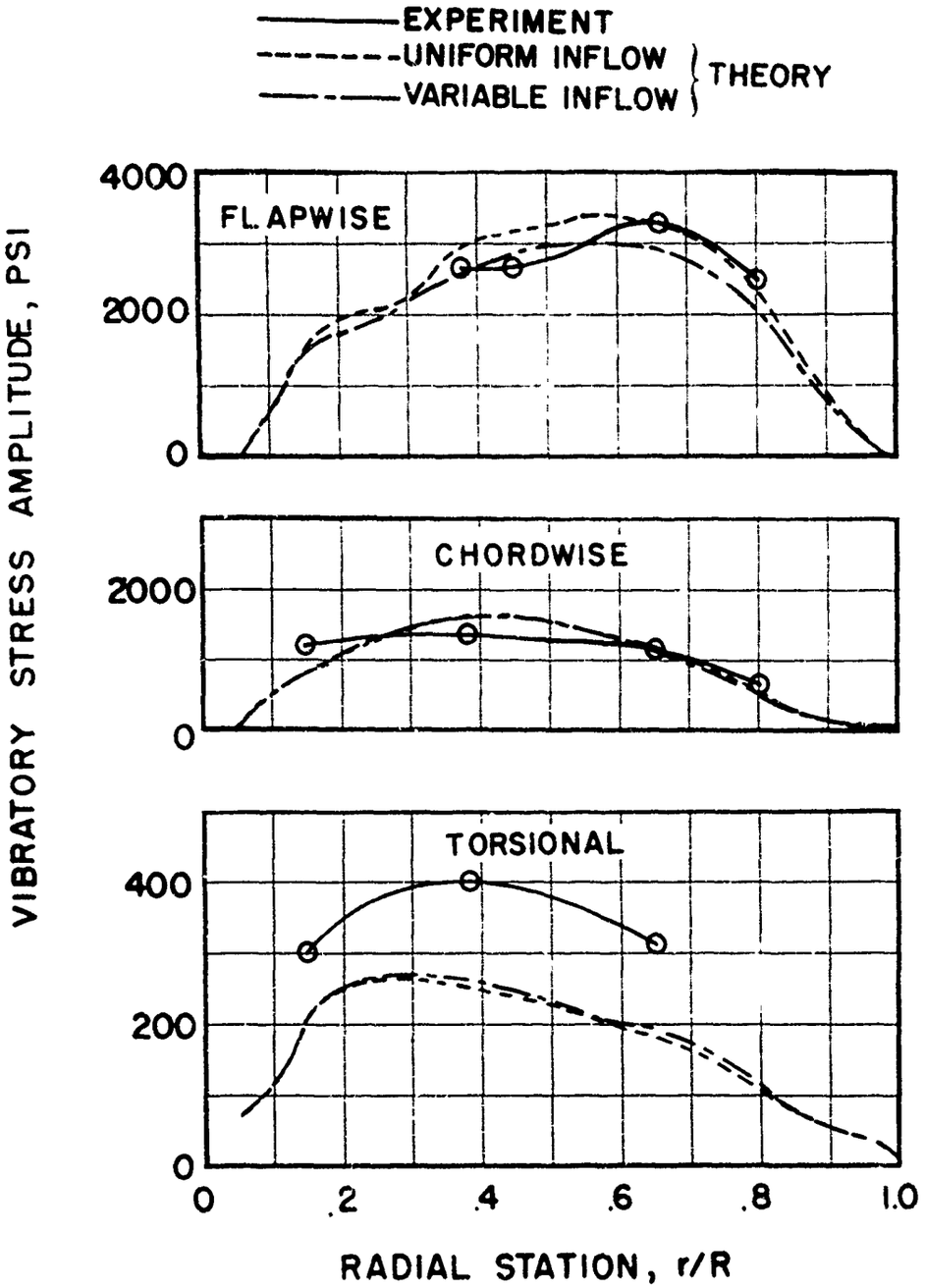

Figure 31. Vibratory Stress Envelope.

V = 150 KT α_s = -5° L = 8500 LB D = -650 LB

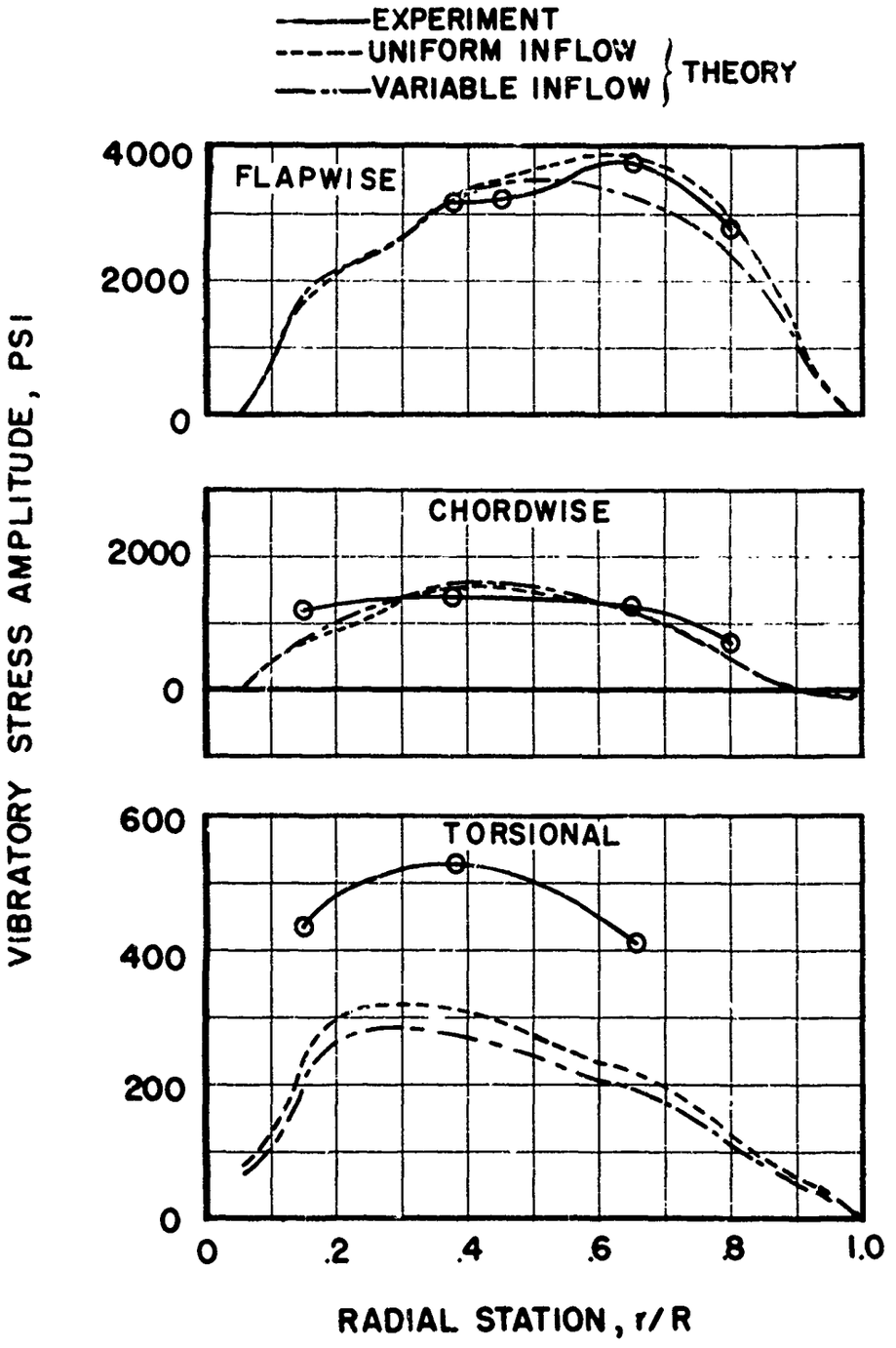

Figure 32. Vibratory Stress Envelope.

V = 175 KT α_s = -5° L = 7100 LB D = -250 LB

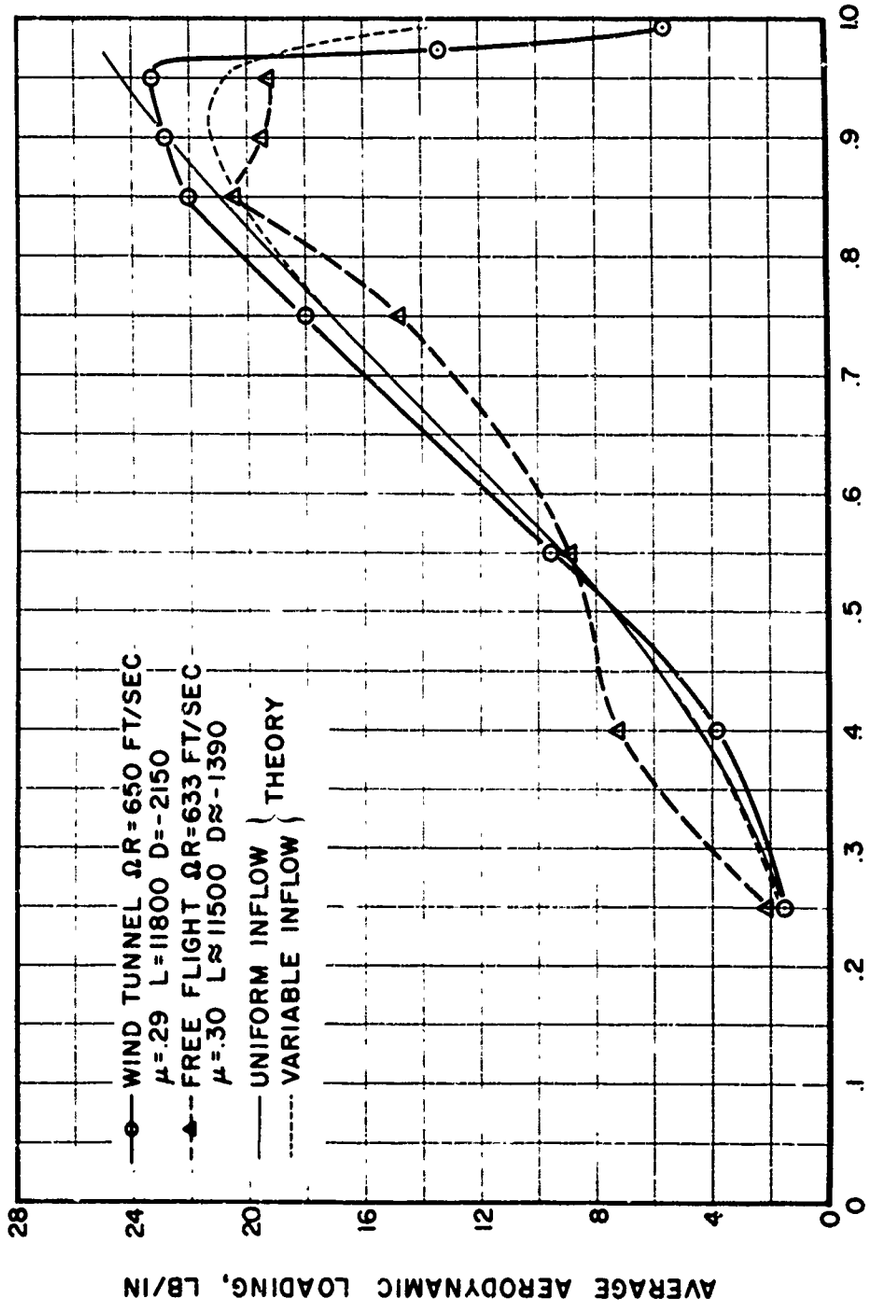

(a) Average Spanwise Aerodynamic Loading

Figure 33. Comparison Of Wind Tunnel And Free Flight Data.

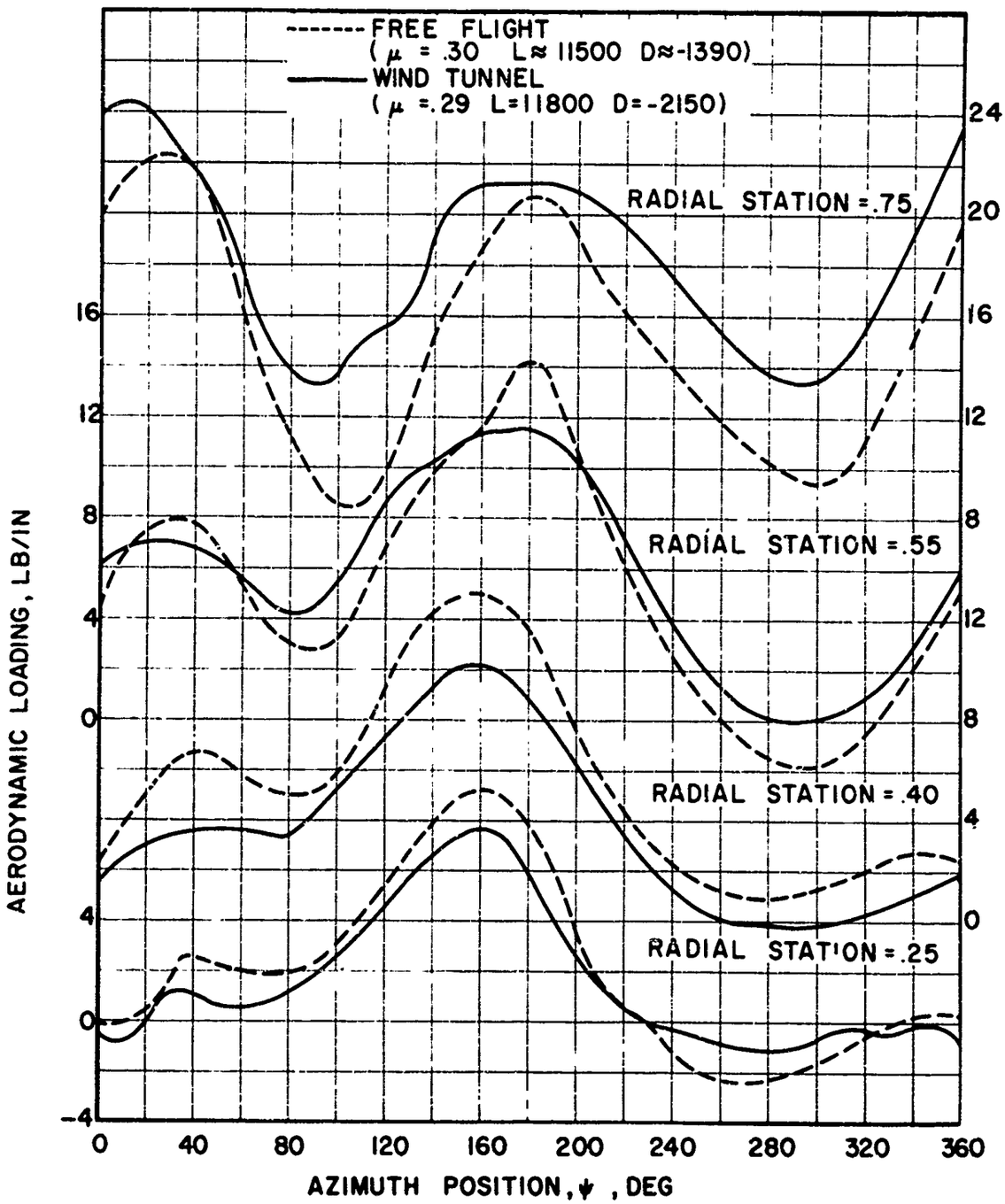

(b) Aerodynamic Loading

Figure 33. Continued.

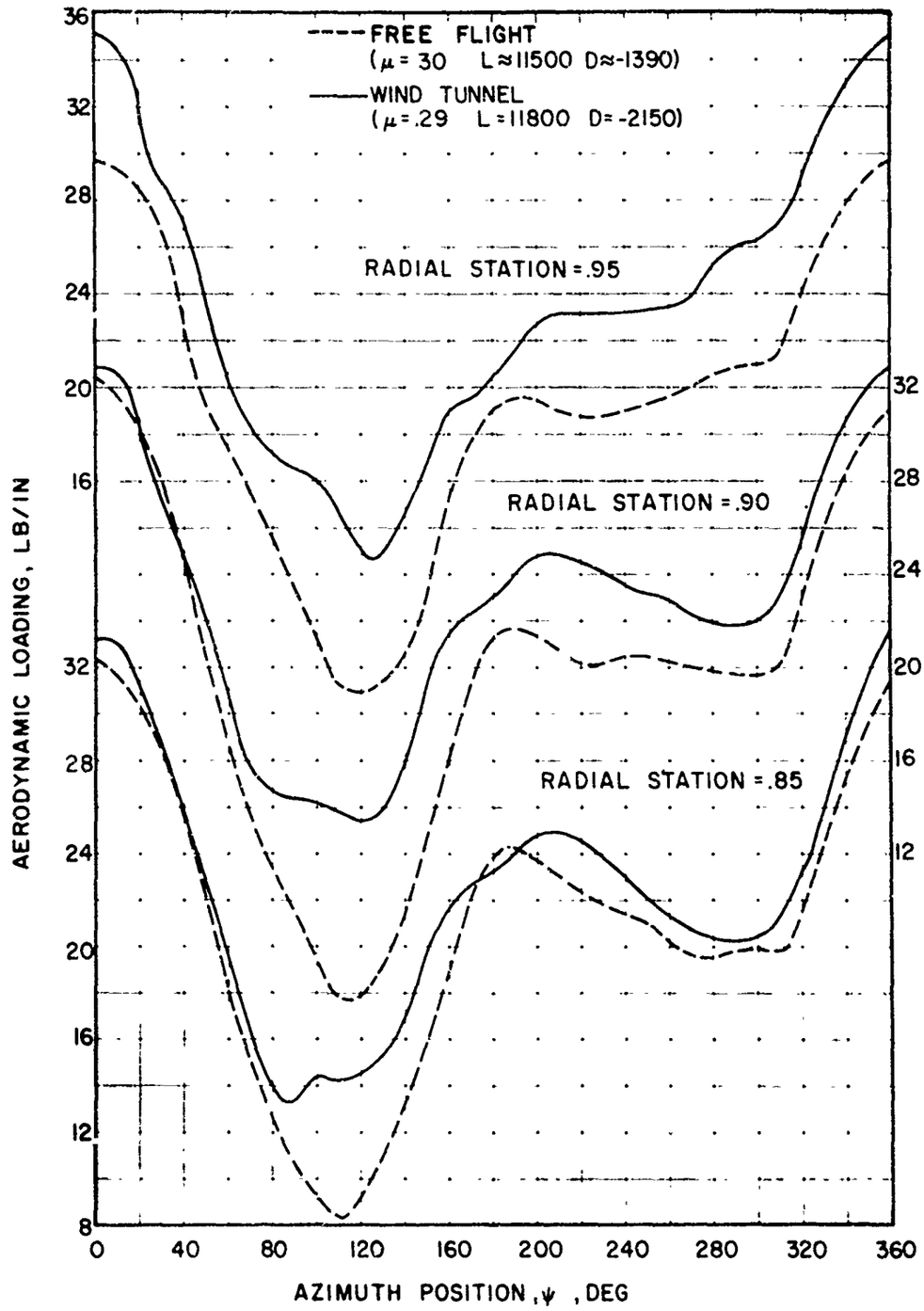

(b) Concluded

Figure 33. Continued.

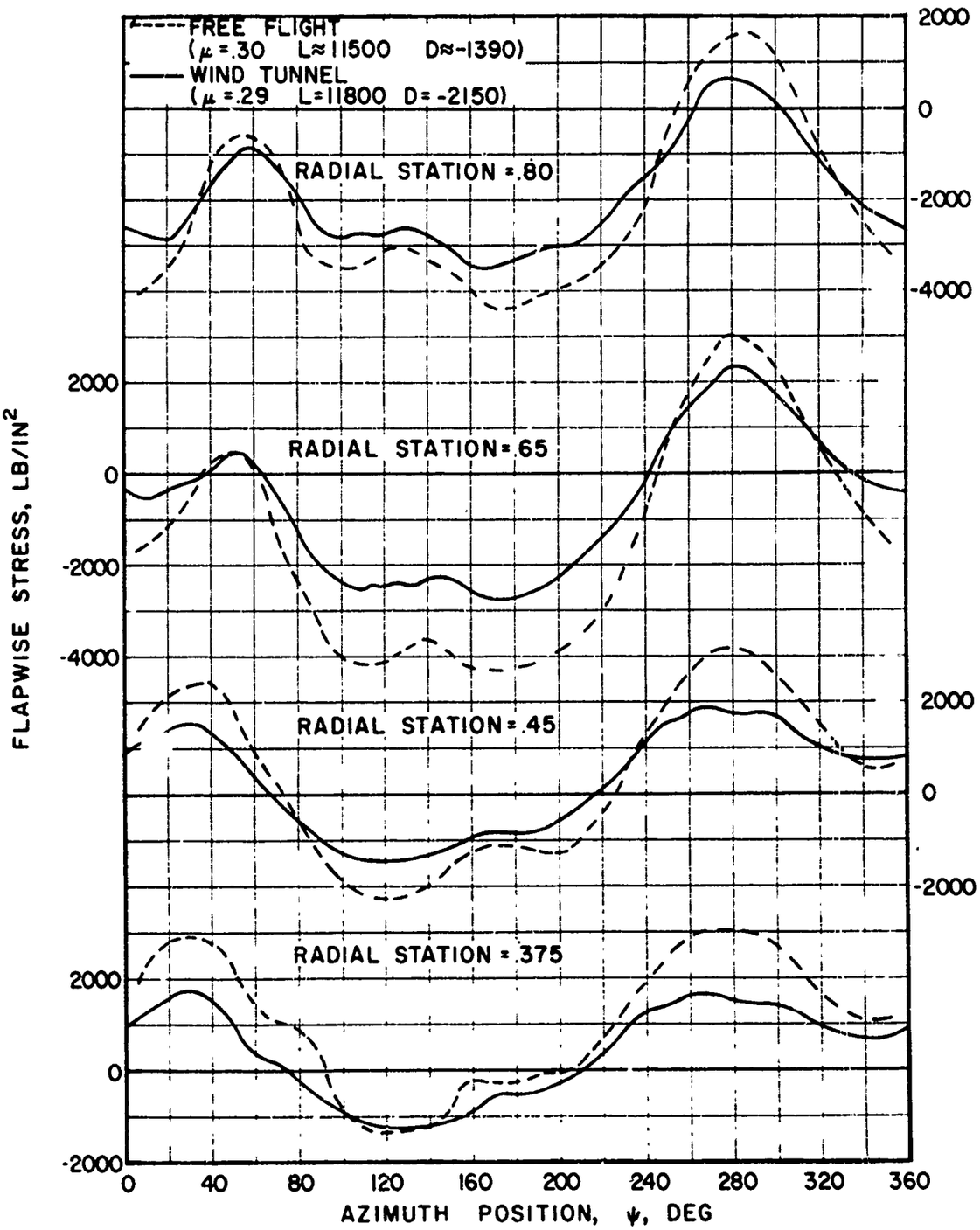

(c) Flapwise Stress

Figure 33. Continued.

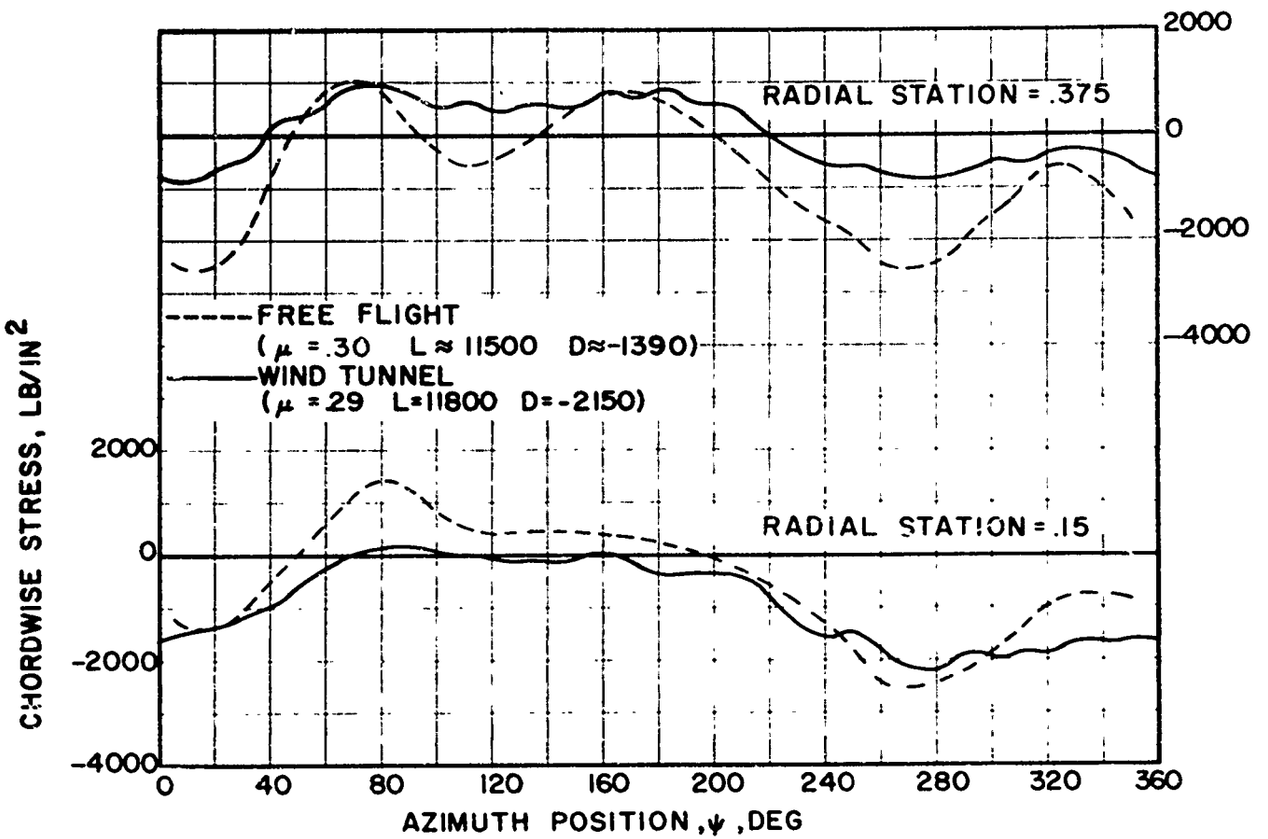

(d) Chordwise Stress

Figure 33. Continued.

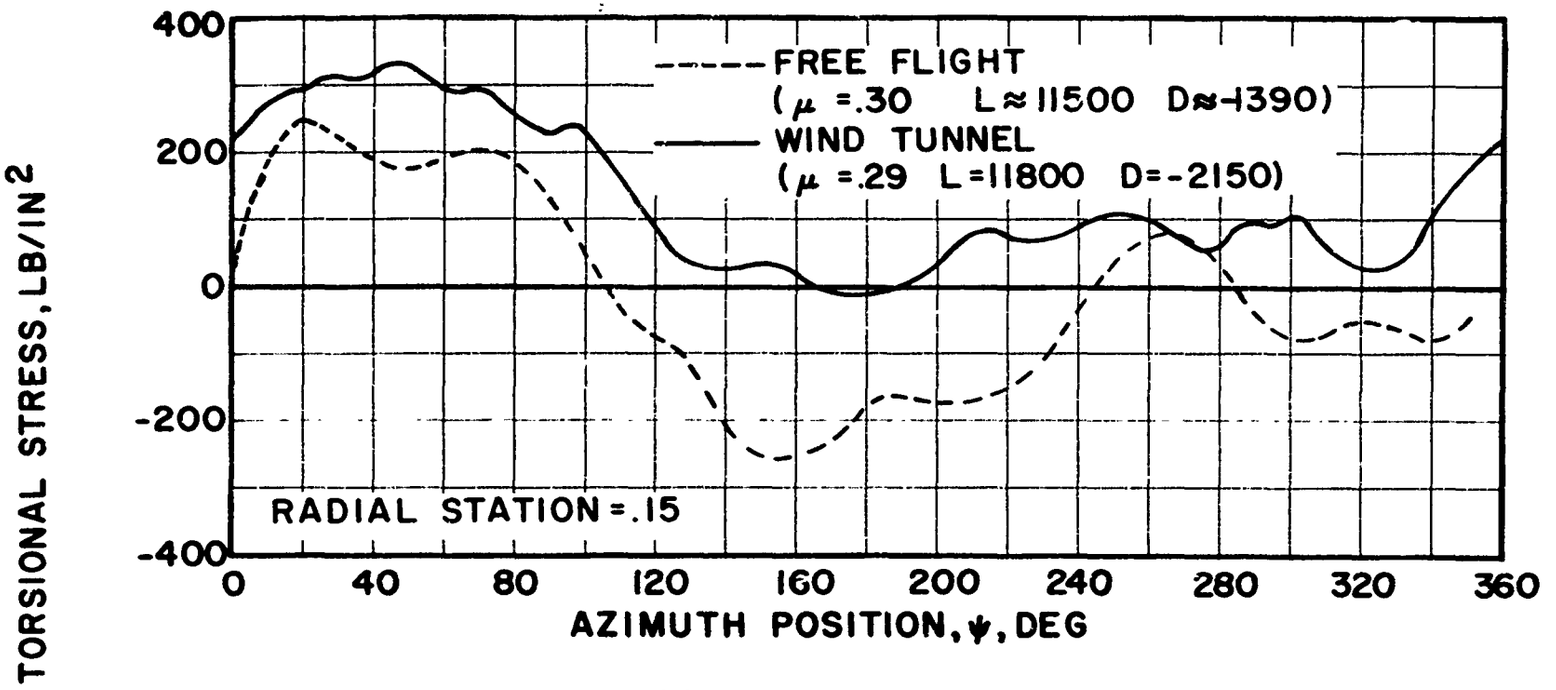

(e) Torsional Stress

Figure 33. Concluded.

TABLE I WIND TUNNEL OPERATING CONDITIONS

μ	ΩR FT/SEC	α_S DEG	L LB	D LB	HP	ρ SLUGS/FT^3	$M_{(1.0,90)}$	q LB/FT^2	$\theta_{.75R}$ DEG	A_{1S} DEG	B_{1S} DEG	a_{1S} DEG	b_{1S} DEG	E_0 DEG	E_1 DEG	F_1 DEG
.45	650	-5	7084	-251	703	.002249	.83	95.6	8.6	33	91	0.2	4.4	6.6	0.3	-0.1
.45	650	0	7129	415	293	.002216	.83	94.7	5.0	39	64	1.0	3.7	3.4	0.2	0.0
.45	650	+5	7323	1173	-61	.002201	.83	940	1.3	32	32	1.8	2.3	0.3	0.1	0.1
.39	650	-5	8463	-629	750	002195	.79	728	8.7	29	95	-1.0	4.4	8.4	0.3	-0.1
.39	650	0	8428	240	326	.002192	.79	71.7	5.4	34	6.5	0.5	3.6	4.4	0.2	0.0
39	650	+5	8553	1083	-20	.002173	.79	70.5	2.7	39	44	1.1	3.6	1.0	0.2	0.1
.29	650	-5	8252	-762	579	.002226	.73	390	6.6	24	60	-0.7	3.5	5.9	0.2	0.0
.29	650	0	8212	31	303	.002227	.73	380	4.5	21	49	-0.5	2.8	3.7	0.2	0.0
.29	650	+5	8144	830	45	.002231	73	380	2.4	2.4	37	0.0	2.8	1.5	0.1	0.1
.29	650	-9	11800	-2144	1187	.002221	.73	39.2	10.4	.7	8.9	-1.4	3.6	10.9	0.5	0.0

TABLE II HARMONICS OF FLAPPING, DEG

	V = 110 KT α_s = 0° L = 8200 LB D = 50 LB				V = 110 KT α_s = +5° L = 8100 LB D = 850 LB			
N	EXPERIMENTAL		UNIFORM INFLOW		EXPERIMENTAL		UNIFORM INFLOW	
	A(N)	B(N)	A(N)	B(N)	A(N)	B(N)	A(N)	B(N)
0	2.6	-	2.8	-	2.7	-	2.8	-
1	-0.5	2.8	0.0	0.0	0.0	2.8	0.0	0.0
2	0.0	0.4	0.3	0.2	-0.1	0.4	0.3	0.3
3	0.1	0.0	0.1	0.0	0.1	-0.1	0.1	0.0
4	0.0	0.0	0.0	0.0	0.1	0.0	0.0	0.0

	V = 150 KT α_s = 0° L = 8400 LB D = 250 LB				V = 150 KT α_s = +5° L = 8600 LB D = 1100 LB			
	EXPERIMENTAL		UNIFORM INFLOW		EXPERIMENTAL		UNIFORM INFLOW	
	A(N)	B(N)	A(N)	B(N)	A(N)	B(N)	A(N)	B(N)
0	3.1	-	2.9	-	3.3	-	2.9	-
1	0.5	3.6	-0.1	0.0	1.1	3.6	0.0	0.0
2	0.2	0.8	0.6	0.5	0.2	0.9	0.5	0.5
3	0.0	0.0	0.3	0.0	0.1	-0.1	0.3	-0.1
4	0.1	0.0	0.1	0.0	0.1	0.0	0.1	0.0

	V = 175 KT α_s = 0° L = 7100 LB D = 400 LB				V = 175 KT α_s = +5° L = 7300 LB D = 1150 LB			
	EXPERIMENTAL		UNIFORM INFLOW		EXPERIMENTAL		UNIFORM INFLOW	
	A(N)	B(N)	A(N)	B(N)	A(N)	B(N)	A(N)	B(N)
0	2.8	-	2.4	-	2.8	-	2.5	-
1	1.0	3.7	-0.1	0.0	1.8	2.3	0.0	0.0
2	0.2	1.1	0.5	0.7	0.2	1.2	0.4	0.8
3	0.1	0.0	0.4	0.0	0.1	-0.2	0.4	-0.2
4	0.2	0.0	0.1	0.1	0.2	0.0	0.2	0.0

V = 110 KT α_s = -9° L = 11,800 LB D = -2150 LB

	EXPERIMENTAL		UNIFORM INFLOW	
	A(N)	B(N)	A(N)	B(N)
0	4.1	-	4.2	-
1	-1.4	3.6	0.0	0.0
2	0.3	0.3	0.5	0.4
3	0.0	0.2	0.1	0.1
4	0.0	0.0	0.0	0.0

NOTE: Harmonics above 4th harmonic are less than 1/10 of a degree.
First harmonic flapping for theoretical calculations set equal to zero for these operating conditions.

TABLE II CONTINUED

V = 175 KT α_S = -5° L = 7100 LB D = -250 LB

N	EXPERIMENTAL A(N)	EXPERIMENTAL B(N)	UNIFORM INFLOW A(N)	UNIFORM INFLOW B(N)	VARIABLE INFLOW A(N)	VARIABLE INFLOW B(N)
0	2.7	-	2.4	-	2.4	-
1	0.2	4.4	0.2	4.4	0.3	4.4
2	0.4	0.9	0.8	0.6	0.7	0.6
3	0.0	0.2	0.4	0.1	0.4	0.0
4	0.1	0.1	0.1	0.1	0.1	0.1

V = 150 KT α_S = -5° L = 8500 LB D = -650 LB

N	EXPERIMENTAL A(N)	EXPERIMENTAL B(N)	UNIFORM INFLOW A(N)	UNIFORM INFLOW B(N)	VARIABLE INFLOW A(N)	VARIABLE INFLOW B(N)
0	2.9	-	2.9	-	2.9	-
1	-1.0	4.4	-1.1	4.4	-1.0	4.4
2	0.4	0.7	0.8	0.5	0.6	0.4
3	0.0	0.2	0.3	0.2	0.3	0.1
4	0.1	0.1	0.1	0.1	0.1	0.0

V = 110 KT α_S = -5° L = 8300 LB D = -750 LB

N	EXPERIMENTAL A(N)	EXPERIMENTAL B(N)	UNIFORM INFLOW A(N)	UNIFORM INFLOW B(N)	VARIABLE INFLOW A(N)	VARIABLE INFLOW B(N)
0	2.6	-	2.8	-	2.8	-
1	-0.7	3.5	-0.8	3.5	-0.7	3.5
2	0.1	0.3	0.4	0.3	0.3	0.1
3	0.1	0.1	0.1	0.1	0.1	0.0
4	0.0	0.0	0.0	0.0	0.0	0.0

NOTE: Harmonic above 4th harmonic are less than 1/10 of a degree. First harmonic flapping for theoretical calculations set equal to experimental values for these operating conditions.

TABLE III TIME HISTORIES OF AERODYNAMIC LOADING, LB/IN
V = 110 KT α_s = 0° L = 8200 LB D = 50 LB

(a) EXPERIMENTAL

	Blade Radial Station								
ψ	.25R	.40R	.55R	.75R	.85R	.90R	.95R	.97R	.99R
0	1.0	1.8	7.4	14.2	16.4	14.9	10.6	7.1	-1.3
5	-0.2	3.2	5.9	13.6	15.0	12.7	8.0	5.8	-2.1
10	-0.6	2.4	6.7	12.5	14.1	12.1	6.2	4.5	-1.7
15	0.3	2.1	7.1	11.4	13.1	11.4	5.5	4.0	-1.4
20	0.9	2.4	6.9	11.0	12.4	10.7	5.0	3.4	-1.2
25	2.1	2.8	7.1	10.9	12.0	9.8	4.2	3.0	-1.5
30	2.7	3.0	7.1	10.8	11.2	9.2	4.2	3.1	-2.1
35	1.9	3.3	7.5	10.7	10.8	9.4	4.2	3.4	-1.8
40	1.8	3.7	8.0	10.7	10.9	10.0	4.3	3.6	-1.6
45	1.9	4.2	8.3	10.8	10.8	10.0	4.6	3.7	-1.6
50	2.3	5.0	8.4	10.6	10.6	9.8	4.3	3.6	-1.2
55	2.5	5.4	8.5	10.5	10.6	10.0	4.7	4.0	-0.9
60	2.8	5.6	8.5	11.3	11.4	9.9	5.3	4.4	-1.3
65	3.1	6.1	8.9	11.3	10.5	9.6	6.4	5.3	-1.2
70	3.6	6.5	9.6	11.4	10.8	10.2	6.5	5.7	-0.8
75	3.9	6.9	10.1	11.8	10.6	10.6	6.6	5.3	-1.0
80	4.5	7.3	10.5	12.2	11.0	11.5	6.1	4.7	-1.6
85	4.7	7.8	10.9	12.5	12.5	11.2	5.3	3.7	-1.7
90	5.3	8.2	11.2	12.7	12.9	9.9	3.5	1.8	-2.3
95	5.7	8.6	11.7	12.9	11.6	7.6	0.9	0.3	-2.6
100	6.1	8.8	11.7	12.9	9.3	4.7	-1.8	-0.9	-2.9
105	6.5	9.0	11.5	12.9	6.4	3.0	-4.2	-2.0	-3.4
110	6.9	9.5	11.3	11.8	3.4	2.1	-6.0	-3.0	-3.4
115	7.3	9.7	11.3	10.3	2.4	1.0	-6.7	-3.4	-4.2
120	7.6	9.9	11.2	8.7	2.3	1.0	-7.2	-3.5	-4.3
125	7.9	10.2	11.4	7.9	2.4	1.7	-6.7	-2.9	-4.2
130	8.2	10.5	11.8	7.9	2.7	2.5	-5.3	-2.0	-4.0
135	8.4	10.6	12.2	8.2	3.6	3.3	-5.2	-1.5	-3.4
140	8.4	10.7	12.6	8.5	4.5	4.4	-4.7	-0.9	-3.0
145	8.3	10.8	12.8	9.1	5.1	5.0	-2.7	0.2	-2.9
150	8.4	10.8	13.7	9.9	6.4	5.9	-3.0	0.8	-2.9
155	8.3	10.6	14.0	10.3	7.7	7.2	-2.2	1.3	-2.5
160	8.1	10.3	13.6	10.5	8.4	8.3	-1.1	2.1	-2.1
165	7.8	9.7	13.4	10.5	8.9	9.0	-0.8	2.3	-1.6
170	7.3	9.2	13.0	10.5	9.4	9.4	-0.4	2.7	-1.2
175	6.8	8.9	12.5	10.6	9.8	9.7	0.0	2.9	-1.5
180	6.1	8.5	12.3	10.8	10.2	10.0	0.2	3.1	-1.1
185	5.3	7.9	12.5	11.2	11.1	10.7	1.2	3.7	-0.9
190	4.4	7.3	12.6	11.3	11.7	11.5	1.7	4.1	-0.9
195	3.6	6.5	12.1	11.3	11.9	11.9	1.7	4.1	-0.6
200	2.9	5.8	11.4	11.5	12.3	12.5	2.5	4.6	0.3
205	2.2	5.2	10.8	11.7	13.2	13.3	3.8	5.4	0.7
210	1.6	4.4	10.2	11.9	13.8	13.4	4.8	5.9	0.6
215	1.2	3.8	9.6	12.1	14.0	13.7	4.5	5.9	0.5
220	0.9	3.2	9.0	12.0	14.2	14.1	4.4	6.0	0.7
225	0.4	2.6	8.5	11.7	14.1	14.3	4.4	6.2	1.1
230	0.2	2.1	8.0	11.4	13.9	14.0	4.9	6.4	1.3
235	0.0	1.7	7.4	11.0	13.5	13.4	5.5	6.6	1.2
240	-0.1	1.3	6.8	10.7	13.3	13.1	6.4	6.9	1.3
245	-0.2	1.1	6.0	10.3	13.2	13.0	7.7	7.3	1.3
250	-0.3	0.8	5.1	10.2	13.1	13.0	7.4	7.4	0.9
255	-0.4	0.7	4.2	10.2	13.2	13.1	7.0	7.5	0.7
260	-0.5	0.5	3.9	10.2	13.3	13.2	7.2	7.8	0.7
265	-0.4	0.3	3.7	10.4	13.5	13.2	8.9	8.3	0.5
270	-0.4	0.2	3.6	10.4	13.6	13.7	11.0	9.0	0.8
275	-0.4	0.3	3.4	9.4	14.1	14.1	12.2	9.3	1.3
280	-0.4	0.4	3.3	8.3	13.8	14.4	11.4	9.4	0.9
285	-0.4	0.4	3.2	8.3	12.3	13.6	10.8	9.6	0.6
290	-0.4	0.5	3.3	8.4	11.9	11.8	9.2	8.8	0.4
295	-0.3	0.6	3.5	8.5	12.2	11.6	8.1	7.5	-0.3
300	-0.2	0.7	3.7	8.8	12.3	12.0	9.3	8.0	-0.4
305	-0.1	0.7	3.9	9.2	13.0	12.5	10.1	8.4	-0.6
310	0.0	0.8	4.2	9.8	13.8	13.2	10.3	8.5	-0.7
315	0.1	1.2	4.5	11.1	15.5	14.4	10.2	8.6	-0.4
320	0.2	1.5	4.9	12.4	14.3	13.7	10.3	8.5	-0.7
325	0.2	1.8	5.2	11.0	14.8	14.7	11.4	9.0	-2.9
330	0.1	1.9	5.8	11.5	16.7	15.7	12.5	9.7	-1.0
335	0.1	1.6	6.5	12.3	18.1	17.3	13.8	10.3	-1.1
340	0.5	1.5	7.6	13.0	19.2	18.5	14.5	10.5	-0.2
345	0.8	1.3	9.1	13.7	19.9	19.6	14.9	10.4	-0.2
350	1.4	1.3	10.4	14.2	19.4	18.5	15.1	10.4	-0.8
355	1.8	1.1	9.2	14.7	18.1	16.9	13.3	9.0	-0.9
360	1.0	1.8	7.4	14.2	16.4	14.9	10.6	7.1	-1.3

TABLE III CONCLUDED

V = 110 KT a_s = 0° L = 8200 LB D = 50 LB

(b) THEORETICAL (UNIFORM INFLOW)

	Blade Radial Station								
ψ	.25R	.40R	.55R	.75R	.85R	.90R	.95R	.97R	.99R
0	1.3	4.4	7.7	12.5	14.7	15.4	15.8	15.9	0.0
5	1.6	4.7	8.0	12.6	14.5	15.0	15.2	15.2	0.0
10	1.9	5.0	8.2	12.5	14.1	15.6	14.6	14.4	0.0
15	2.3	5.3	8.4	12.4	13.8	14.?	13.9	13.6	0.0
20	2.6	5.6	8.5	12.2	13.3	13.4	13.1	12.6	0.0
25	2.9	5.9	8.6	11.9	12.7	12.7	12.2	11.7	0.0
30	3.2	6.1	8.6	11.5	12.1	11.8	11.2	10.7	0.0
35	3.5	6.3	8.6	11.2	11.4	10.9	10.2	9.5	0.0
40	3.9	6.5	8.6	10.7	10.6	10.0	9.0	8.?	0.0
45	4.2	6.7	8.7	10.3	9.8	8.9	7.7	6.7	0.0
50	4.5	7.0	8.8	9.9	8.9	7.8	6.3	5.0	0.0
55	4.9	7.2	8.9	9.4	8.1	6.7	4.9	3.4	0.0
60	5.2	7.5	9.0	9.0	7.2	5.5	3.4	1.6	0.0
65	5.6	7.9	9.2	8.7	6.4	4.3	1.9	-0.1	0.0
70	6.0	8.2	9.5	8.4	5.6	3.3	0.5	-1.7	0.0
75	6.4	8.6	9.8	8.2	5.0	2.3	-0.8	-3.2	0.0
80	6.7	9.0	10.1	8.1	4.4	1.4	-1.9	-4.5	0.0
85	7.1	9.5	10.5	8.1	4.0	0.7	-2.8	-5.6	0.0
90	7.5	9.9	10.9	8.1	3.7	0.2	-3.5	-6.4	0.0
95	7.8	10.3	11.2	8.1	3.5	-0.1	-4.0	-7.0	0.0
100	8.1	10.6	11.6	8.2	3.4	-0.3	-4.2	-7.2	0.0
105	8.3	11.0	11.9	8.4	3.5	-0.3	-4.2	-7.2	0.0
110	8.5	11.2	12.2	8.7	3.6	-0.1	-4.0	-6.9	0.0
115	8.6	11.5	12.5	8.9	3.9	0.2	-3.6	-6.5	0.0
120	8.6	11.6	12.7	9.2	4.3	0.7	-3.0	-5.8	0.0
125	8.6	11.8	12.9	9.6	4.8	1.3	-2.3	-5.0	0.0
130	8.5	11.8	13.1	10.0	5.3	2.0	-1.5	-4.1	0.0
135	8.3	11.7	13.2	10.3	5.8	2.7	-0.6	-3.0	0.0
140	8.1	11.6	13.2	10.7	6.5	3.5	0.4	-1.9	0.0
145	7.7	11.4	13.2	11.1	7.1	4.3	1.4	-0.8	0.0
150	7.3	11.2	13.1	11.4	7.8	5.1	2.4	0.4	0.0
155	6.8	10.8	13.0	11.7	8.4	5.9	3.4	1.5	0.0
160	6.3	10.4	12.8	12.0	9.0	6.7	4.4	2.7	0.0
165	5.8	9.9	12.6	12.3	9.6	7.5	5.3	3.8	0.0
170	5.2	9.4	12.3	12.5	10.1	8.2	6.3	4.8	0.0
175	4.5	8.8	11.9	12.6	10.6	8.9	7.2	5.9	0.0
180	3.9	8.2	11.5	12.6	11.0	9.6	8.0	6.9	0.0
185	3.3	7.5	11.0	12.6	11.4	10.2	8.8	7.8	0.0
190	2.6	6.8	10.4	12.6	11.7	10.7	9.5	8.6	0.0
195	2.1	6.2	9.9	12.5	12.0	11.2	10.2	9.4	0.0
200	1.6	5.5	9.2	12.3	12.2	11.6	10.8	10.1	0.0
205	1.2	4.8	8.6	12.2	12.3	11.9	11.3	10.8	0.0
210	0.9	4.2	8.0	11.9	12.3	12.2	11.8	11.4	0.0
215	0.6	3.6	7.3	11.6	12.3	12.4	12.2	11.9	0.0
220	0.4	3.0	6.7	11.3	12.3	12.5	12.5	12.3	0.0
225	0.2	2.5	6.1	10.9	12.3	12.6	12.8	12.7	0.0
230	0.1	2.1	5.5	10.5	12.2	12.7	13.0	13.1	0.0
235	0.0	1.7	5.0	10.1	12.1	12.7	13.1	13.4	0.0
240	0.0	1.4	4.5	9.8	11.9	12.8	13.3	13.6	0.0
245	0.0	1.1	4.0	9.4	11.8	12.8	13.5	13.9	0.0
250	0.0	0.9	3.7	9.0	11.6	12.7	13.6	14.1	0.0
255	0.0	0.8	3.3	8.7	11.5	12.7	13.7	14.3	0.0
260	0.0	0.6	3.1	8.5	11.4	12.8	13.9	14.5	0.0
265	-0.1	0.5	2.9	8.3	11.3	12.8	14.0	14.8	0.0
270	-0.1	0.5	2.7	8.1	11.3	12.9	14.2	15.0	0.0
275	-0.1	0.4	2.6	8.1	11.3	13.0	14.4	15.3	0.0
280	-0.1	0.4	2.6	8.1	11.4	13.2	14.6	15.5	0.0
285	-0.1	0.4	2.6	8.2	11.6	13.4	14.9	15.8	0.0
290	-0.1	0.4	2.7	8.3	11.8	13.6	15.1	16.1	0.0
295	0.0	0.5	2.8	8.5	12.0	13.9	15.4	16.4	0.0
300	0.0	0.6	3.0	8.8	12.3	14.2	15.7	16.7	0.0
305	0.0	0.7	3.3	9.2	12.7	14.5	15.9	17.0	0.0
310	0.0	0.8	3.6	9.5	13.0	14.8	16.2	17.2	0.0
315	-0.1	1.1	4.0	9.9	13.4	15.1	16.5	17.5	0.0
320	-0.1	1.3	4.4	10.4	13.7	15.4	16.8	17.6	0.0
325	-0.1	1.6	4.8	10.8	14.0	15.6	17.0	17.7	0.0
330	0.0	1.9	5.2	11.2	14.3	15.9	17.1	17.8	0.0
335	0.1	2.3	5.7	11.6	14.5	16.0	17.1	17.7	0.0
340	0.3	2.7	6.2	11.9	14.7	16.1	17.0	17.5	0.0
345	0.5	3.1	6.6	12.1	14.8	16.0	16.8	17.2	0.0
350	0.7	3.6	7.0	12.3	14.9	15.9	16.5	16.9	0.0
355	1.0	4.0	7.4	12.4	14.8	15.7	16.2	16.4	0.0
360	1.3	4.4	7.7	12.5	14.7	15.4	15.8	15.9	0.0

TABLE IV TIME HISTORIES OF AERODYNAMIC LOADING, LB/IN

V = 110 KT α_s=+5° L = 8000 LB D =850 LB

(a) EXPERIMENTAL

	Blade Radial Station								
ψ	.25R	.40R	.55R	.75R	.85R	.90R	.95R	.97R	.99R
0	1.0	2.7	6.6	10.3	12.4	11.2	9.9	3.9	0.0
5	0.3	3.5	6.3	9.4	10.1	9.4	9.9	4.1	-0.4
10	0.3	2.0	7.8	8.5	8.6	7.5	8.0	2.5	0.2
15	1.3	2.2	6.2	8.4	7.2	6.0	6.1	1.0	-0.2
20	2.2	3.0	5.7	9.5	7.9	5.1	5.9	1.2	-0.3
25	3.4	3.2	6.5	9.6	8.3	6.6	6.8	2.1	0.1
30	3.2	3.8	6.9	9.7	7.9	6.7	7.3	2.2	-0.2
35	2.5	4.3	7.7	9.8	8.3	7.4	8.5	2.6	-0.2
40	2.3	4.8	8.2	10.1	8.9	8.2	8.9	3.3	-0.2
45	2.6	5.6	8.5	10.5	9.3	8.6	9.8	3.9	-0.4
50	3.2	6.3	9.1	11.2	10.2	9.6	10.9	4.7	-0.1
55	3.5	6.9	9.8	12.1	11.0	10.3	11.6	5.5	0.5
60	4.3	7.7	10.6	12.6	11.7	11.1	12.4	6.4	0.6
65	4.7	8.4	11.3	13.1	12.0	11.4	12.5	6.7	0.6
70	5.3	8.9	12.0	13.4	11.7	11.7	13.2	6.6	0.7
75	5.8	9.3	12.6	13.4	11.9	12.1	12.7	6.0	0.4
80	6.2	9.9	13.1	13.8	12.2	11.5	10.6	4.4	0.4
85	6.7	10.4	13.4	14.2	12.0	10.1	8.4	2.3	0.2
90	7.2	10.6	13.5	14.1	10.8	7.8	5.3	0.2	-0.8
95	7.6	10.9	13.4	14.1	8.7	4.9	2.3	-1.4	-1.6
100	8.0	11.2	13.2	13.6	6.1	2.4	0.4	-2.5	-2.5
105	8.4	11.4	13.1	12.6	3.7	1.0	-1.2	-3.4	-2.7
110	8.8	11.7	13.0	11.2	1.8	0.3	-1.8	-3.8	-3.1
115	9.2	12.0	12.9	9.7	0.8	-0.2	-2.0	-3.7	-3.2
120	9.5	12.1	12.9	8.3	0.2	-0.1	-2.0	-3.3	-3.0
125	9.8	12.2	13.0	7.1	-0.1	-0.1	-2.0	-2.9	-2.9
130	9.9	12.2	13.1	6.9	-0.3	0.1	-2.0	-2.6	-3.2
135	9.9	12.2	13.5	6.8	0.9	0.8	-1.7	-2.3	-3.0
140	9.9	12.2	13.7	7.0	2.7	1.4	-0.7	-1.5	-2.3
145	9.8	12.3	13.5	7.3	2.0	1.9	-0.2	-0.8	-2.1
150	9.9	12.2	13.8	7.3	2.8	2.6	0.3	-0.4	-1.9
155	9.7	11.8	13.7	7.5	3.3	3.2	0.6	-0.3	-2.2
160	9.4	11.5	13.7	7.5	3.7	3.9	0.6	-0.1	-1.6
165	9.0	11.2	13.5	7.6	4.1	4.3	1.3	0.2	-1.5
170	8.4	10.8	13.3	7.9	5.0	5.2	1.8	0.7	-1.5
175	7.8	10.3	13.0	8.6	6.1	6.2	3.0	1.4	-0.8
180	7.0	9.9	12.8	9.1	7.3	7.3	3.6	2.1	-0.6
185	6.3	9.3	12.7	9.7	8.4	8.4	4.6	2.7	-0.3
190	5.5	8.7	12.5	10.5	9.4	9.4	5.9	3.4	0.6
195	4.8	8.0	12.2	11.2	10.2	10.1	6.7	4.0	0.9
200	4.8	7.3	11.8	11.5	11.0	10.9	7.6	4.7	0.9
205	4.2	6.5	11.4	11.8	11.7	11.9	8.2	5.2	1.1
210	3.2	5.8	10.8	11.9	12.2	12.4	8.5	5.4	1.8
215	2.7	5.1	10.0	11.9	12.4	12.6	9.1	5.7	2.0
220	2.1	4.4	9.2	11.7	12.5	12.8	9.5	6.1	2.4
225	1.4	3.8	8.7	11.4	12.7	12.9	10.2	6.4	2.2
230	1.1	3.1	8.1	11.1	12.6	12.8	10.2	6.4	2.2
235	0.8	2.6	7.5	10.7	12.5	12.8	10.5	6.7	2.6
240	0.6	2.7	6.8	10.5	12.5	12.8	10.8	6.8	2.4
245	0.5	2.4	6.3	10.4	12.5	12.8	10.7	6.8	2.6
250	0.3	1.9	5.9	10.3	12.4	12.7	11.4	7.2	2.4
255	0.1	1.8	5.5	10.3	12.5	12.8	11.4	7.4	2.2
260	0.1	1.7	5.3	10.3	12.7	13.1	12.3	7.8	2.5
265	0.1	1.4	5.0	10.5	12.9	13.3	13.1	8.1	2.3
270	0.0	1.3	4.9	10.4	13.4	13.7	13.3	8.4	2.8
275	0.0	1.5	4.8	10.0	13.8	14.2	14.1	8.9	2.4
280	-0.1	1.3	4.5	9.6	13.3	14.4	14.9	9.5	2.3
285	-0.1	0.8	4.4	9.2	12.3	13.5	15.0	9.6	2.4
290	0.0	0.6	4.4	8.9	11.8	12.3	13.9	8.5	1.2
295	0.0	0.5	4.4	8.8	11.1	11.6	13.2	7.8	1.0
300	0.0	0.7	4.5	9.1	11.5	11.6	12.9	7.5	0.9
305	0.1	1.1	4.5	9.4	12.3	12.3	13.2	7.8	0.9
310	0.1	1.5	4.7	9.9	13.0	12.9	14.1	8.3	1.2
315	0.2	2.0	5.2	10.6	14.0	13.7	15.1	8.6	1.0
320	0.3	2.3	5.7	11.3	14.7	14.0	14.8	8.4	0.9
325	0.4	2.4	6.3	11.9	15.4	14.2	15.9	8.3	0.4
330	0.6	2.4	7.0	12.6	15.9	15.2	15.8	8.6	0.7
335	0.9	2.1	7.8	13.0	16.5	16.0	17.3	9.3	0.9
340	1.3	2.1	8.7	13.3	17.1	17.1	18.2	9.7	1.4
345	2.6	2.1	9.5	13.7	17.1	17.6	18.3	9.6	1.3
350	2.3	1.6	9.2	14.0	15.0	15.6	17.9	9.2	0.7
355	1.3	1.5	8.5	12.3	13.5	12.2	13.3	6.6	1.1
360	1.0	2.7	6.6	10.3	12.4	11.2	9.9	3.9	0.0

TABLE IV CONCLUDED

V = 130 KT a_s=0° L = 6500 LB D = 690 LB

(b) THEORETICAL (UNIFORM INFLOW)

ψ	Blade Radial Station .25R	.40R	.55R	.75R	.85R	.90R	.95R	.97R	.99R
0	2.7	5.8	8.6	11.5	11.8	11.4	10.6	9.9	0.0
5	3.1	6.1	8.8	11.5	11.5	10.9	9.9	9.0	0.0
10	3.5	6.5	9.0	11.4	11.2	10.4	9.2	8.2	0.0
15	3.9	6.8	9.2	11.2	10.7	9.8	8.5	7.4	0.0
20	4.3	7.1	9.3	11.0	10.3	9.2	7.8	6.6	0.0
25	4.7	7.4	9.4	10.6	9.7	8.6	7.1	5.9	0.0
30	5.1	7.7	9.5	10.3	9.2	7.9	6.4	5.1	0.0
35	5.5	8.0	9.6	10.0	8.6	7.2	5.5	4.1	0.0
40	5.9	8.3	9.7	9.6	7.9	6.4	4.5	2.9	0.0
45	6.3	8.6	9.8	9.3	7.2	5.4	3.3	1.5	0.0
50	6.7	8.9	9.9	9.0	6.5	4.4	1.9	-0.1	0.0
55	7.1	9.2	10.1	8.8	5.8	3.3	0.5	-1.8	0.0
60	7.5	9.5	10.4	8.5	5.1	2.2	-1.0	-3.5	0.0
65	7.9	9.9	10.7	8.3	4.3	1.2	-2.4	-5.1	0.0
70	8.3	10.4	11.0	8.1	3.6	0.1	-3.7	-6.7	0.0
75	8.7	10.8	11.4	7.9	3.0	-0.8	-4.9	-8.0	0.0
80	9.2	11.2	11.8	7.8	2.4	-1.6	-5.9	-9.2	0.0
85	9.5	11.7	12.1	7.7	2.0	-2.2	-6.7	-10.2	0.0
90	9.9	12.1	12.4	7.7	1.7	-2.7	-7.4	-11.0	0.0
95	10.3	12.5	12.7	7.7	1.5	-3.0	-7.8	-11.5	0.0
100	10.5	12.8	13.0	7.8	1.4	-3.2	-8.0	-11.7	0.0
105	10.7	13.1	13.3	7.9	1.4	-3.2	-8.0	-11.7	0.0
110	10.9	13.3	13.6	8.0	1.5	-3.1	-7.9	-11.4	0.0
115	10.9	13.5	13.8	8.2	1.7	-2.9	-7.5	-11.0	0.0
120	10.9	13.6	14.0	8.4	2.0	-2.5	-7.1	-10.5	0.0
125	10.7	13.6	14.1	8.7	2.4	2.0	-6.5	-9.8	0.0
130	10.6	13.6	14.2	9.0	2.8	-1.4	-5.7	-8.9	0.0
135	10.3	13.5	14.2	9.4	3.4	-0.7	-4.9	-7.9	0.0
140	9.9	13.3	14.1	9.7	4.0	0.1	-3.9	-6.9	0.0
145	9.5	13.0	14.0	10.0	4.6	0.9	-2.9	-5.7	0.0
150	9.0	12.7	13.9	10.3	5.2	1.7	-1.9	-4.5	0.0
155	8.5	12.3	13.8	10.6	5.9	2.5	-0.9	-3.3	0.0
160	7.8	11.8	13.6	13.1	6.4	3.3	0.2	-2.1	0.0
165	7.0	11.3	13.3	11.1	7.0	4.1	1.2	-1.0	0.0
170	6.2	10.7	13.0	11.3	7.6	4.9	2.1	0.1	0.0
175	5.3	10.1	12.6	11.4	8.1	5.6	3.1	1.2	0.0
180	3.9	9.4	12.1	11.5	8.6	6.3	4.0	2.2	0.0
185	2.3	8.7	11.7	11.5	9.0	6.9	4.9	3.2	0.0
190	1.8	8.1	11.1	11.5	9.3	7.5	5.5	4.0	0.0
195	1.4	7.3	10.6	11.4	9.6	8.0	6.2	4.9	0.0
200	1.1	6.4	10.0	11.4	9.9	8.5	6.9	5.7	0.0
205	0.9	5.6	9.5	11.3	10.1	9.0	7.6	6.6	0.0
210	0.7	4.8	8.9	11.2	10.3	9.4	8.3	7.4	0.0
215	0.5	4.0	8.3	11.1	10.5	9.8	8.8	8.0	0.0
220	0.4	3.2	7.6	10.9	10.7	10.1	9.3	8.6	0.0
225	0.3	2.5	7.0	10.7	10.8	10.3	9.7	9.1	0.0
230	0.2	1.5	6.4	10.3	10.8	10.5	10.0	9.5	0.0
235	0.1	1.2	5.8	10.0	10.7	10.6	10.2	9.9	0.0
240	0.1	1.0	5.3	9.6	10.6	10.7	10.5	10.3	0.0
245	0.1	0.9	4.9	9.2	10.5	10.8	10.8	10.7	0.0
250	0.1	0.8	4.5	8.9	10.4	10.9	11.1	11.1	0.0
255	0.1	0.7	4.2	8.6	10.3	10.9	11.3	11.5	0.0
260	0.1	0.6	4.0	8.4	10.2	11.0	11.6	11.8	0.0
265	0.1	0.6	3.8	8.2	10.2	11.1	11.7	12.1	0.0
270	0.1	0.9	3.7	8.1	10.2	11.2	11.9	12.3	0.0
275	0.1	1.0	3.6	8.1	10.3	11.3	12.0	12.4	0.0
280	0.0	1.0	3.5	8.1	10.4	11.4	12.1	12.5	0.0
285	0.0	1.1	3.6	8.2	10.5	11.5	12.3	12.7	0.0
290	0.0	1.1	3.7	8.4	10.7	11.7	12.4	12.8	0.0
295	0.0	1.3	3.9	8.5	10.9	11.9	12.6	13.0	0.0
300	0.0	1.4	4.1	8.8	11.1	12.1	12.8	13.2	0.0
305	0.0	1.6	4.4	9.0	11.3	12.2	12.9	13.4	0.0
310	0.1	1.9	4.7	9.3	11.5	12.4	13.1	13.5	0.0
315	0.1	2.2	5.0	9.6	11.7	12.5	13.2	13.5	0.0
320	0.2	2.5	5.4	9.9	11.9	12.7	13.2	13.4	0.0
325	0.4	2.8	5.8	10.2	12.0	12.7	13.1	13.2	0.0
330	0.7	3.2	6.2	10.5	12.1	12.7	13.0	13.0	0.0
335	0.9	3.6	6.7	10.8	12.2	12.7	12.8	12.7	0.0
340	1.2	4.1	7.1	11.0	12.3	12.6	12.5	12.3	0.0
345	1.6	4.5	7.6	11.2	12.2	12.4	12.2	11.9	0.0
350	1.9	5.0	8.0	11.3	12.2	12.1	11.8	11.3	0.0
355	2.3	5.4	8.3	11.4	12.0	11.8	11.2	10.7	0.0
360	2.7	5.8	8.6	11.5	11.8	11.4	10.6	9.9	0.0

TABLE V TIME HISTORIES OF AERODYNAMIC LOADING, LB/IN
V = 150 KT α_s = 0° L = 8600 LB D = 250 LB

(a) EXPERIMENTAL

	Blade Radial Station								
ψ	.25R	.40R	.55R	.75R	.85R	.90R	.95R	.97R	.99R
0	-3.2	0.6	4.4	14.6	20.4	17.9	17.6	9.5	-0.5
5	-2.2	-0.6	4.0	14.7	16.0	12.3	12.2	5.7	-1.3
10	1.1	2.4	3.6	14.2	14.8	10.9	10.9	5.1	1.6
15	2.2	2.8	4.5	13.2	13.6	9.6	9.6	4.5	1.7
20	1.6	3.2	5.6	12.6	12.3	8.7	8.3	4.1	-2.2
25	0.9	3.3	7.0	12.4	12.2	8.8	8.7	4.4	-2.0
30	0.5	4.4	7.9	12.8	12.6	9.7	9.8	5.0	-1.8
35	1.0	5.0	8.3	13.4	13.5	10.5	11.0	5.8	-1.4
40	1.7	4.9	8.4	14.3	14.7	11.8	13.2	7.3	-1.0
45	1.5	5.2	8.6	14.6	14.8	12.3	13.3	7.2	-0.8
50	1.7	5.4	8.6	14.2	13.5	11.0	12.1	6.1	-1.1
55	2.1	5.3	8.5	13.0	12.4	10.2	11.2	5.4	-1.2
60	2.5	5.8	8.3	13.1	12.4	9.6	11.1	5.2	-0.8
65	3.0	6.3	8.4	13.4	12.4	8.9	12.5	8.4	-0.2
70	3.4	7.3	9.1	13.8	12.1	9.3	13.3	10.2	-0.5
75	3.9	7.7	10.2	13.6	12.6	10.6	12.5	8.7	-1.7
80	4.4	8.4	11.0	14.0	13.5	11.4	10.6	6.1	-2.7
85	5.1	8.9	11.2	14.6	14.1	9.4	6.4	1.4	-2.9
90	6.1	9.7	11.6	15.2	13.1	5.0	1.8	-1.4	-3.3
95	7.1	10.5	11.7	15.3	8.6	-1.1	-0.5	-3.1	-4.7
100	8.2	11.4	11.5	14.2	0.6	-3.8	-3.0	-5.9	-5.1
105	9.4	12.0	11.3	11.2	-3.3	-5.1	-5.8	-9.9	-5.4
110	10.3	12.6	11.4	7.1	-4.8	-6.6	-7.9	-11.2	-6.2
115	10.9	12.7	11.8	4.2	-5.9	-7.3	-9.0	-11.5	-6.5
120	11.5	13.3	12.5	3.9	-6.0	-7.1	-8.5	-11.5	-6.4
125	12.2	13.9	13.5	4.2	-5.1	-6.5	-8.0	-8.1	-5.9
130	12.7	14.6	14.6	4.7	-3.7	-5.1	-6.7	-4.6	-6.0
135	12.9	15.2	15.0	5.8	-1.6	-3.2	-5.4	-3.3	-5.6
140	12.9	15.7	14.9	7.1	0.8	-0.8	-3.3	-1.7	-4.8
145	13.2	15.7	15.2	8.1	3.0	1.6	-0.9	0.1	-4.0
150	13.3	15.6	15.9	9.3	5.0	3.5	0.0	1.4	-3.2
155	13.1	15.6	16.2	10.6	6.7	4.9	1.5	2.4	-2.1
160	12.7	15.9	16.3	11.8	8.9	6.2	2.5	3.0	-1.7
165	11.8	15.6	16.3	13.0	10.9	8.1	3.2	3.8	-1.0
170	10.6	14.5	16.1	13.6	12.2	9.1	4.0	4.2	-0.7
175	9.4	13.5	15.9	14.2	13.3	10.1	6.1	5.0	0.1
180	8.0	12.6	15.2	14.4	13.6	10.6	7.3	5.6	0.8
185	7.0	11.3	14.4	14.4	13.4	10.7	6.9	5.4	1.1
190	6.5	9.8	13.7	14.5	14.1	11.2	7.1	5.4	1.4
195	5.2	8.0	12.7	14.8	14.9	12.2	7.3	6.0	1.6
200	3.8	6.8	11.4	15.0	15.8	13.1	7.3	6.6	1.7
205	2.5	5.5	10.3	14.9	16.2	13.7	8.1	7.3	2.4
210	1.6	4.6	9.2	14.8	16.5	14.2	9.7	8.0	2.7
215	1.0	4.0	8.2	14.5	16.5	14.0	10.8	8.1	3.4
220	0.6	3.5	7.2	13.6	15.8	14.0	11.5	8.7	3.8
225	0.0	2.6	6.3	12.8	15.4	13.9	12.6	9.0	4.6
230	-0.5	1.8	5.4	12.1	14.6	14.0	11.9	9.3	4.2
235	-1.0	1.4	4.6	11.5	14.3	13.4	10.5	8.9	3.8
240	-1.3	0.9	3.9	10.7	13.7	12.9	10.0	8.9	3.6
245	-1.5	0.5	3.3	10.1	13.1	12.4	10.8	8.9	3.5
250	-1.6	0.2	2.8	9.6	12.5	12.1	11.6	9.2	3.6
255	-1.8	0.2	2.5	9.3	12.1	12.2	12.3	9.3	3.6
260	-2.0	0.0	2.3	9.0	12.0	12.0	12.1	9.2	3.3
265	-2.3	0.0	2.2	8.8	12.0	11.7	12.1	9.3	2.7
270	-2.3	0.1	2.0	9.0	12.1	11.8	13.2	9.8	2.6
275	-2.6	-0.1	1.9	8.6	12.0	12.2	14.0	10.2	2.3
280	-2.5	-0.1	1.9	8.5	12.0	12.5	14.9	10.5	2.6
285	-2.5	0.3	2.0	9.0	12.4	12.7	15.3	10.7	2.3
290	-2.3	0.1	2.0	8.9	12.8	12.5	14.9	10.7	1.7
295	-1.9	0.2	1.6	9.2	13.5	12.8	14.9	10.8	1.1
300	-1.6	0.4	1.5	9.8	14.1	13.4	15.4	11.1	1.0
305	-1.2	0.6	2.1	10.3	14.3	13.4	15.9	10.9	1.0
310	-1.2	1.0	2.7	10.6	13.4	12.7	15.2	10.0	0.5
315	-0.9	1.2	3.4	10.3	13.6	13.0	15.3	10.3	-0.2
320	-0.3	1.6	4.2	10.4	14.6	13.8	16.0	10.8	-0.1
325	0.0	2.1	4.8	11.0	15.8	14.8	16.7	11.1	-0.6
330	0.1	2.4	5.2	12.3	17.1	16.1	18.1	11.7	-0.2
335	0.2	2.8	5.4	14.3	18.8	17.3	19.5	12.2	-0.2
340	0.3	2.1	6.2	16.6	20.3	18.3	20.5	12.5	-0.1
345	0.5	2.5	6.5	18.8	22.3	19.2	21.2	12.6	-0.1
350	-0.4	4.4	5.2	20.2	26.1	21.1	22.3	12.8	0.1
355	-2.0	3.9	4.5	16.8	27.4	23.6	22.4	12.9	-0.2
360	-3.2	0.6	4.4	14.6	20.4	17.9	17.6	9.5	-0.5

TABLE V CONCLUDED

V = 150 KT α_s = 0° L = 8600 LB D = 250 LB

(b) THEORETICAL (UNIFORM INFLOW)

ψ	Blade Radial Station .25R	.40R	.55R	.75R	85R	.90R	.95R	.97R	.99R
0	1.8	5.2	8.8	13.7	15.9	16.7	17.1	17.2	0.0
5	2.3	5.7	9.2	13.8	15.7	16.2	16.4	16.2	0.0
10	2.7	6.1	9.4	13.8	15.3	15.6	15.5	15.2	0.0
15	3.2	6.4	9.5	13.6	14.9	15.0	14.6	14.1	0.0
20	3.6	6.6	9.5	13.3	14.3	14.2	13.7	13.3	0.0
25	4.0	6.8	9.4	12.8	13.6	13.4	12.9	12.4	0.0
30	4.3	7.0	9.3	12.1	12.7	12.5	12.1	11.5	0.0
35	4.7	7.1	9.1	11.3	11.6	11.5	11.0	10.4	0.0
40	5.0	7.2	8.8	10.4	10.5	10.2	9.5	8.8	0.0
45	5.4	7.3	8.6	9.4	9.2	8.6	7.6	6.7	0.0
50	5.8	7.5	8.4	8.6	7.8	6.8	5.3	4.1	0.0
55	6.3	7.7	8.4	7.9	6.4	4.8	2.8	1.0	0.0
60	6.8	8.1	8.6	7.3	4.9	2.7	0.0	-2.3	0.0
65	7.3	8.6	9.0	6.9	3.5	0.6	-2.8	-5.7	0.0
70	7.9	9.3	9.5	6.7	2.3	-1.3	-5.5	-8.8	0.0
75	8.5	10.1	10.3	6.6	1.4	-2.8	-7.5	-11.3	0.0
80	9.1	10.9	11.1	6.8	0.8	-3.8	-9.0	-13.1	0.0
85	9.8	11.8	12.0	7.1	0.6	-4.4	-9.9	-14.3	0.0
90	10.5	12.6	12.7	7.4	0.4	-4.8	-10.6	-15.1	0.0
95	11.1	13.3	13.4	7.6	0.2	-5.2	-11.2	-15.8	0.0
100	11.7	13.9	13.8	7.6	0.1	-5.7	-11.8	-16.5	0.0
105	12.1	14.4	14.1	7.4	-0.5	-6.2	-12.3	-17.1	0.0
110	12.5	14.7	14.4	7.3	-0.7	-6.5	-12.6	-17.3	0.0
115	12.7	15.0	14.6	7.3	-0.7	-6.4	-12.4	-16.9	0.0
120	12.8	15.2	14.8	7.5	-0.5	-6.0	-11.7	-16.1	0.0
125	12.8	15.3	15.1	7.8	0.1	-5.1	-10.6	-14.7	0.0
130	12.6	15.3	15.3	8.4	1.1	-4.0	-9.0	-12.8	0.0
135	12.3	15.3	15.6	9.2	2.3	-2.4	-7.0	-10.5	0.0
140	12.0	15.2	15.8	10.0	3.6	-0.7	-5.0	-8.0	0.0
145	11.5	15.0	15.9	10.8	4.9	1.0	-2.9	-5.7	0.0
150	10.9	14.7	15.8	11.6	6.1	2.6	-0.9	-3.4	0.0
155	10.2	14.2	15.7	12.2	7.3	4.0	0.9	-1.4	0.0
160	9.3	13.7	15.4	12.7	8.3	5.3	2.5	0.5	0.0
165	8.3	12.9	15.2	13.1	9.2	6.5	4.0	2.1	0.0
170	7.2	12.1	14.8	13.4	10.0	7.6	5.3	3.6	0.0
175	6.0	11.2	14.3	13.7	10.7	8.6	6.5	5.0	0.0
180	4.6	10.2	13.6	13.8	11.4	9.5	7.7	6.3	0.0
185	2.5	9.2	12.9	13.8	11.9	10.3	8.7	7.5	0.0
190	1.6	8.0	12.1	13.8	12.4	11.0	9.6	8.5	0.0
195	1.1	6.8	11.2	13.7	12.7	11.6	10.4	9.5	0.0
200	0.8	5.5	10.2	13.4	12.9	12.1	11.1	10.4	0.0
205	0.5	4.2	9.3	13.1	13.0	12.5	11.8	11.2	0.0
210	0.3	2.9	8.3	12.7	13.1	12.7	12.3	11.9	0.0
215	0.1	1.5	7.2	12.2	13.0	13.0	12.7	12.5	0.0
220	0.0	1.1	6.1	11.7	12.9	13.1	13.0	13.0	0.0
225	0.0	0.8	5.1	11.1	12.8	13.2	13.3	13.3	0.0
230	0.0	0.5	4.2	10.4	12.5	13.2	13.6	13.7	0.0
235	-0.1	0.4	3.5	9.7	12.2	13.1	13.7	14.0	0.0
240	-0.3	0.2	2.8	9.0	11.8	13.0	13.8	14.3	0.0
245	-0.4	0.1	2.3	8.3	11.4	12.8	13.9	14.5	0.0
250	-0.5	0.1	1.9	7.6	10.9	12.5	13.9	14.7	0.0
255	-0.6	0.1	1.6	7.0	10.5	12.3	13.8	14.8	0.0
260	-0.7	0.0	1.4	6.5	10.1	12.1	13.8	15.0	0.0
265	-0.8	0.0	1.2	6.2	9.9	11.9	13.8	15.1	0.0
270	-0.8	0.0	1.0	6.0	9.7	11.9	13.9	15.2	0.0
275	-0.8	0.0	1.0	5.9	9.7	12.0	14.0	15.4	0.0
280	-0.8	0.0	0.9	5.9	9.9	12.2	14.2	15.6	0.0
285	-0.7	0.0	1.0	6.1	10.1	12.4	14.3	15.9	0.0
290	-0.6	-0.1	1.1	6.4	10.5	12.8	14.9	16.3	0.0
295	-0.5	-0.1	1.3	6.8	11.0	13.3	15.4	16.8	0.0
300	-0.4	0.0	1.5	7.3	11.5	13.8	15.9	17.3	0.0
305	-0.3	0.0	1.9	7.9	12.1	14.4	16.5	17.8	0.0
310	-0.2	0.2	2.3	8.6	12.8	15.1	17.1	18.3	0.0
315	-0.1	0.4	2.9	9.3	13.5	15.7	17.6	18.8	0.0
320	0.0	0.7	3.5	10.1	14.2	16.3	18.0	19.1	0.0
325	0.0	1.1	4.2	10.8	14.8	16.8	18.3	19.4	0.0
330	-0.1	1.5	4.9	11.6	15.3	17.1	18.6	19.5	0.0
335	0.0	2.1	5.6	12.2	15.7	17.3	18.7	19.4	0.0
340	0.2	2.7	6.4	12.7	15.9	17.5	18.6	19.3	0.0
345	0.5	3.4	7.1	13.1	16.1	17.5	18.4	19.0	0.0
350	0.9	4.0	7.8	13.4	16.1	17.3	18.1	18.5	0.0
355	1.3	4.7	8.3	13.5	16.1	17.1	17.7	17.9	0.0
360	1.8	5.2	8.8	13.7	15.9	16.7	17.1	17.2	0.0

TABLE VI TIME HISTORIES OF AERODYNAMIC LOADING, LB/IN

V = 150 KT α_s=-5° L = 6600 LB D = 1100 LB

(a) EXPERIMENTAL

	Blade Radial Station								
ψ	.25R	.40R	.55R	.75R	.85R	.90R	.95R	.97R	.99R
0	-3.0	0.8	5.6	13.1	11.1	8.3	8.0	2.5	-0.6
5	-0.8	1.0	5.0	12.2	10 8	7.0	8.3	3.2	-0.6
10	0.9	3.8	3.7	9.5	8.3	6 2	7.2	2.3	-1.4
15	1.8	4.7	4.7	9.4	8.4	6.2	7.3	2.9	-2.1
20	2.6	3.2	5.7	10.0	8.5	6.1	7.3	2.9	-2.1
25	1.9	3.9	7.2	10.2	9.1	7.0	6.9	2.8	-2.0
30	1.9	4.7	7.9	11.3	10.8	8.0	7.0	3.3	-2.2
35	2.7	5.3	8.6	13.0	12.6	9.6	9.4	4.5	-1.9
40	2.8	6.1	9.4	14.3	13.4	10.6	11.2	5.0	-1.2
45	2.7	6.4	9.9	14.4	13 3	10.7	11.2	5.4	-1.2
50	3.1	7.0	10.4	14.2	12.9	10.5	11.9	5.4	-1.0
55	3.6	8.0	10.8	14.3	12.7	1.0	11.2	4.8	-0.5
60	4.2	8.9	11.3	14.3	12.4	8.9	10.9	6.3	-0.7
65	5.0	9.8	12.0	14.1	12.2	8.5	11.0	8.3	-0.7
70	5.7	10.9	12.7	14.4	12.1	7.9	10.0	7.0	-0.9
75	6.5	11.5	13.4	14.6	11.6	7.0	8.0	4.1	-1.6
80	7.4	12.1	13.9	14.5	10.8	5.0	3.9	0.0	-2.7
85	8.5	12 7	14.4	14.6	8.9	1.8	-0.7	-3.1	-4.1
90	9.5	13.4	14.7	14.5	5.4	-2.5	3.3	-5.9	-4.9
95	10.4	14.3	14.6	13.8	0.6	-5.3	-5.1	-9.6	-5.2
100	11.3	14.7	14.5	11.9	-3 5	-7.2	-7.8	-11.8	-6.1
105	12.0	15.0	14.6	8.9	-5.6	-8.7	-10.5	-12.9	-6.9
110	12.8	15.5	14.8	5.6	-6.6	-9.7	-12.0	-13.8	-7.4
115	13.5	16.1	15.2	3.6	-7.5	-9.7	-12.5	-14.2	-7.2
120	14.1	16.8	15.9	3.2	-7.3	-9.1	-11.9	-10.9	-7.4
125	14.4	17.3	16.6	3.3	-6.4	-7.9	-10.2	- 6.9	-6.9
130	14.6	17.9	16.9	3.9	-4.9	-6.5	-8.4	-5.9	-6.3
135	14.8	18.4	16.7	4.7	-3.2	-5.2	-7.1	-5.0	-5.9
140	15.0	18.3	16.5	5.7	-1.4	-3.5	-6.8	-4.0	-5.6
145	15.0	18.2	16.2	6.6	0.1	-1.8	-6.1	-2.8	-5.1
150	14.8	18.6	16.0	7.8	1.6	0.0	-4.7	-1.7	-4.3
155	14.5	18.0	16.1	8.2	3.2	1.0	-3.7	-1.2	-3.9
160	14.0	17.4	16.2	9.0	4.7	2.1	-3.3	-0.6	-3.7
165	13 1	16.4	16 1	9.8	6.1	3.4	-2.6	0.0	-3.4
170	12.0	15.4	16.1	10.5	7.6	4.8	-1.6	0 8	-3.0
175	12.1	14.2	16.0	11.5	8.7	6.2	-0.2	1.7	-2.2
180	12.2	13.0	15.6	12.6	10 0	7.4	2.0	2.7	-1.6
185	10.5	11 5	14.9	13.0	10.8	8.5	4.5	3 6	-0.7
190	8.6	10 1	13.8	13.3	11.4	9.2	4.7	3 8	-0.2
195	6.5	8.7	12.5	13.3	12 3	9.7	3.9	4.2	-0.1
200	4.6	8.1	11.6	13 5	13.3	10.5	4.6	4.8	0.3
205	3.3	7.9	10.7	13.6	13 8	11.3	5.2	5.3	0.7
210	2.3	6.5	9.7	13.5	14.0	11.7	6.8	6.2	1.6
215	1.4	5.2	8.6	13.2	14.1	12.2	9.0	7.1	2.6
220	0.7	4.5	7.7	13.0	14.2	12.4	10.0	7.3	3.0
225	0.3	3.7	6.9	12.4	14.0	12.5	10.3	7.7	2.7
230	0.0	2.8	6.2	11.9	13.7	12.3	9.7	7.5	2.6
235	-0.2	1.8	5.8	11.1	13.3	11.8	9.0	7.5	2.5
240	-0.4	1.6	5.3	10.9	12.7	11.5	9.4	7.7	2.6
245	-0.4	1.3	4.9	10.4	12.2	11.4	10.3	8.0	2.8
250	-0.5	1.0	4.4	10.0	11.8	11.4	11.2	8.4	3.0
255	-0.6	0.8	4.1	9.6	11.7	11.3	11.1	8 2	2.7
260	-0.7	0.9	3.8	9.5	11.7	10.9	10.1	8.0	2.0
265	-0.8	0.7	3.5	9.4	11.6	10.8	11.2	8.5	2.0
270	-0.7	0.3	3.1	9.1	11.6	11.1	12.4	8.8	1.7
275	-0.8	0.4	3.0	9.2	11.6	11.5	13.8	9.3	2.3
280	-0.8	0.4	2.4	9.3	11.7	11.7	14.1	9.4	2.3
285	-0.7	0.4	1.6	9.4	12.1	11.3	13.2	9.2	1.2
290	-0.6	0.4	1.6	9.5	12.8	11.5	12.6	9.2	0.4
295	-0.6	0.6	2.0	10.1	13.7	12.4	13.2	9.7	0.4
300	-0.5	0.8	2.3	10.6	14.4	13.2	14.4	10.1	0.3
305	-0.3	0.8	2.8	10.7	14.7	13.3	14.8	9.8	0.2
310	-0.2	1.0	3.4	11.1	14.9	13.2	14.7	9.6	-0.1
315	0.0	1.1	4.3	11.7	15.1	13.4	15.0	9.5	-0.1
320	0.1	1.6	4.9	12.8	15.6	14.0	16.1	9.8	0.0
325	0.2	2.0	5.1	13.8	16.5	14.1	16.4	9.8	-0.4
330	0.3	2.6	5.3	14.7	17.5	14 8	15.8	9.7	-0.7
335	0.7	3.0	5.6	15.4	18.2	15.1	16.2	9.5	-1.1
340	1.3	3.6	6.2	16.0	18.9	15.9	16.8	9.6	-0.8
345	1.1	5.1	6.6	16.2	20.3	17.5	18.5	10.4	-0.3
350	-1.7	5.7	6.1	15.2	24.0	20.4	20.7	10.8	0.0
355	-3.4	3.4	5.4	13.2	19.8	16.6	16.2	7.1	0.1
360	-3.0	0.8	5.6	13.1	11.1	8.3	8.0	2.5	-0.6

TABLE VI CONCLUDED

V = 150 KT θ_0 = +5° L = 8600 LB B = 1100 LB

(b) THEORETICAL (UNIFORM INFLOW)

	Blade Radial Station								
ψ	.25R	.40R	.55R	.75R	.85R	.90R	.95R	.97R	.99R
0	3.7	7.1	10.0	12.2	11.4	10.2	8.6	7.3	0.0
5	4.3	7.6	10.3	12.0	10.9	9.6	7.9	6.6	0.0
10	4.9	8.0	10.4	11.7	10.5	9.2	7.5	6.2	0.0
15	5.4	8.4	10.5	11.4	10.2	8.9	7.3	6.1	0.0
20	6.0	8.7	10.4	11.0	9.9	8.6	7.2	6.0	0.0
25	6.5	8.9	10.2	10.6	9.5	8.3	6.9	5.7	0.0
30	7.0	9.0	10.1	10.2	9.0	7.8	6.3	5.0	0.0
35	7.5	9.2	9.9	9.6	8.2	7.0	5.3	3.8	0.0
40	8.0	9.5	9.9	8.9	7.3	5.7	3.8	2.2	0.0
45	8.5	9.8	10.0	8.3	6.1	4.2	1.9	0.0	0.0
50	9.1	10.2	10.3	7.8	4.9	2.5	-0.3	-2.7	0.0
55	9.7	10.8	10.7	7.5	3.6	0.6	-2.9	-5.8	0.0
60	10.3	11.5	11.3	7.3	2.4	-1.4	-5.7	-9.2	0.0
65	11.0	12.2	11.9	7.2	1.2	-3.4	-8.6	-12.7	0.0
70	11.8	13.1	12.7	7.3	0.4	-4.9	-10.9	-15.7	0.0
75	12.6	14.0	13.6	7.7	0.0	-6.0	-12.6	-17.8	0.0
80	13.4	14.9	14.5	8.0	-0.3	-6.6	-13.6	-19.0	0.0
85	14.2	15.9	15.3	8.1	-0.6	-7.1	-14.2	-19.8	0.0
90	14.8	16.7	15.9	8.0	-1.1	-7.8	-14.9	-20.5	0.0
95	15.4	17.3	16.3	7.6	-1.8	-8.6	-15.9	-21.4	0.0
100	15.9	17.7	16.5	7.2	-2.7	-9.6	-16.8	-22.4	0.0
105	16.2	18.0	16.6	6.7	-3.4	-10.4	-17.7	-23.2	0.0
110	16.4	18.2	16.7	6.5	-3.7	-10.7	-18.0	-23.4	0.0
115	16.5	18.3	16.8	6.6	-3.6	-10.6	-17.8	-23.1	0.0
120	16.4	18.3	16.9	6.7	-3.3	-10.1	-17.1	-22.3	0.0
125	16.2	18.3	17.0	7.0	-2.7	-9.3	-15.9	-20.9	0.0
130	15.9	18.2	17.1	7.5	-1.9	-8.2	-14.3	-19.0	0.0
135	15.5	18.1	17.2	8.0	-0.9	-6.8	-12.6	-16.8	0.0
140	14.8	17.8	17.3	8.7	0.2	-5.3	-10.7	-14.6	0.0
145	14.0	17.5	17.2	9.4	1.5	-3.7	-8.7	-12.2	0.0
150	13.0	17.0	17.1	10.1	2.7	-2.0	-6.6	-9.9	0.0
155	11.6	16.5	16.9	10.7	4.0	-0.4	-4.7	-7.7	0.0
160	9.5	15.9	16.7	11.2	5.1	1.0	-2.9	-5.7	0.0
165	6.8	15.0	16.4	11.6	5.9	2.2	-1.5	-4.1	0.0
170	4.8	14.0	15.9	11.8	6.6	3.1	-0.3	-2.7	0.0
175	3.6	12.8	15.5	12.0	7.2	4.0	0.9	-1.4	0.0
180	2.9	11.2	15.0	12.3	7.9	5.0	2.1	0.0	0.0
185	2.4	8.7	14.4	12.5	8.7	6.0	3.4	1.5	0.0
190	1.9	6.2	13.6	12.8	9.2	6.8	4.4	2.7	0.0
195	1.5	4.4	12.6	13.0	9.8	7.6	5.4	3.8	0.0
200	1.2	3.3	11.4	13.2	10.5	8.5	6.5	5.0	0.0
205	0.8	2.6	10.1	13.3	11.3	9.5	7.6	6.2	0.0
210	0.6	2.1	8.4	13.2	11.9	10.4	8.8	7.5	0.0
215	0.4	1.7	6.2	12.9	12.4	11.2	9.7	8.6	0.0
220	0.3	1.4	4.5	12.3	12.4	11.6	10.4	9.5	0.0
225	0.3	1.1	3.5	11.5	12.2	11.7	10.9	10.2	0.0
230	0.4	0.9	2.8	10.7	11.8	11.8	11.3	10.9	0.0
235	0.3	0.7	2.3	10.0	11.4	11.7	11.7	11.5	0.0
240	0.4	0.5	1.9	9.3	11.1	11.7	12.0	12.1	0.0
245	0.5	0.4	1.6	8.7	10.8	11.6	12.2	12.5	0.0
250	0.6	0.3	1.4	8.1	10.5	11.6	12.4	12.9	0.0
255	0.8	0.2	1.2	7.7	10.3	11.5	12.5	13.1	0.0
260	0.8	0.2	1.1	7.3	10.1	11.4	12.5	13.2	0.0
265	0.7	0.1	1.0	7.0	9.9	11.3	12.5	13.2	0.0
270	0.6	0.1	1.0	6.8	9.7	11.2	12.5	13.3	0.0
275	0.5	0.1	1.0	6.8	9.7	11.3	12.6	13.4	0.0
280	0.4	0.1	1.4	6.8	9.8	11.4	12.8	13.6	0.0
285	0.4	0.1	1.7	7.1	10.1	11.7	13.0	13.9	0.0
290	0.3	0.2	2.1	7.4	10.4	12.0	13.4	14.2	0.0
295	0.4	0.2	2.5	7.8	10.9	12.4	13.7	14.5	0.0
300	0.3	0.3	2.8	8.3	11.3	12.8	13.9	14.6	0.0
305	0.2	0.4	3.3	8.8	11.7	13.1	14.1	14.7	0.0
310	0.1	0.6	3.9	9.3	12.0	13.3	14.1	14.6	0.0
315	0.1	0.8	4.5	9.8	12.3	13.4	14.1	14.4	0.0
320	0.1	1.0	5.2	10.2	12.5	13.4	14.0	14.3	0.0
325	0.1	2.0	6.0	10.6	12.6	13.4	13.8	14.0	0.0
330	0.3	3.1	6.7	11.1	12.7	13.3	13.6	13.6	0.0
335	0.4	3.8	7.4	11.5	12.8	13.2	13.2	13.0	0.0
340	0.7	4.6	8.0	11.9	12.8	12.9	12.6	12.2	0.0
345	0.9	5.4	8.6	12.1	12.7	12.3	11.7	11.0	0.0
350	2.3	6.0	9.1	12.2	12.4	11.7	10.6	9.6	0.0
355	3.0	6.6	9.6	12.2	11.9	10.9	9.5	8.3	0.0
360	3.7	7.1	10.0	12.2	11.4	10.2	8.6	7.3	0.0

TABLE VII TIME HISTORIES OF AERODYNAMIC LOADING, LB/IN

V = 175 KT θ_s = 6° L = 7100 LB B = 400 LB

(a) EXPERIMENTAL

	Blade Radial Station								
ψ	.25R	.40R	.55R	.75R	.85R	.90R	.95R	.97R	.99R
0	-3.7	-0.2	4.3	11.4	13.6	10.6	9.4	4.3	-1.7
5	-0.8	-0.1	2.2	11.2	11.7	7.6	6.7	2.7	-2.5
10	1.5	2.0	2.5	9.9	10.3	6.5	5.4	2.1	-2.9
15	1.5	2.7	4.6	9.4	9.5	6.0	4.3	1.8	-3.3
20	1.6	2.3	5.1	9.7	9.5	6.5	4.6	2.2	-3.2
25	1.0	2.5	6.1	10.6	10.6	7.7	6.2	3.3	-2.8
30	0.9	3.9	7.4	12.3	12.7	9.8	8.7	4.9	-2.0
35	1.4	4.5	8.1	14.0	15.3	12.4	10.9	6.5	-1.7
40	2.1	4.9	8.5	15.0	16.5	13.4	11.2	6.5	-1.7
45	1.7	5.0	8.6	15.5	16.4	13.2	11.3	6.5	-1.6
50	1.7	5.1	8.7	15.6	16.3	13.5	11.8	9.1	-1.7
55	2.0	5.4	8.9	15.7	16.2	13.4	13.4	10.9	-2.8
60	2.2	6.1	9.2	15.8	15.2	12.5	13.9	9.6	1.4
65	2.7	7.0	9.8	15.2	13.9	10.7	18.0	7.5	4.8
70	3.2	7.5	10.4	14.7	13.1	10.7	21.1	5.9	4.3
75	3.8	8.1	10.7	14.4	12.7	13.5	19.0	4.0	3.5
80	4.7	8.7	10.8	14.5	12.9	14.2	13.1	0.5	-0.6
85	5.9	9.2	11.1	15.2	11.9	11.0	-0.9	-0.8	-6.0
90	7.3	10.4	11.5	15.7	6.5	-2.4	-7.2	-0.1	-7.7
95	8.8	11.6	11.9	15.0	-1.8	-16.0	-8.7	-0.8	-8.4
100	10.4	12.4	11.8	11.3	-8.7	-19.3	-13.7	-2.1	-9.6
105	11.4	13.2	11.9	5.1	-11.4	-19.7	-21.8	-3.7	-10.7
110	12.2	13.8	12.3	1.1	-12.8	-22.0	-23.8	-4.8	-10.8
115	13.2	14.4	12.8	-0.3	-13.9	-22.4	-23.9	-6.1	-10.9
120	14.2	15.1	13.8	-0.6	-13.2	-14.6	-23.5	-8.5	-11.7
125	14.8	16.2	15.2	0.3	-11.0	-9.5	-14.9	-10.2	-11.0
130	15.1	17.2	15.1	1.9	7.6	-9.0	-9.9	-10.0	-8.4
135	15.5	18.1	14.8	3.9	-4.0	-5.8	-8.3	-8.3	-7.3
140	15.9	18.6	15.4	5.6	-0.7	-2.1	-5.2	-3.3	-6.2
145	15.9	18.7	15.7	7.0	2.7	0.7	-2.5	-0.1	-4.6
150	16.0	18.6	16.2	8.7	4.3	2.9	-0.9	1.3	-3.0
155	15.8	18.3	16.1	9.9	6.1	4.1	-0.5	1.8	-2.4
160	15.2	17.7	16.0	10.6	7.5	5.2	-1.1	1.6	-2.5
165	14.4	16.7	16.0	11.0	8.5	6.0	-0.8	1.6	-2.6
170	13.2	15.7	15.9	11.5	8.8	6.1	0.4	2.0	-2.4
175	12.8	14.3	15.6	12.2	9.4	6.8	2.5	2.9	-1.7
180	11.5	12.8	15.2	13.1	10.5	8.1	4.8	4.0	-0.3
185	9.3	11.2	14.6	13.7	12.0	9.5	6.3	4.8	0.6
190	7.7	9.7	14.0	14.4	13.5	10.8	6.5	5.2	1.1
195	5.9	8.0	12.6	14.6	14.8	11.7	5.3	5.4	1.4
200	4.0	6.4	11.2	14.6	15.6	13.1	5.0	6.0	1.9
205	2.5	5.1	9.9	14.5	16.1	14.0	6.2	6.7	2.3
210	1.5	4.0	8.6	14.2	16.2	14.1	7.5	7.4	2.8
215	0.7	3.1	7.3	13.6	15.9	14.2	9.7	8.3	3.8
220	-0.1	2.2	6.1	13.0	15.4	14.4	12.0	8.9	4.7
225	-0.7	1.6	5.0	12.2	14.6	14.0	12.1	8.8	5.0
230	-1.2	0.9	4.1	11.1	13.8	13.0	11.0	8.5	4.7
235	-1.8	0.3	3.3	10.1	13.0	12.3	9.8	8.2	4.1
240	-2.1	0.1	2.7	9.6	12.2	12.0	9.5	8.1	3.9
245	-2.3	-0.4	2.2	8.8	11.4	11.4	10.0	8.2	3.6
250	-2.5	-0.4	1.8	8.3	10.9	11.1	10.5	8.2	3.7
255	-2.9	-0.6	1.4	7.9	10.6	10.4	9.5	8.0	2.9
260	-3.5	-0.9	1.2	7.5	10.4	10.0	8.5	7.7	2.3
265	-4.2	-1.1	1.0	7.2	10.3	10.0	9.0	7.9	2.0
270	-4.2	-1.2	1.0	7.1	10.2	9.9	10.4	8.2	1.9
275	-4.2	-1.0	1.0	6.9	10.0	10.5	12.1	8.8	2.2
280	-4.1	-0.8	1.0	6.9	10.0	10.6	12.6	8.8	2.0
285	-3.9	-0.7	1.0	7.0	10.3	10.1	11.3	8.6	1.1
290	-3.5	-0.4	1.1	7.2	10.7	10.1	10.4	8.6	0.3
295	-2.4	-0.1	1.3	7.6	11.3	10.6	10.8	8.8	-3.1
300	-1.3	0.1	1.4	8.1	12.0	11.2	12.5	9.3	-0.2
305	-1.2	0.2	1.7	8.6	12.8	12.6	15.4	10.2	0.2
310	-1.3	0.5	2.1	9.1	13.6	13.3	16.6	10.7	0.5
315	-0.6	1.0	2.5	9.9	14.7	14.3	16.7	11.2	0.2
320	0.1	1.0	2.6	10.7	15.8	15.8	17.5	11.5	-0.4
325	0.3	0.7	2.9	11.6	16.4	16.9	17.8	10.9	-1.8
330	0.3	1.5	4.1	13.0	18.5	17.6	17.5	10.3	-1.4
335	0.4	2.4	5.4	14.2	19.6	18.3	18.1	10.4	-1.5
340	1.2	2.6	5.9	15.3	20.5	18.9	19.3	10.9	-1.4
345	0.3	2.5	5.7	14.6	22.2	19.5	20.5	12.3	-1.7
350	-1.6	3.7	4.2	13.0	21.5	21.1	20.7	12.4	-1.2
355	-2.6	3.1	4.3	12.2	15.6	16.8	17.2	9.4	-1.0
360	-3.7	-0.2	4.3	11.4	13.6	10.6	9.4	4.3	-1.7

TABLE VII CONCLUDED

V = 175 KT a_s = 0° L = 7100 LB D = 400 LB

(b) THEORETICAL (UNIFORM INFLOW)

	Blade Radial Station								
ψ	.25R	.40R	.55R	.75R	.85R	.90R	.95R	.97R	.99R
0	2.1	5.2	8.1	11.0	11.5	11.1	10.3	9.5	0.0
5	2.6	5.7	8.4	11.1	11.1	10.3	9.1	8.0	0.0
10	3.1	6.0	8.6	11.0	10.6	9.5	8.0	6.7	0.0
15	3.6	6.3	8.7	10.8	10.0	8.8	7.1	5.9	0.0
20	4.1	6.6	8.7	10.4	9.5	8.2	6.8	5.6	0.0
25	4.5	6.8	8.6	9.8	8.9	7.9	6.7	5.7	0.0
30	4.9	7.0	8.4	9.1	8.3	7.6	6.6	5.7	0.0
35	5.3	7.0	8.1	8.2	7.6	7.0	6.1	5.2	0.0
40	5.7	7.1	7.7	7.3	6.6	5.9	4.9	3.9	0.0
45	6.1	7.2	7.4	6.5	5.4	4.3	2.9	1.6	0.0
50	6.6	7.4	7.2	5.8	4.0	2.3	0.1	-1.8	0.0
55	7.1	7.8	7.4	5.3	2.5	0.0	-3.2	-5.8	0.0
60	7.7	8.4	7.9	5.1	1.2	-2.1	-6.2	-9.6	0.0
65	8.4	9.3	9.0	5.7	0.8	-3.3	-8.2	-12.1	0.0
70	9.1	10.4	10.4	6.6	1.0	-3.7	-9.4	-13.5	0.0
75	10.0	11.6	11.8	7.4	1.0	-4.2	-10.1	-14.3	0.0
80	10.8	12.7	12.8	7.5	0.2	-5.6	-12.1	-15.9	0.0
85	11.6	13.6	13.5	7.4	-0.8	-7.2	-14.3	-18.0	-0.1
90	12.4	14.4	14.1	7.4	-1.4	-8.4	-16.0	-19.7	-0.1
95	13.2	15.2	14.7	7.6	-1.8	-9.0	-17.0	-20.9	-0.1
100	13.8	15.8	15.2	7.5	-2.1	-9.6	-17.7	-22.1	-0.1
105	14.3	16.3	15.5	7.2	-2.7	-10.2	-18.2	-23.3	-0.1
110	14.6	16.6	15.7	6.7	-3.3	-10.7	-18.6	-24.6	-0.1
115	14.7	16.8	15.7	6.3	-3.9	-11.2	-18.8	-24.6	-0.1
120	14.7	16.8	15.5	5.6	-4.7	-11.9	-19.4	-25.0	-0.1
125	14.6	16.6	15.2	5.1	-5.2	-12.4	-19.6	-25.1	-0.1
130	14.4	16.3	14.9	4.7	-5.5	-12.4	-19.5	-24.7	-0.1
135	14.1	16.0	14.6	4.7	-5.1	-11.7	-18.5	-23.4	0.0
140	13.7	15.7	14.5	5.1	-4.0	-10.2	-16.4	-21.1	0.0
145	13.2	15.5	14.7	6.1	-2.3	-7.9	-13.5	-17.6	0.0
150	12.5	15.3	14.9	7.2	-0.3	-5.3	-10.2	-13.8	0.0
155	11.7	15.0	15.0	8.3	1.6	-2.8	-7.1	-10.1	0.0
160	10.6	14.5	15.0	9.3	3.3	-0.6	-4.2	-6.9	0.0
165	9.5	13.8	14.9	10.1	4.7	1.2	-2.0	-4.3	0.0
170	8.2	12.9	14.6	10.7	5.8	2.7	-0.2	-2.2	0.0
175	6.4	11.9	14.1	11.1	6.7	3.9	1.2	-0.7	0.0
180	3.5	10.8	13.4	11.4	7.5	4.9	2.4	0.6	0.0
185	2.3	9.5	12.7	11.5	8.2	5.8	3.4	1.8	0.0
190	1.6	8.2	11.8	11.6	8.8	6.6	4.3	2.9	0.0
195	1.1	6.6	10.9	11.6	9.3	7.4	5.5	4.2	0.0
200	0.7	4.5	9.9	11.6	9.7	8.2	6.6	5.4	0.0
205	0.4	2.4	8.8	11.4	10.1	8.8	7.5	6.5	0.0
210	0.2	1.6	7.7	11.2	10.4	9.4	8.3	7.5	0.0
215	0.1	1.1	6.4	10.9	10.7	10.0	9.1	8.4	0.0
220	0.1	0.8	5.1	10.4	10.9	10.5	9.8	9.2	0.0
225	0.1	0.5	4.0	9.8	10.9	10.8	10.4	10.0	0.0
230	0.0	0.3	3.6	9.0	10.7	10.9	10.8	10.6	0.0
235	-0.2	0.2	2.4	8.1	10.3	10.8	11.0	11.0	0.0
240	-0.5	0.1	1.9	7.2	9.7	10.6	11.2	11.4	0.0
245	-0.8	0.0	1.4	6.4	9.1	10.3	11.2	11.7	0.0
250	-1.2	0.0	1.1	5.6	8.5	9.9	11.1	11.9	0.0
255	-1.3	0.0	0.9	5.0	7.9	9.6	11.1	12.0	0.0
260	-1.5	0.0	0.7	4.5	7.5	9.3	10.9	12.0	0.0
265	-1.6	-0.1	0.5	4.2	7.3	9.1	10.8	12.0	0.0
270	-1.6	-0.1	0.4	4.0	7.2	9.0	10.8	12.0	0.0
275	-1.6	-0.1	0.4	3.9	7.2	9.1	10.8	11.9	0.0
280	-1.5	-0.1	0.3	4.0	7.3	9.2	10.9	12.0	0.0
285	-1.4	0.0	0.4	4.2	7.5	9.4	11.0	12.1	0.0
290	-1.3	0.0	0.5	4.5	7.8	9.6	11.3	12.4	0.0
295	-1.1	0.0	0.7	4.9	8.2	10.0	11.7	12.8	0.0
300	-0.9	0.0	0.9	5.4	8.7	10.5	12.1	13.2	0.0
305	-0.7	0.0	1.2	6.0	9.2	11.1	12.6	13.6	0.0
310	-0.4	0.1	1.6	6.6	9.9	11.6	13.1	14.0	0.0
315	-0.3	0.2	2.2	7.3	10.5	12.1	13.4	14.2	0.0
320	-0.1	0.5	2.7	8.0	11.1	12.5	13.6	14.3	0.0
325	0.0	0.9	3.4	8.7	11.5	12.8	13.7	14.2	0.0
330	0.0	1.3	4.1	9.3	11.8	12.9	13.6	14.0	0.0
335	0.1	1.9	4.9	9.8	12.0	12.8	13.4	13.7	0.0
340	0.3	2.6	5.7	10.2	12.0	12.8	13.2	13.3	0.0
345	0.7	3.3	6.4	10.5	12.0	12.6	12.8	12.8	0.0
350	1.1	4.0	7.1	10.7	12.0	12.3	12.2	12.0	0.0
355	1.6	4.6	7.6	10.9	11.8	11.8	11.4	10.9	0.0
360	2.1	5.2	8.1	11.0	11.5	11.1	10.3	9.5	0.0

TABLE VIII TIME HISTORIES OF AERODYNAMIC LOADING, LB/IN

V = 175 KT α_s=+3° L = 7500 LB D = 1190 LB

(a) EXPERIMENTAL

	Blade Radial Station								
ψ	.25R	.40R	.55R	.75R	.85R	.90R	.95R	.97R	.99R
0	-2.0	-1.9	2.0	9.7	3.8	-1.6	-1.9	-2.8	-2.5
5	0.4	-0.3	0.9	9.7	5.9	0.4	-0.9	-2.2	-3.0
10	2.3	3.5	2.3	5.7	4.1	0.1	-1.4	-2.1	-3.2
15	3.2	5.2	3.8	4.9	3.2	0.1	-1.3	-2.0	-3.5
20	3.4	3.7	4.8	6.9	5.7	2.5	0.2	-0.8	-3.6
25	2.4	3.7	6.3	8.8	8.1	4.1	3.1	0.7	-3.1
30	2.3	4.3	7.4	10.8	10.6	6.6	5.3	2.1	-2.8
35	3.1	5.0	8.1	12.7	12.7	8.5	7.0	3.1	-2.6
40	4.0	5.6	8.9	14.1	13.6	9.5	9.2	4.2	-2.5
45	3.7	6.5	9.8	14.3	13.4	10.2	12.0	7.5	-2.1
50	3.7	7.7	10.7	14.5	13.1	10.8	14.0	8.5	-1.7
55	4.2	8.8	11.6	14.7	12.8	10.6	14.3	7.6	-2.1
60	4.9	10.1	12.4	14.8	12.4	10.4	14.0	6.2	1.6
65	5.8	11.0	13.2	14.9	12.9	9.5	17.6	4.6	2.9
70	6.8	11.9	13.8	15.5	13.0	10.1	20.1	2.9	2.3
75	7.9	12.8	14.3	16.0	12.1	11.7	16.1	0.9	0.2
80	9.2	13.6	15.1	16.3	10.3	12.2	6.4	-0.2	-2.6
85	10.5	14.7	15.8	16.3	6.9	5.3	-2.2	-0.5	-5.6
90	11.7	15.7	16.4	15.6	2.1	-4.6	-5.3	-0.6	-7.1
95	12.9	16.6	16.9	13.5	-3.7	-14.6	-10.4	-1.4	-8.6
100	14.0	17.2	17.1	9.5	-8.7	-18.8	-19.5	-3.0	-1.0
105	14.8	17.7	17.2	4.3	-11.8	-21.1	-22.7	-4.9	-10.6
110	15.4	18.4	17.3	0.6	-14.1	-21.3	-25.2	-7.2	-11.5
115	16.1	19.1	17.4	-1.1	-15.0	-16.2	-26.1	-11.1	-12.6
120	16.5	19.6	17.4	-1.7	-15.0	-13.4	-20.0	-13.4	-13.0
125	16.9	20.0	17.0	-1.7	-13.6	-14.4	-15.2	-13.6	-11.1
130	17.2	20.4	16.1	-1.4	-11.8	-13.5	-15.7	-13.8	-10.2
135	17.4	20.5	14.8	-0.6	9.4	-10.7	-14.0	-11.1	-9.5
140	17.6	20.4	14.0	1.2	-7.2	-8.2	-10.3	-6.7	-8.0
145	17.4	20.1	14.2	2.8	-5.3	-6.3	-7.3	-5.0	-6.5
150	17.3	19.5	14.7	3.9	-2.9	-4.0	-6.2	-3.9	-5.8
155	17.0	18.8	14.5	4.6	-1.5	-3.0	-4.6	-3.3	-4.9
160	16.7	17.9	14.4	5.3	-0.4	-2.3	-5.4	-3.2	-5.4
165	16.7	16.9	14.8	6.2	0.9	-1.6	-6.0	-3.0	-5.9
170	16.5	15.6	14.8	7.3	2.4	0.0	-3.9	-1.8	-5.0
175	15.2	14.4	14.7	8.4	4.0	2.3	-0.1	-0.3	-3.7
180	13.7	13.0	14.5	9.8	5.8	4.2	1.6	0.9	-2.4
185	12.0	11.5	14.1	10.8	7.7	5.4	1.5	1.5	-1.9
190	9.2	10.1	13.3	11.8	9.9	7.2	0.1	2.2	-1.5
195	6.4	8.9	12.4	12.7	12.1	9.6	1.2	3.3	-0.5
200	4.8	8.4	11.6	13.3	13.5	11.3	2.6	4.4	0.2
205	3.6	6.9	10.5	13.6	14.2	12.2	3.8	5.2	1.0
210	2.3	5.8	9.3	13.0	14.3	12.2	5.0	5.7	1.2
215	1.2	5.0	8.1	12.6	13.8	11.8	6.3	6.0	1.7
220	0.9	3.8	7.2	12.0	13.1	11.7	7.7	6.4	2.3
225	0.6	2.8	6.8	11.3	12.7	11.7	8.7	6.8	2.3
230	0.3	2.3	6.1	10.5	12.2	11.9	9.6	7.1	2.6
235	0.2	1.6	5.1	9.9	11.5	11.7	10.4	7.3	3.2
240	0.1	0.9	4.1	9.2	10.9	11.2	10.5	7.3	3.5
245	0.0	0.6	3.4	8.6	10.4	10.7	10.5	7.4	3.1
250	-0.1	0.4	2.8	8.2	10.1	10.3	10.2	7.2	2.6
255	-0.3	0.3	2.5	7.8	9.9	9.9	1.0	6.9	2.0
260	-0.4	0.3	2.0	7.5	9.6	9.7	9.6	6.9	1.8
265	-0.4	0.2	1.8	7.3	9.3	9.8	10.6	7.1	2.0
270	-0.4	0.3	1.6	7.1	9.4	9.7	10.9	7.1	1.7
275	-0.4	0.4	1.4	7.0	9.2	9.4	10.7	7.2	1.1
280	-0.3	0.3	1.2	7.0	9.3	9.0	9.1	7.0	-0.1
285	-0.2	0.4	1.0	7.0	9.6	8.9	8.9	6.9	-0.4
290	-0.0	0.4	1.1	7.2	10.0	8.9	8.2	6.9	-0.9
295	0.0	0.5	1.3	7.4	10.6	9.1	8.4	7.0	-1.6
300	0.1	0.6	1.5	7.4	11.0	9.7	9.8	7.2	-1.6
305	0.3	0.7	2.0	8.1	11.6	10.5	11.1	7.6	-1.2
310	0.3	0.9	2.4	9.0	12.4	11.4	12.4	8.1	-1.5
315	0.4	1.1	2.9	9.8	13.0	12.7	15.1	8.9	-0.7
320	0.6	1.3	3.4	10.9	14.0	13.6	15.7	9.3	-0.7
325	0.8	1.9	3.8	12.1	15.1	14.2	16.3	9.2	-0.9
330	1.0	2.2	4.3	12.8	16.3	14.9	16.5	9.2	-0.9
335	2.0	2.9	4.8	12.9	16.9	15.2	16.2	9.0	-1.2
340	1.3	4.4	5.4	12.2	16.2	14.6	15.9	8.3	-1.6
345	-1.5	6.5	6.3	10.7	13.2	11.9	14.8	7.1	-1.1
350	-3.0	6.3	5.2	10.7	11.6	7.8	11.5	4.8	-1.2
355	-2.8	1.8	2.3	11.0	9.1	2.0	1.7	-1.1	-1.7
360	-2.0	-1.9	2.0	9.7	3.8	-1.6	-1.9	-2.8	-2.5

TABLE VIII CONCLUDED

V = 175 KT a_s = -5° L = 7300 LB B = 2 [illegible]

(b) THEORETICAL (UNIFORM INFLOW)

	Blade Radial Station								
ψ	.25R	.40R	.55R	.75R	.85R	.90R	.95R	.97R	.99R
0	4.3	7.4	9.3	8.5	4.7	1.5	-2.1	-4.8	0.0
5	5.1	7.8	9.6	8.3	4.1	0.8	-2.7	-5.3	0.0
10	5.7	8.3	9.7	7.9	3.8	0.7	-2.6	-5.0	0.0
15	6.3	8.6	9.7	7.5	3.7	0.9	-1.9	-4.0	0.0
20	6.9	8.9	9.6	7.1	3.8	1.5	-0.9	-2.8	0.0
25	7.5	9.1	9.3	6.8	4.0	2.1	-0.1	-1.8	0.0
30	8.2	9.3	9.0	6.5	4.1	2.4	0.3	-1.3	0.0
35	8.8	9.4	8.8	6.2	4.0	2.2	0.0	-1.8	0.0
40	9.4	9.7	8.8	5.9	3.4	1.3	-1.2	-3.3	0.0
45	10.0	10.3	9.1	5.7	2.4	-0.1	-3.2	-5.8	0.0
50	10.7	11.0	9.8	5.5	1.2	-2.0	-6.0	-9.2	0.0
55	11.4	11.9	10.8	5.7	0.2	-4.0	-8.9	-12.9	0.0
60	12.3	13.1	12.1	6.5	-0.1	-5.2	-11.2	-15.9	0.0
65	13.3	14.4	13.8	7.9	0.3	-5.7	-12.6	-18.1	0.0
70	14.4	15.8	15.3	9.1	0.6	-6.2	-13.9	-19.6	-0.1
75	15.4	17.0	16.5	9.6	0.2	-7.4	-15.8	-21.2	-0.1
80	16.4	18.0	17.2	9.4	-1.0	-9.2	-18.3	-23.3	-0.1
85	17.4	18.9	17.8	8.9	-2.2	-10.9	-20.5	-25.3	-0.1
90	18.2	19.7	18.3	8.4	-3.3	-12.2	-21.9	-26.8	-0.1
95	18.8	20.4	18.7	7.8	-4.3	-13.4	-23.1	-28.3	-0.1
100	19.3	20.8	18.8	7.1	-5.4	-14.6	-24.2	-30.1	-0.1
105	19.6	21.1	18.9	6.4	-6.4	-15.6	-25.1	-32.2	-0.1
110	19.7	21.1	18.7	5.8	-7.3	-16.4	-25.8	-33.0	-0.1
115	19.7	20.9	18.3	4.8	-8.4	-17.5	-26.9	-34.0	-0.1
120	19.5	20.6	17.7	3.9	-9.3	-18.4	-27.7	-34.8	-0.1
125	19.1	20.2	17.1	3.2	-9.9	-18.9	-27.9	-34.7	-0.1
130	18.7	19.8	16.6	2.7	-10.1	-18.7	-27.6	-34.0	-0.1
135	18.1	19.4	16.3	2.7	-9.7	-17.9	-26.2	-32.4	-0.1
140	17.4	19.0	16.2	3.0	-8.7	-16.4	-23.9	-29.7	-0.1
145	16.4	18.8	16.3	3.7	-7.2	-14.4	-21.4	-26.3	0.0
150	15.0	18.5	16.4	4.7	-5.5	-12.0	-18.4	-22.9	0.0
155	12.8	17.9	16.4	5.8	-3.5	-9.4	-15.1	-19.2	0.0
160	9.3	17.4	16.4	6.9	-1.6	-6.9	-12.1	-15.8	0.0
165	6.9	16.6	16.3	7.6	-0.2	-5.2	-9.8	-13.2	0.0
170	5.0	15.3	16.1	8.2	0.9	-3.7	-8.0	-11.1	0.0
175	4.0	13.6	15.8	8.8	2.0	-2.3	-6.4	-9.3	0.0
180	3.4	10.5	15.4	9.4	3.0	-1.1	-4.9	-7.6	0.0
185	2.8	7.5	14.9	9.9	3.8	-0.1	-3.6	-6.2	0.0
190	2.2	5.3	14.0	10.5	4.7	1.0	-2.4	-4.8	0.0
195	1.8	4.0	12.8	11.2	5.9	2.4	-0.8	-3.1	0.0
200	1.3	3.2	10.9	11.9	7.3	4.1	1.0	-1.2	0.0
205	0.9	2.6	8.1	12.3	8.7	5.8	2.9	0.8	0.0
210	0.6	2.1	5.8	12.3	9.6	7.1	4.4	2.4	0.0
215	0.5	1.7	4.2	12.0	10.2	8.1	5.8	4.0	0.0
220	0.6	1.4	3.2	11.4	10.6	9.0	7.0	5.4	0.0
225	0.7	1.1	2.6	10.7	10.6	9.5	8.1	6.8	0.0
230	0.8	0.8	2.2	9.8	10.3	9.8	8.9	8.0	0.0
235	0.8	0.6	1.8	8.9	9.9	9.8	9.4	8.9	0.0
240	0.9	0.5	1.5	8.0	9.4	9.7	9.7	9.5	0.0
245	1.1	0.4	1.2	7.3	8.9	9.4	9.8	9.9	0.0
250	1.3	0.3	1.0	6.6	8.4	9.2	9.7	10.0	0.0
255	1.5	0.3	0.9	6.0	8.0	9.0	9.7	10.1	0.0
260	1.6	0.3	0.8	5.6	7.8	8.8	9.6	10.1	0.0
265	1.7	0.3	0.7	5.4	7.6	8.7	9.5	10.1	0.0
270	1.7	0.3	0.7	5.3	7.6	8.7	9.5	10.1	0.0
275	1.6	0.2	0.6	5.3	7.6	8.7	9.6	10.1	0.0
280	1.5	0.2	0.7	5.4	7.7	8.8	9.7	10.2	0.0
285	1.4	0.2	0.7	5.6	7.8	8.9	9.7	10.2	0.0
290	1.2	0.2	0.9	5.9	8.0	9.0	9.8	10.2	0.0
295	1.0	0.2	1.0	6.2	8.3	9.1	9.8	10.1	0.0
300	0.8	0.2	1.2	6.6	8.5	9.2	9.7	9.9	0.0
305	0.5	0.4	1.5	7.0	8.7	9.2	9.5	9.6	0.0
310	0.4	0.5	3.1	7.4	8.8	9.2	9.3	9.1	0.0
315	0.4	0.7	3.9	7.8	8.9	9.1	8.9	8.7	0.0
320	0.3	0.9	4.7	8.1	8.9	8.8	8.5	8.1	0.0
325	0.3	1.2	5.5	8.4	8.8	8.5	7.9	7.4	0.0
330	0.4	1.6	6.3	8.6	8.5	8.0	7.1	6.4	0.0
335	0.6	3.1	7.0	8.7	8.1	7.2	6.0	4.9	0.0
340	0.8	4.7	7.5	8.7	7.5	6.2	4.5	3.1	0.0
345	1.1	5.6	8.1	8.7	6.9	5.0	2.7	0.9	0.0
350	1.4	6.3	8.5	8.7	6.2	3.8	0.9	-1.4	0.0
355	3.1	6.9	8.9	8.7	5.5	2.5	-0.8	-3.4	0.0
360	4.3	7.4	9.3	8.5	4.7	1.5	-2.1	-4.8	0.0

TABLE IX HARMONICS OF AERODYNAMIC LOADING, LB/IN

V = 110 KT α_s = -5° L = 8300 LB D = -750 LB

BLADE STATION = .25R

N	EXPERIMENTAL A(N)	EXPERIMENTAL B(N)	UNIFORM INFLOW A(N)	UNIFORM INFLOW B(N)	VARIABLE INFLOW A(N)	VARIABLE INFLOW B(N)
0	1.98		2.01		1.63	
1	2.55	-2.49	1.48	-2.93	1.35	-1.90
2	-0.77	1.44	0.53	0.96	0.01	0.75
3	0.24	-0.52	-0.13	-0.33	-0.06	-0.27
4	0.05	0.18	0.07	-0.01	-0.16	-0.10
5	0.19	-0.19	0.05	-0.07	0.01	-0.18
6	0.09	0.11	-0.03	-0.06	0.02	-0.08
7	0.11	0.11	-0.07	-0.00	0.03	-0.07
8	0.12	0.11	-0.01	-0.01	0.07	0.01
9	0.06	0.16	-0.02	0.00	0.01	0.06
10	0.03	0.15	-0.01	0.02	0.00	-0.01

BLADE STATION = .40R

N	EXPERIMENTAL A(N)	EXPERIMENTAL B(N)	UNIFORM INFLOW A(N)	UNIFORM INFLOW B(N)	VARIABLE INFLOW A(N)	VARIABLE INFLOW B(N)
0	3.63		4.33		3.95	
1	2.88	-3.24	2.19	-4.35	1.93	-3.07
2	-0.80	1.26	-0.65	0.84	-0.78	0.58
3	0.21	-0.26	-0.16	-0.37	-0.25	-0.18
4	0.10	0.08	-0.09	-0.08	-0.11	-0.08
5	0.06	0.02	-0.00	-0.01	-0.17	0.06
6	0.09	-0.01	-0.00	-0.00	-0.05	-0.18
7	0.05	-0.02	-0.00	0.00	0.01	0.03
8	0.02	-0.03	-0.00	0.00	-0.13	-0.06
9	-0.	-0.06	-0.00	0.00	0.01	-0.15
10	0.02	-0.	0.00	0.00	0.04	-0.03

BLADE STATION = .55R

N	EXPERIMENTAL A(N)	EXPERIMENTAL B(N)	UNIFORM INFLOW A(N)	UNIFORM INFLOW B(N)	VARIABLE INFLOW A(N)	VARIABLE INFLOW B(N)
0	7.71		7.23		7.20	
1	2.71	-2.71	2.22	-3.88	2.23	-2.66
2	-1.93	0.23	-1.64	0.53	-1.83	-0.04
3	-0.19	0.08	-0.27	-0.16	-0.34	0.47
4	-0.12	0.09	-0.10	-0.10	-0.38	-0.14
5	-0.19	0.04	0.01	-0.01	-0.06	-0.08
6	0.07	0.20	0.01	0.00	0.01	-0.01
7	-0.06	0.20	0.01	-0.00	0.03	0.11
8	0.02	0.07	-0.00	0.00	-0.04	0.00
9	-0.03	0.14	0.00	-0.00	0.03	0.10
10	-0.	0.07	0.00	0.00	-0.08	0.02

BLADE STATION = .75R

N	EXPERIMENTAL A(N)	EXPERIMENTAL B(N)	UNIFORM INFLOW A(N)	UNIFORM INFLOW B(N)	VARIABLE INFLOW A(N)	VARIABLE INFLOW B(N)
0	11.74		11.15		11.59	
1	-0.54	-0.38	0.27	-0.15	0.54	-0.13
2	-1.99	-0.65	-2.68	-0.29	-2.20	0.08
3	-0.60	0.46	-0.22	-0.09	-0.74	0.37
4	-0.69	0.30	0.02	-0.03	-0.16	0.56
5	-0.03	-0.07	0.04	-0.03	-0.06	0.17
6	0.19	0.36	0.03	0.01	-0.01	-0.10
7	-0.19	0.05	0.01	-0.01	-0.00	0.04
8	0.02	-0.	-0.00	-0.00	-0.10	0.02
9	-0.02	0.15	0.00	-0.01	0.12	0.01
10	-0.05	-0.04	-0.00	-0.00	0.03	0.07

BLADE STATION = .85R

N	EXPERIMENTAL A(N)	EXPERIMENTAL B(N)	UNIFORM INFLOW A(N)	UNIFORM INFLOW B(N)	VARIABLE INFLOW A(N)	VARIABLE INFLOW B(N)
0	14.08		12.43		12.62	
1	-2.90	3.02	-1.84	3.23	-1.52	2.17
2	-2.78	-1.09	-3.18	-0.78	-2.06	-0.10
3	-0.42	0.91	-0.39	-0.20	-0.65	0.65
4	-1.23	0.81	0.07	0.02	-0.34	0.62
5	-0.33	-0.28	0.04	0.00	0.20	0.32
6	0.60	0.50	0.00	0.00	0.11	0.11
7	-0.20	0.43	0.00	0.00	-0.08	-0.02
8	-0.27	-0.03	0.00	0.00	-0.07	-0.05
9	0.04	-0.08	-0.01	0.01	0.07	0.14
10	0.16	0.18	0.00	0.00	0.06	0.06

BLADE STATION = .90R

N	EXPERIMENTAL A(N)	EXPERIMENTAL B(N)	UNIFORM INFLOW A(N)	UNIFORM INFLOW B(N)	VARIABLE INFLOW A(N)	VARIABLE INFLOW B(N)
0	12.32		12.73		12.58	
1	-2.59	3.58	-3.15	5.43	-2.81	3.58
2	-2.72	-1.23	-3.50	-1.01	-2.04	-0.21
3	-0.04	0.86	0.02	-0.31	-0.35	0.70
4	-1.30	1.17	0.14	0.07	-0.34	0.76
5	-0.80	-0.26	0.01	0.07	0.14	0.44
6	0.55	0.32	-0.02	0.01	0.17	0.15
7	0.08	0.56	0.00	-0.01	-0.01	0.02
8	-0.33	0.25	0.01	0.00	-0.12	0.01
9	-0.26	-0.16	0.01	-0.01	-0.05	0.09
10	0.26	-0.09	0.01	0.01	0.02	0.02

BLADE STATION = .95R

N	EXPERIMENTAL A(N)	EXPERIMENTAL B(N)	UNIFORM INFLOW A(N)	UNIFORM INFLOW B(N)	VARIABLE INFLOW A(N)	VARIABLE INFLOW B(N)
0	7.94		12.76		11.83	
1	-5.58	4.61	-4.32	7.62	-3.87	4.52
2	-1.36	-0.55	-3.83	-1.19	-2.03	-0.22
3	0.53	0.93	0.15	-0.45	0.01	0.61
4	-1.41	1.20	0.23	0.12	-0.21	0.87
5	-0.99	-0.09	-0.01	0.12	0.03	0.58
6	0.44	0.20	-0.02	0.02	0.16	0.16
7	0.35	0.30	-0.00	-0.01	0.08	0.04
8	-0.22	0.35	-0.01	-0.01	-0.16	0.07
9	-0.40	0.06	0.00	-0.01	-0.19	0.01
10	0.01	-0.11	-0.01	-0.01	-0.03	-0.00

BLADE STATION = .97R

N	EXPERIMENTAL A(N)	EXPERIMENTAL B(N)	UNIFORM INFLOW A(N)	UNIFORM INFLOW B(N)	VARIABLE INFLOW A(N)	VARIABLE INFLOW B(N)
0	5.89		12.64		10.33	
1	-2.61	3.81	-5.12	9.23	-4.44	4.60
2	-0.90	-0.35	-4.09	-1.30	-2.00	-0.12
3	0.50	0.55	0.24	-0.56	0.26	0.47
4	-0.81	1.08	0.30	0.16	-0.01	0.88
5	-1.78	-0.10	-0.00	0.15	0.00	0.68
6	0.29	0.01	-0.03	0.03	0.09	0.15
7	0.27	0.16	-0.01	-0.00	0.12	0.02
8	0.03	0.23	-0.02	-0.01	-0.15	0.15
9	-0.24	0.07	-0.01	-0.00	-0.28	0.01
10	-0.07	-0.17	-0.01	-0.01	-0.09	-0.01

BLADE STATION = .99R

N	EXPERIMENTAL A(N)	EXPERIMENTAL B(N)	UNIFORM INFLOW A(N)	UNIFORM INFLOW B(N)	VARIABLE INFLOW A(N)	VARIABLE INFLOW B(N)
0	0.52		-	-	7.43	
1	0.19	1.93	-	-	-4.03	3.58
2	-0.02	-0.81	-	-	-1.59	-0.02
3	0.36	0.03	-	-	0.29	0.33
4	-0.21	0.38	-	-	0.08	0.70
5	-0.30	-0.06	-	-	-0.02	0.59
6	0.13	0.08	-	-	0.03	0.11
7	0.13	0.05	-	-	0.11	-0.00
8	-0.02	-0.17	-	-	-0.10	0.16
9	-0.09	-0.	-	-	-0.27	0.02
10	0.05	-0.05	-	-	-0.12	-0.01

TABLE X HARMONICS OF AERODYNAMIC LOADING, LB/IN

V = 110 KT α_s = 0° I = 8200 LB D = 50 LB

BLADE STATION = .25R

	EXPERIMENTAL		UNIFORM INFLOW	
N	A(N)	B(N)	A(N)	B(N)
0	2.80		3.15	
1	2.48	-3.17	1.44	-4.07
2	-0.48	1.48	0.58	0.95
3	0.08	-0.37	-0.15	-0.36
4	-0.07	0.15	0.01	-0.01
5	0.12	-0.	0.01	-0.05
6	0.01	0.13	-0.02	-0.00
7	0.06	0.12	-0.01	0.00
8	-0.01	0.20	0.00	0.01
9	-0.02	0.18	0.01	-0.00
10	-0.04	0.19	0.00	0.00

BLADE STATION = .40R

	EXPERIMENTAL		UNIFORM INFLOW	
N	A(N)	B(N)	A(N)	B(N)
0	4.57		5.61	
1	3.30	-3.91	2.11	-4.98
2	-0.48	1.19	-0.55	0.88
3	0.27	-0.	-0.19	-0.28
4	0.31	0.12	-0.10	-0.06
5	-0.	-0.02	-0.00	-0.00
6	0.03	-0.08	-0.00	-0.00
7	-0.04	-0.07	-0.00	0.01
8	-0.03	-0.15	0.00	0.00
9	-0.03	-0.11	-0.00	0.00
10	-0.05	-0.09	0.00	0.00

BLADE STATION = .55R

	EXPERIMENTAL		UNIFORM INFLOW	
N	A(N)	B(N)	A(N)	B(N)
0	8.58		8.08	
1	2.72	-3.07	2.10	-4.12
2	-1.59	0.27	-1.40	0.59
3	-0.12	0.71	-0.24	-0.06
4	-0.28	0.40	-0.11	-0.07
5	-0.18	0.05	0.00	-0.01
6	0.09	0.37	0.00	-0.00
7	-0.10	0.41	0.01	-0.01
8	0.33	0.09	-0.00	0.00
9	-0.04	0.25	0.00	-0.00
10	0.17	0.13	0.00	0.00

BLADE STATION = .75R

	EXPERIMENTAL		UNIFORM INFLOW	
N	A(N)	B(N)	A(N)	B(N)
0	10.96		10.36	
1	-0.66	-0.32	0.19	0.96
2	-0.70	-0.65	-2.27	-0.23
3	-0.53	1.24	-0.18	-0.00
4	-0.82	0.37	0.02	-0.02
5	0.01	-0.19	0.02	-0.03
6	0.21	0.31	0.02	0.00
7	-0.50	-0.05	0.01	-0.01
8	-0.20	-0.03	-0.00	-0.01
9	-0.02	0.30	0.00	-0.01
10	-0.14	0.06	0.00	-0.00

BLADE STATION = .85R

	EXPERIMENTAL		UNIFORM INFLOW	
N	A(N)	B(N)	A(N)	B(N)
0	11.65		10.24	
1	-2.99	3.31	-1.79	3.68
2	-1.22	-1.45	-2.69	-0.70
3	0.11	1.84	-0.05	-0.13
4	-1.31	1.16	0.08	0.01
5	-0.41	-0.20	0.03	-0.00
6	0.75	0.45	-0.00	0.00
7	-0.17	0.44	0.00	0.00
8	-0.39	0.07	0.00	-0.00
9	0.18	-0.	-0.01	0.01
10	0.40	0.28	0.00	0.00

BLADE STATION = .90R

	EXPERIMENTAL		UNIFORM INFLOW	
N	A(N)	B(N)	A(N)	B(N)
0	10.92		9.67	
1	-2.42	4.04	-2.99	6.02
2	-1.30	-1.47	-2.97	-0.93
3	0.51	1.60	0.06	-0.27
4	1.04	1.54	0.15	0.04
5	1.76	0.19	0.02	0.05
6	0.64	0.38	-0.01	0.01
7	0.20	0.42	-0.00	0.00
8	0.30	0.28	0.01	-0.00
9	0.11	0.01	0.00	-0.01
10	0.37	0.14	0.01	0.00

BLADE STATION = .95R

	EXPERIMENTAL		UNIFORM INFLOW	
N	A(N)	B(N)	A(N)	B(N)
0	4.75		8.85	
1	5.30	4.90	-4.06	8.35
2	-0.03	-0.96	-3.27	-1.10
3	0.99	1.41	0.17	-0.42
4	-1.32	1.86	0.24	0.06
5	-1.06	0.45	0.03	0.09
6	0.61	0.24	-0.00	0.03
7	0.29	0.47	-0.00	0.00
8	-0.21	0.24	-0.01	-0.00
9	-0.23	0.17	-0.01	-0.01
10	0.16	0.44	-0.01	-0.01

BLADE STATION = .97R

	EXPERIMENTAL		UNIFORM INFLOW	
N	A(N)	B(N)	A(N)	B(N)
0	4.79		8.13	
1	-2.44	4.06	-4.78	10.06
2	-3.17	-0.66	-3.51	-1.20
3	0.93	0.84	0.26	-0.55
4	-0.62	1.39	0.32	0.08
5	-0.73	0.32	0.04	0.11
6	0.29	0.13	-0.01	0.04
7	0.21	0.19	-0.00	0.00
8	-0.33	0.16	-0.01	0.01
9	-0.13	0.12	-0.02	0.01
10	-0.09	0.15	-0.01	-0.01

BLADE STATION = .99R

	EXPERIMENTAL		UNIFORM INFLOW	
N	A(N)	B(N)	A(N)	B(N)
0	-1.07		-	
1	-0.02	1.67	-	-
2	0.21	-1.02	-	-
3	0.27	0.13	-	-
4	-0.21	0.28	-	-
5	-0.31	-0.01	-	-
6	0.02	0.12	-	-
7	0.05	0.09	-	-
8	0.05	0.05	-	-
9	0.04	0.09	-	-
10	0.16	0.22	-	-

TABLE XI HARMONICS OF AERODYNAMIC LOADING, LB/IN

V = 110 KT α_s = +5° L = 8100 LB D = 850 LB

BLADE STATION = .25R

	EXPERIMENTAL		UNIFORM INFLOW	
N	A(N)	B(N)	A(N)	B(N)
0	3.84		4.20	
1	2.86	-3.75	1.05	-5.36
2	-0.38	1.42	0.83	1.07
3	-0.02	-0.14	-0.38	-0.53
4	-0.09	0.12	0.06	0.15
5	0.01	0.06	-0.07	-0.15
6	0.15	0.09	0.04	0.14
7	0.12	0.10	-0.03	-0.09
8	0.22	0.24	0.03	0.07
9	0.10	0.16	-0.00	-0.06
10	0.11	0.24	0.01	0.05

BLADE STATION = .40R

	EXPERIMENTAL		UNIFORM INFLOW	
N	A(N)	B(N)	A(N)	B(N)
0	5.92		6.84	
1	3.49	-4.55	1.86	-5.90
2	-0.37	1.11	-0.62	1.14
3	0.29	0.26	0.02	-0.19
4	-0.08	0.26	-0.19	-0.15
5	0.37	0.12	-0.01	0.09
6	0.07	-0.13	0.05	-0.02
7	-0.04	-0.11	-0.03	0.00
8	-0.08	-0.09	0.01	0.02
9	-0.11	-0.03	-0.01	-0.02
10	-0.07	-0.	-0.02	0.02

BLADE STATION = .55R

	EXPERIMENTAL		UNIFORM INFLOW	
N	A(N)	B(N)	A(N)	B(N)
0	9.35		9.10	
1	2.75	-3.43	2.01	-4.31
2	-0.71	0.48	-1.18	0.60
3	0.07	1.02	-0.21	0.08
4	-0.38	0.57	-0.10	-0.06
5	-0.23	0.33	-0.03	-0.01
6	0.15	0.20	0.01	-0.01
7	0.05	0.24	-0.00	-0.0.
8	0.06	0.13	-0.01	0.03
9	0.01	0.09	0.00	-0.00
10	0.07	0.04	-0.00	0.00

BLADE STATION = .75R

	EXPERIMENTAL		UNIFORM INFLOW	
N	A(N)	B(N)	A(N)	B(N)
0	10.52		9.70	
1	-0.92	-0.19	0.18	0.36
2	0.68	-0.96	-1.79	-0.23
3	0.07	2.10	-0.13	0.11
4	-0.42	0.57	0.03	0.02
5	0.06	0.35	-0.05	-0.07
6	0.50	0.35	-0.00	0.01
7	-0.15	0.21	0.01	-0.03
8	0.06	-0.01	-0.01	-0.01
9	0.17	0.27	0.02	-0.01
10	0.02	0.20	-0.01	-0.00

BLADE STATION = .85R

	EXPERIMENTAL		UNIFORM INFLOW	
N	A(N)	B(N)	A(N)	B(N)
0	9.77		8.16	
1	-3.35	3.86	-1.66	4.21
2	0.41	-1.84	-2.08	-0.69
3	0.97	2.51	0.03	-0.06
4	-0.74	1.59	0.10	0.06
5	-0.45	0.52	0.00	-0.03
6	0.71	0.13	-0.02	0.04
7	0.17	0.37	0.00	-0.01
8	-0.24	0.03	-0.01	-0.02
9	-0.01	0.09	0.01	0.01
10	0.10	0.19	-0.01	-0.00

BLADE STATION = .90R

	EXPERIMENTAL		UNIFORM INFLOW	
N	A(N)	B(N)	A(N)	B(N)
0	9.37		6.69	
1	-2.70	4.67	-2.74	6.68
2	0.31	-1.83	-2.29	-0.91
3	1.23	2.18	0.16	-0.22
4	-0.52	1.87	0.18	0.08
5	-0.81	0.88	0.05	0.04
6	0.44	0.12	-0.00	0.06
7	0.42	0.32	-0.02	0.01
8	-0.08	0.30	-0.02	0.00
9	-0.17	0.19	0.01	-0.00
10	0.13	0.08	-0.01	0.00

BLADE STATION = .95R

	EXPERIMENTAL		UNIFORM INFLOW	
N	A(N)	B(N)	A(N)	B(N)
0	8.49		5.00	
1	-5.04	4.92	-3.69	9.13
2	0.73	-1.57	-2.53	-1.07
3	1.71	1.84	0.29	-0.40
4	-0.23	2.11	0.27	0.08
5	-0.99	1.16	0.10	0.09
6	0.23	0.19	0.03	0.09
7	0.50	0.27	-0.04	0.02
8	0.08	0.29	-0.04	0.04
9	-0.20	0.32	-0.01	0.01
10	-0.	0.05	-0.03	-0.01

BLADE STATION = .97R

	EXPERIMENTAL		UNIFORM INFLOW	
N	A(N)	B(N)	A(N)	B(N)
0	4.18		3.65	
1	-2.37	4.20	-4.31	10.93
2	0.48	-1.06	-2.72	-1.16
3	1.36	0.98	0.38	-0.55
4	-0.	1.51	0.34	0.08
5	-0.81	0.87	0.15	0.13
6	0.33	0.06	0.04	0.10
7	0.30	0.13	-0.05	0.01
8	0.10	0.16	-0.04	0.08
9	-0.10	0.27	-0.01	0.03
10	-0.04	0.14	-0.03	-0.00

BLADE STATION = .99R

	EXPERIMENTAL		UNIFORM INFLOW	
N	A(N)	B(N)	A(N)	B(N)
0	0.21		-	
1	-0.51	1.87	-	-
2	0.35	-1.10	-	-
3	0.24	0.30	-	-
4	-0.16	0.38	-	-
5	-0.30	0.09	-	-
6	0.11	-0.06	-	-
7	0.15	0.06	-	-
8	-0.	0.04	-	-
9	-0.03	0.11	-	-
10	0.06	0.09	-	-

TABLE XII HARMONICS OF AERODYNAMIC LOADING, LB/IN

V = 150 KT α_s = -5° L = 8500 LB D = -650 LB

BLADE STATION = .25R

N	EXPERIMENTAL A(N)	EXPERIMENTAL B(N)	UNIFORM INFLOW A(N)	UNIFORM INFLOW B(N)	VARIABLE INFLOW A(N)	VARIABLE INFLOW B(N)
0	1.77		2.47		2.36	
1	3.74	-3.91	2.20	-4.21	2.06	-2.32
2	-2.10	2.44	0.21	1.60	0.14	1.65
3	-0.03	-0.77	-0.46	-0.44	-0.34	-0.83
4	0.43	0.44	0.32	0.08	-0.23	-0.13
5	0.30	-0.28	0.17	-0.20	0.02	-0.18
6	0.07	-0.08	0.02	-0.00	-0.04	-0.20
7	0.14	-0.12	0.05	-0.05	0.19	-0.21
8	0.14	0.13	-0.01	-0.04	0.26	-0.10
9	0.28	0.09	-0.00	-0.01	0.16	0.23
10	0.27	-0.06	-0.00	-0.02	-0.12	0.06

BLADE STATION = .40R

N	EXPERIMENTAL A(N)	EXPERIMENTAL B(N)	UNIFORM INFLOW A(N)	UNIFORM INFLOW B(N)	VARIABLE INFLOW A(N)	VARIABLE INFLOW B(N)
0	4.34		4.87		4.42	
1	4.29	-3.74	3.02	-5.26	3.15	-3.95
2	-1.78	2.10	-0.98	1.64	-1.55	1.42
3	0.57	-1.04	-0.35	-1.00	-0.07	-0.62
4	0.23	0.10	-0.32	-0.33	-0.74	-0.43
5	0.37	0.04	0.05	-0.13	0.20	-0.13
6	0.12	0.13	-0.00	0.02	-0.1.	-0.19
7	0.37	0.07	-0.05	0.03	0.04	-0.19
8	0.01	-0.	0.01	0.01	0.16	0.00
9	-0.32	0.17	0.04	0.02	-0.15	0.01
10	-0.08	0.06	0.01	-0.01	-0.01	-0.14

BLADE STATION = .55R

N	EXPERIMENTAL A(N)	EXPERIMENTAL B(N)	UNIFORM INFLOW A(N)	UNIFORM INFLOW B(N)	VARIABLE INFLOW A(N)	VARIABLE INFLOW B(N)
0	6.82		7.32		7.40	
1	3.83	-3.46	3.08	-5.08	3.20	-3.94
2	-3.17	0.59	-2.96	0.99	-2.96	0.88
3	0.55	-0.87	-0.59	-0.54	-0.40	-0.37
4	0.08	0.10	-0.37	-0.37	-0.40	-0.00
5	0.16	0.09	0.09	-0.10	-0.17	-0.09
6	0.17	0.20	0.10	0.06	0.12	0.07
7	-0.	0.22	-0.05	0.05	-0.13	0.01
8	-0.15	-0.01	-0.00	-0.04	-0.03	-0.11
9	0.06	0.06	0.03	0.01	-0.03	-0.08
10	0.04	0.04	-0.01	0.01	0.11	-0.12

BLADE STATION = .75R

N	EXPERIMENTAL A(N)	EXPERIMENTAL B(N)	UNIFORM INFLOW A(N)	UNIFORM INFLOW B(N)	VARIABLE INFLOW A(N)	VARIABLE INFLOW B(N)
0	12.60		11.07		11.28	
1	-0.86	-0.64	0.36	-0.38	0.43	-0.33
2	-4.11	-2.18	-5.04	-0.60	-4.07	-0.27
3	0.41	-0.16	-0.57	-0.15	-0.88	0.28
4	-0.57	0.46	-0.14	-0.22	-0.43	-0.01
5	-0.33	-0.29	0.18	-0.16	0.08	-0.00
6	0.25	0.23	0.19	0.15	0.13	0.28
7	-0.19	0.30	-0.07	0.08	-0.05	0.23
8	-0.16	-0.25	-0.01	-0.01	-0.03	-0.02
9	0.16	0.11	0.02	0.02	0.15	-0.02
10	0.04	0.07	-0.02	0.01	0.04	0.10

BLADE STATION = .85R

N	EXPERIMENTAL A(N)	EXPERIMENTAL B(N)	UNIFORM INFLOW A(N)	UNIFORM INFLOW B(N)	VARIABLE INFLOW A(N)	VARIABLE INFLOW B(N)
0	14.23		12.46		12.30	
1	-4.04	3.72	-2.59	4.15	-2.23	2.91
2	-5.80	-3.37	-4.07	-1.58	-4.40	-1.25
3	1.0.	-0.09	-0.28	-0.38	-0.17	0.16
4	0.92	1.61	0.10	0.01	-0.26	0.51
5	-1.16	-0.76	0.20	-0.07	-0.11	0.16
6	0.54	-0.08	0.15	0.18	0.07	0.29
7	-0.16	0.62	-0.11	0.09	-0.12	0.37
8	-0.56	-0.08	-0.02	-0.05	-0.19	-0.07
9	0.07	-0. 36	0.06	0.03	0.13	-0.13
10	0.27	-0.0.	-0.02	0.03	0.05	0.04

BLADE STATION = .90R

N	EXPERIMENTAL A(N)	EXPERIMENTAL B(N)	UNIFORM INFLOW A(N)	UNIFORM INFLOW B(N)	VARIABLE INFLOW A(N)	VARIABLE INFLOW B(N)
0	11.65		12.85		12.36	
1	-4.46	5.13	-4.40	7.14	-3.90	4.95
2	-5.65	-3.18	-6.72	-2.09	-4.73	-1.58
3	1.29	-0.17	-0.02	-0.67	0.49	-0.08
4	-0.71	1.78	0.25	0.18	-0.01	0.82
5	-1.43	-0.62	0.19	0.02	-0.24	0.37
6	0.44	-0.30	0.13	0.23	-0.06	0.27
7	0.13	0.47	-0.16	0.16	-0.08	0.30
8	-0.41	0.16	-0.00	-0.10	-0.08	0.02
9	-0.32	-0.28	0.07	0.04	0.02	-0.01
10	0.12	-0.33	-0.03	0.03	-0.10	-0.05

BLADE STATION = .95R

N	EXPERIMENTAL A(N)	EXPERIMENTAL B(N)	UNIFORM INFLOW A(N)	UNIFORM INFLOW B(N)	VARIABLE INFLOW A(N)	VARIABLE INFLOW B(N)
0	13.11		12.93		11.77	
1	-7.61	5.09	-6.02	10.14	-5.22	6.39
2	-4.10	-2.80	-7.46	-2.55	-4.96	-1.57
3	1.53	-0.60	0.28	-1.04	0.90	-0.36
4	-0.51	1.34	0.42	0.36	0.30	1.04
5	-1.83	-0.41	0.19	0.13	-0.30	0.62
6	0.17	-0.45	0.12	0.28	-0.22	0.29
7	0.24	0.21	-0.20	0.08	-0.02	0.15
8	-0.19	0.10	0.02	-0.14	0.14	0.10
9	-0.36	0.49	0.08	0.05	-0.04	0.18
10	-0.16	-0.34	-0.04	0.05	-0.24	-0.08

BLADE STATION = .97R

N	EXPERIMENTAL A(N)	EXPERIMENTAL B(N)	UNIFORM INFLOW A(N)	UNIFORM INFLOW B(N)	VARIABLE INFLOW A(N)	VARIABLE INFLOW B(N)
0	7.54		12.83		10.48	
1	-3.97	4.97	-7.11	12.34	-5.79	6.64
2	-2.91	-2.20	-8.05	-2.86	-4.91	-1.23
3	1.97	-0.09	0.51	-1.34	1.21	-0.54
4	-0.50	2.26	0.56	0.51	0.55	1.10
5	-1.98	-0.65	0.19	0.21	-0.27	0.79
6	0.40	-0.75	0.11	0.32	-0.32	0.32
7	0.38	0.36	-0.24	0.07	0.01	0.02
8	-0.11	0.17	0.04	-0.17	0.30	0.12
9	-0.31	0.31	0.10	0.07	-0.03	0.29
10	-0.43	0.07	-0.05	0.07	-0.31	-0.07

BLADE STATION = .99R

N	EXPERIMENTAL A(N)	EXPERIMENTAL B(N)	UNIFORM INFLOW A(N)	UNIFORM INFLOW B(N)	VARIABLE INFLOW A(N)	VARIABLE INFLOW B(N)
0	1.38		—		7.71	
1	0.45	3.44	—	—	-5.37	5.22
2	-0.52	-1.84	—	—	-3.90	-0.79
3	0.72	-0.17	—	—	1.02	-0.43
4	0.09	0.56	—	—	0.54	0.89
5	-0.55	-0.15	—	—	-0.20	0.71
6	-0.06	-0.13	—	—	-0.31	0.28
7	0.08	-0.02	—	—	0.02	-0.05
8	0.06	0.08	—	—	0.31	0.11
9	-0.27	0.23	—	—	-0.02	0.28
10	-0.03	-0.13	—	—	-0.26	-0.05

TABLE XIII HARMONICS OF AERODYNAMIC LOADING, LB/IN

V = 150 KT α_s = 0° L = 8400 LB D = 250 LB

BLADE STATION = .25R

	EXPERIMENTAL		UNIFORM INFLOW	
N	A(N)	B(N)	A(N)	B(N)
0	3.24		4.18	
1	4.35	-4.92	1.92	-6.05
2	-1.07	2.72	0.89	1.79
3	-0.08	-0.66	-0.60	-0.65
4	0.35	0.19	0.24	0.11
5	0.38	-0.12	-0.02	-0.34
6	0.21	-0.04	0.01	0.13
7	0.15	-0.13	-0.03	-0.13
8	0.35	-0.09	-0.01	0.06
9	0.25	-0.01	-0.01	-0.06
10	0.29	-0.10	-0.00	0.06

BLADE STATION = .40R

	EXPERIMENTAL		UNIFORM INFLOW	
N	A(N)	B(N)	A(N)	B(N)
0	6.01		6.47	
1	4.46	-5.31	2.76	-6.87
2	-1.29	2.40	-0.71	1.91
3	0.40	-0.47	-0.35	-0.77
4	-0.31	0.44	-0.55	-0.11
5	0.32	-0.	0.15	-0.10
6	0.19	0.34	-0.03	-0.04
7	0.18	0.14	-0.00	0.11
8	-0.	0.18	0.00	-0.06
9	0.10	0.16	-0.04	0.03
10	-0.02	0.16	0.04	-0.00

BLADE STATION = .55R

	EXPERIMENTAL		UNIFORM INFLOW	
N	A(N)	B(N)	A(N)	B(N)
0	8.17		8.51	
1	4.10	-4.51	2.86	-5.69
2	-1.95	0.97	-2.31	1.19
3	0.82	0.09	-0.47	-0.07
4	-0.02	0.45	-0.50	-0.24
5	0.34	0.19	0.03	-0.13
6	0.48	0.21	0.15	-0.00
7	0.33	0.32	-0.03	0.07
8	-0.10	0.18	-0.04	0.01
9	-0.04	-0.01	0.01	-0.02
10	0.06	0.09	-0.01	0.01

BLADE STATION = .75R

	EXPERIMENTAL		UNIFORM INFLOW	
N	A(N)	B(N)	A(N)	B(N)
0	11.93		9.98	
1	-1.27	-0.26	0.25	0.04
2	-2.20	-2.10	-3.77	-0.45
3	0.86	1.95	-0.32	0.33
4	-1.53	0.82	-0.23	-0.09
5	-0.33	-0.35	0.09	-0.33
6	0.50	0.93	0.23	0.06
7	-0.48	0.88	-0.01	0.09
8	-0.31	0.18	-0.00	-0.06
9	0.37	0.01	0.04	-0.01
10	0.23	0.36	0.01	0.01

BLADE STATION = .85R

	EXPERIMENTAL		UNIFORM INFLOW	
N	A(N)	B(N)	A(N)	B(N)
0	11.82		9.35	
1	-4.12	4.61	-2.44	5.09
2	-3.61	-3.64	-4.49	-1.42
3	1.99	2.32	0.05	0.00
4	-1.95	2.35	0.05	0.10
5	-1.52	-0.36	0.18	-0.26
6	0.52	0.76	0.19	0.15
7	-0.22	1.47	-0.09	0.12
8	-0.89	0.93	-0.04	-0.11
9	-0.33	-0.18	0.04	-0.03
10	0.21	0.23	0.01	0.02

BLADE STATION = .90R

	EXPERIMENTAL		UNIFORM INFLOW	
N	A(N)	B(N)	A(N)	B(N)
0	9.64		8.46	
1	-3.87	6.01	-4.05	8.40
2	-3.04	-3.18	-5.00	-1.92
3	2.05	1.65	0.36	-0.37
4	-1.11	2.52	0.25	0.22
5	-1.48	0.19	0.23	-0.17
6	0.22	0.60	0.20	0.23
7	-0.	1.05	-0.17	0.17
8	-0.53	0.94	-0.09	-0.11
9	-0.66	0.15	0.02	-0.04
10	-0.18	-0.12	0.01	0.02

BLADE STATION = .95R

	EXPERIMENTAL		UNIFORM INFLOW	
N	A(N)	B(N)	A(N)	B(N)
0	9.03		7.31	
1	-6.63	6.42	-5.48	11.75
2	-1.65	-2.65	-5.60	-2.33
3	2.53	1.54	0.70	-0.84
4	-0.76	2.81	0.46	0.33
5	-1.57	0.54	0.29	-0.06
6	0.04	0.74	0.22	0.31
7	0.25	0.71	-0.25	0.22
8	-0.43	0.78	-0.13	-0.10
9	-0.11	0.48	0.03	-0.05
10	-0.53	-0.07	0.01	0.02

BLADE STATION = .97R

	EXPERIMENTAL		UNIFORM INFLOW	
N	A(N)	B(N)	A(N)	B(N)
0	5.59		6.32	
1	-3.36	6.00	-6.44	14.24
2	-1.49	-2.20	-6.10	-2.59
3	2.61	0.56	0.97	-1.24
4	-0.24	2.75	0.62	0.40
5	-1.63	0.13	0.34	0.03
6	0.36	-0.08	0.25	0.38
7	0.46	0.73	-0.30	0.24
8	-0.20	0.61	-0.17	-0.09
9	-0.11	0.25	0.03	-0.06
10	-0.33	0.20	0.00	0.03

BLADE STATION = .99R

	EXPERIMENTAL		UNIFORM INFLOW	
N	A(N)	B(N)	(N)	B(N)
0	-0.45		—	
1	0.24	3.42	—	—
2	-0.11	-1.92	—	—
3	0.68	0.22	—	—
4	-0.16	0.61	—	—
5	-0.32	-0.01	—	—
6	-0.12	0.21	—	—
7	0.02	0.02	—	—
8	-0.04	0.09	—	—
9	0.03	0.11	—	—
10	-0.08	-0.04	—	—

TABLE XIV HARMONICS OF AERODYNAMIC LOADING, LB/IN

V = 150 KT α_s = +5° $\bar{b}$ = 8600 FT-LB $\bar{D}$ = 2100 LB

BLADE STATION = .25R

N	EXPERIMENTAL A(N)	EXPERIMENTAL B(N)	UNIFORM INFLOW A(N)	UNIFORM INFLOW B(N)
0	4.66		5.82	
1	4.89	-5.63	1.29	-7.70
2	-0.45	2.88	2.08	1.59
3	1.34	-0.67	-1.15	-0.74
4	-0.05	0.04	0.34	-0.17
5	0.68	-0.13	-0.33	-0.10
6	0.19	-0.11	0.19	-0.18
7	0.46	0.02	-0.22	0.15
8	0.22	-0.15	0.04	-0.12
9	0.37	-0.	-0.07	0.10
10	0.18	-0.18	-0.03	-0.11

BLADE STATION = .40R

N	EXPERIMENTAL A(N)	EXPERIMENTAL B(N)	UNIFORM INFLOW A(N)	UNIFORM INFLOW B(N)
0	7.44		8.00	
1	4.84	-6.70	2.20	-8.72
2	-0.59	2.48	-0.20	2.25
3	0.11	-0.14	-0.68	-0.84
4	-0.33	0.59	-0.59	0.42
5	0.16	0.16	0.04	-0.40
6	0.25	0.21	-0.07	0.31
7	0.29	0.12	0.16	-0.07
8	0.15	0.23	-0.06	0.10
9	0.12	0.03	0.14	-0.09
10	0.18	0.14	-0.04	0.03

BLADE STATION = .55R

N	EXPERIMENTAL A(N)	EXPERIMENTAL B(N)	UNIFORM INFLOW A(N)	UNIFORM INFLOW B(N)
0	9.33		9.72	
1	4.13	-5.47	2.45	-6.89
2	-0.86	0.91	-2.14	1.78
3	0.40	0.46	0.09	0.37
4	-0.06	0.60	-0.282	-0.220
5	0.38	0.38	0.05	0.03
6	0.11	-0.02	0.09	-0.25
7	0.20	0.18	-0.06	0.18
8	-0.20	0.27	0.10	-0.06
9	-0.05	0.06	-0.05	-0.07
10	0.03	0.13	0.03	0.03

BLADE STATION = .70R

N	EXPERIMENTAL A(N)	EXPERIMENTAL B(N)	UNIFORM INFLOW A(N)	UNIFORM INFLOW B(N)
0	11.70		9.59	
1	-1.69	0.40	0.36	0.70
2	-0.97	-2.03	2.71	-0.54
3	1.59	2.33	-0.73	0.84
4	-0.68	1.25	-0.18	0.00
5	-0.04	0.06	-0.21	-0.30
6	0.65	0.57	0.29	-0.02
7	-0.15	0.17	-0.04	0.08
8	-0.35	-0.12	-0.03	0.10
9	0.16	0.11	-0.02	-0.04
10	-0.03	0.05	0.03	-0.01

BLADE STATION = .85R

N	EXPERIMENTAL A(N)	EXPERIMENTAL B(N)	UNIFORM INFLOW A(N)	UNIFORM INFLOW B(N)
0	9.75		7.13	
1	-4.96	5.86	-2.11	6.31
2	-2.40	-3.44	-3.08	-1.57
3	2.85	2.24	0.39	0.30
4	-0.21	2.59	0.24	0.16
5	-1.30	0.58	-0.01	-0.34
6	0.31	0.47	0.36	0.17
7	0.22	1.13	-0.04	0.14
8	-0.33	0.95	-0.09	0.15
9	-0.20	0.33	0.02	-0.05
10	-0.06	0.12	0.04	-0.02

BLADE STATION = .90R

N	EXPERIMENTAL A(N)	EXPERIMENTAL B(N)	UNIFORM INFLOW A(N)	UNIFORM INFLOW B(N)
0	7.33		5.06	
1	-4.13	7.20	-3.54	9.93
2	-2.36	-3.23	-3.42	-2.09
3	2.64	1.29	0.72	-0.26
4	0.36	2.35	0.52	0.22
5	-0.86	0.96	0.21	-0.32
6	0.01	0.47	0.41	0.27
7	0.19	0.81	-0.05	0.22
8	-0.14	0.83	-0.09	0.11
9	-0.10	0.52	0.05	-0.07
10	-0.04	0.18	0.01	-0.02

BLADE STATION = .95R

N	EXPERIMENTAL A(N)	EXPERIMENTAL B(N)	UNIFORM INFLOW A(N)	UNIFORM INFLOW B(N)
0	6.26		2.75	
1	-7.25	7.71	-4.76	13.59
2	-0.91	-3.16	-3.89	-2.50
3	2.72	1.15	1.05	-0.92
4	0.56	2.53	0.80	0.24
5	-1.07	1.25	0.45	-0.28
6	-0.12	0.29	0.49	0.36
7	0.39	0.47	-0.07	0.30
8	-0.35	0.38	-0.08	0.04
9	0.25	0.53	0.08	-0.11
10	-0.14	0.30	0.11	-0.01

BLADE STATION = .97R

N	EXPERIMENTAL A(N)	EXPERIMENTAL B(N)	UNIFORM INFLOW A(N)	UNIFORM INFLOW B(N)
0	3.69		0.93	
1	-3.40	6.82	-5.54	16.29
2	-1.19	-2.46	-4.30	-2.75
3	2.78	0.02	1.28	-1.45
4	0.92	2.41	1.00	0.23
5	-1.34	0.86	0.44	-0.25
6	-0.09	-0.47	0.55	0.42
7	0.71	0.25	-0.10	0.36
8	0.06	0.54	-0.07	-0.02
9	0.14	0.25	0.11	-0.14
10	-0.	0.26	0.12	-0.01

BLADE STATION = .99R

N	EXPERIMENTAL A(N)	EXPERIMENTAL B(N)	UNIFORM INFLOW A(N)	UNIFORM INFLOW B(N)
0	-1.23			
1	-0.57	3.33		
2	0.02	-1.99		
3	0.53	0.19		
4	-0.	0.63		
5	-0.49	0.18		
6	-0.14	-0.03		
7	-0.07	-0.05		
8	-0.15	-0.		
9	-0.03	0.09		
10	-0.15	0.09		

TABLE XV HARMONICS OF AERODYNAMIC LOADING, LB/IN

V = 175 KT α_S = -5° L = 7100 LB D = -250 LB

BLADE STATION = .25R

	EXPERIMENTAL		UNIFORM INFLOW		VARIABLE INFLOW	
N	A(N)	B(N)	A(N)	B(N)	A(N)	B(N)
0	2.15		2.76		3.02	
1	4.37	-5.16	2.42	-5.13	2.28	-2.68
2	-2.91	3.24	0.17	1.82	0.59	2.05
3	-0.04	-0.85	-0.67	-0.35	-0.43	-0.97
4	0.72	0.48	0.31	0.10	-0.53	-0.08
5	0.32	-0.41	0.20	-0.29	0.03	-0.46
6	-0.20	0.12	0.09	0.04	0.01	-0.14
7	0.02	-0.05	0.06	-0.08	0.24	-0.17
8	0.36	0.05	-0.02	-0.04	0.14	-0.07
9	0.31	-0.17	0.01	-0.02	0.40	0.04
10	0.10	-0.17	-0.01	-0.04	0.05	0.36

BLADE STATION = .40R

	EXPERIMENTAL		UNIFORM INFLOW		VARIABLE INFLOW	
N	A(N)	B(N)	A(N)	B(N)	A(N)	B(N)
0	4.30		5.03		4.63	
1	4.90	-4.54	3.17	-5.71	3.40	-4.52
2	-2.32	2.55	-0.70	2.00	-1.23	2.12
3	0.54	-1.43	-0.49	-0.91	-0.36	-0.76
4	0.23	0.35	-0.54	-0.40	-0.77	-0.29
5	0.37	-0.01	0.21	-0.33	0.09	-0.27
6	0.04	0.32	-0.04	-0.00	-0.08	-0.05
7	-0.06	0.12	-0.04	0.04	-0.17	-0.04
8	0.11	0.06	0.01	0.07	-0.04	-0.21
9	0.14	0.14	-0.04	-0.00	0.13	-0.23
10	0.03	0.13	0.03	-0.01	0.19	0.13

BLADE STATION = .55R

	EXPERIMENTAL		UNIFORM INFLOW		VARIABLE INFLOW	
N	A(N)	B(N)	A(N)	B(N)	A(N)	B(N)
0	6.61		6.76		6.77	
1	4.35	-3.87	3.19	-5.49	3.18	-4.67
2	-3.51	0.82	-2.62	1.29	-2.34	1.24
3	1.00	-1.04	-0.69	-0.26	-0.54	-0.04
4	0.15	0.30	-0.82	-0.60	-0.59	-0.18
5	0.32	0.23	0.23	-0.25	-0.13	0.02
6	0.28	0.43	0.12	0.09	0.02	-0.08
7	9.01	0.26	0.02	0.03	0.04	0.02
8	0.10	0.09	0.01	0.09	-0.21	0.05
9	0.11	0.05	-0.08	-0.01	-0.15	-0.46
10	0.14	0.02	0.02	-0.05	0.45	-0.13

BLADE STATION = .75R

	EXPERIMENTAL		UNIFORM INFLOW		VARIABLE INFLOW	
N	A(N)	B(N)	A(N)	B(N)	A(N)	B(N)
0	11.86		8.81		8.80	
1	-0.83	-0.65	0.35	-0.59	0.22	-0.37
2	-4.76	-2.80	-4.64	-0.70	-3.86	-0.37
3	1.29	0.07	-0.66	0.59	-0.66	1.00
4	-0.64	1.07	-0.61	-0.51	-0.79	-0.08
5	-0.56	-0.24	0.40	-0.40	0.37	-0.47
6	0.35	0.30	0.22	0.27	0.45	0.44
7	-0.19	0.38	0.02	0.01	-0.13	0.27
8	-0.19	-0.08	0.04	0.15	-0.15	-0.09
9	0.27	-0.10	-0.15	-0.02	0.26	-0.22
10	0.14	0.18	0.04	-0.09	0.33	0.27

BLADE STATION = .85R

	EXPERIMENTAL		UNIFORM INFLOW		VARIABLE INFLOW	
N	A(N)	B(N)	A(N)	B(N)	A(N)	B(N)
0	12.80		8.96		8.82	
1	-4.34	4.25	-2.70	4.46	-2.44	3.35
2	-7.26	-4.44	-5.65	-2.01	-4.35	-1.59
3	2.17	-0.06	-0.23	0.41	0.27	0.71
4	-0.83	2.73	-0.34	-0.20	-0.31	0.58
5	-1.78	-0.51	0.57	-0.41	0.38	-0.25
6	0.49	-0.05	0.22	0.43	0.46	0.53
7	-0.13	0.64	-0.04	0.02	-0.10	0.51
8	-0.48	0.01	0.03	0.17	-0.37	0.04
9	-0.	-0.33	-0.23	-0.03	0.15	-0.31
10	0.34	0.06	0.06	-0.14	0.39	0.16

BLADE STATION = .90R

	EXPERIMENTAL		UNIFORM INFLOW		VARIABLE INFLOW	
N	A(N)	B(N)	A(N)	B(N)	A(N)	B(N)
0	11.49		8.56		8.32	
1	-4.75	5.63	-4.60	7.93	-4.02	5.83
2	-7.14	-4.47	-6.37	-2.75	-4.99	-2.07
3	2.77	-0.30	0.20	0.05	0.96	0.05
4	-0.81	3.67	-0.17	0.03	0.27	0.86
5	-3.03	-0.60	0.69	-0.38	0.45	0.14
6	0.68	-0.97	0.22	0.54	0.22	0.64
7	0.92	1.14	-0.08	0.02	-0.08	0.37
8	-0.96	0.88	0.03	0.22	-0.12	0.21
9	-0.75	-0.88	-0.28	-0.04	-0.06	0.04
10	0.85	-0.36	0.08	-0.16	0.05	-0.01

BLADE STATION = .95R

	EXPERIMENTAL		UNIFORM INFLOW		VARIABLE INFLOW	
N	A(N)	B(N)	A(N)	B(N)	A(N)	B(N)
0	10.26		7.87		7.55	
1	-7.82	5.23	-6.32	11.51	-5.16	7.41
2	-5.28	-3.98	-7.22	-3.40	-5.38	-2.19
3	3.60	0.18	0.69	-0.42	1.54	-0.56
4	-1.33	3.07	0.01	0.26	0.69	0.99
5	-3.80	-0.48	0.83	-0.33	0.57	0.41
6	0.27	-1.22	0.23	0.65	0.06	0.77
7	1.00	0.61	-0.13	0.02	-0.12	0.23
8	-0.48	0.37	0.03	0.26	0.13	0.30
9	-0.01	0.52	-0.32	-0.07	-0.14	0.29
10	-0.60	0.13	0.12	-0.17	-0.14	-0.05

BLADE STATION = .97R

	EXPERIMENTAL		UNIFORM INFLOW		VARIABLE INFLOW	
N	A(N)	B(N)	A(N)	B(N)	A(N)	B(N)
0	7.81		7.32		6.62	
1	-3.15	3.91	-7.48	13.98	-5.46	7.49
2	-2.91	-1.52	-7.70	-3.81	-5.32	-1.81
3	1.10	0.15	1.03	-0.63	1.78	-0.89
4	-0.35	1.06	-0.04	0.35	0.85	0.87
5	-0.65	0.15	1.02	-0.45	0.81	0.45
6	-3.42	0.86	0.38	0.83	0.05	0.95
7	-0.67	-0.33	-0.24	0.11	-0.23	0.18
8	0.26	-0.32	-0.05	0.23	0.25	0.25
9	0.04	0.34	-0.28	-0.15	-0.10	0.39
10	0.02	-0.12	0.18	-0.13	-0.18	0.02

BLADE STATION = .99R

	EXPERIMENTAL		UNIFORM INFLOW		VARIABLE INFLOW	
N	A(N)	B(N)	A(N)	B(N)	A(N)	B(N)
0	0.42				4.88	
1	0.76	3.50	–	–	-4.98	5.80
2	-0.61	-2.73	–	–	-4.14	-1.19
3	1.74	0.03	–	–	1.41	-0.69
4	-0.22	1.50	–	–	0.71	0.61
5	-1.41	-0.26	–	–	0.75	0.40
6	-0.16	-0.61	–	–	0.02	0.85
7	0.55	-0.15	–	–	-0.25	0.12
8	0.44	0.25	–	–	0.25	0.17
9	-0.16	0.68	–	–	-0.05	0.36
10	-0.35	0.06	–	–	-0.17	0.04

TABLE XVI HARMONICS OF AERODYNAMIC LOADING, LB/IN

V = 175 KT α_S = 0° L = 7100 LB D = 400 LB

BLADE STATION = .25R

	EXPERIMENTAL		UNIFORM INFLOW	
N	A(N)	B(N)	A(N)	B(N)
0	3.74		4.66	
1	5.24	-6.14	2.12	-7.22
2	-1.71	3.60	1.02	2.06
3	-0.02	-0.69	-0.84	-0.55
4	0.42	0.16	0.36	0.16
5	0.75	-0.35	-0.10	-0.48
6	0.07	-0.02	0.10	0.19
7	0.20	-0.08	-0.09	-0.15
8	0.22	-0.12	0.04	0.05
9	0.34	-0.15	-0.08	-0.05
10	0.16	-0.17	0.06	0.06

BLADE STATION = .40R

	EXPERIMENTAL		UNIFORM INFLOW	
N	A(N)	B(N)	A(N)	B(N)
0	6.15		6.77	
1	5.12	-6.40	2.93	-7.62
2	-1.37	3.21	-0.28	2.27
3	0.26	-0.80	-0.43	-0.69
4	0.14	0.59	-0.84	-0.03
5	0.39	0.01	0.27	-0.33
6	0.14	0.25	-0.14	0.05
7	0.26	0.26	0.13	0.07
8	0.07	0.14	-0.03	0.00
9	0.18	0.15	-0.04	0.10
10	0.02	0.14	-0.01	-0.11

BLADE STATION = .55R

	EXPERIMENTAL		UNIFORM INFLOW	
N	A(N)	B(N)	A(N)	B(N)
0	7.87		8.12	
1	4.30	5.32	3.01	-6.29
2	-1.81	1.13	-1.84	1.35
3	0.98	0.11	-0.42	0.41
4	0.02	0.36	-1.00	-0.39
5	0.31	0.47	0.12	-0.26
6	0.22	0.18	0.16	-0.04
7	0.32	0.35	0.05	-0.01
8	0.12	0.26	0.09	0.15
9	0.07	0.11	-0.10	0.04
10	0.14	0.04	-0.04	-0.02

BLADE STATION = .75R

	EXPERIMENTAL		UNIFORM INFLOW	
N	A(N)	B(N)	A(N)	B(N)
0	10.58		7.87	
1	-1.27	-0.36	0.21	-0.04
2	-1.85	-3.13	-2.86	-0.84
3	2.48	2.22	-0.21	1.38
4	-0.69	1.73	-0.74	-0.25
5	-0.34	-0.24	0.16	-0.61
6	1.19	0.49	0.19	0.13
7	-0.31	1.08	0.09	-0.13
8	-0.51	-0.19	0.10	0.09
9	0.30	-0.34	-0.09	0.08
10	0.27	0.14	-0.06	-0.06

BLADE STATION = .85R

	EXPERIMENTAL		UNIFORM INFLOW	
N	A(N)	B(N)	A(N)	B(N)
0	9.85		5.89	
1	-4.55	5.58	-2.58	5.65
2	-4.04	-5.05	-3.36	-2.21
3	4.25	1.97	0.38	1.09
4	0.20	3.80	-0.44	0.07
5	-1.62	0.41	0.37	-0.59
6	1.43	0.77	0.16	0.37
7	0.26	1.48	0.00	-0.07
8	-0.43	0.71	0.07	0.10
9	-0.28	-0.08	-0.20	0.13
10	0.40	-0.25	-0.09	-0.12

BLADE STATION = .90R

	EXPERIMENTAL		UNIFORM INFLOW	
N	A(N)	B(N)	A(N)	B(N)
0	7.69		4.10	
1	-4.78	7.71	-4.27	9.51
2	-4.29	-4.99	-3.84	-2.98
3	4.73	1.23	0.90	0.63
4	1.07	4.98	-0.21	0.30
5	-2.64	0.97	0.57	-0.50
6	1.13	-0.91	0.17	0.54
7	1.33	1.38	-0.07	-0.01
8	-0.60	1.71	0.06	0.21
9	-1.18	0.03	-0.29	0.16
10	0.30	-0.54	-0.11	-0.14

BLADE STATION = .95R

	EXPERIMENTAL		UNIFORM INFLOW	
N	A(N)	B(N)	A(N)	B(N)
0	6.33		2.05	
1	-7.51	7.95	-5.77	13.49
2	-2.40	-4.62	-4.50	-3.65
3	5.35	1.61	1.45	0.02
4	1.06	5.77	0.07	0.48
5	-2.98	0.92	0.80	-0.39
6	0.39	-0.98	0.21	0.72
7	1.40	0.87	-0.13	0.06
8	-0.57	0.92	0.06	0.36
9	0.09	1.28	-0.38	0.18
10	-0.68	0.60	-0.12	-0.18

BLADE STATION = .97R

	EXPERIMENTAL		UNIFORM INFLOW	
N	A(N)	B(N)	A(N)	B(N)
0	4.90		0.55	
1	-3.15	5.25	-6.76	16.17
2	-3.71	-2.30	-4.78	-4.08
3	2.57	1.28	1.84	-0.20
4	0.46	2.10	-0.08	0.56
5	-3.20	0.47	1.01	-0.55
6	0.29	1.16	0.47	0.88
7	-0.96	0.30	-0.20	0.27
8	0.21	-0.33	-0.08	0.45
9	0.40	0.90	-0.42	0.08
10	-0.24	0.36	-0.06	-0.18

BLADE STATION = .99R

	EXPERIMENTAL		UNIFORM INFLOW	
N	A(N)	B(N)	A(N)	B(N)
0	-1.32		–	
1	0.	4.00	–	–
2	-0.20	-3.17	–	–
3	1.73	0.28	–	–
4	0.20	1.69	–	–
5	-1.33	-0.06	–	–
6	-0.10	-0.58	–	–
7	0.30	-0.21	–	–
8	0.31	0.16	–	–
9	-0.10	0.91	–	–
10	-0.61	0.15	–	–

TABLE XVII HARMONICS OF AERODYNAMIC LOADING, LB/IN

V = 175 KT α_s = +5° L = 7300 LB D = 1150 LB

BLADE STATION = .25R

N	EXPERIMENTAL A(N)	EXPERIMENTAL B(N)	UNIFORM INFLOW A(N)	UNIFORM INFLOW B(N)
0	5.77		7.00	
1	5.38	-0.56	1.43	-8.86
2	-0.37	3.50	2.99	1.79
3	0.35	-0.97	-1.34	-0.79
4	-0.21	0.66	0.31	-0.34
5	0.07	-0.59	-0.40	-0.06
6	0.10	-0.07	0.26	-0.31
7	0.56	-0.27	-0.14	0.15
8	0.09	-0.26	-0.05	-0.20
9	0.28	-0.35	-0.02	0.14
10	0.06	-0.27	-0.12	-0.17

BLADE STATION = .40R

N	EXPERIMENTAL A(N)	EXPERIMENTAL B(N)	UNIFORM INFLOW A(N)	UNIFORM INFLOW B(N)
0	7.93		8.70	
1	5.16	-7.86	2.43	-9.99
2	-0.11	3.11	0.56	2.47
3	-0.03	0.02	-0.82	-0.70
4	0.01	0.49	-0.85	0.52
5	-0.08	0.31	-0.17	-0.66
6	0.31	0.22	-0.04	0.41
7	0.26	0.14	-0.01	-0.22
8	0.37	0.16	0.06	0.30
9	0.44	0.08	0.06	-0.04
10	0.44	0.17	0.02	0.16

BLADE STATION = .55R

N	EXPERIMENTAL A(N)	EXPERIMENTAL B(N)	UNIFORM INFLOW A(N)	UNIFORM INFLOW B(N)
0	8.78		9.56	
1	4.32	-6.47	2.58	-7.93
2	0.08	0.67	-1.40	1.82
3	0.74	1.32	0.19	0.93
4	-0.01	0.19	-1.55	0.16
5	0.74	0.44	0.34	-0.08
6	0.13	0.39	-0.07	-0.35
7	0.34	0.12	0.15	0.02
8	0.23	0.24	0.13	-0.20
9	0.14	0.19	-0.13	0.17
10	0.30	0.08	0.01	-0.04

BLADE STATION = .70R

N	EXPERIMENTAL A(N)	EXPERIMENTAL B(N)	UNIFORM INFLOW A(N)	UNIFORM INFLOW B(N)
0	9.13		7.43	
1	-1.99	0.27	0.31	0.30
2	-0.24	-3.74	-1.16	-1.43
3	2.73	3.10	0.49	2.26
4	-0.65	1.55	-0.63	-0.33
5	-0.20	-0.11	-0.27	-0.45
6	1.16	0.27	0.23	0.06
7	-0.17	0.96	0.02	-0.15
8	-0.60	-0.02	0.13	0.18
9	-0.25	-0.22	-0.14	0.09
10	-0.16	0.	-0.10	-0.02

BLADE STATION = .85R

N	EXPERIMENTAL A(N)	EXPERIMENTAL B(N)	UNIFORM INFLOW A(N)	UNIFORM INFLOW B(N)
0	6.72		3.14	
1	-4.63	6.59	-2.25	7.24
2	-1.64	-5.78	-1.11	-3.05
3	4.75	2.68	1.29	1.54
4	0.45	2.80	0.01	0.24
5	-0.72	0.65	0.11	-0.59
6	1.42	-0.25	0.39	0.35
7	0.61	0.98	0.09	-0.10
8	0.12	0.57	0.15	0.30
9	-0.29	0.05	-0.14	0.14
10	-0.03	-0.21	-0.14	-0.01

BLADE STATION = .90R

N	EXPERIMENTAL A(N)	EXPERIMENTAL B(N)	UNIFORM INFLOW A(N)	UNIFORM INFLOW B(N)
0	4.49		-0.16	
1	-3.95	8.31	-3.73	11.53
2	-1.27	-5.59	-1.36	-3.96
3	5.22	1.98	1.83	0.76
4	1.89	3.79	0.43	0.35
5	-1.01	1.23	0.53	-0.62
6	1.24	-1.13	0.50	0.55
7	1.66	0.53	0.14	-0.06
8	0.36	1.12	0.22	0.30
9	-0.62	0.06	-0.12	0.17
10	0.36	-0.91	-0.14	-0.01

BLADE STATION = .93R

N	EXPERIMENTAL A(N)	EXPERIMENTAL B(N)	UNIFORM INFLOW A(N)	UNIFORM INFLOW B(N)
0	3.44		-3.71	
1	-6.92	8.25	-4.99	15.34
2	0.19	-5.31	-1.34	-4.74
3	6.03	1.54	2.41	-0.14
4	2.17	0.17	0.83	0.39
5	-1.49	1.49	1.02	-0.60
6	0.78	-1.03	0.62	0.72
7	1.68	0.25	0.18	-0.00
8	0.07	0.47	0.31	0.26
9	0.24	0.57	-0.11	0.19
10	0.13	0.13	-0.13	-0.03

BLADE STATION = .97R

N	EXPERIMENTAL A(N)	EXPERIMENTAL B(N)	UNIFORM INFLOW A(N)	UNIFORM INFLOW B(N)
0	2.21		-0.27	
1	-2.87	5.76	-5.82	16.89
2	0.77	-3.09	-1.99	-5.30
3	3.11	1.67	2.88	-0.61
4	0.82	1.89	0.79	0.43
5	0.68	0.23	1.33	-0.96
6	1.08	0.98	0.96	0.76
7	-0.52	0.56	0.25	0.24
8	0.13	-0.76	0.22	0.27
9	0.62	0.13	-0.14	0.07
10	0.10	0.09	-0.03	-0.06

BLADE STATION = .99R

N	EXPERIMENTAL A(N)	EXPERIMENTAL B(N)	UNIFORM INFLOW A(N)	UNIFORM INFLOW B(N)
0	-2.42		—	
1	-0.90	3.97	—	—
2	0.01	-3.20	—	—
3	1.30	0.47	—	—
4	0.13	1.73	—	—
5	0.86	0.24	—	—
6	0.07	-0.55	—	—
7	0.15	-0.12	—	—
8	0.22	-0.10	—	—
9	0.02	0.54	—	—
10	-0.30	0.24	—	—

TABLE XVIII TIME HISTORIES OF BLADE STRESS, PSI

V = 110 KT α_s = -5° L = 8300 LB D = -750 LB

	Chordwise Stress		Flapwise Stress		Torsional Stress
ψ, DEG	r/R .15	r/R .80	r/R .45	r/R .80	r/R .15
0	-1790	1111	5209	-1393	133
5	-1697	1076	5262	-1351	150
10	-1597	1053	5315	-1279	164
15	-1547	1036	5432	-1081	176
20	-1460	1094	5532	-817	217
25	-1354	1215	5526	-547	251
30	-1279	1278	5509	-354	251
35	-1192	1244	5385	-150	256
40	-1073	1232	5127	-96	251
45	-911	1261	4863	-18	233
50	-811	1255	4675	78	231
55	-805	1215	4481	6	239
60	-824	1226	4211	-180	243
65	-780	1284	4041	-487	249
70	-761	1342	3917	-925	255
75	-792	1272	3771	-1255	266
80	-799	1186	3618	-1567	270
85	-780	1163	3412	-1808	270
90	-742	1163	3266	-1988	262
95	-749	1134	3183	-2162	249
100	-774	1134	3172	-2174	207
105	-742	1146	3136	-2036	176
110	-711	1146	3019	-1880	147
115	-705	1122	2913	-1706	97
120	-749	1099	2831	-1501	56
125	-730	1174	2672	-1429	27
130	-693	1313	2590	-1339	-3
135	-624	1393	2573	-1327	-18
140	-543	1405	2620	-1363	-9
145	-418	1405	2690	-1429	-9
150	-356	1388	2796	-1567	-3

TABLE XVIII CONCLUDED

V = 110 KT. α_s = -5° L = 8300 LB D = -750 LB

	Chordwise Stress		Flapwise Stress		Torsional Stress
ψ, DEG	r/R .15	r/R .80	r/R .45	r/R .80	r/R .15
155	-337	1347	2813	-1784	3
160	-337	1405	2860	-1916	15
165	-343	1532	2925	-2042	5
170	-393	1566	3025	-2084	3
175	-493	1503	3113	-2078	7
180	-530	1440	3177	-2072	1
185	-505	1370	3336	-1994	-9
190	-468	1301	3506	-1934	-5
195	-480	1238	3694	-1874	-1
200	-524	1220	3888	-1766	11
205	-655	1203	4076	-1597	35
210	-805	1215	4240	-1357	58
215	-936	1249	4493	-1051	68
220	-1017	1295	4734	-817	80
225	-1110	1284	4957	-601	84
230	-1179	1232	5180	-439	80
235	-1260	1174	5403	-300	78
240	-1291	1151	5614	-162	82
245	-1285	1197	5785	6	92
250	-1310	1272	5902	132	86
255	-1435	1255	5943	294	74
260	-1535	1215	5937	408	86
265	-1566	1278	5896	540	94
270	-1566	1342	5867	667	103
275	-1578	1313	5808	721	113
280	-1584	1272	5720	745	133
285	-1578	1238	5620	703	121
290	-1584	1209	5509	643	88
295	-1653	1163	5403	558	76
300	-1691	1192	5291	390	54
305	-1734	1261	5168	150	37
310	-1747	1255	5098	-78	29
315	-1784	1163	5033	-396	31
320	-1753	999	4957	-697	29
325	-1697	871	4892	-961	41
330	-1684	1042	4851	-1171	62
335	-1747	1030	4810	-1285	90
340	-1809	1053	4839	-1357	99
345	-1834	1128	4904	-1381	123
350	-1840	1163	5033	-1417	127
355	-1834	1151	5133	-1429	125
360	-1790	1111	5209	-1393	133

TABLE XIX TIME HISTORIES OF BLADE STRESS, PSI

V = 110 KT α_S = 0° L = 8200 LB D = 50 LB

	Chordwise Stress				Flapwise Stress				Torsional Stress		
ψ_{DEG}	r/R .15	r/R .375	r/R .65	r/R .80	r/R .375	r/R .45	r/R .65	r/R .80	r/R .15	r/R .375	r/R .65
0	-1678	-145	264	1157	6757	5233	730	-1189	198	330	394
5	-1597	-364	220	1088	6585	5051	1064	-1267	164	316	405
10	-1572	-510	220	1088	6407	4910	1626	-1477	164	301	402
15	-1560	-212	276	1140	6388	4775	2157	-1309	145	289	363
20	-1516	56	433	1192	6222	4833	1873	-535	147	265	392
25	-1491	-108	515	1330	6394	4974	1539	150	194	273	376
30	-1429	-419	546	1313	6726	5010	1342	576	215	320	376
35	-1298	-108	527	1203	6431	4786	1335	504	256	366	440
40	-1142	299	446	1151	6081	4340	1743	-126	258	422	487
45	-1011	13	358	1122	5670	4252	1866	-607	235	424	491
50	-992	-47	333	1071	5381	4199	1453	-793	213	384	454
55	-1054	439	408	1105	5541	4070	1101	-985	213	356	425
60	-1148	172	521	1249	5762	3982	521	-895	192	316	431
65	-1198	-267	634	1353	5756	3941	-23	-961	198	326	466
70	-1173	7	671	1318	5559	3665	-227	-1339	233	360	477
75	-1129	348	565	1261	5043	3301	-245	-1712	262	406	505
80	-1029	26	421	1146	4669	3019	-190	-2018	288	448	522
85	-961	-90	295	1030	4644	2960	-196	-2186	300	488	557
-90	-986	263	270	1047	4656	2990	-480	-2162	319	488	553
95	-979	360	377	1174	4681	3025	-764	-2198	315	502	553
100	-1004	-163	515	1301	4675	3037	-937	-2270	282	466	501
105	-1023	-273	584	1318	4429	2849	-1054	-2324	221	392	450
110	-1011	44	559	1249	4227	2573	-986	-2366	162	299	398
115	-986	421	458	1174	4104	2402	-1159	-2096	107	233	330
120	-886	377	458	1128	4098	2391	-1535	-1663	56	175	308
125	-799	166	496	1180	4178	2256	-1770	-1387	29	121	295
130	-730	220	621	1295	4116	2150	-1795	-1273	13	82	244
135	-661	476	759	1353	3975	2050	-1640	-1381	7	44	221
140	-649	865	885	1399	3778	1991	-1325	-1651	-9	42	207
145	-636	780	960	1428	3570	1968	-955	-1832	-20	36	223
150	-599	537	1010	1428	3570	2068	-1091	-1916	-7	30	233

TABLE XIX CONCLUDED

V = 110 KT α_s = 0° L = 8200 LB D = 50 LB

	Chordwise Stress				Flapwise Stress				Torsional Stress		
ψ, DEG	r/R .15	r/R .375	r/R .65	r/R .80	r/R .375	r/R .45	r/R .65	r/R .80	r/R .15	r/R .375	r/R .65
155	-574	811	1085	1457	3803	2220	-1146	-1814	-10	38	229
160	-480	1109	1110	1509	3987	2320	-1282	-1706	-34	14	221
165	-487	786	1098	1526	4092	2338	-1307	-1730	-28	-12	178
170	-505	537	1010	1411	4159	2361	-1214	-1802	-44	-12	151
175	-524	750	928	1336	4227	2420	-1066	-1922	-56	-30	182
180	-524	993	860	1365	4435	2561	-912	-2030	-34	-4	161
185	-574	658	803	1353	4755	2866	-850	-1988	-14	16	141
190	-674	287	784	1318	5080	3277	-881	-1904	-5	6	157
195	-755	251	778	1324	5479	3659	-714	-1880	21	26	161
200	-811	439	734	1359	5657	3906	-418	-1844	46	42	135
205	-880	464	671	1318	5762	4064	45	-1808	68	86	155
210	-986	93	596	1238	5891	4199	558	-1597	72	111	192
215	-1042	-187	540	1215	6001	4428	934	-1207	84	117	209
220	-1073	-157	515	1295	6259	4675	1231	-715	94	119	170
225	-1123	-108	502	1278	6585	5004	1422	-258	84	111	159
230	-1204	7	477	1238	6843	5233	1626	60	86	99	168
235	-1304	-78	458	1244	6978	5397	2002	84	90	115	159
240	-1335	-267	452	1232	6941	5497	2329	66	72	113	180
245	-1366	-455	471	1244	7008	5638	2583	-18	62	91	188
250	-1404	-382	508	1307	7125	5779	2737	48	86	82	151
255	-1422	-230	571	1342	7236	5890	2632	186	74	82	157
260	-1416	-17	584	1365	7322	5914	2607	240	80	76	188
265	-1366	-60	590	1388	7279	5826	2706	210	88	99	182
270	-1347	-291	508	1342	7057	5644	2848	12	76	99	176
275	-1422	-212	465	1220	6867	5391	2984	-96	60	91	198
280	-1472	208	465	1180	6714	5291	2959	60	90	95	205
285	-1472	214	521	1284	6689	5303	2700	294	107	111	200
290	-1466	-260	609	1382	6677	5286	2366	558	111	141	227
295	-1503	-437	590	1359	6560	5151	2107	685	96	153	258
300	-1541	-163	471	1249	6394	4904	2231	342	88	143	238
305	-1528	99	339	1157	6149	4599	2416	-144	54	111	219
310	-1485	-35	226	1117	5903	4587	2286	-499	33	121	227
315	-1478	-473	145	1099	5909	4728	1953	-805	33	117	238
320	-1491	-607	145	1122	6179	4839	1533	-973	52	137	244
325	-1572	-577	170	1140	6300	4880	619	-1099	72	160	269
330	-1691	-431	182	1099	6511	4892	737	-1327	78	193	308
335	-1821	-200	157	1094	6578	4739	811	-1567	99	215	326
340	-1846	-321	176	1094	6364	4557	903	-1724	149	261	349
345	-1834	-668	245	1163	6345	4628	1064	-1742	172	316	390
350	-1778	-741	289	1169	6517	4951	934	-1447	190	338	421
355	-1715	-479	289	1186	6671	5192	576	-1057	217	334	400
360	-1678	-145	264	1157	6757	5233	730	-1189	198	330	394

TABLE XX TIME HISTORIES OF BLADE STRESS, PSI

V = 110 KT α_s = +5° L = 8100 LB D = 850 LB

	Chordwise Stress				Flapwise Stress				Torsional Stress		
ψ, DEG	r/R .15	r/R .375	r/R .65	r/R .80	r/R .375	r/R .45	r/R .65	r/R .80	r/R .15	r/R .375	r/R .65
0	-1912	-394	358	1192	6886	5033	595	-1177	190	299	359
5	-1884	-309	414	1215	6683	4681	1041	-1435	172	295	372
10	-1772	-303	439	1209	6419	4575	1607	-1465	168	277	351
15	-1678	-285	396	1197	6210	4722	1416	-697	147	255	310
20	-1572	-206	339	1134	6057	4822	965	42	131	225	339
25	-1485	-78	333	1088	6327	4722	1126	348	164	223	334
30	-1397	-102	352	1163	6259	4499	1397	408	200	283	345
35	-1354	-151	389	1169	5725	4141	1737	12	196	326	404
40	-1366	-60	439	1180	5172	3911	1873	-336	200	364	450
45	-1360	-11	465	1209	4773	3882	1453	-372	243	374	442
50	-1304	-114	465	1226	4964	3635	1033	-559	268	410	431
55	-1285	-151	402	1186	5314	3406	656	-745	300	440	477
60	-1254	56	327	1088	5424	3477	-165	-949	329	472	540
65	-1241	-11	289	1059	5387	3571	-758	-1579	357	516	538
70	-1229	-96	308	1099	5111	3354	-949	-2324	355	553	586
75	-1241	-23	364	1146	4792	3072	-912	-3063	368	559	611
80	-1316	32	446	1215	4890	2990	-770	-3593	358	553	578
85	-1366	-54	502	1261	4884	3095	-1140	-3177	331	516	553
90	-1335	-157	527	1272	4687	3066	-1560	-2804	309	472	524
95	-1273	7	540	1267	4546	2837	-1628	-2492	272	440	485
100	-1204	129	502	1220	4282	2479	-1474	-2246	233	392	450
105	-1098	141	477	1174	3938	2073	-1227	-2066	180	340	417
110	-1048	153	446	1203	3643	1868	-1220	-1802	135	277	361
115	-986	239	508	1215	3422	1897	-1603	-1375	88	213	320
120	-955	409	609	1255	3490	1833	-1875	-1177	60	153	289
125	-917	403	722	1353	3570	1651	-1900	-1225	48	121	264
130	-842	433	816	1411	3434	1516	-1924	-1387	39	103	244
135	-805	488	866	1376	3244	1498	-1887	-1682	11	74	287
140	-736	750	822	1336	3042	1433	-1856	-1922	-10	60	225
145	-655	774	841	1324	2974	1339	-1819	-2084	-12	50	223
150	-587	792	897	1376	3232	1369	-1758	-2102	-10	40	221

TABLE XX CONCLUDED

V = 110 KT a_s = +5° L = 8100 LB D = 850 LB

	Chordwise Stress				Flapwise Stress				Torsional Stress		
ψ, DEG	r/R .15	r/R .375	r/R .65	r/R .80	r/R .375	r/R .45	r/R .65	r/R .80	r/R .15	r/R .375	r/R .65
155	-549	762	891	1393	3459	1539	-1887	-1928	-18	32	198
160	-555	890	928	1388	3539	1698	-2023	-1796	-32	6	190
165	-568	829	966	1416	3600	1792	-1912	-1826	-50	-14	161
170	-574	798	916	1399	3632	1839	-1585	-1904	-69	-28	151
175	-605	780	916	1376	3809	1956	-1177	-1988	-85	-44	139
180	-630	829	910	1376	4012	2220	-906	-1904	-87	-48	118
185	-661	725	872	1370	4270	2667	-906	-1676	-77	-58	106
190	-711	585	872	1359	4718	3042	-819	-1513	-4	-40	102
195	-716	452	860	1353	5113	3359	-523	-1489	13	988	126
200	-749	464	759	1359	5326	3571	-146	-1501	46	543	157
205	-848	415	690	1295	5516	3859	230	-1537	52	125	180
210	-967	281	628	1197	5707	4158	502	-1387	56	119	207
215	-1073	147	634	1272	5995	4434	700	-1153	80	103	190
220	-1117	-5	684	1393	6400	4734	977	-907	92	127	163
225	-1154	-84	703	1382	6714	5027	1144	-595	80	121	190
230	-1229	-133	609	1313	6861	5239	1428	-439	96	125	196
235	-1266	-175	471	1232	6843	5344	1817	-354	78	149	176
240	-1248	-139	402	1174	6714	5368	2163	-234	39	105	203
245	-1285	-175	414	1215	6818	5403	2521	-102	50	101	186
250	-1329	-193	496	1290	6892	5479	2620	180	58	99	147
255	-1372	-157	609	1365	6922	5538	2490	474	46	82	178
260	-1404	-267	646	1422	6971	5562	2453	492	64	105	198
265	-1366	-236	640	1399	6843	5415	2453	366	70	115	200
270	-1360	-133	571	1336	6689	5209	2589	-12	68	119	225
275	-1397	32	502	1238	6591	5074	2576	-306	58	125	238
280	-1422	20	452	1174	6462	5092	2255	-390	56	121	258
285	-1422	-133	496	1267	6554	5104	1941	-481	52	121	254
290	-1429	-151	533	1342	6591	5033	1595	-390	48	115	233
295	-1472	-193	515	1295	6529	4910	1360	-378	46	103	211
300	-1560	-139	446	1197	6431	4693	1410	-583	31	97	205
305	-1578	-169	333	1146	6124	4540	1391	-763	33	107	235
310	-1584	-285	276	1134	5934	4499	1379	-919	68	135	242
315	-1597	-273	270	1146	6001	4522	1447	-1087	121	209	266
320	-1634	-382	264	1163	6020	4546	1342	-1069	137	251	320
325	-1691	-382	276	1197	6106	4599	1261	-1129	147	256	341
330	-1715	-498	258	1151	6155	4634	1187	-1111	139	261	326
335	-1728	-510	201	1094	6143	4651	1126	-1117	137	249	324
340	-1722	-461	164	1088	6222	4610	1169	-1159	137	269	357
345	-1734	-461	164	1082	6370	4710	1119	-1099	143	283	380
350	-1778	-388	220	1099	6486	4998	768	-943	168	291	371
355	-1859	-419	276	1146	6707	5145	403	-931	178	291	361
360	-1921	-394	358	1192	6886	5033	595	-1177	190	299	359

TABLE XXI TIME HISTORIES OF BLADE STRESS, PSI

V = 150 KT α_s = -5° L = 8500 LB D = -650 LB

	Chordwise Stress		Flapwise Stress		Torsional Stress
ψ, DEG	r/R .15	r/R .80	r/R .45	r/R .80	r/R .15
0	-1797	704	5728	-1453	205
5	-1685	785	6018	-1236	223
10	-1635	924	6475	-856	233
15	-1585	1074	6866	-482	276
20	-1566	1236	6961	-332	314
25	-1504	1351	6860	-410	310
30	-1397	1369	6635	-332	318
35	-1191	1421	6398	-108	353
40	-897	1501	6315	398	389
45	-685	1542	6131	826	413
50	-610	1403	5680	814	437
55	-566	1288	5164	422	431
60	-497	1340	4809	-96	419
65	-466	1369	4566	-717	419
70	-510	1247	4269	-1170	423
75	-560	1166	3955	-1471	415
80	-497	1097	3694	-1507	409
85	-403	1005	3403	-1682	415
90	-385	912	2977	-2207	383
95	-397	855	2662	-2623	332
100	-353	953	2650	-2563	258
105	-391	1114	2793	-2267	173
110	-447	1230	2728	-1875	98
115	-572	1288	2431	-1538	15
120	-566	1455	2093	-1399	-80
125	-460	1571	1779	-1212	-128
130	-285	1646	1548	-1194	-140
135	-66	1623	1583	-1103	-136
140	178	1611	1785	-1061	-124
145	272	1576	1986	-1248	-106
150	228	1484	2141	-1622	-98

TABLE XXI CONCLUDED

V = 150 KT α_s = -5° L = 8500 LB D = -650 LB

	Chordwise Stress		Flapwise Stress		Torsional Stress
ψ, DEG	r/R .15	r/R .80	r/R .45	r/R .80	r/R .15
155	66	1507	2218	-2122	-100
160	-84	1675	2224	-2665	-74
165	-216	1802	2265	-2979	-49
170	-303	1761	2502	-2955	-35
175	-285	1542	2828	-2810	-33
180	-197	1299	3101	-2659	-13
185	-109	1126	3249	-2707	-7
190	-159	1039	3439	-2744	-5
195	-316	1091	3676	-2629	11
200	-522	1276	3961	-2261	27
205	-697	1496	4269	-1640	23
210	-860	1553	4637	-886	33
215	-947	1444	4915	-326	56
220	-1028	1276	5159	60	76
225	-1078	1149	5419	223	112
230	-1153	1132	5740	338	171
235	-1303	1207	6149	495	213
240	-1472	1334	6582	724	239
245	-1697	1351	6896	935	252
250	-1879	1259	6979	1086	268
255	-1985	1178	6914	1188	270
260	-1972	1143	6825	1315	282
265	-1891	1143	6759	1574	306
270	-1835	1201	6641	1773	336
275	-1835	1218	6463	1900	342
280	-1797	1247	6255	1845	342
285	-1835	1340	5995	1610	322
290	-1841	1369	5787	1260	262
295	-1860	1351	5585	844	219
300	-1841	1432	5408	422	191
305	-1741	1426	5277	36	155
310	-1641	1363	5170	-271	108
315	-1579	1224	5064	-615	74
320	-1479	1062	4862	-898	27
325	-1516	982	4672	-1170	-17
330	-1629	947	4655	-1242	-3
335	-1804	970	4803	-1164	27
340	-1897	1057	4987	-1121	66
345	-1891	1143	5212	-1127	130
350	-1885	1074	5449	-1206	165
355	-1866	866	5591	-1393	181
360	-1797	704	5728	-1453	205

TABLE XXII TIME HISTORIES OF BLADE STRESS, PSI

V = 150 KT a_s = 0° L = 8400 LB D = 250 LB

	Chordwise Stress				Flapwise Stress				Torsional Stress		
ψ, DEG	r/R .15	r/R .375	r/R .65	r/R .80	r/R .375	r/R .45	r/R .65	r/R .80	r/R .15	r/R .375	r/R .65
0	-1635	-513	-432	635	6463	5277	2636	-2744	225	410	505
5	-1597	-379	-325	722	6958	5680	2289	-1218	203	378	448
10	-1554	-324	39	1062	7440	6392	1290	567	142	317	425
15	-1654	-372	51[illegible]	1369	7928	6398	1302	1369	173	274	419
20	-1810	-238	912	1484	7798	5663	2506	965	249	315	376
25	-1772	-18	1113	1519	6797	5081	3629	404	254	335	427
30	-1560	141	1101	1576	6365	5277	3982	133	249	386	493
35	-1260	227	994	1449	6408	5674	3461	434	318	457	503
40	-978	337	799	1247	6692	5591	2524	743	373	508	530
45	-816	319	598	1137	7088	5378	2065	537	359	530	591
50	-803	331	435	1109	6847	5016	1526	127	322	548	634
55	-941	276	435	1045	5981	4370	1191	-778	332	524	599
60	-1191	56	467	1132	5190	3611	973	-1670	320	508	589
65	-1272	-165	554	1282	4900	3332	440	-2062	350	520	617
70	-1241	-305	580	1340	5166	3237	-336	-2056	435	599	638
75	-1235	-440	360	1189	5271	3261	-1260	-2032	506	705	675
80	-113[illegible]	-317	65	860	4980	3143	-1880	-2177	512	769	781
85	-985	-183	-193	751	4511	2751	-1638	-2973	504	816	852
90	-853	-177	-262	831	3825	2093	-909	-4004	498	818	791
95	-828	-183	-92	912	3268	1785	-751	-4317	431	731	713
100	-972	-12	153	1080	3275	2152	-1533	-3546	314	571	621
105	-1060	-91	498	1276	3757	2449	-2799	-2201	211	404	505
110	-1035	31	793	1432	4127	2135	-3469	-1326	132	242	379
115	-1053	416	931	1478	4022	1447	-3220	-971	9	118	278
120	-1010	673	1000	1363	3268	866	-2588	-953	-112	-24	236
125	-828	930	1088	1397	2261	386	-1911	-1097	-183	-123	185
130	-516	1052	1201	1553	1717	172	-1452	-1176	-211	-170	123
135	-203	1107	1346	1646	1853	356	-1397	-989	-209	-188	127
140	-53	1260	1383	1617	2453	777	-1620	-856	-197	-178	152
145	9	1382	1314	1524	2756	1073	-1607	-959	-197	-154	156
150	3	1468	1302	1467	2527	1156	-1973	-1459	-227	-160	172

TABLE XXII CONCLUDED

V = 150 KT α_s = 0° L = 8400 LB D = 250 LB

	Chordwise Stress				Flapwise Stress				Torsional Stress		
ψ, DEG	r/R .15	r/R .375	r/R .65	r/R .80	r/R .375	r/R .45	r/R .65	r/R .80	r/R .15	r/R .375	r/R .65
155	-134	1492	1302	1507	2329	984	-1669	-2189	-221	-164	168
160	-260	1394	1415	1600	2323	777	-1334	-2719	-165	-158	156
165	-310	1040	1503	1725	2626	830	-1440	-2864	-106	-135	136
170	-272	887	1434	1744	3417	1435	-2054	-2587	-82	-95	131
175	-191	869	1157	1524	4171	2158	-2774	-2406	-51	-62	138
180	-191	783	749	1207	4733	2526	-2885	-2689	-33	-16	154
135	-260	795	423	1016	5005	2775	-2228	-3353	-27	25	180
190	-341	783	372	1005	5048	3107	-1465	-3738	-20	33	185
195	-510	557	567	1247	5110	3581	-751	-3660	-9	27	144
200	-785	160	862	1501	5357	4002	-243	-2900	-1	19	105
205	-978	-67	1094	1600	5833	4411	142	-1755	9	3	113
210	-1097	-146	1044	1605	6389	4708	750	-597	35	3	107
215	-1097	-165	755	1421	6544	4850	1457	223	54	41	97
220	-1091	-91	397	1120	6395	4939	2264	676	66	68	134
225	-1166	-158	115	976	6414	5212	3052	808	92	102	178
230	-1247	-342	71	1045	6748	5597	3591	953	157	126	182
235	-1403	-629	209	1253	7298	6036	3846	1007	187	149	158
240	-1697	-868	391	1386	7891	6611	3796	1152	167	114	178
245	-1866	-929	460	1374	8237	7056	3591	1200	149	49	148
250	-1922	-917	372	1293	8231	7014	3734	965	136	13	93
255	-1891	-782	159	1189	8027	6599	4106	718	118	-22	93
260	-1797	-635	65	1050	7823	6321	4354	736	183	-26	101
265	-1697	-525	33	1022	7767	6250	4144	1104	243	39	119
270	-1610	-421	159	1184	7712	6208	3635	1496	282	80	183
275	-1560	-476	372	1334	7607	6078	3232	1598	328	124	223
280	-1635	-262	586	1397	7390	5817	3145	1285	336	151	229
285	-1735	-36	711	1455	7007	5431	3300	670	280	118	238
290	-1785	-12	818	1444	6445	5099	3318	79	201	76	248
295	-1804	92	843	1478	6043	4945	2977	-193	138	25	219
300	-1747	62	837	1461	6093	4910	2469	-265	98	5	183
305	-1622	-177	724	1426	6191	4720	1960	-283	70	11	183
310	-1485	-305	510	1317	6179	4542	1594	-410	64	41	195
315	-1422	-434	196	1080	5988	4406	1228	-573	43	74	221
320	-1554	-397	-124	849	5747	4305	930	-904	37	114	258
325	-1704	-482	-293	739	5503	4156	887	-1230	50	173	287
330	-1847	-721	-187	889	5975	4239	781	-1435	120	232	344
335	-1991	-917	-17	1132	6284	4637	545	-1544	169	319	381
340	-2079	-1113	102	1201	6531	5058	452	-1815	197	347	444
345	-2079	-1113	109	1213	6525	5289	744	-2352	235	382	450
350	-1929	-935	-55	1143	6414	5212	1246	-2979	249	373	450
355	-1710	-751	-268	883	6297	5129	2096	-3142	235	396	493
360	-1635	-513	-432	635	6463	5277	2636	-2744	225	410	505

TABLE XXIII TIME HISTORIES OF BLADE STRESS, PSI

V = 150 KT α_s = 5° L = 8600 LB D = 1100 LB

	Chordwise Stress				Flapwise Stress				Torsional Stress		
ψ, DEG	r/R .15	r/R .375	r/R .65	r/R .80	r/R .375	r/R .45	r/R .65	r/R .80	r/R .15	r/R .375	r/R .65
0	-1791	-648	58	1068	6847	5372	2425	-1007	213	394	440
5	-1816	-85	240	1184	7285	5757	1848	410	213	341	399
10	-1822	-305	504	1241	7526	6030	1240	1206	219	307	405
15	-1810	-366	680	1357	7539	5562	1978	784	249	315	381
20	-1747	441	818	1421	6754	5159	2723	296	231	321	409
25	-1675	-48	900	1409	6111	5105	3076	-121	252	358	475
30	-1585	105	900	1392	6179	5087	3151	-241	336	445	501
35	-1391	245	862	1421	6093	5016	2369	163	423	536	542
40	-1247	-244	755	1380	6247	4886	1575	259	427	599	626
45	-1216	208	498	1149	6204	4471	1091	-48	427	629	654
50	-1228	-146	240	941	5450	3753	552	-675	427	619	664
55	-1228	-116	109	924	4912	3095	415	-1706	423	613	666
60	-1272	-18	65	999	4727	2882	-94	-2340	433	658	668
65	-1429	-568	134	1022	4677	2917	-1130	-2623	472	698	719
70	-1641	-599	153	1057	4912	2870	-1856	-3027	508	741	742
75	-1666	-201	266	1103	4844	2840	-2340	-3298	516	755	773
80	-1560	-434	266	1166	4443	2567	-2476	-3745	494	751	766
85	-1466	-684	184	1143	3924	2040	-2054	-4281	456	727	705
90	-1360	-183	178	1010	3219	1648	-1942	-4185	415	646	658
95	-1266	239	203	1028	3009	1571	-2327	-3491	350	575	605
100	-1153	-134	341	1184	3262	1524	-2885	-2418	270	494	528
105	-1103	19	561	1282	3262	1263	-3493	-1453	183	372	460
110	-1128	630	774	1334	3077	836	-3605	-1067	74	208	360
115	-1110	655	994	1461	2595	380	-3251	-1103	-43	59	268
120	-928	490	1182	1559	1804	-71	-2805	-1326	-114	-60	193
125	-741	985	1314	1646	1322	-451	-2296	-1604	-138	-95	140
130	-578	1382	1327	1594	1217	-480	-2191	-1507	-173	-117	180
135	-391	1174	1289	1501	1433	-255	-2532	-1302	-185	-131	219
140	-241	1297	1264	1507	1711	-71	-2761	-1369	-195	-137	201
145	-141	1350	1270	1536	1674	18	-2879	-1628	-205	-150	164
150	-172	1376	1327	1542	1569	24	-2656	-2183	-209	-176	170

TABLE XXIII CONCLUDED

V = 150 kt α_s = +5° L = 8600 LB D = 1100 LB

	Chordwise Stress				Flapwise Stress				Torsional Stress		
ψ, DEG	r/R .15	r/R .375	r/R .65	r/R .80	r/R .375	r/R .45	r/R .65	r/R .80	r/R .15	r/R .375	r/R .65
155	-241	1327	1390	1576	1625	24	-2265	-2756	-203	-168	162
160	-266	1694	1415	1640	1822	279	-2259	-2912	-177	-160	138
165	-285	1144	1365	1628	2385	771	-2507	-2786	-175	-139	127
170	-347	1040	1214	1478	3170	1322	-2755	-2593	-165	-135	127
175	-391	1413	1057	1322	3788	1803	-2836	-2520	-146	-125	121
180	-416	997	969	1340	4208	2218	-2439	-2756	-128	-56	129
185	-435	496	963	1409	4387	2579	-1763	-3009	-142	-16	170
190	-572	539	982	1449	4449	2941	-1080	-3045	-128	-22	158
195	-778	661	956	1426	4838	3392	-454	-2695	-112	-34	95
200	-842	312	956	1403	5400	3902	-69	-1948	-104	-62	87
205	-885	-189	850	1467	6006	4382	279	-1115	-59	-24	107
210	-910	-379	667	1357	6432	4785	762	-446	-3	45	131
215	-1035	-338	485	1172	6575	5022	1451	-54	29	90	185
220	-1185	-183	322	1143	6674	5206	2301	42	50	110	195
225	-1210	-262	310	1207	6797	5419	3058	175	70	118	183
230	-1303	-617	322	1345	7211	5882	3430	422	72	114	180
235	-1416	-959	353	1288	7712	6463	3424	862	50	90	195
240	-1547	-1039	322	1270	8070	6795	3343	1140	23	43	183
245	-1604	-892	253	1247	8181	6801	3560	1128	-1	7	140
250	-1535	-611	259	1195	7959	6564	3858	1013	-31	-28	127
255	-1566	-232	259	1236	7712	6315	4137	869	-21	-46	138
260	-1616	-256	341	1305	7452	6107	4088	965	19	-24	146
265	-1560	-690	492	1322	7347	6042	3666	1176	58	9	193
270	-1504	-654	592	1501	7465	6000	3194	1248	78	51	250
275	-1441	1	649	1496	7359	5811	2754	1025	84	63	274
280	-1447	263	592	1357	7032	5461	2599	452	37	27	266
285	-1541	-207	498	1276	6593	5182	2549	-283	-37	-38	217
290	-1535	-189	536	1293	6148	4915	2363	-844	-57	-74	160
295	-1529	215	611	1432	6012	4708	2227	-1278	-35	-48	148
300	-1541	-18	592	1467	6025	4607	1873	-1230	13	25	211
305	-1597	-599	498	1305	6056	4619	1321	-995	74	135	291
310	-1660	-764	291	1161	6062	4530	1054	-910	126	210	311
315	-1672	-403	14	993	5913	4411	887	-935	153	283	356
320	-1704	-226	-149	935	5845	4311	1004	-1200	185	345	407
325	-1866	-825	-174	976	5957	4376	1191	-1525	209	375	401
330	-1960	-1216	-86	1045	6093	4690	1097	-1682	199	408	456
335	-2047	-1161	-23	1155	6402	5099	992	-1839	167	380	434
340	-2079	-886	2	1143	6711	5443	1085	-1984	149	329	401
345	-2091	-641	-48	1039	6809	5497	1333	-2050	138	283	391
350	-2041	-727	-136	947	6711	5372	1811	-1948	169	285	409
355	-1885	-935	-74	930	6568	5253	2270	-1598	183	337	440
360	-1791	-648	58	1068	6347	5372	2425	-1007	213	394	440

TABLE XXIV TIME HISTORIES OF BLADE STRESS, PSI

V = 175 KT α_s = -5° L = 7100 LB D = -250 LB

	Chordwise Stress		Flapwise Stress		Torsional Stress
ψ, DEG	r/R .15	r/R .80	r/R .45	r/R .80	r/R .15
0	-1324	498	5694	-1575	227
5	-1298	567	6103	-1032	259
10	-1267	764	6685	-267	269
15	-1280	1105	6988	239	293
20	-1342	1331	6922	372	327
25	-1280	1475	6804	396	321
30	-1129	1620	6715	547	331
35	-846	1695	6548	872	404
40	-538	1655	6483	1294	479
45	-369	1579	6305	1385	503
50	-256	1487	5646	987	519
55	-218	1469	4999	191	531
60	-318	1423	4643	-544	509
65	-362	1377	4459	-1147	515
70	-375	1365	4150	-1701	525
75	-356	1232	3753	-1912	533
80	-369	932	3492	-1846	533
85	-381	746	3040	-2099	517
90	-325	723	2411	-2606	479
95	-312	816	2186	-2600	420
100	-406	995	2465	-2093	297
105	-557	1128	2554	-1533	188
110	-670	1284	2144	-1093	75
115	-746	1464	1746	-864	-38
120	-670	1631	1444	-755	-161
125	-469	1707	1058	-731	-221
130	-161	1782	779	-828	-245
135	153	1764	945	-737	-256
140	366	1660	1189	-797	-264
145	329	1533	1331	-1153	-243
150	285	1545	1444	-1744	-217

TABLE XXIV CONCLUDED

V = 175 KT α_s = -5° L = 7100 LB D = -250 LB

	Chordwise Stress		Flapwise Stress		Torsional Stress
ψ, DEG	r/R .15	r/R .80	r/R .45	r/R .80	r/R .15
155	197	1817	1533	-2425	-183
160	40	1967	1456	-3021	-120
165	-168	1863	1592	-3238	-62
170	-243	1672	2067	-3124	-48
175	-86	1533	2536	-2979	-16
180	40	1336	2708	-3028	13
185	2	1082	2874	-3142	-7
190	-86	995	3207	-3058	-36
195	-199	1209	3503	-2744	-54
200	-457	1417	3776	-2117	-52
205	-702	1441	4216	-1274	-38
210	-909	1475	4691	-448	17
215	-978	1458	4993	40	81
220	-1053	1267	5278	342	152
225	-1173	1099	5700	499	237
230	-1261	1128	6103	722	305
235	-1324	1273	6477	987	333
240	-1619	1331	6916	1324	339
245	-1964	1215	7261	1674	337
250	-2147	1227	7219	1800	335
255	-2153	1319	6988	1855	370
260	-2027	1238	6928	2017	436
265	-1958	1140	6910	2240	489
270	-1883	1093	6738	2337	557
275	-1688	1099	6495	2355	610
280	-1613	1261	6293	2102	612
285	-1606	1348	5943	1692	547
290	-1631	1400	5611	1131	456
295	-1606	1539	5409	667	358
300	-1424	1620	5290	276	275
305	-1242	1550	5064	-98	180
310	-1085	1388	4827	-454	97
315	-909	1209	4601	-701	5
320	-896	1111	4323	-906	-48
325	-1022	1012	4091	-978	-50
330	-1223	1041	4186	-864	-20
335	-1430	1203	4542	-779	51
340	-1518	1215	4827	-858	128
345	-1575	1024	5017	-1153	182
350	-1543	822	5260	-1485	208
355	-1424	631	5504	-1620	224
360	-1324	408	5694	-1575	227

TABLE XXV TIME HISTORIES OF BLADE STRESS, PSI

V = 175 KT a_s = 0° L = 7100 LB D = 400 LB

	Chordwise Stress				Flapwise Stress				Torsional Stress		
ψ, DEG	r/R .15	r/R .375	r/R .65	r/R .80	r/R .375	r/R .45	r/R .65	r/R .80	r/R .15	r/R .375	r/R .65
0	-1386	-451	-516	556	6882	5385	3112	46	148	266	377
5	-1280	-163	-283	781	7396	5860	2653	1427	148	274	358
10	-1267	52	303	1209	7910	6358	2672	1909	160	257	379
15	-1462	-46	902	1550	7817	6305	3013	1788	218	337	399
20	-1631	64	1399	1718	7365	6228	3611	1137	265	341	423
25	-1638	383	1626	1880	7309	6163	4184	571	249	356	433
30	-1411	395	1569	1834	7036	6097	4017	499	309	394	450
35	-1041	511	1336	1608	6875	5830	3378	673	366	469	480
40	-727	432	952	1371	6888	5569	2709	655	390	552	596
45	-538	530	518	1163	6541	4969	1859	535	457	656	706
50	-570	401	221	932	6021	4186	1363	-291	515	753	738
55	-790	180	102	874	5686	3723	929	-1219	507	775	793
60	-1122	94	127	1012	5271	3598	-19	-2033	517	777	832
65	-1355	-733	316	1209	5191	3444	-776	-2883	600	840	821
70	-1462	-604	354	1284	5110	3343	-1501	-3238	624	901	823
75	-1430	-598	190	1140	4906	3124	-2047	-3353	622	921	895
80	-1292	-886	-112	949	4627	2619	-1942	-3504	618	952	915
85	-1148	-665	-434	729	3896	2031	-1613	-3956	604	946	911
90	-991	-89	-472	648	3258	1646	-1309	-4209	549	915	903
95	-922	-157	-232	856	3010	1794	-1867	-3461	467	834	836
100	-959	-390	127	1174	3252	2156	-3101	-2154	342	646	655
105	-1085	-59	612	1423	3884	1936	-3833	-1286	184	404	474
110	-1267	389	1047	1562	3828	1224	-3789	-773	13	149	287
115	-1292	585	1324	1689	3016	441	-3318	-586	-195	-97	145
120	-1091	713	1506	1759	1908	-200	-2506	-695	-312	-316	27
125	-720	1075	1620	1811	941	-735	-1923	-683	-365	-381	-46
130	-256	1492	1576	1776	675	-907	-1644	-623	-369	-391	7
135	159	1620	1450	1655	1115	-586	-1706	-442	-332	-318	78
140	373	1590	1292	1522	1369	-123	-2245	-406	-284	-204	137
145	310	1914	1198	1400	1301	79	-2462	-1026	-280	-150	224
150	84	2110	1355	1504	1090	-10	-2233	-1997	-272	-135	269

TABLE XXV CONCLUDED

V = 175 KT α_s = 0° L = 7100 LB D = 400 LB

	Chordwise Stress				Flapwise Stress				Torsional Stress		
ψ, DEG	r/R .15	r/R .375	r/R .65	r/R .80	r/R .375	r/R .45	r/R .65	r/R .80	r/R .15	r/R .375	r/R .65
155	-136	1510	1645	1817	1041	-105	-1979	-2805	-221	-168	220
160	-356	1277	1884	2054	1487	-22	-1979	-3251	-187	-168	125
165	-425	1253	1847	2019	2162	476	-2524	-3100	-209	-200	104
170	-375	965	1431	1730	3066	1212	-3399	-2756	-213	-231	84
175	-274	677	826	1290	3964	1794	-3634	-2786	-183	-174	27
180	-168	836	341	943	4453	2120	-3213	-3124	-181	-111	76
185	-168	922	102	932	4509	2435	-2326	-2570	-147	-52	145
190	-293	597	203	1088	4571	2928	-1371	-3709	-88	11	106
195	-651	64	473	1296	4751	3527	-652	-3166	-64	11	84
200	-1022	-347	769	1464	5364	4020	-75	-2172	-12	-24	76
205	-1236	-506	877	1562	6138	4566	526	-960	53	19	68
210	-1280	-408	681	1504	6566	4981	1084	125	93	76	110
215	-1298	-255	360	1232	6671	5248	1927	709	140	141	167
220	-1236	-396	39	978	6578	5379	2920	963	176	189	198
225	-1185	-684	-157	989	6795	5646	3837	1101	192	183	204
230	-1236	-886	-150	1070	7414	6210	4401	1288	208	155	155
235	-1449	-935	45	1163	8034	6875	4265	1764	186	86	131
240	-1751	-757	215	1325	8535	7439	4116	1891	156	-8	94
245	-1902	-659	398	1383	8802	7575	4228	1861	164	-60	44
250	-2033	-757	455	1441	8616	7290	4594	1595	222	-79	10
255	-2027	-843	442	1348	8368	6863	5059	1336	337	-34	43
260	-1832	-433	448	1261	8052	6661	4966	1547	461	92	113
265	-1625	-249	385	1354	7916	6164	4395	1963	563	199	202
270	-1399	-267	442	1351	7941	6412	3881	2156	626	295	243
275	-1273	3	518	1296	7724	5979	3502	2048	624	305	263
280	-1273	58	574	1394	7377	5569	3341	1475	515	254	249
285	-1330	370	732	1394	6782	5195	3168	703	370	151	210
290	-1512	291	864	1458	6188	4821	2827	58	245	45	157
295	-1619	272	1009	1579	6008	4637	2461	-460	160	-28	137
300	-1455	70	1040	1660	6076	4518	1810	-550	111	-30	135
305	-1267	-279	776	1574	6045	4382	1171	-719	120	39	151
310	-1091	-482	335	1209	5835	4150	911	-906	114	92	204
315	-965	-267	-251	758	5476	3943	743	-1123	107	151	269
320	-1028	-102	-742	527	5271	3735	911	-1382	112	238	310
325	-1135	-537	-717	504	5296	3699	1078	-1491	146	305	393
330	-1437	-1021	-591	810	5550	4067	1016	-1424	184	349	399
335	-1820	-1248	-251	1134	5996	4649	929	-1378	204	370	297
340	-2040	-1284	14	1198	6268	5017	1047	-1485	202	351	413
345	-1996	-1223	64	1146	6405	5159	1493	-1617	196	327	450
350	-1751	-929	-138	1007	6448	5171	2076	-1298	186	315	407
355	-1518	-580	-446	706	6603	5177	2709	-1045	156	295	381
360	-1386	-451	-516	556	6882	5385	3112	46	148	266	377

TABLE XXVI TIME HISTORIES OF BLADE STRESS, PSI

V = 175 KT α_s = +5° L = 7300 LB D = 1150 LB

	Chordwise Stress				Flapwise Stress				Torsional Stress		
ψ, DEG	r/R .15	r/R .375	r/R .65	r/R .80	r/R .375	r/R .45	r/R .65	r/R .80	r/R .15	r/R .375	r/R .65
0	-1738	-322	763	1539	7173	5421	2517	1234	105	149	238
5	-1587	82	738	1388	7551	6073	1927	1770	146	224	316
10	-1443	199	719	1174	7718	6222	2362	1113	261	347	409
15	-1254	438	662	1267	7284	5895	3050	511	339	439	472
20	-1217	481	751	1377	6560	5717	3763	-92	331	477	476
25	-1317	419	958	1406	6256	5432	3806	209	327	469	505
30	-1443	266	1185	1562	5897	5177	3044	1017	392	493	533
35	-1380	-40	1198	1741	6052	4607	2306	1535	426	562	551
40	-1317	21	908	1522	5990	4097	1667	1354	432	597	628
45	-1336	-114	404	1018	5271	3497	793	499	469	642	687
50	-1273	-77	-31	741	4776	3106	384	-1105	479	698	720
55	-1154	-163	-333	718	4491	2928	-218	-2515	521	755	763
60	-1217	-555	-371	793	4472	2898	-1222	-3570	596	871	811
65	-1550	-629	-251	845	4745	2856	-2028	-4227	644	950	874
70	-1826	-690	-49	966	4646	2708	-2965	-4245	666	960	931
75	-1908	-904	95	1157	4218	2316	-3318	-4281	668	970	931
80	-1908	-800	177	1221	3716	1628	-3027	-4378	616	950	889
85	-1851	-574	158	1082	3004	1117	-2816	-4209	576	877	862
90	-1675	-353	152	1036	2707	927	-2878	-3684	541	820	813
95	-1374	-218	177	1105	2713	1117	-3411	-2720	473	757	710
100	-1110	-22	297	1169	2762	1171	-4149	-1641	370	650	610
105	-1041	303	448	1209	2824	791	-4285	-1141	222	469	486
110	-1066	530	681	1279	2385	61	-3882	-882	53	252	346
115	-1009	750	1040	1493	1456	-723	-3312	-761	-104	9	192
120	-878	1044	1418	1788	619	-1411	-2673	-671	-241	-170	76
125	-746	1259	1683	1909	25	-1839	-2425	-400	-334	-308	27
130	-607	1436	1752	1857	-74	-1898	-2481	-237	-360	-395	33
135	-369	1712	1689	1753	105	-1655	-2661	-243	-346	-373	68
140	-80	2006	1588	1689	74	-1275	-2865	-635	-312	-275	129
145	140	1933	1481	1614	--09	-1019	-2841	-1412	-290	-194	180
150	134	1976	1412	1585	62	-830	-2586	-2268	-268	-127	226

TABLE XXVI CONCLUDED

V = 175 KT α_s = +5° L = 7300 LB D = 1100 LB

	Chordwise Stress				Flapwise Stress				Torsional Stress		
ψ, DEG	r/R .15	r/R .375	r/R .65	r/R .80	r/R .375	r/R .45	r/R .65	r/R .80	r/R .15	r/R .375	r/R .65
155	21	1878	1399	1585	322	-663	-2481	-2774	-272	-148	204
160	-136	1577	1437	1672	886	-426	-2617	-2871	-318	-206	147
165	-413	1424	1412	1695	1728	96	-3089	-2527	-379	-282	64
170	-702	1271	1349	1562	2552	749	-3566	-2190	-405	-306	3
175	-852	848	1223	1545	3270	1141	-3479	-2262	-385	-286	41
180	-808	542	1047	1533	3605	1515	-2822	-2714	-322	-229	46
185	-752	358	782	1388	3840	2067	-2028	-3046	-241	-137	17
190	-746	137	423	1134	4274	2839	-1309	-3136	-185	-97	27
195	-714	-16	184	972	4899	3604	-708	-2738	-92	-32	108
200	-739	-175	89	1007	5599	4305	-218	-2209	37	104	147
205	-903	-390	121	1111	6275	4869	415	-1129	83	228	218
210	-1179	-567	253	1169	6609	5118	1214	-351	55	220	273
215	-1506	-653	410	1313	6634	5159	2188	282	33	124	202
220	-1656	-806	568	1458	6813	5391	3099	854	-26	27	96
225	-1638	-825	625	1504	7222	5860	3651	1445	-88	-30	106
230	-1493	-733	518	1441	7656	6335	3887	1861	-64	-44	131
235	-1298	-653	373	1267	8052	6762	3992	1987	-30	-22	98
240	-1129	-469	171	1163	8263	7136	4116	1897	-30	-12	104
245	-1035	-249	108	1076	8133	7106	4364	1565	9	27	157
250	-1116	-132	253	1209	7848	6744	4656	1192	43	78	165
255	-1330	-71	562	1452	7495	6430	4606	1210	71	94	180
260	-1506	-126	940	1655	7414	6174	4141	1517	89	88	200
265	-1518	-145	1204	1799	7396	5913	3515	1710	122	106	212
270	-1386	70	1198	1817	7148	5510	2808	1680	105	112	234
275	-1185	180	946	1574	6832	5177	2448	1065	61	82	251
280	-991	266	581	1238	6423	4821	2213	245	17	35	230
285	-840	407	297	1076	5866	4524	1946	-653	-44	-10	175
290	-827	352	190	1099	5531	4257	1717	-1400	-124	-40	159
295	-1003	94	253	1192	5407	4204	1283	-1569	-139	-58	145
300	-1267	-273	373	1319	5333	4020	780	-1436	-100	-58	112
305	-1506	-555	448	1412	5234	3693	545	-1255	-88	-2	155
310	-1625	-586	379	1331	4999	3462	433	-1014	-22	45	220
315	-1644	-653	108	1088	4881	3420	384	-924	118	195	267
320	-1543	-696	-220	937	4949	3509	557	-1069	229	372	375
325	-1455	-733	-478	822	5172	3788	669	-1292	309	633	478
330	-1437	-794	-547	746	5624	4334	842	-1593	378	625	563
335	-1518	-868	-516	781	6132	4952	979	-1834	319	603	559
340	-1613	-849	-358	880	6392	5278	1252	-1882	216	485	535
345	-1807	-727	-106	995	6553	5219	1803	-1593	144	349	417
350	-1983	-567	209	1157	6652	5011	2306	-810	101	209	297
355	-1920	-426	530	1394	6776	4999	2641	167	89	132	243
360	-1738	-322	763	1539	7173	5421	2517	1234	105	149	238

TABLE XXVII a HARMONICS OF FLAPWISE STRESS, PSI

V = 110 KT α_s = -5° L = 8300 LB D = -750 LB

BLADE STATION = .375R

N	EXPERIMENTAL A(N)	EXPERIMENTAL B(N)	UNIFORM INFLOW A(N)	UNIFORM INFLOW B(N)	VARIABLE INFLOW A(N)	VARIABLE INFLOW B(N)
0	-243.		472.		570.	
1	-811.	942.	-765.	1444.	-680.	964.
2	124.	-571.	-329.	-549.	7.	-250.
3	-140.	-204.	-218.	-65.	-320.	-44.
4	-39.	-72.	-29.	-25.	-46.	50.
5	67.	-38.	-33.	-22.	-118.	40.
6	-11.	-25.	-10.	-8.	7.	-13.
7	29.	-6.	-3.	-1.	1.	-31.
8	30.	19.	-1.	1.	-95.	1.
9	4.	30.	1.	0.	-24.	-13.
10	-7.	1.	0.	0.	-7.	-6.

BLADE STATION = .45R

EXPERIMENTAL A(N)	EXPERIMENTAL B(N)	UNIFORM INFLOW A(N)	UNIFORM INFLOW B(N)	VARIABLE INFLOW A(N)	VARIABLE INFLOW B(N)
-395.		309.		396.	
-899.	1060.	-924.	1707.	-844.	1152.
191.	-565.	-262.	-595.	109.	-228.
-133.	-259.	-249.	-107.	-346.	-105.
-12.	-51.	-12.	-17.	-45.	28.
60.	-55.	-13.	-22.	-61.	6.
15.	2.	-5.	-8.	9.	-16.
-9.	2.	-2.	-3.	-11.	-47.
28.	7.	-1.	3.	-198.	2.
-16.	28.	2.	1.	-41.	-23.
-22.	8.	0.	-1.	-13.	-9.

BLADE STATION = .65R

N	EXPERIMENTAL A(N)	EXPERIMENTAL B(N)	UNIFORM INFLOW A(N)	UNIFORM INFLOW B(N)	VARIABLE INFLOW A(N)	VARIABLE INFLOW B(N)
0	-881.		-1176.		-1068.	
1	-1105.	1297.	-964.	1649.	-1104.	1175.
2	586.	-459.	204.	-485.	475.	-145.
3	94.	-474.	-262.	-241.	-189.	-291.
4	171.	-1.	12.	-1.	-13.	-200.
5	-14.	37.	56.	13.	159.	-124.
6	30.	66.	16.	8.	-12.	-4.
7	-51.	17.	3.	1.	-11.	24.
8	-21.	-24.	1.	0.	25.	-1.
9	0.	-27.	0.	0.	16.	6.
10	17.	-4.	0.	0.	2.	4.

BLADE STATION = .80R

EXPERIMENTAL A(N)	EXPERIMENTAL B(N)	UNIFORM INFLOW A(N)	UNIFORM INFLOW B(N)	VARIABLE INFLOW A(N)	VARIABLE INFLOW B(N)
-1555.		-1451.		-1342.	
-470.	701.	-551.	892.	-765.	668.
590.	-266.	307.	-258.	418.	-98.
181.	-515.	-168.	-200.	-31.	-239.
325.	-27.	-1.	-2.	6.	-242.
-68.	119.	52.	29.	160.	-118.
-71.	23.	17.	15.	-23.	7.
13.	4.	5.	4.	8.	76.
-13.	11.	2.	-4.	270.	-5.
27.	26.	-3.	-1.	65.	33.
0.	3.	0.	2.	18.	13.

TABLE XXVII.b HARMONICS OF CHORDWISE STRESS, PSI

V = 110 KT α_s = -5° L = 8300 LB D = -750 LB

BLADE STATION = .15R

N	EXPERIMENTAL A(N)	EXPERIMENTAL B(N)	UNIFORM INFLOW A(N)	UNIFORM INFLOW B(N)	VARIABLE INFLOW A(N)	VARIABLE INFLOW B(N)
0	-1101.		244.		265.	
1	522.	-416.	31.	-166.	40.	-169.
2	-42.	-66.	9.	22.	-38.	11.
3	146.	-20.	108.	-80.	115.	-42.
4	21.	21.	28.	-10.	17.	16.
5	8.	13.	-2.	- 7.	-14.	-3.
6	22.	5.	-3.	- 2.	- 7.	11.
7	-23.	12.	-1.	- 1.	- 6.	6.
8	35.	-34.	1.	- 0.	-16.	39.
9	-15.	-14.	2.	- 0.	0.	11.
10	2.	-11.	2.	- 1.	- 6.	-1.

BLADE STATION = .375R

N	EXPERIMENTAL A(N)	EXPERIMENTAL B(N)	UNIFORM INFLOW A(N)	UNIFORM INFLOW B(N)	VARIABLE INFLOW A(N)	VARIABLE INFLOW B(N)
0	10.		162.		204.	
1	387.	-316.	94.	-289.	125.	-254.
2	-55.	19.	11.	53.	-82.	18.
3	258.	-113.	210.	-201.	230.	-114.
4	3.	75.	64.	- 41.	74.	36.
5	-28.	-2.	- 2.	- 5.	1.	21.
6	6.	6.	-4.	- 2.	2.	12.
7	-3.	0.	-1.	- 1.	0.	4.
8	15.	-11.	1.	0.	-5.	27.
9	-6.	-20.	1.	- 1.	1.	7.
10	17.	-27.	1.	- 1.	-4.	-1.

BLADE STATION = .65R

N	EXPERIMENTAL A(N)	EXPERIMENTAL B(N)	UNIFORM INFLOW A(N)	UNIFORM INFLOW B(N)	VARIABLE INFLOW A(N)	VARIABLE INFLOW B(N)
0	483.		105.		148.	
1	259.	-119.	114.	-110.	151.	-29.
2	-38.	-6.	-5.	42.	-57.	6.
3	186.	-130.	114.	-174.	133.	-106.
4	-6.	73.	47.	-53.	99.	26.
5	-28.	-14.	1.	9.	42.	50.
6	-8.	13.	3.	3.	24.	-7.
7	16.	-4.	0.	0.	18.	-9.
8	-46.	39.	-2.	-2.	33.	-57.
9	19.	23.	-4.	0.	0.	-16.
10	-23.	31.	-3.	0.	9.	2.

BLADE STATION = .80R

N	EXPERIMENTAL A(N)	EXPERIMENTAL B(N)	UNIFORM INFLOW A(N)	UNIFORM INFLOW B(N)	VARIABLE INFLOW A(N)	VARIABLE INFLOW B(N)
0	1231.		51.		72.	
1	100.	-10.	58.	-28.	76.	18.
2	-16.	0.	-4.	18.	-24.	1.
3	68.	-70.	41.	-80.	-50.	-49.
4	-3.	35.	20.	-27.	51.	11.
5	-12.	-6.	1.	6.	26.	28.
6	-2.	11.	2.	2.	14.	-6.
7	8.	-3.	0.	0.	11.	-6.
8	-30.	32.	-2.	-1.	21.	-39.
9	16.	20.	-3.	0.	0.	-11.
10	-15.	30.	-2.	0.	6.	-1.

TABLE XXVII c HARMONICS OF TORSIONAL STRESS, PSI

V = 110 KT α_s = -5° L = 8300 LB D = -750 LB

BLADE STATION .15R

N	EXPERIMENTAL A(N)	EXPERIMENTAL B(N)	UNIFORM INFLOW A(N)	UNIFORM INFLOW B(N)	VARIABLE INFLOW A(N)	VARIABLE INFLOW B(N)
0	108.		-129.		-127.	
1	-75.	-59.	-86.	-17.	-91.	-30.
2	46.	-63.	34.	-14.	31.	-16.
3	3.	5.	1.	2.	5.	-3.
4	-20.	-3.	-3.	-2.	3.	-6.
5	-3.	-12.	1.	0.	2.	-3.
6	14.	16.	1.	0.	-1.	0.
7	6.	3.	0.	0.	0.	1.
8	4.	2.	-0.	-0.	-2.	3.
9	0.	1.	-0.	-0.	1.	2.
10	-1.	4.	-0.	-0.	1.	0.

BLADE STATION .375R

N	EXPERIMENTAL A(N)	EXPERIMENTAL B(N)	UNIFORM INFLOW A(N)	UNIFORM INFLOW B(N)	VARIABLE INFLOW A(N)	VARIABLE INFLOW B(N)
0	185.		-157.		-155.	
1	-132.	-122.	-105.	-20.	-111.	-37.
2	37.	-53.	42.	-17.	38.	-20.
3	-4.	34.	2.	2.	6.	-4.
4	-15.	4.	-3.	-2.	4.	-7.
5	8.	-13.	1.	0.	3.	-3.
6	19.	23.	1.	0.	-2.	0.
7	13.	-1.	1.	0.	0.	1.
8	7.	-5.	-0.	-0.	-2.	4.
9	-7.	-4.	-0.	-0.	2.	2.
10	-5.	-2.	-0.	-0.	1.	0.

BLADE STATION .65R

EXPERIMENTAL A(N)	EXPERIMENTAL B(N)	UNIFORM INFLOW A(N)	UNIFORM INFLOW B(N)	VARIABLE INFLOW A(N)	VARIABLE INFLOW B(N)
292.		-111.		-109.	
-107.	-133.	-74.	-14.	-78.	-26.
20.	-30.	29.	-12.	27.	-14.
7.	10.	1.	2.	4.	-3.
-20.	11.	-3.	-2.	3.	-5.
-1.	-12.	1.	0.	2.	-2.
9.	16.	1.	0.	-1.	0.
6.	3.	-0.	-0.	0.	1.
4.	1.	-0.	-0.	-1.	3.
-2.	-2.	-0.	-0.	1.	1.
1.	-1.	-0.	-0.	1.	0.

TABLE XXVIII a. HARMONICS OF FLAPWISE STRESS, PSI

V = 110 KT α_s = 0° L = 8200 LB D = 50 LB

BLADE STATION = .375R

N	EXPERIMENTAL A(N)	EXPERIMENTAL B(N)	UNIFORM INFLOW A(N)	UNIFORM INFLOW B(N)
0	-555.		-52.	
1	-742.	1057.	-743.	1728.
2	190.	-701.	-302.	-555.
3	-247.	-103.	-217.	-19.
4	-120.	-63.	-25.	-13.
5	-66.	74.	-26.	-8.
6	-77.	31.	-8.	1.
7	6.	77.	-1.	0.
8	73.	84.	-5.	2.
9	66.	79.	-1.	1.
10	68.	37.	0.	0.

BLADE STATION = .45R

EXPERIMENTAL A(N)	EXPERIMENTAL B(N)	UNIFORM INFLOW A(N)	UNIFORM INFLOW B(N)
-716.		-279.	
-908.	1225.	-892.	1964.
230.	-643.	-235.	-604.
-230.	-78.	-253.	-66.
-32.	-15.	-16.	-9.
33.	18.	-13.	-13.
11.	2.	-6.	1.
-57.	-9.	-1.	-1.
43.	-32.	-9.	2.
-23.	16.	-3.	2.
-37.	25.	0.	0.

BLADE STATION = .65R

N	EXPERIMENTAL A(N)	EXPERIMENTAL B(N)	UNIFORM INFLOW A(N)	UNIFORM INFLOW B(N)
0	-1289.		-1609.	
1	-1045.	1422.	-905.	1755.
2	526.	-651.	166.	-505.
3	-1.	-430.	-291.	-217.
4	112.	-73.	-14.	-6.
5	20.	-167.	39.	-4.
6	47.	46.	11.	-2.
7	-95.	15.	2.	-1.
8	-52.	-43.	1.	-1.
9	41.	-3.	0.	-1.
10	75.	-28.	0.	0.

BLADE STATION = .80R

EXPERIMENTAL A(N)	EXPERIMENTAL B(N)	UNIFORM INFLOW A(N)	UNIFORM INFLOW B(N)
-1685.		-1622.	
-404.	742.	-506.	932.
376.	-340.	244.	-273.
40.	-567.	-195.	-182.
337.	-106.	-21.	-8.
13.	-103.	39.	7.
-89.	47.	14.	-3.
140.	96.	2.	1.
6.	139.	13.	-3.
5.	64.	4.	-3.
-45.	43.	0.	0.

TABLE XXVIII b HARMONICS OF CHORDWISE STRESS, PSI

V = 110 KT α_s = 0° L = 8200 LB D = 50 LB

BLADE STATION = .15R

N	EXPERIMENTAL A(N)	EXPERIMENTAL B(N)	UNIFORM INFLOW A(N)	UNIFORM INFLOW B(N)
0	-1170.		155.	
1	440.	-247.	112.	-151.
2	-50.	12.	-29.	38.
3	135.	-61.	76.	-69.
4	22.	-3.	24.	-9.
5	18.	-7.	0.	-4.
6	5.	-3.	-3.	-1.
7	-19.	-2.	-1.	0.
8	-63.	-7.	-1.	0.
9	-21.	-26.	-1.	1.
10	7.	-10.	0.	0.

BLADE STATION = .375R

EXPERIMENTAL A(N)	EXPERIMENTAL B(N)	UNIFORM INFLOW A(N)	UNIFORM INFLOW B(N)
42.		162.	
389.	-222.	227.	-262.
-87.	69.	-68.	73.
186.	-148.	143.	-162.
-14.	5.	56.	-44.
-28.	-7.	0.	-4.
15.	11.	-2.	0.
4.	5.	-1.	0.
-15.	-16.	-1.	0.
1.	-12.	-1.	1.
52.	-36.	0.	0.

BLADE STATION = .65R

N	EXPERIMENTAL A(N)	EXPERIMENTAL B(N)	UNIFORM INFLOW A(N)	UNIFORM INFLOW B(N)
0	524.		135.	
1	262.	-56.	148.	-86.
2	-55.	13.	-53.	40.
3	91.	-135.	71.	-126.
4	-27.	28.	43.	-61.
5	-32.	-15.	0.	4.
6	11.	14.	5.	3.
7	-9.	10.	1.	0.
8	64.	16.	2.	-1.
9	27.	40.	1.	-2.
10	-34.	16.	0.	0.

BLADE STATION = .80R

EXPERIMENTAL A(N)	EXPERIMENTAL B(N)	UNIFORM INFLOW A(N)	UNIFORM INFLOW B(N)
1249.		66.	
103.	11.	60.	-16.
-13.	10.	-23.	14.
27.	-67.	24.	-55.
-17.	15.	19.	-31.
-15.	-9.	0.	3.
10.	2.	3.	2.
-7.	0.	1.	0.
45.	7.	2.	0.
30.	33.	1.	-1.
-25.	19.	0.	0.

TABLE XXVIII c HARMONICS OF TORSIONAL STRESS, PSI

V = 110 KT α_s = 0° L = 8200 LB D = 50 LB

BLADE STATION .15R

N	EXPERIMENTAL A(N)	EXPERIMENTAL B(N)	UNIFORM INFLOW A(N)	UNIFORM INFLOW B(N)
0	111.		-106.	
1	-82.	-59.	-70.	-6.
2	47.	-52.	26.	-14.
3	-13.	32.	1.	3.
4	-23.	-9.	-3.	-1.
5	-8.	-8.	1.	0.
6	16.	21.	1.	0.
7	-8.	23.	1.	0.
8	-4.	6.	-0.	-0.
9	-3.	0.	-0.	-0.
10	-5.	0.	-0.	-0.

BLADE STATION .375R

N	EXPERIMENTAL A(N)	EXPERIMENTAL B(N)	UNIFORM INFLOW A(N)	UNIFORM INFLOW B(N)
0	201.		-129.	
1	-127.	-119.	-86.	-7.
2	48.	-35.	31.	-17.
3	-22.	49.	1.	4.
4	-13.	4.	-3.	-1.
5	-9.	-13.	1.	0.
6	32.	22.	1.	0.
7	-15.	30.	1.	0.
8	-14.	-16.	-0.	-0.
9	-1.	-1.	-0.	-0.
10	-21.	-11.	-0.	-0.

BLADE STATION .65R

EXPERIMENTAL A(N)	EXPERIMENTAL B(N)	UNIFORM INFLOW A(N)	UNIFORM INFLOW B(N)
297.		-91.	
-105.	-126.	-61.	-5.
34.	-23.	22.	-12.
-5.	33.	1.	3.
-24.	5.	-2.	-1.
-7.	-10.	1.	0.
12.	19.	1.	0.
-9.	16.	-0.	-0.
-6.	5.	-0.	-0.
-4.	-5.	-0.	-0.
-2.	-5.	-0.	-0.

TABLE XXIX a HARMONICS OF FLAPWISE STRESS, PSI

V = 110 KT α_s = +5° L = 8100 LB D = 850 LB

BLADE STATION = .375R

N	EXPERIMENTAL A(N)	EXPERIMENTAL B(N)	UNIFORM INFLOW A(N)	UNIFORM INFLOW B(N)
0	-789.		-556.	
1	-919.	1251.	-650.	2070.
2	167.	-664.	-258.	-631.
3	-248.	133.	-233.	23.
4	-134.	-8.	-24.	-17.
5	-131.	-80.	-64.	55.
6	-19.	-29.	17.	36.
7	24.	-4.	-8.	-20.
8	33.	15.	-31.	8.
9	20.	18.	-3.	3.
10	33.	30.	-1.	0.

BLADE STATION = .45R

N	EXPERIMENTAL A(N)	EXPERIMENTAL B(N)	UNIFORM INFLOW A(N)	UNIFORM INFLOW B(N)
0	-1019.		-858.	
1	-904.	1370.	-805.	2271.
2	210.	-718.	-172.	-682.
3	-256.	91.	-294.	-45.
4	-79.	-15.	-9.	4.
5	-47.	-47.	-50.	11.
6	26.	-12.	11.	39.
7	24.	41.	-8.	-33.
8	11.	15.	-66.	9.
9	-4.	6.	-4.	0.
10	17.	13.	-2.	-1.

BLADE STATION = .65R

N	EXPERIMENTAL A(N)	EXPERIMENTAL B(N)	UNIFORM INFLOW A(N)	UNIFORM INFLOW B(N)
0	-1612.		-2072.	
1	-1048.	1549.	-842.	1856.
2	299.	-739.	159.	-548.
3	-143.	-320.	-354.	-243.
4	149.	-55.	-16.	19.
5	245.	79.	70.	-108.
6	90.	44.	-20.	-37.
7	-24.	27.	8.	8.
8	-52.	-48.	7.	-6.
9	-40.	-37.	2.	1.
10	-33.	-37.	0.	-1.

BLADE STATION = .80R

N	EXPERIMENTAL A(N)	EXPERIMENTAL B(N)	UNIFORM INFLOW A(N)	UNIFORM INFLOW B(N)
0	-1781.		-1820.	
1	-374.	741.	-463.	950.
2	75.	-353.	179.	-285.
3	-219.	-576.	-221.	-199.
4	297.	-173.	-35.	-5.
5	307.	188.	97.	-85.
6	-78.	94.	-24.	-72.
7	-19.	-17.	14.	46.
8	94.	65.	89.	-14.
9	111.	58.	7.	-12.
10	74.	38.	3.	2.

TABLE XXIX b HARMONICS OF CHORDWISE STRESS, PSI

V = 110 KT α_s = +5° L = 8100 LB D = 850 LB

BLADE STATION = .15R

N	EXPERIMENTAL A(N)	EXPERIMENTAL B(N)	UNIFORM INFLOW A(N)	UNIFORM INFLOW B(N)
0	-1238.		73.	
1	477.	-150.	158.	-174.
2	-62.	25.	-65.	80.
3	114.	-79.	62.	-68.
4	34.	1.	22.	-7.
5	22.	23.	-7.	-6.
6	12.	7.	-0.	12.
7	9.	1.	-2.	-6.
8	36.	-1.	-3.	14.
9	1.	24.	9.	-4.
10	1.	12.	-6.	2.

BLADE STATION = .375R

EXPERIMENTAL A(N)	EXPERIMENTAL B(N)	UNIFORM INFLOW A(N)	UNIFORM INFLOW B(N)
51.		180.	
444.	-179.	303.	-286.
-128.	89.	-141.	147.
131.	-125.	124.	-148.
-12.	-29.	41.	-49.
-10.	2.	2.	-1.
3.	-5.	-1.	6.
-4.	-4.	-1.	-3.
7.	-1.	-2.	9.
-11.	14.	6.	-3.
-12.	24.	-5.	1.

BLADE STATION = .65R

N	EXPERIMENTAL A(N)	EXPERIMENTAL B(N)	UNIFORM INFLOW A(N)	UNIFORM INFLOW B(N)
0	533.		193.	
1	271.	-26.	166.	-67.
2	-56.	24.	-96.	67.
3	37.	-87.	73.	-101.
4	-25.	-22.	19.	-76.
5	-15.	-3.	24.	13.
6	14.	-7.	-1.	-22.
7	-8.	5.	5.	11.
8	-45.	4.	5.	-21.
9	10.	-32.	-11.	5.
10	6.	-39.	8.	-3.

BLADE STATION = .80R

EXPERIMENTAL A(N)	EXPERIMENTAL B(N)	UNIFORM INFLOW A(N)	UNIFORM INFLOW B(N)
1248.		95.	
112.	18.	60.	-1.
-6.	13.	-40.	21.
2.	-41.	28.	-41.
-16.	-5.	6.	-40.
-2.	-2.	15.	9.
10.	-4.	-0.	-14.
-6.	1.	3.	7.
-34.	8.	4.	-15.
3.	-29.	-8.	3.
4.	-37.	5.	-2.

TABLE XXIX c HARMONICS OF TORSIONAL STRESS, PSI

V = 110 KT α_s = +5° L = 8100 LB D = 850 LB

BLADE STATION .15R

N	EXPERIMENTAL A(N)	EXPERIMENTAL B(N)	UNIFORM INFLOW A(N)	UNIFORM INFLOW B(N)
0	111.		-87.	
1	-99.	-76.	-58.	5.
2	57.	-56.	18.	-11.
3	3.	49.	1.	3.
4	-3.	22.	-2.	-1.
5	-21.	1.	0.	-2.
6	14.	-2.	1.	2.
7	-5.	-6.	0.	-2.
8	-3.	-3.	-3.	2.
9	-8.	0.	2.	1.
10	-1.	3.	0.	-1.

BLADE STATION .375R

N	EXPERIMENTAL A(N)	EXPERIMENTAL B(N)	UNIFORM INFLOW A(N)	UNIFORM INFLOW B(N)
0	207.		-106.	
1	-140.	-119.	-71.	6.
2	76.	-46.	22.	-13.
3	1.	72.	1.	4.
4	1.	41.	-3.	-1.
5	-23.	0.	0.	-2.
6	28.	-2.	1.	2.
7	-5.	-7.	0.	-3.
8	-5.	-17.	-3.	2.
9	-15.	-2.	2.	2.
10	-19.	2.	-1.	-1.

BLADE STATION .65R

EXPERIMENTAL A(N)	EXPERIMENTAL B(N)	UNIFORM INFLOW A(N)	UNIFORM INFLOW B(N)
292.		-75.	
-113.	-112.	-50.	4.
60.	-32.	15.	-9.
12.	49.	1.	3.
-18.	23.	-2.	-1.
-15.	2.	0.	-1.
9.	10.	1.	2.
4.	-8.	0.	-2.
0.	6.	-2.	1.
16.	-3.	1.	1.
-1.	5.	0.	-1.

TABLE XXX a HARMONICS OF FLAPWISE STRESS, PSI

V = 150 KT α_s = -5° L = 8500 LB D = -650 LB

BLADE STATION = .375R

N	EXPERIMENTAL A(N)	EXPERIMENTAL B(N)	UNIFORM INFLOW A(N)	UNIFORM INFLOW B(N)	VARIABLE INFLOW A(N)	VARIABLE INFLOW B(N)
0	-22.		357.		395.	
1	-1190.	1220.	-1085.	1872.	-1058.	1261.
2	225.	-1204.	-549.	-1033.	-154.	-885.
3	-113.	-431.	-516.	-169.	-701.	-167.
4	-114.	-176.	-122.	-117.	-120.	-83.
5	210.	-51.	-65.	-23.	-60.	-128.
6	-61.	-14.	-20.	-8.	-56.	-84.
7	3.	-27.	14.	-11.	55.	-16.
8	62.	48.	26.	-2.	5.	56.
9	31.	31.	2.	0.	-47.	-4.
10	22.	-43.	1.	-1.	-3.	-21.

BLADE STATION = .45R

EXPERIMENTAL A(N)	EXPERIMENTAL B(N)	UNIFORM INFLOW A(N)	UNIFORM INFLOW B(N)	VARIABLE INFLOW A(N)	VARIABLE INFLOW B(N)
-166.		210.		240.	
-1355.	1351.	-1299.	2191.	-1284.	1564.
220.	-1221.	-479.	-1138.	-29.	-951.
-192.	-478.	-608.	-239.	-792.	-285.
-57.	-95.	-56.	-76.	-126.	-96.
120.	-89.	-20.	-36.	-21.	-108.
-5.	-27.	3.	4.	-13.	-48.
-39.	-10.	21.	-10.	79.	31.
76.	-6.	53.	-2.	-27.	116.
1.	52.	4.	1.	-93.	-27.
-28.	-14.	1.	0.	4.	-39.

BLADE STATION = .65R

N	EXPERIMENTAL A(N)	EXPERIMENTAL B(N)	UNIFORM INFLOW A(N)	UNIFORM INFLOW B(N)	VARIABLE INFLOW A(N)	VARIABLE INFLOW B(N)
0	-566.		-1165.		-1047.	
1	-1550.	1752.	-1344.	2188.	-1491.	1706.
2	764.	-1110.	338.	-954.	482.	-793.
3	-82.	-802.	-654.	-556.	-617.	-731.
4	254.	47.	93.	44.	-88.	-110.
5	-206.	40.	118.	-19.	117.	93.
6	77.	70.	43.	15.	101.	104.
7	-46.	82.	-8.	14.	-42.	44.
8	-47.	-14.	-8.	3.	-26.	-22.
9	-9.	-23.	-1.	0.	16.	-15.
10	25.	66.	0.	1.	12.	7.

BLADE STATION = .80R

EXPERIMENTAL A(N)	EXPERIMENTAL B(N)	UNIFORM INFLOW A(N)	UNIFORM INFLOW B(N)	VARIABLE INFLOW A(N)	VARIABLE INFLOW B(N)
-1391.		-1408.		-1263.	
-621.	1025.	-774.	1260.	-952.	1011.
923.	-508.	586.	-502.	468.	-442.
-124.	-750.	-404.	-498.	-265.	-634.
470.	-37.	61.	42.	-40.	-75.
-208.	255.	103.	11.	109.	149.
-6.	107.	23.	1.	79.	109.
61.	-13.	-30.	22.	-125.	-23.
-80.	-18.	-74.	5.	22.	-165.
57.	-57.	-5.	-1.	129.	25.
4.	-68.	-1.	0.	4.	54.

TABLE XXX b HARMONICS OF CHORDWISE STRESS, PSI

V = 150 KT α_s = -5° L = 8500 LB D = -650 LB

BLADE STATION = .15R

N	EXPERIMENTAL A(N)	EXPERIMENTAL B(N)	UNIFORM INFLOW A(N)	UNIFORM INFLOW B(N)	VARIABLE INFLOW A(N)	VARIABLE INFLOW B(N)
0	-1017.		274.		303.	
1	623.	-690.	45.	-209.	60.	-246.
2	-102.	47.	62.	84.	- 1.	53.
3	218.	46.	307.	-210.	343.	-172.
4	98.	51.	105.	-34.	137.	-19.
5	-34.	0.	-13.	-16.	25.	-24.
6	38.	-18.	-12.	-8.	2.	-38.
7	-22.	30.	- 2.	-3.	10.	- 4.
8	-68.	-124.	4.	- 13.	17.	8.
9	0.	31.	-4.	-5.	-15.	4.
10	-11.	-16.	-2.	1.	2.	-2.

BLADE STATION = .375R

N	EXPERIMENTAL A(N)	EXPERIMENTAL B(N)	UNIFORM INFLOW A(N)	UNIFORM INFLOW B(N)	VARIABLE INFLOW A(N)	VARIABLE INFLOW B(N)
0	32.		161.		223.	
1	498.	-515.	132.	-389.	167.	-399.
2	-75.	162.	107.	179.	- 12.	121.
3	368.	-198.	579.	- 522.	653.	-449.
4	304.	30.	236.	- 122.	326.	-135.
5	-66.	15.	- 2.	- 6.	8.	-27.
6	-7.	-2.	-10.	- 1.	- 8.	-21.
7	-7.	-2.	-2.	- 2.	5.	-5.
8	-15.	-54.	1.	- 9.	14.	4.
9	6.	21.	-3.	- 3.	-10.	3.
10	-3.	-27.	-2.	1.	1.	-1.

BLADE STATION = .65R

N	EXPERIMENTAL A(N)	EXPERIMENTAL B(N)	UNIFORM INFLOW A(N)	UNIFORM INFLOW B(N)	VARIABLE INFLOW A(N)	VARIABLE INFLOW B(N)
0	505.		91.		163.	
1	344.	-242.	154.	-187.	183.	-100.
2	-41.	62.	37.	119.	-23.	94.
3	264.	-300.	286.	-442.	334.	-401.
4	339.	15.	172.	-146.	261.	-215.
5	-25.	15.	33.	34.	-55.	15.
6	-23.	45.	15.	19.	-21.	65.
7	9.	-17.	2.	6.	-18.	2.
8	61.	163.	-9.	20.	- 22.	-14.
9	3.	-40.	6.	8.	24.	-4.
10	17.	82.	3.	-1.	-2.	3.

BLADE STATION = .80R

N	EXPERIMENTAL A(N)	EXPERIMENTAL B(N)	UNIFORM INFLOW A(N)	UNIFORM INFLOW B(N)	VARIABLE INFLOW A(N)	VARIABLE INFLOW B(N)
0	1266.		44.		80.	
1	153.	-37.	77.	-61.	90.	- 5.
2	-16.	30.	8.	49.	-12.	41.
3	94.	-153.	96.	-201.	115.	- 186.
4	155.	-3.	73.	-73.	116.	- 114.
5	-15.	7.	21.	22.	-35.	13.
6	-11.	35.	11.	12.	-12.	43.
7	7.	-10.	1.	4.	-12.	2.
8	57.	104.	-6.	14.	-16.	-9.
9	-4.	-33.	4.	6.	16.	-3.
10	19.	71.	2.	- 1.	-1.	2.

TABLE XXX c HARMONICS OF TORSIONAL STRESS, PSI

V = 150 KT α_s = -5° L = 8500 LB D = -650 LB

BLADE STATION .15R

N	EXPERIMENTAL A(N)	EXPERIMENTAL B(N)	UNIFORM INFLOW A(N)	UNIFORM INFLOW B(N)	VARIABLE INFLOW A(N)	VARIABLE INFLOW B(N)
0	164.		-129.		-138.	
1	-136.	-16.	-128.	-21.	-135.	-48.
2	126.	-141.	86.	-24.	58.	-34.
3	39.	-22.	2.	6.	0.	9.
4	-57.	4.	-17.	-13.	-2.	-10.
5	-11.	-20.	11.	0.	14.	0.
6	9.	15.	7.	5.	8.	1.
7	-6.	16.	-3.	-1.	2.	-1.
8	-6.	-7.	1.	-2.	3.	-3.
9	-1.	4.	0.	2.	2.	-2.
10	6.	7.	-1.	1.	-2.	0.

BLADE STATION .375R

N	EXPERIMENTAL A(N)	EXPERIMENTAL B(N)	UNIFORM INFLOW A(N)	UNIFORM INFLOW B(N)	VARIABLE INFLOW A(N)	VARIABLE INFLOW B(N)
0	203.		-157.		-169.	
1	-197.	-190.	-156.	-26.	-165.	-58.
2	71.	-160.	105.	-30.	71.	-41.
3	40.	40.	2.	8.	1.	11.
4	-51.	6.	-21.	-15.	-2.	-12.
5	-20.	-44.	13.	0.	17.	0.
6	5.	17.	9.	7.	10.	1.
7	-13.	27.	-4.	-1.	3.	-1.
8	-4.	-33.	1.	-2.	4.	-4.
9	5.	11.	0.	2.	3.	-2.
10	3.	1.	-1.	1.	-2.	0.

BLADE STATION .65R

EXPERIMENTAL A(N)	EXPERIMENTAL B(N)	UNIFORM INFLOW A(N)	UNIFORM INFLOW B(N)	VARIABLE INFLOW A(N)	VARIABLE INFLOW B(N)
318.		-111.		-119.	
-160.	-202.	-110.	-18.	-116.	-41.
38.	-80.	74.	-21.	50.	-29.
37.	22.	2.	5.	0.	8.
-33.	21.	-15.	-11.	-1.	-8.
-19.	-31.	9.	0.	12.	0.
1.	7.	6.	5.	7.	1.
-5.	13.	-3.	-1.	2.	-1.
-1.	-17.	1.	-2.	3.	-3.
0.	3.	0.	2.	2.	-1.
10.	-4.	0.	1.	-2.	0.

TABLE XXXI a HARMONICS OF FLAPWISE STRESS, PSI

V = 150 KT α_s = 0° L = 8400 LB D = 250 LB

BLADE STATION = .375R

N	EXPERIMENTAL A(N)	EXPERIMENTAL B(N)	UNIFORM INFLOW A(N)	UNIFORM INFLOW B(N)
0	-630.		-373.	
1	-1202.	1561.	-1002.	2446.
2	209.	-1326.	-529.	-1130.
3	-223.	-157.	-571.	8.
4	-226.	-120.	-136.	-86.
5	177.	82.	-124.	27.
6	-91.	-53.	-29.	37.
7	-18.	-39.	-8.	-40.
8	75.	-47.	-39.	-19.
9	8.	16.	-7.	6.
10	-55.	-141.	0.	-2.

BLADE STATION = .45R

N	EXPERIMENTAL A(N)	EXPERIMENTAL B(N)	UNIFORM INFLOW A(N)	UNIFORM INFLOW B(N)
0	-773.		-600.	
1	-1356.	1728.	-1204.	2750.
2	195.	-1392.	-427.	-1242.
3	-318.	-186.	-695.	-94.
4	-152.	-86.	-73.	-49.
5	116.	0.	-80.	-31.
6	-16.	10.	-4.	44.
7	-131.	114.	-8.	-65.
8	61.	-96.	-80.	-44.
9	-18.	21.	-11.	14.
10	-84.	-74.	0.	-6.

BLADE STATION = .65R

N	EXPERIMENTAL A(N)	EXPERIMENTAL B(N)	UNIFORM INFLOW A(N)	UNIFORM INFLOW B(N)
0	-1171.		-1783.	
1	-1415.	2060.	-1230.	2453.
2	537.	1350.	238.	-1051.
3	390.	-899.	-844.	-547.
4	412.	-22.	50.	61.
5	-177.	-187.	168.	-115.
6	167.	112.	54.	-42.
7	-72.	228.	12.	23.
8	-115.	79.	12.	3.
9	-7.	7.	4.	0.
10	71.	168.	-1.	0.

BLADE STATION = .80R

N	EXPERIMENTAL A(N)	EXPERIMENTAL B(N)	UNIFORM INFLOW A(N)	UNIFORM INFLOW B(N)
0	-1625.		-1679.	
1	-435.	1073.	-691.	1333.
2	644.	-619.	389.	-563.
3	-476.	-1076.	-562.	-518.
4	864.	-288.	17.	54.
5	10.	-95.	199.	-54.
6	101.	-12.	38.	-85.
7	268.	-434.	19.	96.
8	2.	-29.	111.	60.
9	52.	-71.	16.	-18.
10	-64.	-156.	0.	8.

TABLE XXXI b HARMONICS OF CHORDWISE STRESS, PSI

V = 150 KT α_s = 0° L = 8400 LB D = 250 LB

BLADE STATION = .15R

N	EXPERIMENTAL A(N)	EXPERIMENTAL B(N)	UNIFORM INFLOW A(N)	UNIFORM INFLOW B(N)
0	-1185.		121.	
1	582.	-423.	171.	-201.
2	-191.	93.	-28.	134.
3	217.	-98.	195.	-222.
4	70.	13.	96.	-47.
5	-27.	-12.	-19.	-17.
6	27.	4.	-16.	10.
7	-53.	37.	-11.	-6.
8	-195.	-86.	-19.	15.
9	-16.	9.	8.	6.
10	-5.	-25.	-7.	1.

BLADE STATION = .375R

EXPERIMENTAL A(N)	EXPERIMENTAL B(N)	UNIFORM INFLOW A(N)	UNIFORM INFLOW B(N)
3.		136.	
536.	-425.	202.	-167.
-224.	246.	-71.	135.
273.	-358.	149.	-354.
182.	-132.	116.	-253.
-59.	-14.	37.	36.
-9.	17.	26.	-9.
-10.	15.	17.	15.
-71.	-41.	30.	-20.
-14.	-4.	-10.	-10.
-5.	-93.	9.	-0.

BLADE STATION = .65R

N	EXPERIMENTAL A(N)	EXPERIMENTAL B(N)	UNIFORM INFLOW A(N)	UNIFORM INFLOW B(N)
0	536.		70.	
1	350.	-172.	78.	-50.
2	-123.	109.	-33.	47.
3	159.	-342.	43.	-150.
4	228.	-159.	44.	-129.
5	-41.	-21.	24.	23.
6	8.	38.	17.	-7.
7	38.	1.	12.	9.
8	230.	140.	20.	-14.
9	27.	-6.	-7.	-7.
10	7.	133.	6.	-0.

BLADE STATION = .80R

EXPERIMENTAL A(N)	EXPERIMENTAL B(N)	UNIFORM INFLOW A(N)	UNIFORM INFLOW B(N)
1257.		133.	
149.	-10.	337.	-375.
-35.	51.	-74.	259.
40.	-160.	352.	-495.
94.	-82.	195.	-195.
-27.	-10.	-9.	-5.
3.	32.	-10.	10.
31.	6.	-7.	-1.
172.	81.	-11.	12.
26.	1.	7.	4.
23.	118.	-6.	1.

TABLE XXXI c HARMONICS OF TORSIONAL STRESS, PSI

V = 150 KT α_s = 0° L = 8400 LB D = 250 LB

BLADE STATION .15R

N	EXPERIMENTAL A(N)	EXPERIMENTAL B(N)	UNIFORM INFLOW A(N)	UNIFORM INFLOW B(N)
0	140.		-98.	
1	-160.	-30.	-109.	-13.
2	122.	-127.	65.	-23.
3	29.	49.	-2.	15.
4	-85.	11.	-22.	-8.
5	-9.	-10.	13.	-7.
6	26.	38.	6.	4.
7	22.	23.	-4.	0.
8	-17.	-2.	-2.	-1.
9	-10.	8.	2.	2.
10	2.	8.	0.	0.

BLADE STATION .375R

N	EXPERIMENTAL A(N)	EXPERIMENTAL B(N)	UNIFORM INFLOW A(N)	UNIFORM INFLOW B(N)
0	195.		-120.	
1	-224.	-169.	-122.	-15.
2	92.	-136.	79.	-27.
3	23.	131.	-2.	18.
4	-86.	30.	-26.	-9.
5	0.	-24.	16.	-9.
6	38.	42.	8.	5.
7	17.	36.	-5.	0.
8	-33.	-26.	-3.	-1.
9	-20.	-2.	2.	2.
10	-4.	-6.	0.	0.

BLADE STATION .65R

EXPERIMENTAL A(N)	EXPERIMENTAL B(N)	UNIFORM INFLOW A(N)	UNIFORM INFLOW B(N)
319.		-85.	
-166.	-182.	-86.	-11.
60.	-63.	56.	-19.
25.	70.	-2.	13.
-61.	28.	-19.	-6.
-16.	-21.	11.	-6.
19.	32.	6.	4.
7.	34.	-4.	0.
-21.	-15.	-2.	-1.
-11.	-3.	1.	1.
5.	-7.	0.	0.

TABLE XXXII a HARMONICS OF FLAPWISE STRESS, PSI

V = 150 KT α_s = +5° L = 8600 LB D = 1100 LB

BLADE STATION = .375R

N	EXPERIMENTAL A(N)	EXPERIMENTAL B(N)	UNIFORM INFLOW A(N)	UNIFORM INFLOW B(N)
0	-925.		-978.	
1	-1339.	1939.	-793.	3099.
2	61.	-1392.	-616.	-1285.
3	-317.	120.	-595.	236.
4	-253.	-15.	-197.	-53.
5	78.	-31.	-43.	250.
6	-64.	-17.	24.	2.
7	8.	-34.	-47.	20.
8	17.	-44.	74.	7.
9	-23.	-7.	13.	-15.
10	-101.	-15.	-1.	5.

BLADE STATION = .45R

EXPERIMENTAL A(N)	EXPERIMENTAL B(N)	UNIFORM INFLOW A(N)	UNIFORM INFLOW B(N)
-1097.		-1277.	
-1446.	2149.	-991.	3428.
12.	-1447.	-439.	-1462.
-368.	63.	-818.	124.
-205.	-6.	-96.	-54.
80.	-65.	-84.	134.
29.	21.	59.	-23.
21.	108.	-83.	35.
25.	-12.	151.	28.
-22.	27.	22.	-36.
-57.	17.	2.	15.

BLADE STATION = .65R

N	EXPERIMENTAL A(N)	EXPERIMENTAL B(N)	UNIFORM INFLOW A(N)	UNIFORM INFLOW B(N)
0	-1569.		-2384.	
1	-1436.	2434.	-1095.	2798.
2	153.	-1370.	194.	-1260.
3	-622.	-640.	-1231.	-502.
4	272.	-76.	78.	31.
5	-2.	-31.	-26.	-393.
6	123.	31.	-4.	-40.
7	20.	164.	22.	-9.
8	-38.	92.	-17.	6.
9	1.	-7.	-7.	1.
10	118.	-3.	2.	1.

BLADE STATION = .80R

EXPERIMENTAL A(N)	EXPERIMENTAL B(N)	UNIFORM INFLOW A(N)	UNIFORM INFLOW B(N)
-1803.		-2007.	
-380.	1130.	-635.	1394.
253.	-643.	240.	-632.
-861.	-883.	-864.	-559.
458.	-406.	17.	70.
179.	55.	64.	-420.
-18.	3.	-81.	-7.
-139.	-349.	118.	-50.
-101.	-129.	-202.	-33.
-26.	-25.	-33.	47.
-129.	24.	-3.	-19.

TABLE XXXII b HARMONICS OF CHORDWISE STRESS, PSI

V = 150 KT α_s = +5° L = 8600 LB D = 1100 LB

BLADE STATION = .15R

	EXPERIMENTAL		UNIFORM INFLOW	
N	A(N)	B(N)	A(N)	B(N)
0	-1264.		-19.	
1	622.	-239.	234.	-279.
2	-149.	113.	-83.	198.
3	152.	-187.	78.	-220.
4	84.	-28.	93.	-47.
5	-17.	12.	-27.	-7.
6	8.	30.	7.	20.
7	-52.	20.	-1.	11.
8	-71.	-37.	15.	-21.
9	15.	-10.	-19.	-3.
10	-14.	12.	12.	-4.

BLADE STATION = .375R

	EXPERIMENTAL		UNIFORM INFLOW	
	A(N)	B(N)	A(N)	B(N)
	5.		111.	
	596.	-434.	428.	-519.
	-233.	326.	-203.	398.
	166.	-449.	157.	-450.
	43.	-155.	147.	-208.
	-25.	-7.	-1.	-13.
	8.	17.	5.	17.
	-12.	11.	3.	5.
	-31.	-7.	7.	-16.
	33.	-12.	-14.	-0.
	48.	-16.	10.	-4.

BLADE STATION = .65R

	EXPERIMENTAL		UNIFORM INFLOW	
N	A(N)	B(N)	A(N)	B(N)
0	560.		195.	
1	399.	-169.	200.	-225.
2	-146.	127.	-170.	230.
3	43.	327.	92.	-272.
4	46.	-195.	27.	-278.
5	2.	-13.	73.	-7.
6	32.	-26.	-11.	-23.
7	54.	8.	9.	-21.
8	71.	60.	-28.	27.
9	-31.	27.	27.	8.
10	54.	-24.	-14.	5.

BLADE STATION = .80R

	EXPERIMENTAL		UNIFORM INFLOW	
	A(N)	B(N)	A(N)	B(N)
	1281.		104.	
	159.	-4.	64.	-66.
	-33.	61.	-77.	87.
	-14.	-146.	35.	-105.
	10.	-93.	-4.	-143.
	1.	-9.	45.	-3.
	25.	-14.	-7.	-17.
	42.	6.	5.	-14.
	57.	32.	-18.	19.
	-25.	21.	19.	5.
	45.	-33.	-10.	4.

TABLE XXXII c HARMONICS OF TORSIONAL STRESS, PSI

V = 150 KT α_s = +5° L = 8600 LB D = 1100 LB

BLADE STATION .15R

N	EXPERIMENTAL A(N)	EXPERIMENTAL B(N)	UNIFORM INFLOW A(N)	UNIFORM INFLOW B(N)
0	102.		-92.	
1	-207.	-107.	-92.	-20.
2	79.	-129.	45.	-10.
3	38.	72.	-2.	24.
4	-9.	31.	-21.	-8.
5	44.	-20.	6.	-13.
6	31.	4.	10.	4.
7	2.	-13.	-8.	1.
8	-30.	-1.	1.	8.
9	-8.	10.	6.	-2.
10	-4.	2.	1.	-2.

BLADE STATION .375R

N	EXPERIMENTAL A(N)	EXPERIMENTAL B(N)	UNIFORM INFLOW A(N)	UNIFORM INFLOW B(N)
0	205.		-113.	
1	-267.	-177.	-112.	-24.
2	74.	-13.	55.	-12.
3	55.	144.	-2.	29.
4	0.	62.	-26.	-10.
5	21.	-18.	7.	-16.
6	49.	-1.	12.	5.
7	9.	-14.	-10.	1.
8	-43.	-29.	1.	10.
9	-17.	5.	7.	-3.
10	-25.	-5.	1.	-2.

BLADE STATION .65R

EXPERIMENTAL A(N)	EXPERIMENTAL B(N)	UNIFORM INFLOW A(N)	UNIFORM INFLOW B(N)
332.		-79.	
-181.	-162.	-79.	-17.
66.	-68.	38.	-9.
47.	61.	-1.	20.
-11.	48.	-18.	-7.
-7.	-6.	5.	-12.
27.	7.	9.	3.
7.	0.	-7.	1.
-28.	-11.	0.	7.
-5.	13.	5.	-2.
-8.	4.	1.	-1.

TABLE XXXIII a HARMONICS OF FLAPWISE STRESS, PSI

V = 175 KT α_s = -5° L = 7100 LB D = -250 LB

BLADE STATION = .375R

	EXPERIMENTAL		UNIFORM INFLOW		VARIABLE INFLOW	
N	A(N)	B(N)	A(N)	B(N)	A(N)	B(N)
0	-263.		-50.		-46.	
1	-1291.	1460.	-1150.	2093.	-1133.	1498.
2	339.	-1484.	-570.	-1279.	-389.	-1222.
3	-120.	-467.	-733.	-99.	-945.	76.
4	-160.	-200.	-224.	-202.	-235.	-113.
5	180.	-90.	-66.	82.	-157.	-13.
6	-94.	6.	-7.	-3.	-41.	-42.
7	-16.	-26.	13.	-22.	54.	-11.
8	74.	17.	-26.	-4.	6.	94.
9	37.	38.	10.	0.	-64.	-9.
10	-44.	-56.	0.	5.	-6.	-27.

BLADE STATION = .45R

	EXPERIMENTAL		UNIFORM INFLOW		VARIABLE INFLOW	
N	A(N)	B(N)	A(N)	B(N)	A(N)	B(N)
0	-354.		-233.		-208.	
1	-1466.	1551.	-1366.	2414.	-1348.	1826.
2	268.	-1554.	-524.	-1429.	-309.	-1329.
3	-260.	-512.	-873.	-182.	-1084.	-61.
4	-79.	-122.	-126.	-136.	-250.	-102.
5	102.	-108.	-22.	22.	-84.	-94.
6	-38.	10.	18.	19.	29.	-12.
7	-38.	19.	28.	-39.	87.	26.
8	63.	-17.	-49.	1.	-15.	198.
9	21.	68.	15.	0.	-147.	-34.
10	-46.	-14.	1.	9.	-3.	-66.

BLADE STATION = .65R

	EXPERIMENTAL		UNIFORM INFLOW		VARIABLE INFLOW	
N	A(N)	B(N)	A(N)	B(N)	A(N)	B(N)
0	-627.		-1309.		-1149.	
1	-1679.	1939.	-1400.	2441.	-1437.	1983.
2	741.	-1422.	217.	-1252.	128.	-1123.
3	-332.	-1006.	-974.	-694.	-1074.	-803.
4	388.	-8.	180.	128.	-87.	-52.
5	-122.	86.	105.	-183.	191.	-125.
6	143.	41.	27.	9.	98.	34.
7	-20.	108.	1.	11.	-28.	30.
8	-67.	13.	10.	8.	-27.	-31.
9	-27.	-22.	-6.	1.	12.	-24.
10	64.	61.	0.	-3.	19.	3.

BLADE STATION = .80R

	EXPERIMENTAL		UNIFORM INFLOW		VARIABLE INFLOW	
N	A(N)	B(N)	A(N)	B(N)	A(N)	B(N)
0	-1203.		-1317.		-1155.	
1	-672.	1102.	-810.	1468.	-867.	1171.
2	997.	-636.	485.	-674.	218.	-616.
3	-471.	-929.	-617.	-686.	-637.	-817.
4	606.	-228.	165.	148.	37.	-29.
5	27.	313.	89.	-166.	191.	-5.
6	132.	126.	-8.	-28.	18.	11.
7	78.	-55.	-32.	56.	-123.	-23.
8	-21.	-17.	69.	3.	1.	-279.
9	61.	-96.	-22.	0.	201.	20.
10	-30.	-63.	-2.	-13.	21.	90.

TABLE XXXIII b HARMONICS OF CHORDWISE STRESS, PSI

V = 175 KT α_s = -5° L = 7100 LB D = -250 LB

BLADE STATION = .15R

	EXPERIMENTAL		UNIFORM INFLOW		VARIABLE INFLOW	
N	A(N)	B(N)	A(N)	B(N)	A(N)	B(N)
0	-861.		277.		265.	
1	416.	-677.	90.	-111.	118.	-160.
2	-220.	131.	84.	144.	35.	76.
3	332.	55.	306.	-301.	274.	-335.
4	143.	50.	153.	-58.	168.	-71.
5	-59.	-7.	-32.	-6.	-11.	-23.
6	32.	-42.	-6.	4.	-17.	-10.
7	-23.	41.	-14.	-8.	1.	-0.
8	-144.	-134.	-6.	11.	17.	10.
9	-16.	28.	6.	4.	-17.	7.
10	-3.	-1.	-0.	1.	-7.	-7.

BLADE STATION = .375R

	EXPERIMENTAL		UNIFORM INFLOW		VARIABLE INFLOW	
	A(N)	B(N)	A(N)	B(N)	A(N)	B(N)
	93.		221.		222.	
	408.	-507.	183.	-252.	233.	-294.
	-145.	252.	175.	294.	87.	172.
	508.	-311.	533.	-679.	436.	-729.
	464.	-7.	336.	-210.	351.	-289.
	-13.	12.	1.	3.	3.	-9.
	-23.	8.	-5.	3.	-15.	-1.
	24.	13.	-9.	-4.	-0.	-0.
	-62.	-55.	-3.	7.	14.	5.
	-13.	0.	2.	2.	-11.	8.
	-29.	-32.	-0.	1.	-5.	-5.

BLADE STATION = .65R

	EXPERIMENTAL		UNIFORM INFLOW		VARIABLE INFLOW	
N	A(N)	B(N)	A(N)	B(N)	A(N)	B(N)
0	516.		132.		172.	
1	315.	-268.	124.	-180.	145.	-126.
2	-37.	113.	111.	179.	75.	129.
3	367.	-401.	201.	-494.	97.	-499.
4	518.	-19.	237.	-250.	225.	-372.
5	55.	38.	94.	21.	37.	-48.
6	-14.	64.	7.	-5.	19.	25.
7	22.	-36.	20.	15.	-3.	-0.
8	174.	197.	12.	-16.	-23.	-18.
9	26.	-26.	-5.	-7.	26.	-6.
10	47.	51.	-0.	-3.	10.	10.

BLADE STATION = .80R

	EXPERIMENTAL		UNIFORM INFLOW		VARIABLE INFLOW	
	A(N)	B(N)	A(N)	B(N)	A(N)	B(N)
	1298.		59.		84.	
	167.	-58.	51.	-76.	57.	-36.
	-14.	54.	44.	69.	34.	56.
	132.	-201.	49.	-211.	-1.	-207.
	242.	-18.	99.	-126.	90.	-190.
	34.	21.	58.	13.	23.	31.
	1.	44.	5.	-4.	14.	16.
	19.	-16.	14.	10.	-2.	-0.
	135.	116.	8.	-11.	-16.	-12.
	19.	-23.	-4.	-5.	18.	-5.
	35.	35.	-0.	-2.	7.	7.

TABLE XXXIII c HARMONICS OF TORSIONAL STRESS, PSI

V = 175 KT α_s = -5° L = 7100 LB D = -250 LB

BLADE STATION .15R

N	EXPERIMENTAL A(N)	EXPERIMENTAL B(N)	UNIFORM INFLOW A(N)	UNIFORM INFLOW B(N)	VARIABLE INFLOW A(N)	VARIABLE INFLOW B(N)
0	203.		-69.		-100.	
1	-175.	32.	-119.	-53.	-122.	-71.
2	196.	-192.	132.	-11.	67.	-31.
3	57.	-35.	-22.	27.	-22.	30.
4	-102.	12.	-35.	-33.	-11.	-23.
5	-28.	-19.	29.	-3.	35.	-11.
6	-3.	58.	2.	6.	7.	6.
7	18.	12.	0.	-5.	1.	-5.
8	-18.	-9.	-3.	10.	2.	-1.
9	3.	3.	-3.	-3.	3.	-5.
10	10.	1.	3.	-1.	4.	2.

BLADE STATION .375R

N	EXPERIMENTAL A(N)	EXPERIMENTAL B(N)	UNIFORM INFLOW A(N)	UNIFORM INFLOW B(N)	VARIABLE INFLOW A(N)	VARIABLE INFLOW B(N)
0	218.		-84.		-122.	
1	-238.	-203.	-145.	-64.	-149.	-86.
2	112.	-204.	160.	-14.	82.	-38.
3	79.	60.	-27.	33.	-27.	36.
4	-96.	1.	-42.	-40.	-13.	-28.
5	-52.	-58.	36.	-4.	42.	-13.
6	-4.	62.	2.	8.	9.	7.
7	23.	33.	1.	-6.	1.	-6.
8	-27.	-43.	-3.	13.	2.	-2.
9	15.	10.	-4.	-4.	4.	-6.
10	10.	-4.	4.	-2.	5.	2.

BLADE STATION .65R

EXPERIMENTAL A(N)	EXPERIMENTAL B(N)	UNIFORM INFLOW A(N)	UNIFORM INFLOW B(N)	VARIABLE INFLOW A(N)	VARIABLE INFLOW B(N)
315.		-60.		-86	
-190.	-230.	-102.	-45.	-105.	-61.
57.	-112.	113.	-10.	58.	-27.
65.	43.	-19.	23.	-19.	25.
-60.	32.	-30.	-28.	-10.	-20.
-37.	-46.	25.	-3.	30.	-9.
-6.	33.	2.	5.	6.	5.
15.	18.	0.	-4.	1.	-5.
-19.	-26.	-2.	9.	2.	-1.
4.	-2.	-3.	-3.	3.	-5.
13.	-4.	3.	-1.	3.	2.

TABLE XXXIV a HARMONICS OF FLAPWISE STRESS, PSI

V = 175 KT $\alpha_s = 0^\circ$ L = 7100 LB D = 400 LB

BLADE STATION = .375R

N	EXPERIMENTAL A(N)	EXPERIMENTAL B(N)	UNIFORM INFLOW A(N)	UNIFORM INFLOW B(N)
0	-803.		-813.	
1	-1424.	1905.	-1075.	2774.
2	241.	-1778.	-504.	-1442.
3	-343.	-76.	-783.	138.
4	-341.	-157.	-261.	-170.
5	232.	-27.	-183.	198.
6	-145.	4.	-8.	66.
7	-18.	-65.	-32.	-48.
8	98.	-32.	-98.	43.
9	49.	58.	4.	3.
10	-151.	48.	1.	-2.

BLADE STATION = .45R

EXPERIMENTAL A(N)	EXPERIMENTAL B(N)	UNIFORM INFLOW A(N)	UNIFORM INFLOW B(N)
-946.		-1078.	
-1499.	2057.	-1284.	3088.
160.	-1884.	-407.	-1598.
-458.	-138.	-966.	17.
-243.	-100.	-143.	-107.
161.	-128.	-135.	57.
44.	9.	17.	69.
-40.	112.	-46.	-103.
136.	-60.	-195.	90.
75.	102.	11.	10.
-88.	81.	-3.	-7.

BLADE STATION = .65R

N	EXPERIMENTAL A(N)	EXPERIMENTAL B(N)	UNIFORM INFLOW A(N)	UNIFORM INFLOW B(N)
0	-1202.		-1985.	
1	-1627.	2457.	-1292.	2765.
2	295.	-1678.	133.	-1361.
3	-904.	-946.	-1224.	-706.
4	375.	-96.	185.	150.
5	-193.	-76.	221.	-391.
6	265.	-20.	29.	-85.
7	44.	212.	30.	6.
8	-90.	82.	36.	-12.
9	-68.	-75.	2.	1.
10	173.	-41.	-3.	0.

BLADE STATION = .80R

EXPERIMENTAL A(N)	EXPERIMENTAL B(N)	UNIFORM INFLOW A(N)	UNIFORM INFLOW B(N)
-1389.		-1644.	
-554.	1286.	-722.	1546.
403.	-701.	251.	-720.
-1232.	-1112.	-831.	-756.
582.	-543.	156.	163.
-40.	94.	289.	-343.
-11.	101.	-5.	-150.
-41.	-345.	80.	133.
-162.	-125.	273.	-122.
14.	-136.	-12.	-12.
-115.	-5.	2.	9.

TABLE XXXIV b HARMONICS OF CHORDWISE STRESS, PSI

V = 175 KT α_s = 0° L = 7100 LB D = 400 LB

BLADE STATION = .15R

N	EXPERIMENTAL A(N)	EXPERIMENTAL B(N)	UNIFORM INFLOW A(N)	UNIFORM INFLOW B(N)
0	-1098.		139.	
1	422.	-355.	216.	-134.
2	-228.	219.	-37.	191.
3	248.	-188.	153.	-257.
4	154.	-8.	126.	-63.
5	-32.	1.	-39.	-12.
6	32.	-19.	-14.	32.
7	-32.	54.	-21.	2.
8	-302.	-174.	-0.	38.
9	-18.	-2.	19.	-6.
10	-29.	-7.	-7.	6.

BLADE STATION = .375R

EXPERIMENTAL A(N)	EXPERIMENTAL B(N)	UNIFORM INFLOW A(N)	UNIFORM INFLOW B(N)
34.		194.	
477.	-436.	394.	-294.
-216.	381.	-65.	362.
197.	-650.	249.	-530.
180.	-209.	244.	-265.
-37.	-15.	-11.	5.
6.	7.	-6.	25.
-21.	30.	-11.	5.
-115.	-85.	3.	24.
-17.	-27.	13.	-5.
-80.	-31.	-5.	5.

BLADE STATION = .65R

N	EXPERIMENTAL A(N)	EXPERIMENTAL B(N)	UNIFORM INFLOW A(N)	UNIFORM INFLOW B(N)
0	525.		179.	
1	342.	-231.	176.	-188.
2	-86.	165.	-28.	182.
3	34.	-602.	67.	-287.
4	181.	-278.	129.	-347.
5	2.	-40.	86.	43.
6	23.	31.	27.	-42.
7	36.	-18.	38.	5.
8	356.	246.	5.	-60.
9	9.	26.	-29.	6.
10	101.	76.	8.	-7.

BLADE STATION = .85R

EXPERIMENTAL A(N)	EXPERIMENTAL B(N)	UNIFORM INFLOW A(N)	UNIFORM INFLOW B(N)
1285.		87.	
172.	-49.	54.	-75.
-10.	66.	-8.	62.
-22.	-278.	6.	-106.
76.	-140.	45.	-178.
8.	-30.	55.	26.
18.	24.	18.	-29.
29.	-13.	25.	-2.
265.	152.	3.	-41.
17.	21.	-20.	4.
98.	42.	6.	-5.

TABLE XXXIV c HARMONICS OF TORSIONAL STRESS, PSI

V = 175 KT α_s = 0° L = 7100 LB D = 400 LB

BLADE STATION .15R

	EXPERIMENTAL		UNIFORM INFLOW	
N	A(N)	B(N)	A(N)	B(N)
0	171.		-32.	
1	-212.	24.	-85.	-64.
2	208.	195.	118.	0.
3	73.	36.	-30.	42.
4	-94.	48.	-42.	-27.
5	-28.	10.	28.	-11.
6	85.	27.	0.	6.
7	-2.	-15.	4.	-9.
8	-27.	-13.	-4.	12.
9	10.	16.	-3.	3.
10	12.	4.	0.	-3.

BLADE STATION .375R

	EXPERIMENTAL		UNIFORM INFLOW	
N	A(N)	B(N)	A(N)	B(N)
0	216.		-39.	
1	-274.	-178.	-104.	-76.
2	151.	-203.	144.	0.
3	102.	148.	-36.	51.
4	-85.	73.	-51.	-33.
5	-43.	-16.	34.	-13.
6	105.	37.	0.	8.
7	-2.	1.	5.	-10.
8	-45.	-56.	-5.	15.
9	17.	23.	-4.	4.
10	4.	-6.	0.	-4.

BLADE STATION .65R

EXPERIMENTAL		UNIFORM INFLOW	
A(N)	B(N)	A(N)	B(N)
321.		-27.	
-198.	-212.	-73.	-55.
95.	-102.	101.	0.
82.	89.	-26.	36.
-48.	79.	-36.	-24.
-41.	-22.	24.	9.
72.	28.	0.	6.
-5.	12.	4.	-7.
-32.	-42.	-4.	10.
13.	12.	-3.	3.
6.	-7.	0.	-3.

TABLE XXXV a HARMONICS OF FLAPWISE STRESS, PSI

V = 175 KT α_s = +5° L = 7300 LB D = 1150 LB

BLADE STATION = .375R

N	EXPERIMENTAL A(N)	EXPERIMENTAL B(N)	UNIFORM INFLOW A(N)	UNIFORM INFLOW B(N)
0	-1364.		-1585.	
1	-1458.	2198.	-872.	3565.
2	-55.	-1918.	-685.	-1673.
3	-473.	297.	-845.	489.
4	-434.	-60.	-363.	-52.
5	65.	-41.	22.	492.
6	-109.	9.	64.	-9.
7	-13.	82.	-39.	39.
8	74.	-44.	79.	40.
9	25.	34.	10.	-8.
10	-78.	57.	13.	8.

BLADE STATION = .45R

EXPERIMENTAL A(N)	EXPERIMENTAL B(N)	UNIFORM INFLOW A(N)	UNIFORM INFLOW B(N)
-1474.		-1923.	
-1507.	2418.	-1077.	3941.
-155.	-1969.	-478.	-1913.
-533.	175.	-1147.	354.
-325.	-7.	-208.	-83.
40.	-142.	-70.	293.
57.	-13.	90.	-41.
-39.	47.	-64.	48.
242.	-136.	174.	99.
92.	37.	12.	-14.
-28.	50.	28.	19.

BLADE STATION = .65R

N	EXPERIMENTAL A(N)	EXPERIMENTAL B(N)	UNIFORM INFLOW A(N)	UNIFORM INFLOW B(N)
0	-1719.		-2723.	
1	-1436.	2682.	-1155.	3245.
2	-165.	-1669.	28.	-1630.
3	-1161.	-774.	-1813.	-653.
4	391.	-97.	165.	19.
5	-17.	-36.	-166.	-734.
6	166.	-35.	-63.	-52.
7	67.	53.	21.	-40.
8	38.	111.	-12.	-5.
9	9.	-10.	-10.	5.
10	13.	-50.	-3.	-1.

BLADE STATION = .80R

EXPERIMENTAL A(N)	EXPERIMENTAL B(N)	UNIFORM INFLOW A(N)	UNIFORM INFLOW B(N)
-1530.		-2059.	
-328.	1197.	-657.	1642.
32.	-625.	8.	-792.
-1497.	-967.	-1338.	-840.
514.	-519.	113.	108.
306.	4.	-55.	-828.
3.	208.	-162.	-2.
-147.	-148.	92.	-87.
-552.	56.	-232.	-135.
-202.	-5.	-21.	22.
-178.	57.	-38.	-26.

TABLE XXXV b HARMONICS OF CHORDWISE STRESS, PSI

V = 175 KT α_s = +5° L = 7300 LB D = 1150 LB

BLADE STATION = .15R

N	EXPERIMENTAL A(N)	EXPERIMENTAL B(N)	UNIFORM INFLOW A(N)	UNIFORM INFLOW B(N)
0	-1182.		13.	
1	451.	-100.	306.	-246.
2	-130.	236.	-110.	224.
3	71.	-329.	-16.	-188.
4	100.	-43.	122.	-61.
5	-8.	22.	-28.	-22.
6	27.	7.	15.	16.
7	-43.	84.	-12.	10.
8	140.	-199.	-0.	-12.
9	-6.	-61.	-14.	7.
10	6.	15.	8.	-16.

BLADE STATION = .375R

EXPERIMENTAL A(N)	EXPERIMENTAL B(N)	UNIFORM INFLOW A(N)	UNIFORM INFLOW B(N)
70.		191.	
512.	-376.	522.	-501.
-202.	466.	-223.	447.
-68.	-718.	-16.	-310.
11.	-107.	163.	-272.
-39.	-29.	-18.	-30.
12.	-4.	8.	20.
-16.	11.	-6.	5.
58.	-89.	-1.	-8.
0.	-69.	-9.	6.
-7.	20.	6.	-13.

BLADE STATION = .65R

N	EXPERIMENTAL A(N)	EXPERIMENTAL B(N)	UNIFORM INFLOW A(N)	UNIFORM INFLOW B(N)
0	558.		261.	
1	371.	-168.	180.	-276.
2	-118.	188.	-137.	252.
3	-185.	-548.	12.	-86.
4	-9.	-158.	-22.	-367.
5	-18.	-69.	44.	3.
6	23.	-20.	-28.	-7.
7	50.	-65.	22.	-20.
8	-188.	213.	-4.	19.
9	-25.	110.	21.	-8.
10	-2.	-21.	-12.	19.

BLADE STATION = .80R

EXPERIMENTAL A(N)	EXPERIMENTAL B(N)	UNIFORM INFLOW A(N)	UNIFORM INFLOW B(N)
1299.		134.	
171.	-13.	38.	-100.
-22.	84.	-53.	93.
-125.	-241.	9.	-10.
-10.	-74.	-37.	-189.
-10.	-44.	30.	6.
14.	-15.	-18.	-7.
29.	-47.	15.	-13.
-116.	173.	-2.	13.
-8.	87.	14.	-6.
-7.	-21.	-8.	14.

TABLE XXXV c HARMONICS OF TORSIONAL STRESS, PSI

V = 175 KT α_s = +5° L = 7300 LB D = 1150 LB

BLADE STATION .15R

N	EXPERIMENTAL A(N)	EXPERIMENTAL B(N)	UNIFORM INFLOW A(N)	UNIFORM INFLOW B(N)
0	93.		-31.	
1	-271.	-129.	-73.	-101.
2	122.	-190.	92.	19.
3	47.	117.	-34.	63.
4	-29.	49.	-41.	-26.
5	14.	9.	18.	-21.
6	100.	-32.	3.	6.
7	-14.	-15.	8.	-8.
8	21.	-34.	8.	7.
9	-2.	-4.	-4.	-4.
10	-7.	0.	-3.	0.

BLADE STATION .375R

N	EXPERIMENTAL A(N)	EXPERIMENTAL B(N)	UNIFORM INFLOW A(N)	UNIFORM INFLOW B(N)
0	216.		-38.	
1	-317.	-204.	-89.	-124.
2	133.	-197.	112.	23.
3	87.	187.	-42.	77.
4	-39.	82.	-50.	-32.
5	25.	4.	22.	-25.
6	135.	-17.	3.	7.
7	-11.	-21.	10.	-10.
8	51.	-49.	10.	9.
9	11.	-14.	-5.	-5.
10	-16.	-8.	-4.	0.

BLADE STATION .65R

EXPERIMENTAL A(N)	EXPERIMENTAL B(N)	UNIFORM INFLOW A(N)	UNIFORM INFLOW B(N)
328.		-27.	
-213.	-193.	-63.	-87.
103.	-116.	79.	16.
76.	96.	-29.	54.
-27.	75.	-35.	-23.
-4.	-1.	15.	-18.
88.	-2.	2.	5.
4.	-12.	7.	-7.
29.	-21.	7.	6.
5.	-17.	-4.	-3.
5.	-4.	-3.	0.

TABLE XXXVI TIME HISTORIES OF AERODYNAMIC LOADING, LB/IN

V = 110 KT α_s = -9° L = 11800 LB D = -2150 LB

(a) EXPERIMENTAL

	Blade Radial Station								
ψ	.25R	.40R	.55R	75R	.85R	.90R	.95R	.97R	.99R
0	-0.6	1.7	10.0	23.7	33.2	32.9	35.0	19.5	5.9
5	-0.8	2.1	10.4	24.3	33.3	33.0	35.1	19.5	5.5
10	-0.7	2.6	10.6	24.4	33.1	32.7	34.5	19.2	5.2
15	-0.5	2.9	10.7	24.3	32.2	31.8	33.5	18.5	4.7
20	-0.1	3.1	11.0	23.7	30.9	30.1	31.9	17.2	4.9
25	0.7	3.3	11.0	23.1	29.7	28.5	30.1	16.0	4.5
30	1.2	3.4	10.9	22.5	28.3	27.3	28.8	15.2	4.0
35	1.2	3.5	10.8	22.0	27.0	26.1	27.9	14.5	3.8
40	1.0	3.6	10.8	21.4	25.4	24.9	26.7	14.0	3.5
45	0.8	3.6	10.5	20.8	24.3	23.5	25.1	13.0	3.3
50	0.7	3.6	10.2	19.8	22.6	21.7	22.9	12.0	3.4
55	0.7	3.6	9.8	18.6	20.8	20.2	21.6	11.1	3.4
60	0.7	3.6	9.5	17.3	19.1	18.5	20.0	10.2	2.9
65	0.8	3.5	9.0	16.2	17.5	16.8	18.9	9.5	2.9
70	0.8	3.5	8.6	15.1	16.1	15.6	18.5	9.1	2.8
75	1.0	3.4	8.2	14.3	14.6	14.9	18.0	8.9	3.7
80	1.2	3.5	8.1	13.7	13.7	14.5	17.5	8.7	3.0
85	1.4	3.9	8.3	13.3	13.3	14.5	16.8	8.3	2.8
90	1.7	4.3	8.7	13.2	13.5	14.7	16.7	8.3	2.8
95	2.1	4.8	9.1	13.4	14.3	14.5	16.5	8.3	3.1
100	2.5	5.3	9.6	13.9	14.5	14.0	16.4	8.2	2.4
105	3.0	5.8	10.2	14.5	14.2	14.1	15.6	7.6	2.4
110	3.6	6.4	10.9	15.1	14.0	14.1	14.6	6.9	2.0
115	4.1	6.9	11.7	15.3	14.3	13.6	13.9	6.4	2.0
120	4.6	7.6	12.6	15.4	14.7	13.4	12.8	6.2	1.9
125	5.2	8.2	13.1	15.5	14.9	13.5	12.7	6.2	2.0
130	5.7	8.9	13.5	16.2	15.2	14.0	13.1	6.5	2.2
135	6.2	9.4	13.8	17.5	16.2	15.0	13.9	7.3	2.5
140	6.6	9.8	14.2	18.9	17.3	16.0	14.7	8.2	2.9
145	7.0	10.1	14.6	20.0	18.8	17.6	16.0	9.0	2.7
150	7.3	10.2	14.9	20.6	20.2	19.2	17.2	10.1	3.8
155	7.6	10.2	15.1	20.9	21.2	20.6	18.3	11.0	4.3
160	7.7	10.1	15.1	21.0	21.9	21.6	19.3	11.6	4.8
165	7.6	10.0	15.2	21.1	22.4	22.2	19.8	11.9	5.3
170	7.4	9.7	15.4	21.1	22.7	22.5	19.5	11.9	5.7
175	7.0	9.1	15.5	21.1	23.0	22.7	20.1	12.1	6.1
180	6.4	8.5	15.5	21.3	23.4	23.0	20.4	12.3	6.5
185	5.7	8.0	15.4	21.3	23.7	23.5	21.4	13.0	7.0
190	4.9	7.4	15.1	21.2	24.1	23.8	21.9	13.4	6.8
195	4.1	6.8	14.7	21.1	24.6	24.6	22.2	13.8	7.6
200	3.3	6.1	14.3	21.1	25.0	25.0	22.9	14.2	8.3
205	2.5	5.4	13.7	20.8	24.9	25.0	23.3	14.4	8.6
210	1.8	4.6	13.0	20.4	24.9	25.0	23.2	14.6	8.8
215	1.2	4.0	12.0	20.1	24.7	24.8	23.1	14.6	9.0
220	0.7	3.3	11.1	19.6	24.4	24.7	23.5	14.7	9.3
225	0.3	2.7	10.3	19.1	24.2	24.4	23.7	14.8	9.6
230	0.0	2.2	9.4	18.5	23.7	24.3	23.3	14.8	9.4
235	-0.2	1.7	8.6	18.0	23.3	24.0	23.3	14.8	9.2
240	-0.4	1.2	7.9	17.4	23.0	23.7	23.3	14.7	9.2
245	-0.5	0.8	7.1	16.9	22.6	23.4	23.5	14.9	9.0
250	-0.6	0.6	6.4	16.3	22.2	23.3	23.3	15.0	9.1
255	-0.8	0.3	5.8	15.8	21.9	23.2	23.2	15.1	8.8
260	-0.9	0.1	5.2	15.3	21.5	23.2	23.9	15.3	8.4
265	-1.0	0.0	4.8	14.8	21.3	22.9	24.0	15.3	8.0
270	-1.0	-0.1	4.5	14.4	20.8	22.3	23.7	15.5	7.8
275	-1.1	0.0	4.3	14.1	20.4	22.1	24.8	15.9	7.9
280	-1.1	-0.1	4.1	13.7	20.3	22.2	25.6	16.1	8.0
285	-1.0	-0.1	3.9	13.4	20.2	22.0	26.0	16.4	7.6
290	-0.9	0.0	3.8	13.3	20.2	22.0	26.0	16.6	7.6
295	-0.9	0.0	3.9	13.4	20.1	22.1	26.4	16.6	7.3
300	-0.8	0.1	4.0	13.5	20.3	22.1	26.5	16.4	7.3
305	-0.6	0.1	4.1	13.8	20.9	22.5	26.7	16.4	6.6
310	-0.5	0.2	4.3	14.3	21.6	23.2	27.4	16.4	6.0
315	-0.3	0.3	4.6	14.9	22.7	24.3	28.2	16.8	5.5
320	-0.3	0.5	5.0	15.6	23.7	25.6	28.9	17.3	5.9
325	-0.5	0.7	5.3	16.3	25.2	26.7	30.4	17.8	5.7
330	-0.7	0.9	6.0	17.4	26.4	28.3	31.2	18.2	6.0
335	-0.3	1.0	6.7	18.5	28.0	29.4	32.4	18.6	5.8
340	-0.1	1.2	7.3	19.5	29.5	30.7	33.5	19.2	6.2
345	-0.1	1.3	8.0	20.7	30.7	31.4	34.2	19.4	6.2
350	-0.1	1.3	8.7	21.9	31.7	32.0	34.4	19.4	6.1
355	-0.2	1.4	9.3	22.9	32.7	32.6	35.2	19.6	5.8
360	-0.6	1.7	10.0	23.7	33.2	32.9	35.0	19.5	5.9

TABLE XXXVI CONCLUDED

V = 110 KT a_s = -7° L = 11800 LB D = -2150 LB

(b) THEORETICAL (UNIFORM INFLOW)

ψ	Blade Radial Station .25R	.40R	.55R	.75R	.85R	.90R	.95R	.97R	.99R
0	0.8	3.2	9.3	21.4	29.1	33.1	36.4	38.1	0.1
5	-0.6	3.6	9.6	21.4	28.9	32.8	35.6	37.5	0.1
10	-0.3	4.0	9.9	21.3	28.4	32.0	34.9	36.8	0.1
15	-0.1	4.3	10.1	21.0	27.7	31.1	33.9	35.7	0.1
20	0.1	4.6	10.2	20.6	26.9	30.2	32.9	34.5	0.0
25	0.4	4.8	10.2	20.2	26.2	29.2	31.5	33.0	0.0
30	0.6	4.9	10.1	19.7	25.3	28.1	30.2	31.5	0.0
35	0.8	5.0	10.0	19.1	24.4	26.9	28.8	30.0	0.0
40	0.9	5.0	9.7	18.4	23.3	25.6	27.4	28.5	0.0
45	1.1	5.0	9.4	17.5	22.0	24.1	25.9	27.0	0.0
50	1.3	5.0	9.2	16.6	20.7	22.7	24.4	25.4	0.0
55	1.4	5.0	8.9	15.6	19.3	21.2	22.6	23.4	0.0
60	1.6	5.0	8.6	14.7	17.9	19.6	20.7	21.3	0.0
65	1.8	5.1	8.5	13.9	16.6	17.9	18.7	19.0	0.0
70	2.1	5.3	8.5	13.3	15.4	16.3	16.7	16.7	0.0
75	2.4	5.5	8.6	12.8	14.4	14.8	14.8	14.6	0.0
80	2.7	5.8	8.8	12.5	13.6	13.6	13.2	12.7	0.0
85	3.0	6.2	9.2	12.4	12.9	12.6	11.9	11.2	0.0
90	3.4	6.7	9.6	12.4	12.5	11.9	10.8	10.0	0.0
95	3.8	7.2	10.2	12.5	12.2	11.4	10.1	9.1	0.0
100	4.2	7.8	10.7	12.8	12.1	11.1	9.7	8.5	0.0
105	4.6	8.3	11.3	13.1	12.3	11.1	9.6	8.3	0.0
110	5.0	8.8	11.9	13.6	12.6	11.3	9.7	8.5	0.0
115	5.4	9.4	12.5	14.1	13.0	11.8	10.2	8.9	0.0
120	5.7	9.8	13.0	14.7	13.6	12.4	10.9	9.7	0.0
125	5.9	10.2	13.6	15.3	14.3	13.2	11.8	10.7	0.0
130	6.0	10.5	14.0	16.0	15.1	14.1	12.9	11.9	0.0
135	6.1	10.8	14.5	16.7	16.0	15.2	14.1	13.2	0.0
140	6.1	10.9	14.8	17.4	16.8	16.2	15.4	14.7	0.0
145	6.0	11.0	15.1	18.1	17.8	17.3	16.7	16.1	0.0
150	5.8	10.9	15.2	18.8	18.7	18.3	17.9	17.5	0.0
155	5.5	10.8	15.3	19.3	19.7	19.3	19.2	19.0	0.0
160	5.2	10.6	15.3	19.8	20.6	20.4	20.4	20.3	0.0
165	4.8	10.2	15.2	20.3	21.4	21.5	21.5	21.6	0.0
170	4.3	9.8	15.0	20.6	22.1	22.4	22.6	22.7	0.0
175	3.8	9.3	14.8	20.8	22.7	23.3	23.7	23.9	0.0
180	3.3	8.8	14.4	21.0	23.1	24.0	24.6	25.0	0.0
185	2.8	8.2	13.9	21.0	23.5	24.6	25.4	26.0	0.0
190	2.2	7.5	13.4	20.9	23.8	25.0	26.1	26.8	0.0
195	1.7	6.8	12.7	20.7	24.0	25.4	26.7	27.5	0.0
200	1.2	6.1	12.1	20.4	24.1	25.7	27.1	28.1	0.0
205	0.8	5.3	11.3	20.1	24.0	25.9	27.5	28.5	0.0
210	0.4	4.6	10.5	19.7	23.9	26.0	27.8	28.9	0.0
215	0.1	3.9	9.7	19.3	23.7	25.9	27.9	29.2	0.0
220	-0.1	3.2	8.9	18.7	23.4	25.8	27.9	29.2	0.0
225	-0.3	2.6	8.1	18.0	23.1	25.5	27.8	29.3	0.0
230	-0.4	2.0	7.3	17.4	22.7	25.4	27.6	29.1	0.1
235	-0.2	1.5	6.6	16.8	22.3	25.1	27.5	29.1	0.1
240	-0.2	1.1	5.9	16.2	21.8	24.8	27.2	28.9	0.1
245	-0.2	0.7	5.2	15.6	21.3	24.5	27.1	28.7	0.1
250	-0.2	0.4	4.6	15.0	20.9	24.1	26.9	28.6	0.1
255	-0.3	0.1	4.1	14.4	20.5	23.7	26.6	28.4	0.1
260	-0.3	-0.1	3.6	13.9	20.2	23.5	26.4	28.3	0.1
265	-0.4	-0.3	3.3	13.5	19.9	23.3	26.2	28.2	0.1
270	-0.4	-0.4	3.0	13.2	19.8	23.1	26.1	28.1	0.1
275	-0.5	-0.5	2.7	13.0	19.7	23.1	26.1	28.1	0.1
280	-0.5	-0.6	2.6	12.9	19.7	23.2	26.2	28.2	0.1
285	-0.5	-0.7	2.5	12.9	19.9	23.4	26.4	28.4	0.1
290	-0.5	-0.7	2.5	13.1	20.1	23.7	26.7	28.6	0.2
295	-0.5	-0.7	2.6	13.3	20.4	24.0	27.0	29.0	0.2
300	-0.5	-0.7	2.8	13.7	20.9	24.5	27.6	29.5	0.2
305	-0.5	-0.6	3.0	14.2	21.4	25.1	28.2	30.2	0.2
310	-0.5	-0.5	3.3	14.8	22.1	25.8	29.0	30.9	0.2
315	-0.5	-0.4	3.8	15.5	22.9	26.6	29.8	31.6	0.2
320	-0.6	-0.2	4.3	16.3	23.7	27.5	30.6	32.5	0.2
325	-0.6	0.1	4.8	17.0	24.7	28.6	31.5	33.4	0.2
330	-0.6	0.4	5.5	17.8	25.5	29.4	32.4	34.3	0.2
335	-0.6	0.8	6.1	18.6	26.4	30.1	33.2	35.2	0.2
340	-1.0	1.2	6.8	19.3	27.2	31.0	34.1	36.2	0.1
345	-1.3	1.7	7.5	20.0	27.8	31.6	34.9	37.1	0.1
350	-1.2	2.2	8.1	20.7	28.4	32.4	35.9	38.2	0.1
355	-1.0	2.7	8.7	21.1	28.8	32.8	36.3	38.3	0.1
360	-0.8	3.2	9.3	21.4	29.1	33.1	36.4	38.1	0.1

TABLE XXXVII HARMONICS OF AERODYNAMIC LOADING, LB/IN

V = 110 KT α_s = -6° L = 11800 LB D = -2150 LB

BLADE STATION = .25R

N	EXPERIMENTAL A(N)	EXPERIMENTAL B(N)	UNIFORM INFLOW A(N)	UNIFORM INFLOW B(N)	VARIABLE INFLOW A(N)	VARIABLE INFLOW B(N)
0	1.70		1.50		1.57	
1	2.77	-1.94	1.96	-2.36	1.79	-1.68
2	-1.31	1.17	0.12	1.14	-0.19	0.81
3	0.45	-0.62	-0.02	-0.48	0.13	-0.41
4	0.06	0.19	0.13	0.03	-0.01	-0.08
5	0.24	-0.01	0.13	-0.04	0.05	-0.13
6	0.03	0.09	0.01	-0.06	0.06	-0.06
7	0.06	0.10	0.01	-0.01	-0.01	-0.04
8	0.01	0.13	0.02	-0.03	0.03	-0.
9	-0.02	0.10	-0.01	-0.03	-0.04	0.03
10	-0.02	0.08	-0.01	-0.01	-0.02	-0.03

BLADE STATION = .40R

N	EXPERIMENTAL A(N)	EXPERIMENTAL B(N)	UNIFORM INFLOW A(N)	UNIFORM INFLOW B(N)	VARIABLE INFLOW A(N)	VARIABLE INFLOW B(N)
0	3.85		4.52		4.52	
1	3.11	-2.82	2.96	-4.18	2.60	-3.19
2	-1.60	0.85	-1.41	0.71	-1.26	0.30
3	0.24	-0.65	-0.16	-0.63	-0.23	-0.50
4	0.17	-0.03	-0.04	-0.17	0.05	-0.25
5	0.04	0.01	0.01	0.	-0.05	0.07
6	0.06	0.02	-0.01	0.	-0.02	-0.08
7	0.01	0.	-0.01	0.	-0.01	0.01
8	0.03	-0.04	-0.01	-0.	-0.05	-0.01
9	0.04	-0.03	-0.	-0.	-0.02	-0.05
10	0.03	0.01	-0.	0.	0.01	-0.02

BLADE STATION = .55R

N	EXPERIMENTAL A(N)	EXPERIMENTAL B(N)	UNIFORM INFLOW A(N)	UNIFORM INFLOW B(N)	VARIABLE INFLOW A(N)	VARIABLE INFLOW B(N)
0	9.71		8.99		9.15	
1	3.06	-2.70	2.95	-3.78	2.79	-2.73
2	-2.98	-0.55	-2.75	0.19	-2.69	-0.58
3	-0.22	-0.47	-0.39	-0.45	-0.39	-0.01
4	0.12	-0.33	-0.05	-0.20	-0.21	-0.34
5	-0.02	0.20	0.03	0.01	0.04	0.05
6	-0.11	0.01	0.	0.03	-0.04	0.
7	-0.05	0.01	-0.01	0.02	0.03	0.05
8	0.	-0.02	-0.02	-0.01	-0.03	0.02
9	-0.01	0.	-0.	-0.01	-0.02	0.03
10	0.02	0.01	0.01	0.	0.	-0.02

BLADE STATION = .75R

N	EXPERIMENTAL A(N)	EXPERIMENTAL B(N)	UNIFORM INFLOW A(N)	UNIFORM INFLOW B(N)	VARIABLE INFLOW A(N)	VARIABLE INFLOW B(N)
0	18.11		16.92		17.22	
1	-0.14	-0.54	0.27	0.12	0.81	-0.03
2	-4.27	-1.64	-4.17	-0.77	-3.83	-0.52
3	-0.74	-1.03	-0.45	-0.31	-0.92	-0.30
4	-0.05	-0.05	-0.	-0.04	-0.03	0.47
5	-0.14	0.	0.04	0.02	-0.09	0.14
6	0.	0.14	-0.	0.07	0.02	-0.10
7	-0.31	-0.02	-0.04	0.03	0.05	0.13
8	0.02	-0.17	-0.04	0.01	-0.11	0.05
9	0.	0.08	-0.02	-0.01	0.06	-0.04
10	-0.09	-0.08	-0.02	0.01	0.03	0.06

BLADE STATION = .85R

N	EXPERIMENTAL A(N)	EXPERIMENTAL B(N)	UNIFORM INFLOW A(N)	UNIFORM INFLOW B(N)	VARIABLE INFLOW A(N)	VARIABLE INFLOW B(N)
0	22.32		21.00		20.32	
1	-3.25	2.87	-2.43	3.28	-1.71	2.26
2	-5.59	-2.01	-4.90	-1.48	-3.71	-0.75
3	-1.29	-0.71	-0.38	-0.34	-1.01	0.11
4	-0.49	-0.07	-0.05	0.04	-0.34	0.36
5	-0.05	-0.01	-0.03	0.08	0.19	0.31
6	0.76	0.31	-0.05	0.09	-0.03	0.16
7	-0.36	-0.06	-0.04	0.02	-0.06	-0.04
8	0.06	-0.17	-0.04	0.	-0.	-0.01
9	0.01	0.	-0.05	-0.02	0.	0.07
10	0.02	-0.02	-0.01	-0.01	0.02	0.03

BLADE STATION = .90R

N	EXPERIMENTAL A(N)	EXPERIMENTAL B(N)	UNIFORM INFLOW A(N)	UNIFORM INFLOW B(N)	VARIABLE INFLOW A(N)	VARIABLE INFLOW B(N)
0	22.56		22.89		21.31	
1	-3.59	3.91	-3.94	5.13	-3.42	3.68
2	-5.06	-1.76	-5.33	-1.97	-3.63	-0.87
3	-1.03	-0.32	-0.33	-0.42	-0.79	0.33
4	-0.77	0.78	-0.03	0.13	-0.51	0.47
5	0.	-0.15	-0.11	0.12	0.13	0.33
6	0.24	0.36	-0.13	0.09	0.09	0.18
7	-0.34	-0.02	-0.07	0.	-0.10	0.01
8	0.06	-0.15	-0.06	-0.03	-0.08	-0.05
9	-0.05	-0.12	-0.04	-0.03	0.01	0.03
10	0.06	-0.13	-0.04	0.02	-0.01	0.07

BLADE STATION = .95R

N	EXPERIMENTAL A(N)	EXPERIMENTAL B(N)	UNIFORM INFLOW A(N)	UNIFORM INFLOW B(N)	VARIABLE INFLOW A(N)	VARIABLE INFLOW B(N)
0	23.48		24.36		20.98	
1	-6.16	4.30	-5.20	6.92	-4.99	4.85
2	-3.91	-1.15	-5.77	-2.46	-3.53	-0.81
3	-0.66	0.10	-0.24	-0.56	-0.40	0.46
4	-0.88	-0.13	-0.01	0.24	-0.59	0.69
5	-0.21	-0.57	-0.21	0.19	-0.07	0.43
6	0.25	0.40	-0.18	0.02	0.12	0.17
7	-0.21	0.12	-0.14	0.	-0.04	0.12
8	0.08	-0.20	-0.06	-0.02	-0.20	-0.
9	-0.10	-0.03	-0.02	-0.	-0.05	-0.03
10	-0.07	-0.10	-0.03	0.03	0.06	0.02

BLADE STATION = .97R

N	EXPERIMENTAL A(N)	EXPERIMENTAL B(N)	UNIFORM INFLOW A(N)	UNIFORM INFLOW B(N)	VARIABLE INFLOW A(N)	VARIABLE INFLOW B(N)
0	13.53		25.24		18.84	
1	-2.95	3.94	-6.01	8.18	-5.95	5.26
2	-2.22	-0.63	-6.09	-2.80	-3.44	-0.55
3	-0.22	-0.03	-0.17	-0.68	-0.05	0.59
4	-0.58	0.	-0.	0.31	-0.48	0.89
5	-0.20	-0.27	-0.27	0.24	-0.17	0.56
6	0.20	0.24	-0.19	0.05	0.14	0.16
7	-0.19	0.07	-0.16	-0.01	0.05	0.16
8	0.06	-0.15	-0.06	-0.03	-0.20	0.04
9	-0.04	-0.08	0.02	0.	-0.12	-0.06
10	0.	-0.08	0.02	0.02	0.05	-0.01

BLADE STATION = .99R

N	EXPERIMENTAL A(N)	EXPERIMENTAL B(N)	UNIFORM INFLOW		VARIABLE INFLOW A(N)	VARIABLE INFLOW B(N)
0	5.56		-		13.83	
1	0.60	3.12	-	-	-5.56	4.05
2	-0.30	-1.01	-	-	-2.68	-0.34
3	-0.07	0.30	-	-	0.09	0.51
4	-0.27	0.04	-	-	-0.34	0.74
5	-0.18	-0.13	-	-	-0.20	0.47
6	-0.02	0.16	-	-	0.10	0.10
7	0.16	0.07	-	-	0.07	0.13
8	0.07	0.06	-	-	-0.16	0.08
9	0.04	-0.06	-	-	-0.14	-0.06
10	0.	0.	-	-	0.01	-0.03

TABLE XXXVIII TIME HISTORIES OF BLADE STRESS, PSI

V = 110 KT α_s = -9° L = 11800 LB D = -2150 LB

	Chordwise Stress				Flapwise Stress				Torsional Stress		
ψ, DEG	r/R .15	r/R .375	r/R .65	r/R .80	r/R .375	r/R .45	r/R .65	r/R .80	r/R .15	r/R .375	r/R .65
0	-1634	-772	-18	1099	7266	5703	1687	-1988	229	412	536
5	-1566	-832	-106	1082	7420	5867	1552	-2072	253	430	538
10	-1485	-869	-156	1071	7573	6002	1527	-2144	280	470	553
15	-1416	-747	-150	1024	7727	6090	1589	-2222	290	492	565
20	-1379	-662	-119	984	7936	6172	1749	-2180	300	508	584
25	-1223	-571	13	1082	7960	6260	1780	-1934	315	508	565
30	-1117	-443	151	1174	7960	6331	1879	-1579	315	506	565
35	-1023	-163	352	1220	7825	6231	1984	-1273	313	490	565
40	-992	111	527	1278	7690	6072	2206	-901	330	496	574
45	-767	196	803	1434	7426	5808	2397	-703	330	498	567
50	-543	336	966	1538	7143	5597	2508	-439	325	496	563
55	-393	695	1041	1555	6830	5362	2373	-306	307	482	557
60	-287	652	1029	1382	6628	5139	2132	-243	306	440	547
65	-112	944	1010	1405	6499	4828	1860	-372	296	444	590
70	68	926	1004	1480	6345	4616	1508	-583	296	444	545
75	193	798	972	1428	6179	4399	1070	-925	274	454	561
80	168	963	916	1342	5940	4205	588	-1273	256	404	545
85	187	707	860	1330	5762	3982	304	-1682	237	394	536
90	199	786	816	1359	5614	3765	82	-1994	231	370	503
95	131	841	759	1313	5528	3635	-85	-2120	241	384	503
100	62	549	747	1278	5332	3524	-375	-2174	227	366	508
105	6	531	678	1284	5258	3465	-436	-2132	202	372	524
110	31	677	678	1324	5123	3365	-529	-2132	166	316	458
115	-31	531	640	1278	5154	3359	-406	-2096	137	265	419
120	-75	470	659	1301	5092	3295	-378	-2138	82	205	369
125	-119	403	678	1272	5117	3371	-338	-2036	56	141	313
130	-937	585	715	1370	5105	3377	-399	-2054	35	101	303
135	-131	561	765	1382	5154	3436	-288	-2054	37	84	271
140	-131	573	816	1399	5123	3401	-251	-2192	31	78	275
145	-131	409	847	1393	5092	3477	-227	-2300	37	72	285
150	-13	543	873	1457	5166	3583	-294	-2510	41	84	287

TABLE XXXVIII CONCLUDED

V = 110 KT α_s = -9° L = 11800 LB D = -2150 LB

	Chordwise Stress				Flapwise Stress				Torsional Stress		
ψ, DEG	r/R .15	r/R .375	r/R .65	r/R .80	r/R .375	r/R .45	r/R .65	r/R .80	r/R .15	r/R .375	r/R .65
155	31	756	897	1451	5271	3712	-424	-2672	37	84	273
160	12	853	922	1440	5430	3800	-529	-2822	19	80	277
165	-44	713	972	1428	5535	3888	-671	-2871	3	44	250
170	-144	768	1060	1514	5670	3929	-714	-2877	-9	30	242
175	-268	975	1254	1618	5670	3882	-733	-2834	-12	10	205
180	-387	890	1380	1710	5713	3870	-659	-2726	-12	6	209
185	-406	689	1461	1780	5725	3870	-560	-2660	-16	-16	190
190	-393	616	1399	1768	5829	3958	-436	-2516	7	-8	178
195	-337	725	1280	1682	5885	4064	-356	-2450	19	6	159
200	-349	634	1010	1509	6032	4211	-146	-2372	44	54	190
205	-331	518	872	1416	6106	4370	57	-2372	68	88	215
210	-418	348	740	1422	6253	4534	304	-2[illegible]	88	123	221
215	-580	208	722	1445	6400	4681	558	-2126	86	125	200
220	-842	7	715	1457	6591	4916	768	-1844	84	115	186
225	-1098	-175	709	1497	6861	5156	984	-1585	70	105	178
230	-1310	-303	634	1463	7150	5427	1268	-1321	78	103	172
235	-1360	-437	533	1416	7346	5685	1595	-1093	90	119	182
240	-1354	-577	370	1342	7512	5961	2015	-919	103	123	184
245	-1366	-583	189	1244	7616	6172	2441	-709	115	147	194
250	-1497	-571	-6	1111	7659	6325	2867	-414	117	145	200
255	-1678	-577	-37	1059	7770	6448	3317	-18	117	129	217
260	-1828	-705	95	1203	7899	6566	3601	450	99	105	198
265	-1952	-838	239	1393	7923	6607	3811	883	86	84	176
270	-2108	-887	333	1422	7874	6595	4052	1147	78	56	159
275	-2271	-772	320	1347	7807	6542	4280	1267	56	50	180
280	-2227	-729	251	1284	7764	6513	4422	1225	68	40	192
285	-2015	-753	157	1272	7751	6513	4422	1171	97	80	194
290	-1884	-650	107	1226	7696	6536	4237	1063	99	121	219
295	-1903	-522	57	1117	7702	6501	4003	913	103	141	279
300	-1928	-437	95	1099	7665	6372	3786	685	113	151	277
305	-1903	-534	214	1278	7592	6184	3558	396	105	149	275
310	-1865	-546	383	1411	7487	6026	3305	102	84	153	273
315	-1884	-492	452	1399	7340	5932	3002	-180	56	141	289
320	-1878	-321	421	1324	7236	5814	2737	-523	41	127	293
325	-1778	-285	370	1284	7174	5703	2484	-823	41	338	409
330	-1641	-242	295	1290	7113	5609	2286	-1117	46	155	320
335	-1622	-321	201	1220	7064	5567	2101	-1339	70	193	359
340	-1628	-370	220	1186	7014	5538	1978	-1537	112	243	409
345	-1616	-522	214	1278	6947	5509	1860	-1663	150	293	433
350	-1591	-607	170	1301	6990	5491	1823	-1778	176	354	473
355	-1622	-705	95	1203	7088	5567	1768	-1862	207	380	495
360	-1634	-772	-18	1099	7266	5703	1687	-1988	229	412	536

TABLE XXXIX a HARMONICS OF FLAPWISE STRESS, PSI

V = 110 KT α_s = -9° L = 11800 LB D = 2150 LB

BLADE STATION = .375R

N	EXPERIMENTAL A(N)	EXPERIMENTAL B(N)	UNIFORM INFLOW A(N)	UNIFORM INFLOW B(N)
0	454.		1350.	
1	-908.	864.	-1023.	1344.
2	122.	-474.	-266.	-654.
3	34.	-337.	-199.	-217.
4	38.	-52.	-15.	-45.
5	90.	-93.	-36.	-41.
6	9.	-25.	-6.	-18.
7	42.	2.	4.	-3.
8	4.	26.	8.	1.
9	-4.	2.	5.	3.
10	13.	1.	2.	0.

BLADE STATION = .45R

N	EXPERIMENTAL A(N)	EXPERIMENTAL B(N)	UNIFORM INFLOW A(N)	UNIFORM INFLOW B(N)
0	259.		1253.	
1	-1022.	1036.	-1232.	1622.
2	190.	-421.	-169.	-693.
3	61.	-431.	-212.	-282.
4	47.	-11.	4.	-25.
5	60.	-65.	-6.	-29.
6	6.	0.	-1.	-9.
7	4.	5.	5.	0.
8	27.	27.	13.	6.
9	-7.	-16.	9.	7.
10	4.	-2.	3	1.

BLADE STATION = .65R

N	EXPERIMENTAL A(N)	EXPERIMENTAL B(N)	UNIFORM INFLOW A(N)	UNIFORM INFLOW B(N)
0	-544.		-990.	
1	-1366.	1359.	-1220.	1519.
2	824.	-143.	496.	-538.
3	335.	-517.	-146.	-450.
4	120.	64.	39.	3.
5	-105.	175.	83.	45.
6	-23.	20.	15.	27.
7	-47.	2.	-1.	6.
8	2.	-20.	-4.	2.
9	10.	-11.	-2.	0.
10	-11.	9.	-1.	0.

BLADE STATION = .80R

N	EXPERIMENTAL A(N)	EXPERIMENTAL B(N)	UNIFORM INFLOW A(N)	UNIFORM INFLOW B(N)
0	-1952.		-1786.	
1	-687.	861.	-656.	747.
2	1056.	7.	595.	-284.
3	440.	-334.	-61.	-348.
4	127.	48.	22.	-9.
5	-121.	251.	70.	57.
6	-84.	8.	13.	27.
7	2.	-24.	-6.	4.
8	-46.	-23.	-19.	-6.
9	-4.	60.	-13.	-10.
10	-1.	-7.	-5.	-1.

TABLE XXXIX b HARMONICS OF CHORDWISE STRESS, PSI

V = 110 KT α_s = -9° L = 11800 LB D = -2150 LB

BLADE STATION = .15R

N	EXPERIMENTAL A(N)	EXPERIMENTAL B(N)	UNIFORM INFLOW A(N)	UNIFORM INFLOW B(N)
0	-901.		460.	
1	605.	-889.	-22.	-405.
2	-19.	-68.	38.	25.
3	101.	193.	258.	-19.
4	9.	61.	44.	8.
5	-42.	-21.	-2.	-15.
6	23.	-21.	-4.	- 6.
7	-38.	19.	1.	- 1.
8	82.	39.	4.	2.
9	-5.	-43.	4.	6.
10	-7.	-1.	1.	5.

BLADE STATION = .375R

EXPERIMENTAL A(N)	EXPERIMENTAL B(N)	UNIFORM INFLOW A(N)	UNIFORM INFLOW B(N)
40.		256.	
489.	-607.	38.	-685.
-17.	5.	67.	74.
301.	218.	565.	-123.
19.	99.	112.	8.
16.	60.	-4.	-6.
-2.	10.	-6.	-5.
-6.	-2.	0.	-1.
33.	11.	2.	1.
16.	-36.	3.	4.
-9.	7.	1.	4.

BLADE STATION = .65R

N	EXPERIMENTAL A(N)	EXPERIMENTAL B(N)	UNIFORM INFLOW A(N)	UNIFORM INFLOW B(N)
0	564.		140.	
1	377.	-260.	171.	-227.
2	-51.	-54.	27.	77.
3	269.	143.	394.	-187.
4	22.	77.	99.	-6.
5	21.	91.	-2.	31.
6	-29.	22.	1.	9.
7	26.	-4.	-4.	1.
8	-88.	-52.	-6.	-3.
9	-10.	60.	-6.	-8.
10	18.	0.	-2.	-5.

BLADE STATION = .80R

EXPERIMENTAL A(N)	EXPERIMENTAL B(N)	UNIFORM INFLOW A(N)	UNIFORM INFLOW B(N)
1342.		67.	
144.	-21.	102.	-44.
-34.	-27.	8.	38.
112.	51.	165.	-99.
10.	35.	46.	-5.
11.	53.	-1.	20.
-16.	17.	1.	6.
14.	-4.	-2.	1.
-68.	-33.	-4.	-2.
-6.	51.	-4.	-5.
16.	-2.	-1.	-4.

TABLE XXXIX c HARMONICS OF TORSIONAL STRESS, PSI

V = 110 KT α_s = -9° L = 11800 LB D = -2150 LB

BLADE STATION .15R

N	EXPERIMENTAL A(N)	EXPERIMENTAL B(N)	UNIFORM INFLOW A(N)	UNIFORM INFLOW B(N)
0	136.		-206.	
1	-98.	-74.	-132.	-46.
2	28.	-74.	61.	-9.
3	-7.	-10.	5.	1.
4	-4.	-12.	-2.	-5.
5	-8.	-13.	-1.	4.
6	-3.	5.	-2.	4.
7	-17.	7.	-2.	2.
8	9.	3.	-1.	-1.
9	4.	0.	-2.	-2.
10	-3.	1.	-2.	0.

BLADE STATION .375R

N	EXPERIMENTAL A(N)	EXPERIMENTAL B(N)	UNIFORM INFLOW A(N)	UNIFORM INFLOW B(N)
0	226.		-252.	
1	-170.	-135.	-161.	-56.
2	15.	-81.	74.	-11.
3	-24.	9.	6.	1.
4	2.	-8.	-2.	-6.
5	3.	-24.	-1.	5.
6	2.	5.	-2.	5.
7	-19.	-6.	-2.	2.
8	13.	1.	-1.	-1.
9	-1.	-5.	-2.	-2.
10	-12.	-1.	-2.	0.

BLADE STATION .65R

N	EXPERIMENTAL A(N)	EXPERIMENTAL B(N)	UNIFORM INFLOW A(N)	UNIFORM INFLOW B(N)
0	352.		-177.	
1	-141.	-152.	-113.	-39.
2	-1.	-34.	52.	-8.
3	-11.	10.	5.	1.
4	-10.	-3.	-2.	-4.
5	1.	-15.	-1.	4.
6	0.	4.	-1.	4.
7	-14.	-3.	-2.	1.
8	10.	2.	-1.	-1.
9	0.	-3.	-1.	-2.
10	-9.	-2.	-2.	0.

DISTRIBUTION

US Army Materiel Command	5
US Army Mobility Command	5
US Army Aviation Materiel Command	6
US Army Aviation Materiel Laboratories	24
US Army R&D Group (Europe)	2
US Army Limited War Laboratory	1
US Army Human Engineering Laboratories	1
US Army Research Office-Durham	1
US Army Test and Evaluation Command	1
Plastics Technical Evaluation Center	1
US Army Medical R&D Command	1
US Army Engineer Waterways Experiment Station	1
US Army Combat Developments Command, Fort Belvoir	2
US Army Combat Developments Command Experimentation Command	3
US Army War College	1
US Army Command and General Staff College	1
US Army Aviation School	1
US Army Infantry Center	2
US Army Tank-Automotive Center	2
US Army Aviation Maintenance Center	2
US Army Armor and Engineer Board	1
US Army Electronics Command	2
US Army Aviation Test Activity	2
Air Force Flight Test Center, Edwards AFB	2
US Army Field Office, AFSC, Andrews AFB	1
Air Force Flight Dynamics Laboratory, Wright-Patterson AFB	1
Systems Engineering Group (RTD), Wright-Patterson AFB	3
Air Proving Ground Center, Eglin AFB	1
Naval Air Systems Command, DN	2
Bureau of Naval Weapons, DN	4
Chief of Naval Research	4
David Taylor Model Basin	1
Marine Corps Liaison Officer, US Army Transportation School	1
Testing and Development Division, US Coast Guard	1
Ames Research Center, NASA	1
Lewis Research Center, NASA	1
Manned Spacecraft Center, NASA	1
NASA Representative, Scientific and Technical Information Facility	2
NAFEC Library (FAA)	2
National Tillage Machinery Laboratory	1
US Army Aviation Human Research Unit	2
US Army Board for Aviation Accident Research	1

Bureau of Safety, Civil Aeronautics Board	2
US Naval Aviation Safety Center, Norfolk	1
Federal Aviation Agency, Washington, D. C.	1
Bureau of Flight Standards, FAA	1
Civil Aeromedical Research Institute, FAA	2
The Surgeon General	1
Defense Documentation Center	20

Unclassified

Security Classification

DOCUMENT CONTROL DATA - R&D

(Security classification of title, body of abstract and indexing annotation must be entered when the overall report is classified)

1 ORIGINATING ACTIVITY (Corporate author)	2a. REPORT SECURITY CLASSIFICATION
Sikorsky Aircraft Division of United Aircraft Corp. Stratford, Connecticut	Unclassified
	2b GROUP

3. REPORT TITLE

A Presentation of Measured and Calculated Full-Scale Rotor Blade Aerodynamic and Structural Loads

4 DESCRIPTIVE NOTES (Type of report and inclusive dates)

Final Report

5. AUTHOR(S) (Last name, first name, initial)

Rabbott, J. P., Jr. Paglino, V. M.
Lizak, A. A.

6. REPORT DATE	7a. TOTAL NO. OF PAGES	7b. NO. OF REFS
July 1966	176	18

8a. CONTRACT OR GRANT NO.	9a. ORIGINATOR'S REPORT NUMBER(S)
DA 44-177-AMC-53(T) b. PROJECT NO. c. Task 1P125901A14604 d	USAAVLABS Technical Report 66-31
	9b. OTHER REPORT NO(S) (Any other numbers that may be assigned this report) SER-58398

10. AVAILABILITY/LIMITATION NOTICES

Distribution of this document is unlimited.

11. SUPPLEMENTARY NOTES	12. SPONSORING MILITARY ACTIVITY
	US Army Aviation Materiel Laboratories Fort Eustis, Virginia

13. ABSTRACT

A test of a set of Sikorsky CH-34 rotor blades was conducted in the NASA/Ames full-scale wind tunnel at speeds of 110 to 175 knots. One blade of the set was instrumented to measure differential chordwise pressures, as well as flapwise, chordwise and torsional stress. The test results are presented, two- and three-dimensional pressure distributions are compared, and a correlation of airloads and blade stresses is made with a flexible blade aeroelastic theory, including both uniform and variable inflow assumptions.

Correlation of airloads and stresses with theoretical results was generally good. Inclusion of variable inflow improved correlation on both advancing and retreating sides of the disk at speeds as high as 175 knots, but the need for a more precise wake treatment is indicated. There is also evidence of a requirement for including lifting surface effects in the calculation at the advancing blade tip.

A comparison of some of the wind tunnel data with flight test results shows good agreement.

DD FORM 1 JAN 64 1473

Unclassified

Security Classification

Unclassified

Security Classification

14. KEY WORDS	LINK A		LINK B		LINK C	
	ROLE	WT	ROLE	WT	ROLE	WT
Helicopter Rotor Full-scale Tests Airloads Stress Correlation						

INSTRUCTIONS

1. ORIGINATING ACTIVITY: Enter the name and address of the contractor, subcontractor, grantee, Department of Defense activity or other organization *(corporate author)* issuing the report.

2*a*. REPORT SECURITY CLASSIFICATION: Enter the overall security classification of the report. Indicate whether "Restricted Data" is included. Marking is to be in accordance with appropriate security regulations.

2*b*. GROUP: Automatic downgrading is specified in DoD Directive 5200.10 and Armed Forces Industrial Manual. Enter the group number. Also, when applicable, show that optional markings have been used for Group 3 and Group 4 as authorized.

3. REPORT TITLE: Enter the complete report title in all capital letters. Titles in all cases should be unclassified. If a meaningful title cannot be selected without classification, show title classification in all capitals in parenthesis immediately following the title.

4. DESCRIPTIVE NOTES: If appropriate, enter the type of report, e.g., interim, progress, summary, annual, or final. Give the inclusive dates when a specific reporting period is covered.

5. AUTHOR(S): Enter the name(s) of author(s) as shown on or in the report. Enter last name, first name, middle initial. If military, show rank and branch of service. The name of the principal author is an absolute minimum requirement.

6. REPORT DATE: Enter the date of the report as day, month, year, or month, year. If more than one date appears on the report, use date of publication.

7*a*. TOTAL NUMBER OF PAGES: The total page count should follow normal pagination procedures, i.e., enter the number of pages containing information.

7*b*. NUMBER OF REFERENCES: Enter the total number of references cited in the report.

8*a*. CONTRACT OR GRANT NUMBER: If appropriate, enter the applicable number of the contract or grant under which the report was written.

8*b*, 8*c*, & 8*d*. PROJECT NUMBER: Enter the appropriate military department identification, such as project number, subproject number, system numbers, task number, etc.

9*a*. ORIGINATOR'S REPORT NUMBER(S): Enter the official report number by which the document will be identified and controlled by the originating activity. This number must be unique to this report.

9*b*. OTHER REPORT NUMBER(S): If the report has been assigned any other report numbers *(either by the originator or by the sponsor)*, also enter this number(s).

10. AVAILABILITY/LIMITATION NOTICES: Enter any limitations on further dissemination of the report, other than those imposed by security classification, using standard statements such as:

(1) "Qualified requesters may obtain copies of this report from DDC."

(2) "Foreign announcement and dissemination of this report by DDC is not authorized."

(3) "U. S. Government agencies may obtain copies of this report directly from DDC. Other qualified DDC users shall request through _____."

(4) "U. S. military agencies may obtain copies of this report directly from DDC. Other qualified users shall request through _____."

(5) "All distribution of this report is controlled. Qualified DDC users shall request through _____."

If the report has been furnished to the Office of Technical Services, Department of Commerce, for sale to the public, indicate this fact and enter the price, if known.

11. SUPPLEMENTARY NOTES: Use for additional explanatory notes.

12. SPONSORING MILITARY ACTIVITY: Enter the name of the departmental project office or laboratory sponsoring *(paying for)* the research and development. Include address.

13 ABSTRACT Enter an abstract giving a brief and factual summary of the document indicative of the report, even though it may also appear elsewhere in the body of the technical report. If additional space is required, a continuation sheet shall be attached.

It is highly desirable that the abstract of classified reports be unclassified. Each paragraph of the abstract shall end with an indication of the military security classification of the information in the paragraph, represented as *(TS)*, *(S)*, *(C)*, or *(U)*.

There is no limitation on the length of the abstract. However, the suggested length is from 150 to 225 words.

14. KEY WORDS: Key words are technically meaningful terms or short phrases that characterize a report and may be used as index entries for cataloging the report. Key words must be selected so that no security classification is required. Identifiers, such as equipment model designation, trade name, military project code name, geographic location, may be used as key words but will be followed by an indication of technical context. The assignment of links, rules, and weights is optional.

Unclassified

Security Classification